MINISTÉRIO DA SAÚDE
FUNDAÇÃO OSWALDO CRUZ
INSTITUTO OSWALDO CRUZ

Doutorado em Biologia Celular e Molecular

ESTUDO *IN VITRO* E *IN VIVO* DA AÇÃO DE NOVAS DROGAS SOBRE A REPLICAÇÃO DO VÍRUS INFLUENZA

CAROLINA DE QUEIROZ SACRAMENTO

Rio de Janeiro
Setembro de 2017

Ministério da Saúde

FIOCRUZ
Fundação Oswaldo Cruz

INSTITUTO OSWALDO CRUZ
Programa de Pós-Graduação em Biologia Celular e Molecular

CAROLINA DE QUEIROZ SACRAMENTO

Estudo *in vitro* e *in vivo* da ação de novas drogas sobre a replicação do vírus influenza.

Tese apresentada ao Instituto Oswaldo Cruz como parte dos requisitos para obtenção do título Doutor em Ciências pela Pós-graduação em Biologia Celular e Molecular

Orientador (es): Prof. Dr. Thiago Moreno Lopes e Souza

Prof. Dr. Fernando Augusto Bozza

RIO DE JANEIRO
Setembro de 2017

Sacramento, Carolina de Queiroz .

Estudo in vitro e in vivo da ação de novas drogas sobre a replicação do vírus influenza. / Carolina de Queiroz Sacramento. - Rio de janeiro, 2017.
88 f.; il.

Tese (Doutorado) – Instituto Oswaldo Cruz, Pós-Graduação em Biologia Celular e Molecular, 2017.

Orientador: Thiago Moreno Lopes e Souza.
Co-orientador: Fernando Augusto Bozza.

Bibliografia: Inclui Bibliografias.

1. Antivirais. 2. Vírus influenza. 3. Hemaglutinina. 4. Neuraminidase. 5. RNA polimerase. I. Título.

Elaborada pelo Sistema de Geração Automática de Ficha Catalográfica da Biblioteca de Manguinhos/ICICT com os dados fornecidos pelo(a) autor(a).

Ministério da Saúde

FIOCRUZ
Fundação Oswaldo Cruz

INSTITUTO OSWALDO CRUZ

Programa de Pós-Graduação em Biologia Celular e Molecular

AUTOR: CAROLINA DE QUEIROZ SACRAMENTO

ESTUDO *IN VITRO* E *IN VIVO* DA AÇÃO DE NOVAS DROGAS SOBRE A REPLICAÇÃO DO VÍRUS INFLUENZA

ORIENTADOR (ES): Prof. Dr. Thiago Moreno Lopes e Souza
Prof. Dr. Fernando Augusto Bozza

Aprovada em: 13/09/2017

EXAMINADORES:

Prof. Dr. Flavia Barreto dos Santos - Presidente – Pesquisadora do Laboratório de Imunologia Viral / IOC-FIOCRUZ
Prof. Dr. Marcio Lourenço Rodrigues – Vice Coordenador Geral do Centro de Desenvolvimento Tecnológico em Saúde / CDTS-FIOCRUZ
Prof. Dr. Luciana Barros de Arruda – Pesquisadora do Departamento de Virologia / Instituto de Microbiologia-UFRJ
Prof. Dr. Vinicius de Farias Carvalho – Pesquisador do Laboratório de Inflamação / IOC-FIOCRUZ (Suplente)
Prof. Dr. Eduardo de Mello Volotão – Pesquisador do Laboratório de Virologia Comparada e Ambiental / IOC-FIOCRUZ (Revisor e Suplente)

Rio de Janeiro, 13 de setembro de 2017

AGRADECIMENTOS

Ao Dr. Thiago Moreno, meu orientador, por desde a iniciação científica me dar a oportunidade de trabalhar com ele, pelos projetos que desenvolvemos juntos, por tantos ensinamentos, conselhos e confiança no meu desempenho e trabalho;

Ao meu co-orientador Dr. Fernando Bozza pelo apoio durante o desenvolvimento da tese;

Aos chefes e equipe do Laboratório de Vírus Respiratórios e do Sarampo (LVRS) e do Laboratório de Imunofarmacologia pela contribuição e troca de conhecimentos;

Ao grupo “as alunas do Thiago e...”: André, Andressa, Carol, Gabi, Milene, Natália, Natasha e Priscila, por todo companheirismo, discussões científicas, bate papo, momentos de confraternização e risadas. Acrescento um agradecimento especial à Natália pelas escritas de artigos com guloseimas, por sempre me ajudar e principalmente pela amizade. Outro a Carol Freitas, pela imensa ajuda, pelo trabalho que desenvolvemos juntas, por ser uma aluna tão carinhosa e dedicada, e por ter me permitido ser sua co-orientadora;

Aos amigos da pós-graduação que estiveram comigo em disciplinas, congressos e seminários. Um agradecimento especial a Juliana Melgaço, pelo apoio pessoal e científico;

À minha mãe Aliane por ser sempre meu apoio e minha amiga, por acreditar em mim, se orgulhar e me dar força em todas as escolhas e decisões. Aos meus irmãos Katherine e Rafael pelos bons momentos, carinho e amizade. À amiga-irmã Flávia pelas longas conversas e aconselhamentos pessoais e profissionais;

Ao meu noivo, namorado e amigo Thiago Faria por todo o carinho, amor, companheirismo, amizade e compreensão até nos momentos mais atarefados;

À todos os nossos colaboradores que nos forneceram os compostos que foram utilizados neste trabalho, como o grupo da Dra. Gisela da Costa (IOC-FIOCRUZ), os grupos da Dra. Maria Cecília de Souza e do Dr. Vitor Ferreira (Departamento de Química Orgânica-UFF), e o grupo da Dra. Nubia Boechat e do Dr. Luiz Pinheiro (Farmanguinhos-FIOCRUZ);

À banca por terem aceitado o convite de avaliar o meu trabalho;

À Pós-Graduação em Biologia Celular e Molecular, coordenadores, funcionários e corpo docente por todo aprendizado e oportunidade de crescimento;

À Coordenação de Aperfeiçoamento de Pessoal de Nível Superior – CAPES pelo auxílio financeiro;

E a todos que contribuíram direta ou indiretamente para a conclusão deste trabalho.

Muito obrigada!

“A tarefa não é tanto ver aquilo que ninguém viu, mas pensar o que ninguém ainda pensou sobre aquilo que todo mundo vê.” (Arthur Schopenhauer)

Ministério da Saúde

FIOCRUZ
Fundação Oswaldo Cruz

INSTITUTO OSWALDO CRUZ

ESTUDO *IN VITRO* E *IN VIVO* DA AÇÃO DE NOVAS DROGAS SOBRE A REPLICAÇÃO DO VÍRUS INFLUENZA

RESUMO

TESE DE DOUTORADO EM BIOLOGIA CELULAR E MOLECULAR

Carolina de Queiroz Sacramento

Os vírus influenza são um dos principais causadores das infecções respiratórias agudas e apresentam grande impacto na saúde pública. Existe somente uma classe de drogas anti-influenza em uso atualmente, os inibidores de neuraminidase, como o oseltamivir. Como já foram descritas cepas circulantes resistentes a este composto, torna-se necessária a busca por novas moléculas capazes de inibir essas cepas e/ou atuar sobre outros alvos durante a replicação viral. Este trabalho visa estudar o mecanismo de ação de quatro novos compostos contra o vírus influenza: aureonitol, composto **1i**, tritempo e composto **5b**. Todos os compostos inibiram a replicação do vírus influenza em células MDCK com baixa toxicidade e apresentaram alto índice de seletividade para utilização *in vitro*. O aureonitol, um produto natural derivado de espécies do fungo *Chaetomium*, é um potente inibidor da hemaglutinina do vírus influenza, bloqueando a entrada do vírus na célula hospedeira. O composto **1i** é um composto oxoquinolínico capaz de inibir a neuraminidase do vírus influenza. Embora seja menos potente que o oseltamivir em inibir cepas sensíveis, nosso composto foi capaz de inibir cepas resistentes nas quais o oseltamivir não possui efeito inibitório. O tritempo possui uma estrutura química semelhante ao **1i** e se mostrou ainda mais potente em inibir a neuraminidase viral de cepas sensíveis e resistentes ao oseltamivir além de não apresentar resistência cruzada com o composto de referência. O composto **5b** é um análogo da ribavirina e tem como alvo a RNA polimerase do influenza, desregulando o balanço entre os processos de duplicação e transcrição do genoma viral. Este também possui propriedades imunomoduladoras *in vitro* e em camundongos infectados pelo vírus influenza. Os quatro compostos se mostraram potentes inibidores do vírus influenza, com mecanismos de ação inovadores, tornando suas estruturas químicas promissoras para o desenvolvimento de novas drogas anti-influenza. Estudamos também a atividade natural endógena da RNA polimerase do vírus influenza e descrevemos suas aplicações para melhorar a sensibilidade do diagnóstico e como ferramenta para triagem de novas drogas com alvo na RNA polimerase viral.

Ministério da Saúde

FIOCRUZ
Fundação Oswaldo Cruz

INSTITUTO OSWALDO CRUZ

IN VITRO AND *IN VIVO* STUDY OF THE ACTION OF NEW DRUGS AGAINST INFLUENZA VIRUS REPLICATION

ABSTRACT

PHD THESIS IN CELLULAR AND MOLECULAR BIOLOGY

Carolina de Queiroz Sacramento

Influenza virus represents one of the main causes of acute respiratory infections, being a major cause of burden to public health. The sole class of anti-influenza drugs currently in clinical use is represented by neuraminidase inhibitors such as oseltamivir. Nevertheless, oseltamivir-resistant strains have been described, motivating the search for novel compounds with different targets and able to inhibit them. This work aims to study the mechanism of action of four new compounds against influenza virus: aureonitol, compound **1i**, tritempo and compound **5b**. All of them inhibited influenza replication in MDCK cells with low cytotoxicity and presented high selective index for *in vitro* use. Aureonitol, a natural product derived from species of the fungus *Chaetomium*, is a potent inhibitor of influenza hemagglutinin and blocks viral entry. Compound 1i is an oxoquinoline able to inhibit viral neuraminidase. Although less potent than oseltamivir in the inhibition of wild-type strains, our compound inhibited oseltamivir-resistant influenza strains. Tritempo`s chemical structure is similar to compound **1i**`s. Tritempo is even more potent in inhibiting influenza virus wild-type and oseltamivir-resistant neuraminidases and does not present cross-resistance with oseltamivir. Compound **5b** is a ribavirin analogue and targets viral RNA polymerase, disrupting the balance between replication and transcription of influenza genome. This compound also possesses immunomodulatory properties *in vitro* and in mice infected with influenza virus. The four tested compounds are potent inhibitors of influenza virus and have innovative mechanisms of action. Their chemical structures are promising for the development of novel anti-influenza drugs. We also studied the natural endogenous RNA polymerase activity of influenza virus and described its applicability in improving the sensibility of diagnosis and as a tool for screening of novel drugs targeting viral RNA polymerase.

ÍNDICE

ÍNDICE DE FIGURAS

LISTA DE TABELAS

LISTA DE SIGLAS E ABREVIATURAS

A549 - Células de linhagem de epitélio pulmonar humano

aa - Aminoácidos

ARDS - Do inglês, *Adult respiratory distress syndrome*

AS – Ácido siálico

BAL – Lavado broncoalveolar (do inglês, *Bronchoalveolar lavage*)

CC_{50} - Concentração da droga que mantém 50% das células viáveis

CD – Cluster de diferenciação (do inglês, *Cluster of differentiation*)

CDC – Centro de Controle e Prevenção de Doenças (do inglês, *Center for Disease Control and Prevention)*

DANA – Ácido 2-deoxi-2,3-dehidro-N-acetilneuramínico

DNA - Ácido desoxirribonucleico

EC_{50} - Concentração da droga capaz de inibir 50% da replicação viral

FDA - Administração de Alimentos e Medicamentos (do inglês, *Food and Drug Administration*)

FF-3 – Flufirvitida-3

FIOCRUZ - Fundação Oswaldo Cruz

GTP - Guanosina trifosfato

HA - Hemaglutinina

HCV - Vírus da hepatite C (do inglês, *Hepatitis C virus*)

HIV – Vírus da imunodeficiência humana (do inglês, *Human immunodeficiency virus*)

HSV - Vírus Herpes Simplex (do inglês, *herpes simplex virus*)

IC_{50} - Concentração da droga capaz de inibir 50% da atividade enzimática

ICTV - Comitê Internacional de Taxonomia de Vírus

IFN-α/β/γ - Interferon alfa/beta/gama

IL - Interleucina

IMPDH – Inosina monofosfato desidrogenase

Kb - Kilobases

mAb – Anticorpo monoclonal (do inglês, *monoclonal antibody*)

MCP-1 - Proteína quimiotática para monócitos

MDCK - Células epiteliais de rim canino

MIP-1α – Proteína inflamatória de macrófagos 1 alfa (do ingles, *Macrophage inflammatory protein 1 alpha*)

MOI - Multiplicidade de infecção (relação vírus/célula)

NA - Neuraminidase

NAIs - Inibidores de neuraminidase

NEP/NS2 - Proteína de exportação nuclear/proteína não estrutural 2

NERP – Atividade natural endógena da RNA polimerase (do inglês, *Natural endogenous RNA polimerase*)

NK – Células *Natural Killer*

NP - Nucleoproteína

NS1 - Proteína não estrutural 1 (do inglês, *nonstructural protein 1*)

nt - Nucleotídeos

NTPs - Nucleotídeos trifosfatados

OMS - Organização Mundial de Saúde

OST - Oseltamivir

PA - Polimerase ácida

PB1 - Polimerase básica 1

PB2 - Polimerase básica 2

PCR - Reação em cadeia da polimerase

PF – Peptídeo de fusão

pH - Potencial hidrogeniônico

PKR – Proteína kinase R

RANTES – Quimiocina regulada sob ativação, expressa e secretada por células T normais (do ingles, *Regulated on Activation, Normal T cell Expressed and Secreted*)

RAP – Receptor ativado por proteinase

RB - Ribavirina

RDP - Ribavirina defosfatada

RE - Retículo endoplasmático

RMP - Ribavirina monofostato

RNA - Ácido ribonucleico

RNAc - Ácido ribonucleico complementar

RNAmc - Ácido ribonucleico mensageiro celular

RNAmv - Ácido ribonucleico mensageiro viral

RNAv - Ácido ribonucleico viral

RNP - Ribonucleoproteína

RpRd - RNA polimerase RNA dependente

RSV - Vírus Sincicial Respiratório (do inglês, *Respiratory syncytial virus*)

RTP - Ribavirina trifosfato

SE – Semana Epidemiológica

SG – Síndrome gripal

SI - Índice de seletividade

SIVEP - Sistemas de Informações da Vigilância em Saúde e Análise de Situação de Saúde

SRAG – Síndrome respiratória aguda grave

SVS – Sistema de Vigilância em Saúde

Th - Linfócitos T helper

THF – Tetrahidrofurano

TNFR – Receptor de TNF

TNF-α - Fator de necrose tumoral alfa

TR – Transcriptase reversa

UFF – Universidade Federal Fluminense

UTI – Unidade de tratamento intensivo

ZAN – Zanamivir

1 INTRODUÇÃO

1.1 Histórico

Os primeiros relatos de infecções do trato respiratório ocorreram no ano 412 a.C., na Grécia antiga, quando Hipócrates, considerado o “pai da medicina”, relatou casos de uma doença respiratória com sintomatologia semelhante à ocasionada pelo influenza, que, em algumas semanas, levou a muitos óbitos e depois desapareceu. Posteriormente, encontraram-se relatos históricos de infecções durante a Guerra de Peloponeso em Atenas (430 a.C.) e durante a Guerra dos Cem dias (Nicholson, 1998).

O termo “influenza”, ou “influência”, data da Idade Média, na Itália, quando acreditava-se que os sinais clínicos causados pela infecção, como febre, tosse e calafrios, ocorriam por influência astrológica devido à sua associação com determinadas épocas do ano. Mais tarde, ocorreu uma alteração de significado para "influência do frio", já que os surtos eram mais comuns durante os meses de inverno. Já o termo “gripe” tem origem francesa (“grippe"). O vocábulo francês "grippe" era empregado no início do século XIV com o sentido de "gancho" ou "garra". No século XVII, o termo era utilizado com o sentido de "capricho, desejo repentino" e, no século XVIII, passou a denominar "o catarro epidêmico", em uma extensão do sentido de "capricho", provavelmente pelo fato da doença ser adquirida de modo repentino, como um desejo caprichoso do destino (Ws, 1997).

Desde o século XVI foram relatadas epidemias e pandemias causadas pelo vírus influenza. No século XX ocorreram três notáveis pandemias nos anos de 1918, 1957 e 1968 e, de menor impacto em 1977 (Who, 1999). A Tabela 1.1 e a Figura 1.1 resumem as quatro pandemias do século XX, identificando o subtipo viral e a possível origem do vírus influenza A que causou cada uma delas, além do impacto gerado pelas pandemias (Who, 1999).

Tabela 1.1 - Pandemias humanas de influenza ocorridas no século XX.

Ano	Nome	Vírus	Origem	Impacto
1918	"Gripe Espanhola"	H1N1	Recombinação do vírus suíno ou aviário ou adaptação direta do vírus aviário em humanos.	20 a 40 milhões de óbitos.
1957	"Gripe Asiática"	H2N2	Possível recombinação genética do vírus humano (H1N1) e aviário (H2N2).	1 milhão de óbitos. Vírus H1N1 desapareceu.
1968	"Gripe de Hong Kong"	H3N2	Alta probabilidade de recombinação genética do vírus humano (H2N2) e do vírus aviário (H3Nx).	1 milhão de óbitos. Vírus H2N2 desapareceu.
1977	"Gripe Russa"	H1N1	Origem desconhecida, mas o vírus H1N1 é idêntico ao de 1950.	Potencial pandêmico. Envolveu inicialmente pessoas nascidas após 1950. O vírus H1N1 co-circulou com o H3N2.

Fonte: Adaptado de Organização Mundial da Saúde – *Influenza Pandemic Plan* (Who, 1999).

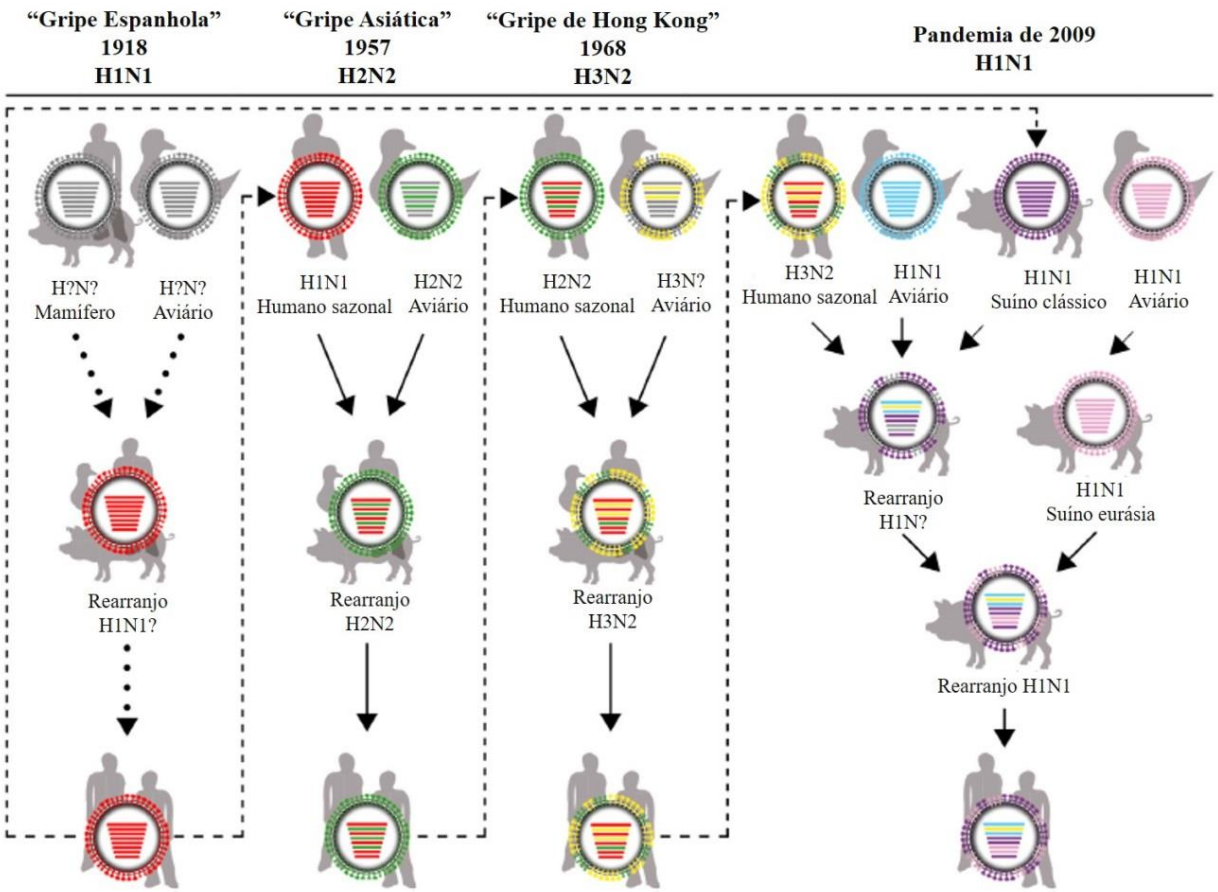

Figura 1.1 - Rearranjo e adaptação dos vírus influenza que causaram as pandemias de 1918, 1957, 1968 e 2009.
Humanos, aves e suínos podem ser infectados simultaneamente por vírus influenza de diferentes cepas do gênero A. Este fato, combinado ao genoma segmentado do vírus influenza, pode levar ao rearranjo gênico e o surgimento de cepas pandêmicas, como foram os casos dos vírus H1N1 (1918), H2N2 (1957), H3N2 (1968) e H1N1 (2009). Os genes identificados com a cor cinza dentro das partículas virais indicam origem incerta dos segmentos genômicos ou ausência de dados. As setas pontilhadas indicam cenários incertos e, as setas cheias, eventos com evidência científica. As setas tracejadas representam os vírus pandêmicos que circularam de forma sazonal posteriormente a pandemia. Fonte: Adaptado de Schrauwen, E. J. A. et al Eur J Clin Microbiol Infect Dis, 2014 (Schrauwen *et al.*, 2014).

No ano de 2009 ocorreu a emergência de nova linhagem do vírus influenza A/H1N1, que provocou a primeira pandemia do século XXI, e ficou conhecido como A(H1N1)pdm09. A circulação deste vírus teve início no México e Canadá, se espalhando rapidamente por todo o mundo (Cdc, 2010). Este novo vírus foi produto de um rearranjo gênico entre dois genes derivados da linhagem aviária norte-americana (PA e PB2), um gene da linhagem sazonal de H3N2 (PB1), três genes da linhagem suína clássica norte-americana (HA, NP e NS) e dois genes da linhagem suína euro-asiática (NA e M) (Figura 1.1) (Ha *et al.*, 2011). Este vírus teve alta transmissibilidade entre humanos, afetando 74 países entre 2009 e 2010 (Belshe, 2009). O Centro de Controle de Doenças dos Estados Unidos (CDC – sigla em inglês para *Center of*

Disease Control) estimou que entre 43 e 89 milhões de pessoas foram infectadas pelo vírus A(H1N1)pdm09, de oito a 18 mil óbitos de Abril de 2009 a Abril de 2010 (Flu.Gov, 2011). Em Agosto de 2010, a Organização Mundial de Saúde (OMS) declarou o fim da pandemia e, desde então, o vírus A(H1N1)pdm09 passou a co-circular na população juntamente com o H3N2, tornando-se portanto, um influenza sazonal, que foi incluído nas vacinas de 2010 a 2016 (Who, 2009a; 2010a; b; 2011; 2012a; 2013a; 2014c; 2015a). É interessante ressaltar, que a cepa do vírus influenza A(H1N1)pdm09 que tem circulado desde 2009 (A/California/7/2009), foi modificada pela primeira vez nos últimos sete anos. Portanto, na campanha de vacinação anual de 2017, ocorreu uma mudança para a cepa A/Michigan/45/2015 (Saúde, M. D., 2017b).

Além das quatro pandemias que ocorreram nos séculos XX e XX1, vem sendo reportadas ameaças de pandemias. Em 1976, um vírus influenza suíno muito semelhante à cepa causadora da Gripe Espanhola foi descrito em Nova Jersey, nos Estados Unidos. Em 1977, na China, um novo vírus foi detectado e se espalhou muito rapidamente tornando-se uma epidemia mundial. Este fato não foi considerado como pandemia porque a maioria das pessoas infectadas eram crianças (Flu.Gov, 2011). Em ambos os casos, campanhas de vacinação foram implementadas a fim de prevenir surtos futuros causados por estes subtipos virais.

Em 1996, um novo vírus influenza aviário H5N1 altamente patogênico foi isolado de alguns gansos na província de Guangdong na China. Em 1997, foi detectado um surto deste mesmo subtipo em aves domésticas em Hong Kong e, neste mesmo ano, foram reportados 18 casos de infecção em seres humanos, sendo seis casos fatais, confirmando o rompimento da barreira animal-humano. Embora até o momento as evidências epidemiológicas e virológicas ainda não tenham confirmado a transmissão sustentada entre humanos deste subtipo viral, a emergência de um vírus aviário de alta patogenicidade capaz de infectar seres humanos é de significativa importância para a saúde pública, sendo necessária a vigilância contínua. Em 2013, na Ásia, houve um aumento significativo de surtos causados pelo vírus H5N1 altamente patogênico (Who, 2015b). De acordo com o último reporte da OMS, de 2013 a maio de 2017, 859 casos de infecção foram confirmados em laboratório incluindo 453 mortes em 16 países asiáticos (Who, 2017a).

Também em 2013, foi detectada pela primeira vez a infecção de seres humanos com o vírus influenza aviário A(H7N9). Foram confirmados 132 casos na China. A maioria dos casos foi considerada grave e 37 pessoas morreram. Embora seja um vírus aviário, o H7N9 não causa doença grave em aves domésticas, o que torna difícil a confirmação da procedência aviária dos casos reportados. O vírus H7N9 ainda é pouco conhecido com relação aos seus

reservatórios e sua capacidade de transmissão de aves para humanos e entre humanos, porém, por ser um vírus altamente patogênico, a OMS recomenda que os países se mantenham em alerta para uma possível circulação maciça desse subtipo viral (Who, 2013b). Em 2014, o número de casos detectados teve um aumento: 454 casos de infecção em humanos pelo vírus A(H7N9) foram reportados em toda a China, sendo importados para Hong Kong, Taiwan e Malásia (Blachere *et al.*, 2007). Desde 2015 até último boletim liberado pela OMS (maio de 2017), dados epidemiológicos mostram que o número de novos casos de infecção em humanos pelo vírus H7N9 e sua distribuição geográfica continua aumentando, enfatizando a necessidade de intensa vigilância e medidas de controle tanto em humanos como em animais. Porém, a sustentabilidade de infecção entre humanos não foi comprovada e, por isso, o risco de espalhamento pela comunidade é pequeno (Who, 2017a).

Um terceiro subtipo de vírus influenza aviário A(H9N2) segue circulando na China, porém, esse subtipo viral causa doença leve em seres humanos. Sua situação epidemiológica segue sendo monitorada pela OMS, embora até o momento não tenham sido reportados *clusters* de casos e esse vírus não tenha adquirido a capacidade de transmissão entre humanos (Who, 2017a).

1.2 Classificação e nomenclatura dos vírus influenza

Os vírus influenza estão classificados na família *Orthomyxoviridae*, gênero *Influenzavirus* (Murphy e Webster, 1996). Atualmente, existem cinco gêneros de vírus influenza: *Influenzavirus A, B e C,* considerados como vírus influenza propriamente ditos, além dos *Isavirus* e *Thogotovírus* (Fauquet e Fargette, 2005). Os *Thogotovírus* foram isolados de carrapatos e são agentes infecciosos capazes de causar meningite e meningoencefalite em seres humanos. Já os *Isavirus* estão relacionados a quadros clínicos de anemia infecciosa em salmões (Fauquet e Fargette, 2005). A característica geral dos 5 gêneros é apresentação do genoma na forma de RNA fita simples, segmentado com polaridade negativa (Palese, P. e Shaw, M. L., 2007).

Os três gêneros de vírus influenza propriamente ditos diferem na gama de hospedeiros e na patogenicidade. Os gêneros B e C são isolados quase exclusivamente de humanos, enquanto o gênero A possui uma ampla variedade de hospedeiros (Webster *et al.*, 1992). As aves aquáticas representam o reservatório natural dos vírus influenza A, que podem ser então transmitidos para cavalos, gatos, cachorros, baleias, focas, aves silvestres migratórias, galinhas, porcos, humanos e, mais recentemente, este gênero também foi encontrado em morcegos, embora sua origem ainda seja desconhecida (Manz *et al.*, 2013). Enquanto os vírus

influenza A são responsáveis por causar de surtos epidêmicos a pandemias, os vírus influenza B causam epidemias periódicas, e o gênero C causa somente endemias e doenças respiratórias leves (Taubenberger e Morens, 2008).

Os vírus influenza A são divididos em subtipos de acordo com a combinação das suas glicoproteínas de superfície, a hemaglutinina (HA) e a neuraminidase (NA) (Murphy e Webster, 1996). Até o presente momento, já foram descritos 18 tipos de HA (H1 a H18) e 11 tipos de NA (N1 a N11), encontrados em diferentes espécies animais (Webster e Govorkova, 2014). Estes números levam a 198 possíveis combinações de HA e NA, porém, nem todas são viáveis na natureza e algumas geram subtipos virais restritos a alguns hospedeiros (Cardona *et al.*, 2009).

Os tipos são divididos em dois grupos filogenéticos devido a suas diferenças antigênicas: grupo 1 (H1, H2, H5, H6, H8, H9, H11–H13, H16-H18) e grupo 2 (H3, H4, H7, H10, H14 e H15) (Webster e Govorkova, 2014). Vírus contendo três subtipos de HA adquiriram a habilidade de serem transmitidos eficientemente entre humanos (H1, H2 e H3), embora, atualmente circulam sazonalmente os subtipos contendo as HAs tipo 1 e 3 (Schrauwen *et al.*, 2014). Entretanto, outros subtipos de HA, como H5, H6, H7 e H9, ocasionalmente acometem humanos e são considerados possíveis ameaças para uma futura pandemia (Beigel *et al.*, 2005; Gao *et al.*, 2013; Wang *et al.*, 2014; Shen *et al.*, 2015).

De acordo com a OMS, a nomenclatura das amostras humanas é representada da seguinte maneira: indica-se o gênero do vírus ao qual pertence (A, B ou C), a origem geográfica de isolamento (cidade ou país), número da amostra do laboratório e ano de isolamento e, finalmente, coloca-se entre parênteses o subtipo de HA e NA. Por exemplo, uma amostra designada como influenza A/England/42/1972 (H3N2) pertence ao gênero A, subtipo H3N2, isolada na Inglaterra no ano de 1972 e recebeu o número 42.

Além da nomenclatura clássica, algumas terminologias especiais foram adotadas recentemente para se referir e diferenciar algumas variantes importantes, como o vírus pandêmico de 2009 do subtipo H1N1, que ficou estabelecido como A(H1N1)pdm09 (Who, 2011a).

Em contraste com o vírus influenza A, não existem subtipos de influenza B. Este gênero é constituído por duas linhagens principais (Yamagata e Victoria). Embora existam diferenças consideráveis entre as linhagens, seja em termos genéticos ou antigênicos, elas não são suficientes para a designação em diferentes subtipos (Ictvdb, 2006). Assim, a nomenclatura adotada para o vírus influenza B descreve apenas o gênero, local de detecção, número de origem e ano (exemplo: B/Florida/4/2006).

1.3 Epidemiologia e infecções causadas pelo vírus influenza

As infecções pelos vírus influenza ocorrem mundialmente, sob a forma de surtos localizados ou regionais, epidemias sazonais ou pandemias associadas aos subtipos do vírus influenza A. São consideradas epidemias sazonais aquelas que acontecem anualmente durantes os meses de inverno, por um vírus igual ou ligeiramente diferente ao que circulou no ano anterior. Já as pandemias são causadas por um subtipo viral novo, ao qual a população não possui imunidade contra este vírus emergente. Como resultado, a taxa de mortalidade associada a uma pandemia é geralmente maior da que estamos habituados a associar às epidemias sazonais.

Dados da OMS estimam de dois a cinco milhões de casos severos e de 250 a 500 mil óbitos anualmente e apontam que as taxas de infecção global anual são de 5-10% em adultos e de 20-30% em crianças (Who, 2014a).

As infecções apresentam um padrão sazonal, ocorrendo surtos principalmente durante o período de inverno. Desta maneira, os surtos epidêmicos nos hemisférios Norte e Sul ocorrem em períodos do ano diferentes (Figura 1.2) (Who, 2017b). No Brasil, devido à grande diversidade climática, são observados diferentes padrões de sazonalidade, cujo o pico da epidemia no Norte do país costuma ocorrer cerca de três meses antes (março-abril) daquele observado na região Sul (Figura 1.3) (Saúde, M. D., 2017a).

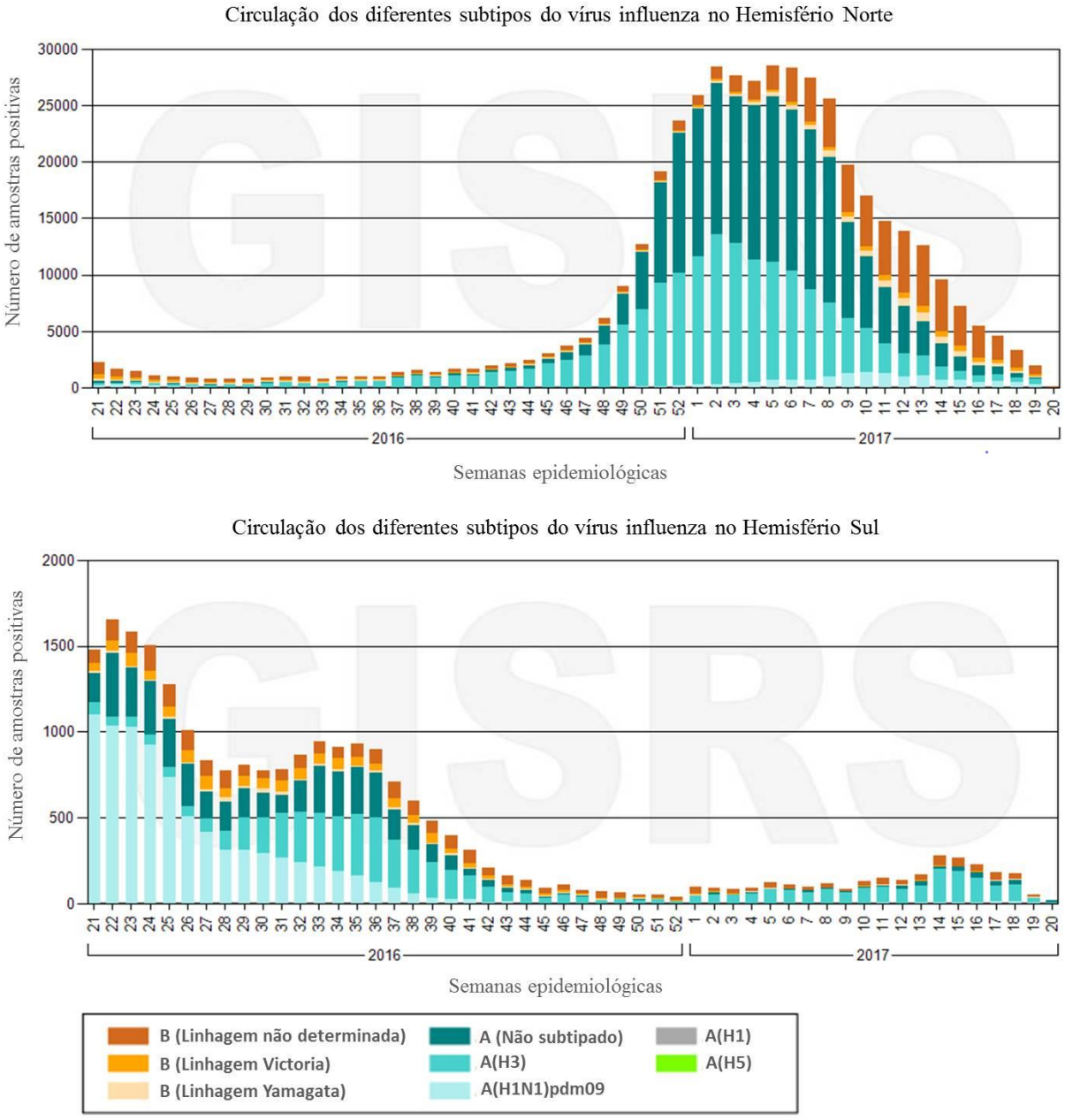

Figura 1.2 - Incidência de Infecção por Influenza nos hemisférios Norte e Sul.
Número de amostras positivas para os diferentes subtipos do vírus influenza em função das semanas epidemiológicas nos hemisférios Norte (gráfico de cima) e Sul (gráfico de baixo), no período 2016/2017. Fonte: Adaptado de OMS (maio de 2017) (Who, 2017b).

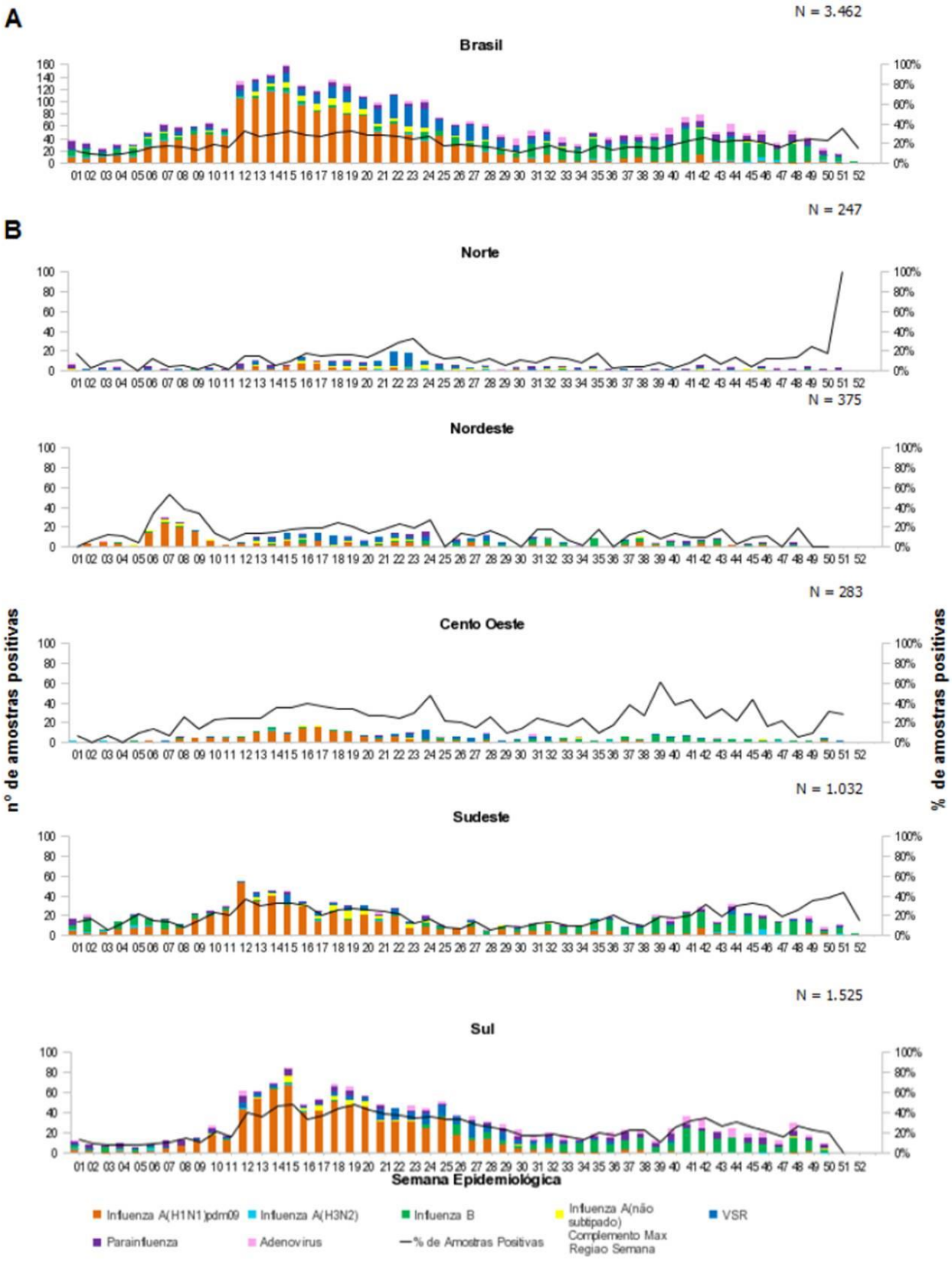

Figura 1.3 - Distribuição dos vírus respiratórios em função das semanas epidemiológicas no Brasil (A) e regiões (B) no ano de 2016.
Fonte: Sistemas de Informações da Vigilância em Saúde e Análise de Situação de Saúde (SIVEP) – Gripe (janeiro de 2017) (Saúde, M. D., 2017b).

A vigilância da circulação dos vírus influenza no Brasil é composta pela vigilância sentinela de Síndrome Gripal (SG), de Síndrome Respiratória Aguda Grave (SRAG) em pacientes internados em Unidade de Terapia Intensiva (UTI) e pela vigilância universal de SRAG. A SG é caracterizada pela presença de febre, acompanhada de tosse ou dor de garganta e início dos sintomas nos últimos sete dias. A vigilância de SG tem como objetivos principais identificar os vírus respiratórios circulantes e permitir o monitoramento da demanda de atendimento por essa doença, e se dá através de uma rede de unidades distribuídas em todas as regiões geográficas do país. Na SRAG, o indivíduo infectado é hospitalizado com febre, acompanhada de tosse ou dor de garganta e que apresente dispneia. Além disso, podem ser observados os seguintes sinais: saturação de O_2 menor que 95% ou desconforto respiratório ou aumento da frequência respiratória A vigilância universal de SRAG monitora os casos hospitalizados e óbitos a fim de identificar o comportamento da influenza no país para orientar na tomada de decisão em situações que requeiram novos posicionamentos do Ministério da Saúde e Secretarias de Saúde Estaduais e Municipais. Como exemplo, na tabela 1.2 e figura 1.4 encontram-se os dados de vigilância de unidades sentinela de SG, SRAG em UTI e SRAG universal no Brasil no ano de 2016 (até a última semana epidemiológica - SE 52) (Saúde, M. D., 2017b); e, na tabela 1.3 e figura 1.5, os dados até a SE 19 de 2017 (Saúde, M. D., 2017a).

Tabela 1.2 - Dados obtidos através da vigilância de unidades sentinela de SG, SRAG em UTI e SRAG universal no Brasil em 2016 (até a última semana epidemiológica - SE 52).

Vigilância por unidades sentinela	Número total de amostras coletadas	Número de amostras processadas N (%)	Número de amostras positivas para vírus respiratórios N (%)	Número de amostras prositivas para os vírus influeza N (%)	Número de amostras positivas de acordo com os subtipos de vírus influenza N (%)			
					A não subtipado	A(H1N1)pdm09	A(H3N2)	B
SG	20.385	16.705 (81,9)	3.462 (20,7)	2.499 (72,2)	137 (5,5)	1.561 (62,5)	43 (1,7%)	757 (30,3)
SRAG em UTI	3.192	2.821 (88,4)	806 (28,6)	447 (55,5)	41 (9,2)	372 (83,2)	4 (0,9)	30 (6,7)
SRAG universal	54.224	44.252 (81,6)	-	12.174 (27,5)*	858 (7,0)	10.625 (87,3)	49 (0,4)	642 (5,3)

* Número de amostras positivas para os vírus influenza obtido diretamente do total de amostras processadas.
Fonte: Adaptado do Boletim Epidemiológico do Sistema de Vigilância em Saúde (SVS – janeiro de 2017) (Saúde, M. D., 2017b).

Tabela 1.3 - Dados obtidos através da vigilância de unidades sentinela de SG, SRAG em UTI e SRAG universal no Brasil até a semana epidemiológica 19 do ano de 2017).

Vigilância por unidades sentinela	Número total de amostras coletadas	Número de amostras processadas N (%)	Número de amostras positivas para vírus respiratórios N (%)	Número de amostras prositivas para os vírus influeza N (%)	Número de amostras positivas de acordo com os subtipos de vírus influenza N (%)			
					A não subtipado	A(H1N1)pdm09	A(H3N2)	B
SG	7.755	5.204 (67,1)	1.660 (31,9)	1.017 (61,3)	38 (3,7)	14 (1,4)	757 (74,4)	207 (20,4)
SRAG em UTI	692	525 (75,9)	146 (27,8)	61 (41,8)	6 (9,8)	2 (3,3)	45 (73,8)	8 (13,1)
SRAG universal	6.840	4.498 (65,7)	-	716 (15,9)*	78 (10,9)	30 (4,2)	481 (67,2)	127 (17,7)

* Número de amostras positivas para os vírus influenza obtido diretamente do total de amostras processadas
Fonte: Adaptado do Boletim Epidemiológico do Sistema de Vigilância em Saúde (SVS – maio de 2017) (Saúde, M. D., 2017a).

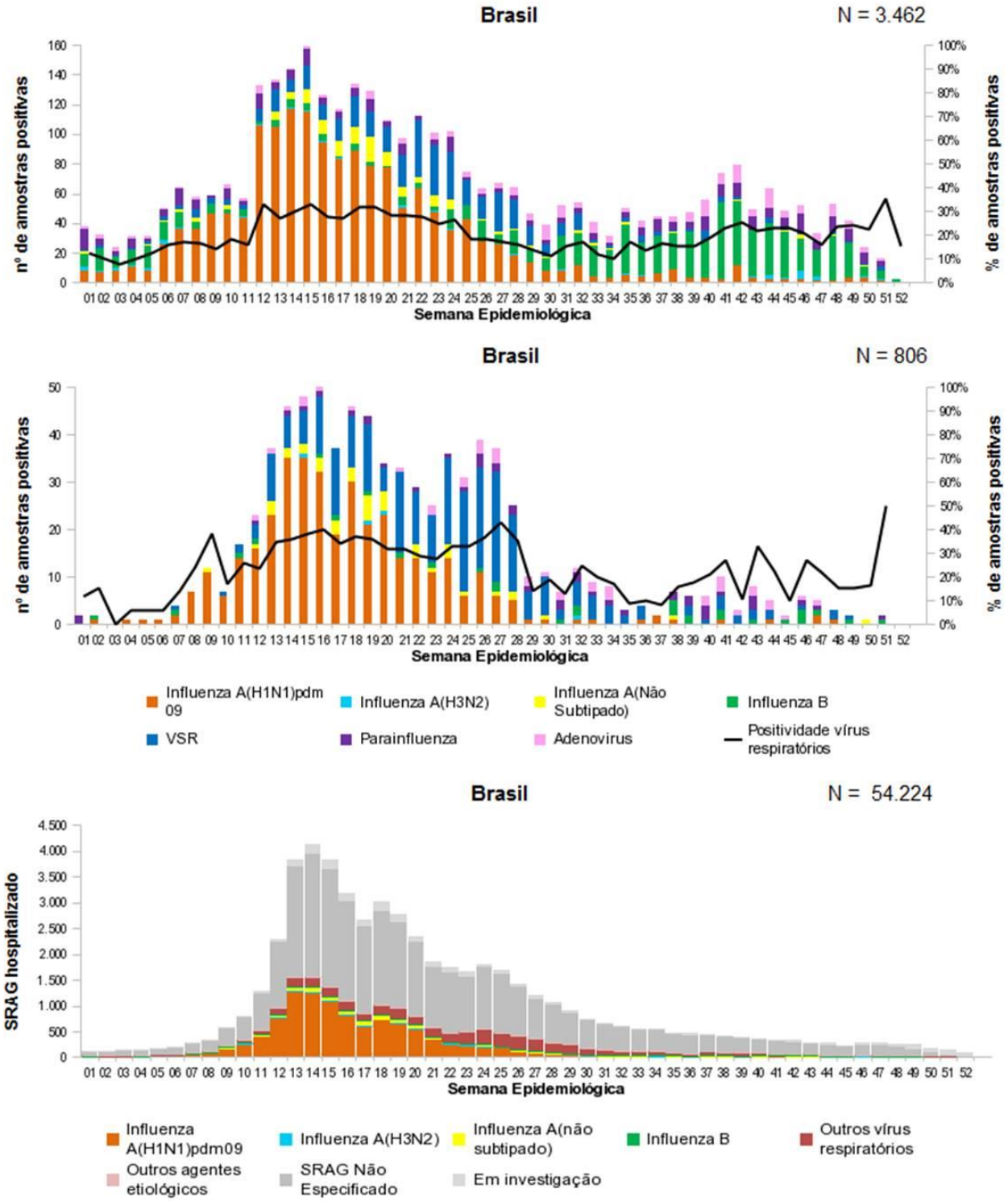

Figura 1.4 - Distribuição dos vírus respiratórios identificados nas unidades sentinelas de Síndrome Gripal (A), Síndrome Respiratória Aguda Grave em Unidade de Terapia Intensiva (B), e distribuição dos casos de Síndrome Respiratória Aguda Grave (C).
Os dados estão distribuídos em função das semanas epidemiológicas de 2016 (até a última semana – SE 52) e dos agentes etiológicos. Fonte: Boletim Epidemiológico do Sistema de Vigilância em Saúde (SVS – janeiro de 2017) (Saúde, M. D., 2017b).

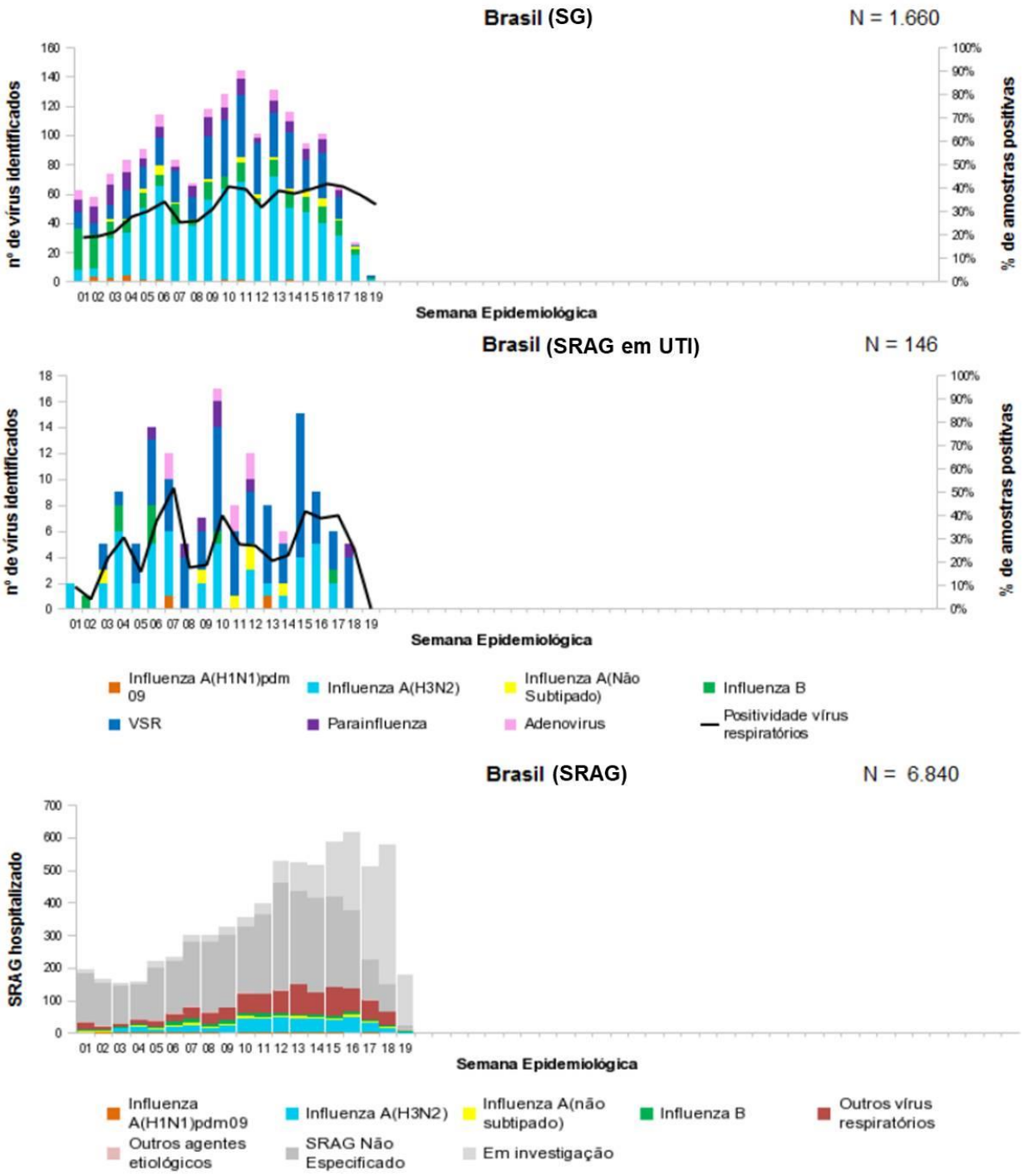

Figura 1.5 - Distribuição dos vírus respiratórios identificados nas unidades sentinelas de Síndrome Gripal (A), Síndrome Respiratória Aguda Grave em Unidade de Terapia Intensiva (B), e distribuição dos casos de Síndrome Respiratória Aguda Grave (C).
Os dados estão distribuídos em função das semanas epidemiológicas (até a semana 19 de 2017) e dos agentes etiológicos. Fonte: Boletim Epidemiológico do Sistema de Vigilância em Saúde (SVS – janeiro de 2017) (Saúde, M. D., 2017a).

As infecções causadas pelos vírus influenza são infecções agudas do trato respiratório. Apesar de geralmente auto-limitadas, as infecções causadas pelo vírus influenza apresentam grande impacto na saúde pública, pois constituem uma das principais causas de morbidade e mortalidade. Tanto a morbidade quanto a mortalidade por influenza podem variar ano a ano,

dependendo das cepas circulantes, do grau de imunidade da população geral e da população susceptível. Normalmente, as infecções são de leve a moderadas, porém, em determinados grupos de risco, pode ocorrer infeção grave, levando à hospitalização e até a morte. Os grupos mais vulneráveis a complicações devido são crianças menores de dois anos de idade, idosos com mais de 65 anos, portadores de doenças crônicas e imunodeprimidos (Who, 2003).

As infecções agudas do trato respiratório podem se manifestar sob diferentes formas clínicas. O período de incubação pode variar de 24 horas até quatro dias, dependendo da carga viral e do estado imunológico do hospedeiro. A transmissibilidade em adultos ocorre principalmente 24 horas antes do início dos sintomas e dura até três dias após o final da febre. Nas crianças pode durar em média dez dias, podendo se prolongar por mais tempo em pacientes imunossuprimidos (Souza *et al.*, 2010; Saúde, 2015).

Normalmente, os primeiros sintomas da infeção pelo vírus influenza se iniciam de dois a três dias após a infecção. Entre eles estão calafrios, cefaleia e tosse seca, seguidos de febre entre 38 e 40ºC. Além disso, os pacientes infectados podem apresentar mialgia generalizada, prostração intensa, fatiga, anorexia, dor de garganta, coriza e congestão nasal, sendo os três últimos sintomas associados à liberação de produtos celulares e virais e a uma resposta imunológica à lesão tecidual. Geralmente, a evolução da infecção tem resolução espontânea em sete dias, mas a tosse e a prostração podem persistir por uma ou duas semanas adicionais, o que caracteriza a alta taxa de morbidade da infecção (Wright *et al.*, 2007). Alguns casos podem evoluir para complicações como pneumonia primária por influenza, pneumonia secundária bacteriana ou por outros vírus, sinusite, otite, desidratação e piora de doenças crônicas (Saúde, M. D., 2015).

Altas taxas de infecção e complicações causadas pelos vírus influenza ocorrem principalmente entre os indivíduos pertencentes aos grupos de risco, por exemplo, os imunocomprometidos como indivíduos com câncer, HIV positivos (vírus da imunodeficiência humana, ou, do inglês, *human immunodeficiency virus*) e submetidos a transplante de órgãos. Este grupo de pacientes geralmente apresenta os sinais e sintomas clínicos de infecção do trato respiratório superior, porém, sintomas sistêmicos como febre, mialgia e fatiga são ausentes (Casper *et al.*, 2010; Memoli *et al.*, 2014). A infecção muitas vezes progride para o trato respiratório inferior, gerando danos pulmonares, pneumonia entre 70-80% dos indivíduos imunocomprometidos e mortalidade acima de 30%. Isto leva a maiores índices de hospitalização, necessidade de cuidado intensivo e ventilação mecânica quando comparado aos indivíduos imunocompetentes (Saúde, 2015). Além disso, como mencionado anteriormente, este grupo apresenta períodos prolongados de excreção viral, muitas vezes associados à evolução viral dentro do hospedeiro, como co-infecção simultânea de dois

subtipos virais e *shift* genético (rearranjo entre os segmentos genômicos de diferentes subtipos de influenza), *drift* antigênico (mutações pontuais na HA e NA, proteínas mais antigênicas do vírus influenza), e desenvolvimento de resistência antiviral; sendo considerada uma fonte importante de propagação comunitária destas cepas virais (Souza *et al.*, 2010). É interessante ressaltar, que um estudo demonstrou que o perfil e os níveis de citocinas relacionadas à infecção com o vírus influenza foram semelhantes entre indivíduos imunocompetentes e imunocomprometidos. Apesar da similaridade, a sintomatologia geral dos dois grupos foi bastante diferente e a tendência geral de sintomas mais inflamatórios e sistémicos ocorreu mais frequentemente entre os indivíduos imunocompetentes. Este fato sugere que uma manifestação clínica atenuada da infecção deve ser levada em consideração no momento da avaliação e manejo de pacientes imunocomprometidos, já mais complicações e excreção viral prolongada e assintomática estão presentes nestes pacientes. Além disso, neste estudo, praticamente metade dos indivíduos recrutados, 59% dos indivíduos imunocompetentes e 25% dos imunocomprometidos, foram vacinados contra o vírus influenza antes de adquirirem a infecção (Memoli *et al.*, 2014). A vacina anti-influenza é considerada a base para prevenção das infecções e complicações associadas e, quando esta não é dada ou não é eficiente, a prevenção deve ser feita através do uso de antivirais.

1.4 Os vírus influenza

1.4.1 Morfologia, genoma e proteínas virais

Os vírus influenza apresentam-se como estruturas pleomórficas, podendo variar de um formato esférico a filamentoso, e medem 80-120 nm de diâmetro (Murphy e Webster, 1996). São vírus envelopados com membrana proveniente da membrana celular do hospedeiro (Palese, P. e Shaw, M. L., 2007) e apresentam capsídeo proteico com simetria helicoidal de aproximadamente 100 nm de diâmetro (Murphy e Webster, 1996). São constituídos de 0,8 a 1% de RNA, 70% de proteína, 20% de lipídios e 5 a 8% de carboidratos (Figura 1.6).

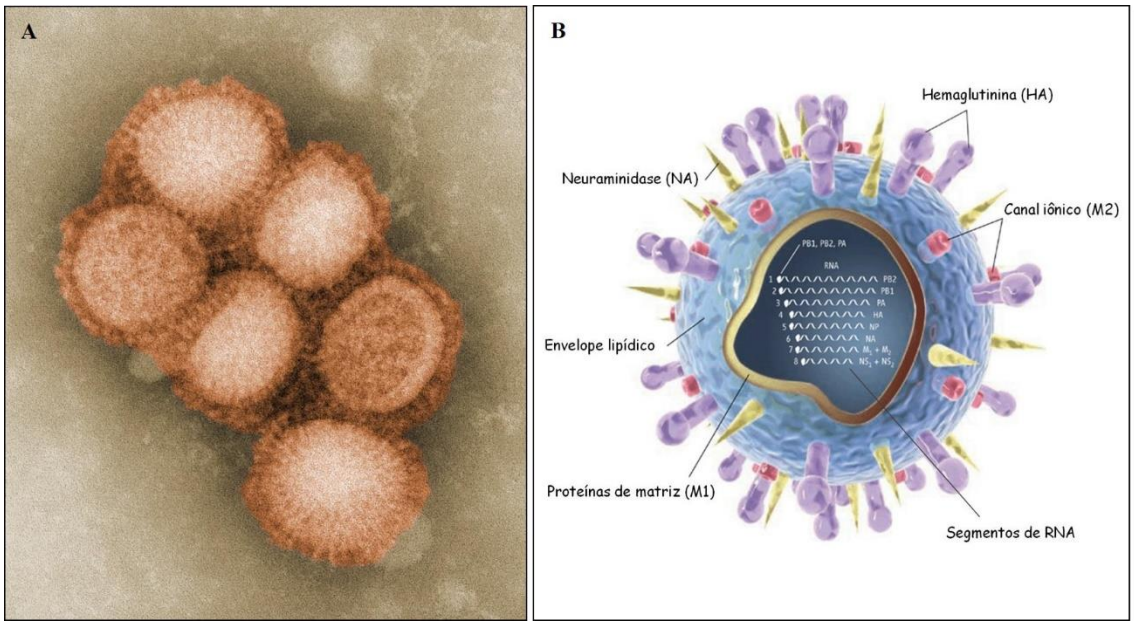

Figura 1.6 - Micrografia eletrônica (A) e esquema representativo do vírus influenza A (B).
As glicoproteínas HA e NA encontram-se inseridas no envelope lipídico, assim como a proteína M2, que forma o canal iônico viral. Abaixo do envelope encontra-se a proteína de matriz M1 e, internamente à matriz estão os segmentos de RNAv fita simples. Fontes: CDC (A) (Goldsmith e A., 2009) e adaptado de *Kaiser, J.* Science, 2006 (B) (Kaiser, 2006).

Inseridas no envelope viral estão presentes duas glicoproteínas, a HA e a NA, e a proteína de membrana M2 (Figura 1.6 B) (Murphy e Webster, 1996). As glicoproteínas HA e NA conferem à partícula viral uma morfologia espiculada quando observadas à microscopia eletrônica (Figura 1.6 A) (Palese, P. e Shaw, M. L., 2007).

A HA é uma proteína trimérica e participa da adsorção viral, já que contém o sítio de ligação que interage com os resíduos de ácido siálico presentes na membrana plasmática da célula hospedeira. Esta proteína também é importante para fusão do envelope viral com a membrana endossomal, já que possui peptídeo de fusão (ou peptídeo fusogênico) na sua extremidade N-terminal (Nakada *et al.*, 1984).

A NA catalisa a clivagem de resíduos de acido siálico presentes na membrana plasmática, permitindo a liberação das novas partículas virais formadas. Além disso, a NA também remove o ácido siálico presente nas próprias glicoproteínas virais impedindo a agregação das novas partículas formada durante a replicação. Este processo é importante para a mobilidade dos vírus no trato respiratório (Von Itzstein, 2007b).

Abaixo do envelope viral há um arranjo de proteínas de matriz M1, que delimitam a porção interna da partícula viral, conferem rigidez ao envelope e atuam como a força motriz do brotamento viral. (Gomez-Puertas *et al.*, 2000) Além disso, as proteínas M1 ancoram o material genético internamente ao envelope lipídico, que é fragmentado em oito segmentos de

RNA fita simples negativa. As moléculas de RNA nunca se encontram desnudas dentro das partículas virais ou das células infectadas. Cada segmento encontra-se associado a um número nucleoproteínas virais (NP), dependendo do comprimento do RNA viral (RNAv), e forma uma estrutura no qual RNAv enovela-se adquirindo uma forma helicoidal. Além das NPs, o RNAv também está associado a um complexo polimerase, e este conjunto recebe o nome de ribonucleoproteína (RNP) (Figura 1.7) (Mikulásová *et al.*, 2000).

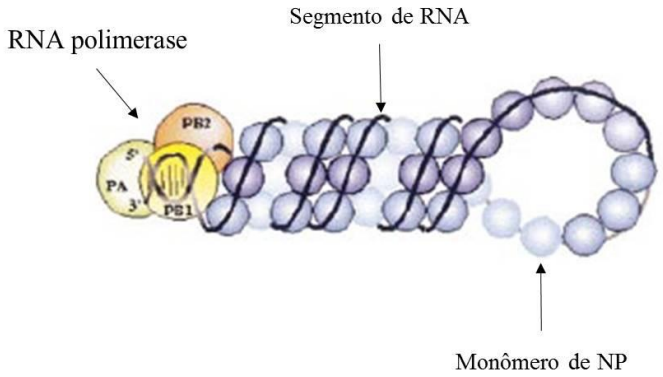

Figura 1.7 - Representação de uma ribonucleoproteína viral.
Os monômeros de NP se associam a um segmento de RNAv e ao complexo polimerase formando uma estrutura com forma helicoidal conhecida como RNP. Fonte: Adaptado de Portela, A. & Digard, P. J Gen Virol, 2002 (Portela e Digard, 2002).

A proteína M2 atravessa o envelope viral formando o canal iônico do vírion (Lamb e Krug, 1996). Após a endocitose do vírus, este canal permite o influxo de prótons e a acidificação do interior do vírion, necessária para a exposição do peptídeo de fusão presente na HA e para a dissociação entre as RNPs e as proteínas M1. Após este processo, as RNPs são então liberadas para migrarem para o núcleo e darem início à transcrição e replicação viral (Nayak *et al.*, 2004).

O genoma do vírus influenza A apresenta cerca de 13 Kb. Dos oito segmentos, seis codificam uma proteína cada, enquanto os outros dois (genes M e NS) codificam para mais de uma proteína. Os três maiores fragmentos genômicos codificam as três subunidades da RNA polimerase viral, uma subunidade ácida, chamada de PA (do inglês *polymerase acid*) e duas subunidades básicas, chamadas PB1 e PB2 (do inglês *polymerase basic 1 e 2*). O gene PB1 pode ainda gerar dois produtos gênicos menores: uma forma truncada da subunidade PB1 originada a partir de um códon de iniciação alternativo e um pequeno peptídeo, PB1-F2 (Mcauley *et al.*, 2010). As proteínas codificadas pelos segmentos genômicos do vírus influenza A e suas respectivas funções estão resumidas na tabela abaixo (Tabela 1.4).

Tabela 1.4 - Proteínas codificadas pelos segmentos genômicos do vírus influenza A e suas respectivas funções.
A tabela relaciona a numeração (de 1 a 8) referente ao segmento de RNAv à(s) proteína(s) por eles codificadas, com suas respectivas funções. Entre parênteses estão representados o tamanho dos genes (em número de nucleotídeos) e das proteínas (em número de aminoácidos).

RNA	Proteína	Função
Segmento 1 (2341 nt)	PB2 (759 aa)	RNA polimerase – reconhecimento do *cap*
Segmento 2 (2341 nt)	PB1 (757 aa)	RNA polimerase – alongamento da cadeia
Segmento 3 (2233 nt)	PA (716 aa)	RNA polimerase – atividade endonuclease
Segmento 4 (1778 nt)	HA (566 aa)	Adsorção e fusão
Segmento 5 (1565 nt)	NP (498 aa)	Ligação de RNA e forma o nucleocapsídeo
Segmento 6 (1413 nt)	NA (454 aa)	Atividade sialidásica
Segmento 7 (1027 nt)	M1 (252 aa) M2 (366 aa)	Interação com RNP e importante para brotamento Canal iônico
Segmento 8 (890 nt)	NS1 (230 aa) NEP/NS2 (121 aa)	Proteína multifuncional Exportação da RNP

Fonte: Adaptado de *Lamb, R.A. & Krug, R.M.* Fields Virol, 2001 (Lamb e Krug, 2001).

Proteínas não estruturais também estão presentes nas partículas virais, como a NS1 e a NEP/NS2 (do inglês *nuclear export protein/nonstructural protein 1 e 2*). A proteína NS1 possui diversas funções dentro do vírion. Ela está envolvida na regulação do *splicing* do segmento 8 do RNA viral, na inibição da poliadenilação e clivagem do RNA mensageiro celular (RNAmc), tornando-o disponível como fonte de iniciadores para a síntese de RNA mensageiro viral (RNAmv) e no escape viral ao sistema imunológico do hospedeiro. Neste último processo, a NS1 estimula inibidores celulares da proteína kinase R (PKR), que participa da resposta imunológica inata e inibe a síntese de proteínas virais e celulares durante a infecção (Hale *et al.*, 2008). Já a proteína NS2 participa da exportação do RNAmv do núcleo celular para o citoplasma, onde será traduzido em proteínas virais e parece estar envolvida na regulação da replicação viral (Robb *et al.*, 2009).

1.4.2 Ciclo replicativo

O principal alvo da infecção pelos vírus influenza em humanos são as células epiteliais ciliadas do trato respiratório superior e inferior. Estas células apresentam alta abundância de resíduos de ácido N-acetil-neuramínico, também chamado de ácido siálico (AS), nas suas membranas plasmáticas (Palese, P. e Shaw, M. L., 2007). Os resíduos de AS presentes nas glicoproteínas e glicolipídios da membrana ficam associados a resíduos de galactose por ligações α-2,3 ou α-2,6, que se encontram preferencialmente no trato respiratório superior e inferior, respectivamente (Liu *et al.*, 2010). Essas ligações são reconhecidas de maneira distinta por hemaglutininas de vírus humanos e animais e são críticos na determinação do hospedeiro e no tropismo tecidual. Tanto a HA quanto a NA viral possuem alta afinidade pelo AS (Palese, P. e Shaw, M. L., 2007).

O ciclo replicativo viral se inicia com a adsorção do vírus influenza à célula hospedeira, através da ligação da HA aos resíduos de AS, o que permite o desencadeamento de diferentes etapas até a liberação da partícula viral recém-formada. As etapas do ciclo replicativo do vírus influenza A encontram-se esquematicamente apresentadas na figura 1.8 (Das *et al.*, 2010).

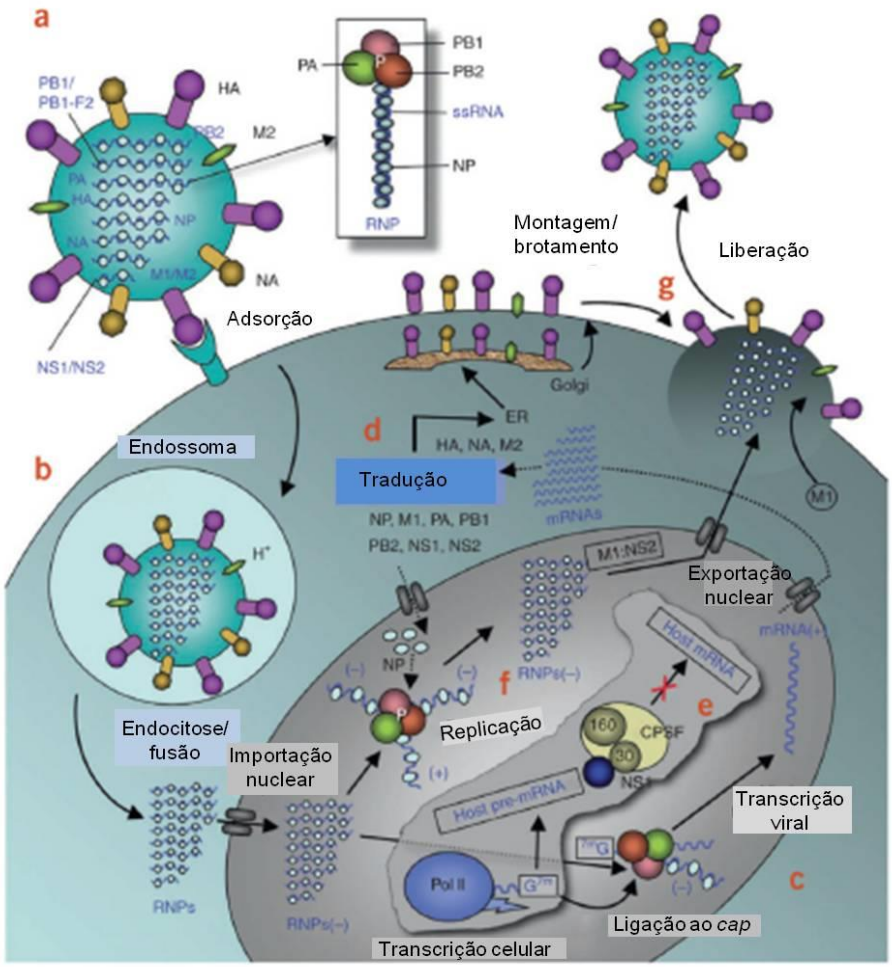

Figura 1.8 - Representação esquemática do ciclo replicativo do vírus influenza A.
(a) A adsorção do vírus influenza à célula hospedeira se dá através da ligação da HA aos resíduos de AS presentes na membrana citoplasmática. **(b)** O vírus é endocitado e ocorre a fusão do envelope viral com a membrana endossomal. As RNPs são liberadas e migram para o núcleo celular, onde ocorrem os processos de transcrição **(c)** e replicação **(f)** do genoma viral pela RNA polimerase. As novas moléculas de RNAmv são exportadas para o citoplasma celular com auxílio da proteína NEP/NS2. **(d)** No citoplasma, os RNAmv são traduzidos nas proteínas virais. As novas proteínas de superfície viral são transportadas e ancoradas na membrana plasmática celular. **(e)** A proteína NS1 tem um papel fundamental para a transcrição viral, já que impede a saída do RNAmc do núcleo. **(f)** Após a replicação do genoma viral, as NPs já se ligam aos novos RNAv formados gerando novas RNPs, que são transportadas para o citoplasma com ajuda das proteínas M1 e NEP/NS2. **(g)** As RNPs são direcionadas para a membrana plasmática celular, onde já estão ancoradas as proteínas de envelope viral, ocorre a montagem e liberação das novas partículas virais pela ação da NA. Fonte: Adaptado de *Das, K. et al* Nat Struct Mol Biol, 2010 (Das *et al.*, 2010).

Após a adsorção viral (Figura 1.8, etapa a), o vírus é endocitado (Figura 1.8, etapa b). O processo de endocitose que pode ser mediado através de quatro mecanismos: vesículas revestidas por clatrina, através de caveolina, através de vias sem clatrina e sem caveolina, ou através de macropinocitose (Edinger *et al.*, 2014). Contudo, a endocitose mediada por clatrina parece ser o modelo mais comum para a entrada dos vírus influenza na célula hospedeira

(Edinger *et al.*, 2014). O endossoma celular já é um ambiente fisiologicamente ácido, permitindo então a entrada de prótons para o interior do vírion através do canal iônico M2 (Kollerova e Betakova, 2006). A acidificação (pH entre 5,0 e 6,0) do interior da partícula viral causa uma mudança conformacional na HA, que leva à exposição de seu domínio hidrofóbico contendo o peptídeo de fusão (PF). Este, por sua vez, se insere na membrana do endossoma e leva a fusão do envelope viral com a membrana endossomal criando um poro por onde as RNPs passarão para o citoplasma. A acidificação do vírion também permite que as RNPs se dissociem das proteínas de matriz M1 e sejam liberadas para o citoplasma celular (Nayak *et al.*, 2004) (Figura 1.8, etapa b).

Os vírus influenza são uma exceção ente os vírus de RNA, pois seu material genético é replicado e transcrito no núcleo celular pelo complexo polimerase (Palese, P. e Shaw, M. L., 2007). Assim, uma vez no citoplasma, as RNPs migram para o núcleo celular através da ligação a nucleoporinas (Figura 1.8, etapa b). A penetração no núcleo é dependente de importinas celulares α e β, que reconhecem sinais de localização nuclear (SLNs) presentes tanto na proteína viral NP (Das *et al.*, 2010) quanto na subunidade PB2 da RNA polimerase (Boivin *et al.*, 2010a) (importina- α) e permitem a interação com proteínas do poro nuclear (importina-β) para internalização das RNPs (Palese, P. e Shaw, M. L., 2007).

A transcrição do genoma viral (Figura 1.8, etapa c) ocorre em momentos iniciais do ciclo replicativo e é um processo dependente de uma sequência iniciadora, que é obtida a partir do pré-RNAmc. Os RNAmv formados são transportados para o citoplasma celular com auxílio da proteína NEP/NS2 e de fatores celulares, onde serão traduzidos em proteínas virais utilizando-se da maquinaria celular. As proteínas virais de superfície, como a HA, NA e M2, são processadas no retículo endoplasmático (RE) da célula, glicosiladas no complexo de Golgi e são direcionadas para a membrana plasmática celular (Figura 1.8, etapa d). A proteína M1 é sintetizada na fase inicial da replicação, a partir do RNAmv codificado pelo segmento 7, que, em uma fase mais tardia, sofre o mecanismo de *splicing*, originando a proteína M2. O mesmo acontece com as proteínas NS1 e NEP/NS2, sendo a segunda dependente do *splicing* (Lamb e Krug, 1996).

A replicação do genoma viral (Figura 1.8, etapa f) se dá através da síntese de uma fita intermediária de RNA complementar (RNAc) com polaridade positiva, para posterior geração das novas fitas de RNAv polaridade negativa. Logo após a formação dos novos RNAv, as NP se ligam e dão origem às novas RNPs, que se associam às proteínas M1 e NEP/NS2. Juntamente com a maquinaria de exportação nuclear da célula, o complexo RNP-M1-NEP/NS2 é exportado para o citoplasma celular até a região da membrana plasmática onde estão inseridas as proteínas de superfície virais. A proteína M1 é a responsável por recrutar

todos os componentes virais para o sítio de brotamento, além de se associar à membrana plasmática celular (Lamb e Krug, 1996).

A liberação das novas partículas virais ocorre por brotamento (Figura 1.8, etapa g). Este processo requer uma curvatura da membrana plasmática, que é estimulada pelo acúmulo de proteínas M1 no interior da mesma (Gomez-Puertas *et al.*, 2000). O brotamento termina quando ocorre a fissão da membrana plasmática celular. Nesse momento, as novas partículas virais estão prontas para serem liberadas e a NA cliva os resíduos de ácido siálico presentes na membrana celular e remove o ácido siálico presente nas próprias glicoproteínas, impedindo a reinfecção da célula já infectada e a agregação das partículas virais (Figura 1.8, etapa g) (Von Itzstein, 2007b).

1.4.3 A hemaglutinina

Como mencionado anteriormente, a HA do vírus influenza é a proteína responsável pela entrada dos vírus na célula hospedeira e se encontra amplamente distribuída no envelope viral (aproximadamente 80 %). O termo "hemaglutinina" vem da sua capacidade de aglutinar os glóbulos vermelhos sanguíneos (eritrócitos) *in vitro*.

A HA é uma proteína trimérica formada por monômeros ligados de forma não covalente. Cada monômero de hemaglutinina (HA0) é composto pelas subunidades HA1 e HA2 (Nakada *et al.*, 1984). A HA0 (566 aa – Figura 1.9 A) é codificada pelo segmento gênico de RNA número 4 dos vírus influenza A. Após sua síntese no retículo endoplasmático da célula infectada, a HA0 é processada através da adição açúcares (glicosilação) e ácidos graxos e, posteriormente, é clivada por proteases intra- e extra-celulares em duas subunidades monoméricas, HA1 (327 aa) e HA2 (222 aa), que se mantem ligadas através de pontes dissulfeto (Figura 1.9 B) (Yang *et al.*, 2013).

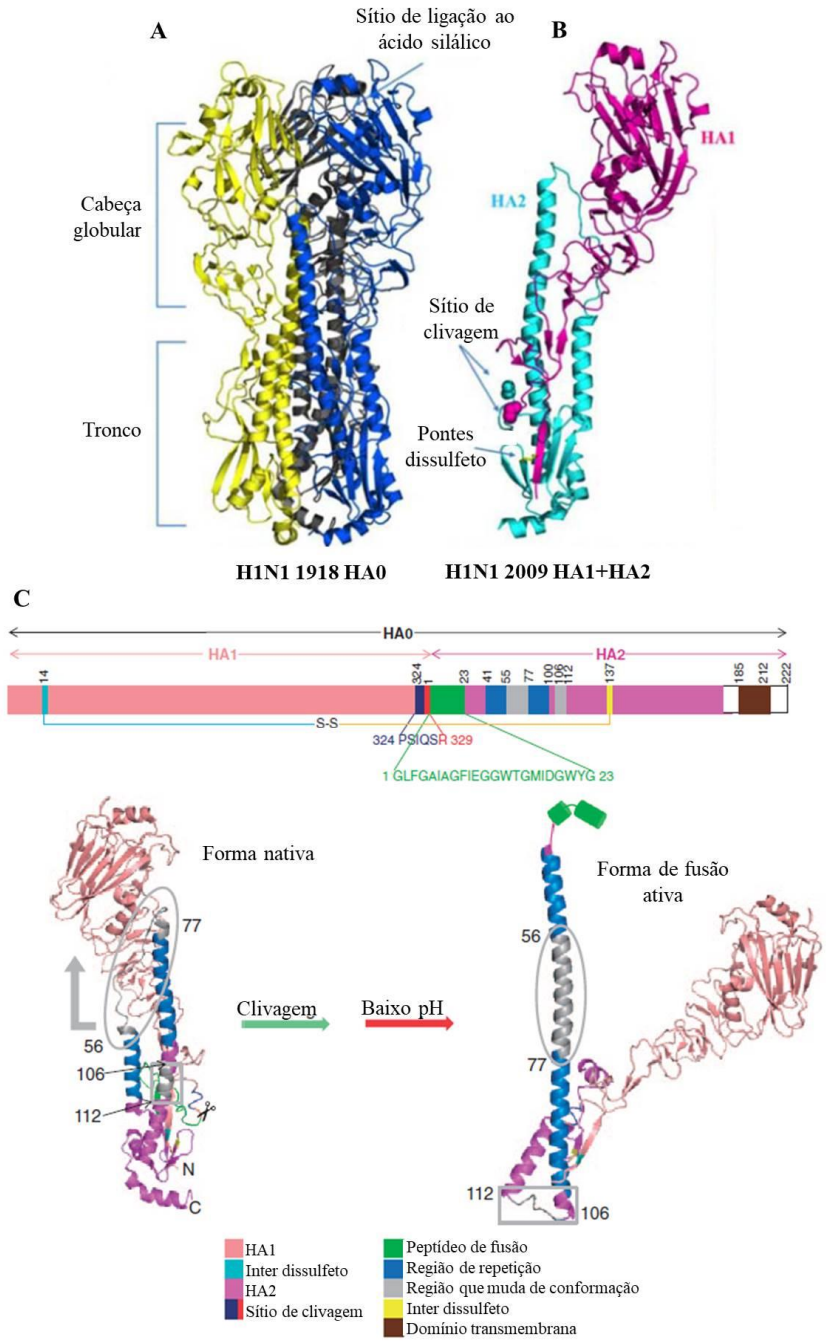

Figura 1.9 – Representação da estrutura da HA do vírus influenza A.
(A) Estrutura cristalizada da HA0 trimérica do vírus influenza H1N1 causador da pandemia de 1918. Cada monômero está representado por uma cor (amarelo, azul e cinza). O sítio de ligação ao ácido siálico é localizado em um "bolsão" na cabeça globular da HA. **(B)** Clivagem proteolítica do trímero HA0. Os resíduos presentes nos sítios de clivagem estão representados em esferas. Após a clivagem, as subunidades HA1 (rosa) e HA2 (verde) permanecem ligadas através de pontes dissulfeto entre duas folhas beta pregueada. **(C)** Estrutura primária da HA0 com suas diferentes regiões mostradas em cores distintas de acordo com a legenda da figura; estrutura terciária do monômero de HA clivado (seta verde) na presença de baixo pH (seta vermelha) na forma sua fusogênica HA1-S-S-HA2 (HA1 ligada a HA2 por ponte dissulfeto). Sequência de 23aa e peptídeo de fusão estão representados em verde na estrutura primária e terciária, respectivamente. As cores representadas na estrutura primária da HA0 correspondem às mesmas estruturas representadas pela mesma cor nas estruturas terciárias. Fonte: Adaptado de *Wang, J. et al*, 2015 (Li *et al.*, 2015) e *Suzuki, Y. & Sriwilaijaroen, N.*, 2012 (Sriwilaijaroen e Suzuki, 2012).

Duas subunidades estruturais da HA estão envolvidas na adsorção e fusão viral, o sítio de ligação ao AS e o peptídeo de fusão, respectivamente. Em um "bolsão" da HA1, localizada na cabeça globular da HA0, se encontra o sítio de ligação ao AS (Figura 1.9 B) (Yang *et al.*, 2013), que é formado por resíduos de aminoácidos relativamente conservados entre as diferentes isoformas de HA presentes na natureza, como Tyr95, Thr136, Phe147, Trp153, His183, e Leu194 (Yang *et al.*, 2013).

A HA2, presente no tronco da HA0, contém o peptídeo de fusão de 23aa (Figura 1.9 C). Este peptídeo fica localizado em uma região hidrofóbica da HA2. Após a acidificação do endossoma celular durante a replicação viral, ocorre um rearranjo estrutural de HA1 e o PF é exposto (Figura 1.9 C). A subsequente alteração conformacional de HA2 permite a fusão do envelope viral com a membrana do endossoma, levando a liberação das RNPs e a continuação do ciclo replicativo (Yang *et al.*, 2013; Li *et al.*, 2015).

A HA é a proteína viral para o qual os anticorpos monoclonais neutralizantes (mAb) do hospedeiro são direcionados e, consequentemente, apresenta uma grande variabilidade genética. Mutações na HA são a peça chave para a emergência de novas variantes virais e escape do sistema imunológico do hospedeiro (Wiley e Skehel, 1987). Desta maneira, os anticorpos produzidos contra uma determinada sequência de HA, desenvolvidos em exposições anteriores como infecção natural ou vacinação, não são capazes de neutralizar os epítopos de uma linhagem variante, mesmo se produzidos em altos títulos (Carrat e Flahault, 2007). Esse fato explica também a necessidade de revisão anual da composição das vacinas sazonais. Portanto, é de grande interesse o desenvolvimento de novos anticorpos amplamente neutralizantes (do inglês *new broadly neutralizing antibodies* – nbnAb) que reconhecem regiões altamente conservadas da HA para serem utilizados como estratégias de vacinação ou tratamento contra os vírus influenza (Laursen e Wilson, 2013).

Como exemplos de anticorpos amplamente neutralizantes, temos dois anticorpos isolados de células B humanas cujos alvos são regiões antigênicas que se sobrepõem ao sítio de ligação ao AS na cabeça globular da HA1 (Laursen e Wilson, 2013; Shen *et al.*, 2013). Este fato sugere que anticorpos que reconhecem o sítio de ligação ao receptor ocorrem naturalmente em seres humanos e podem ser utilizados como estratégias de vacinação. Anticorpos reconhecendo epítopos mais conservados na região membrana-proximal do tronco da HA2 também já foram encontrados em células B de memória de indivíduos vacinados contra influenza (Shen *et al.*, 2013). Estes anticorpos poderiam neutralizar diferentes subtipos de vírus influenza e evitar o surgimento de cepas com mutações de escape.

Além disso, a HA possui diversas regiões em sua estrutura que representam alvos em potencial para o desenvolvimento de compostos com atividade antiviral. Embora drogas com

alvo na NA e no canal M2 estejam disponíveis, a emergência de cepas virais resistentes torna necessária a busca por moléculas capazes de inibir outros alvos da replicação viral. Já foram descritas diversas moléculas capazes de inibir a clivagem de HA0 e regiões específicas de HA1 e HA2. Entre as regiões presentes na HA1 estão o sítio de ligação ao AS, os sítios de glicosilação e regiões antigênicas alvos de anticorpos neutralizantes. Já em HA2, temos como exemplos de alvos promissores a alteração conformacional pH-dependente para exibição do peptídeo de fusão, o peptídeo de fusão em si, e o processo de fusão de membranas mediada pela HA.

Existem dois novos compostos em fase mais avançada de desenvolvimento que são capazes de inibir a HA e, consequentemente, a entrada do vírus influenza na célula hospedeira: o arbidol e a flufirvitida-3. Embora não aprovado em países ocidentais, o arbidol é licenciado para utilização clínica como profilaxia e tratamento de influenza na Rússia e na China (Leneva *et al.*, 2009; Liu *et al.*, 2009; Brooks *et al.*, 2012). O arbidol parece não inibir diretamente a atividade da HA viral, porém, inibiu a fusão do envelope viral com eritrócitos de galinha (Brooks *et al.*, 2012). Outro trabalho demontrou a presença de mutações na subunidade HA2 após a passagens sequenciais do vírus influenza na presença do composto. Essas mutações levaram a um aumento no pH necessário a mudança conformacional da HA que leva a exposição do peptídeo de fusão (Leneva *et al.*, 2009).

A flufirvitida-3 (FF-3), sequencia peptídica de 16 aa derivada de uma região altamente conservada de HA2, está em sendo utilizada em estudos clínicos de fase 1 e 2. Esse peptídeo se mostrou eficaz em inibir a infecção pelo vírus influenza em ensaios de placa e estudos em animais, embora seu mecanismo de ação ainda não seja completamente conhecido (Badani, 2014). Estudos sugerem que o FF-3 não interage com HA nem com a partícula viral, além de não alterar a estrutura ou estabilidade da proteína nem do vírus. Por ser um peptídeo hidrofóbico, parece interagir com a membrana celular e/ou envelope viral dentro do endossoma, após a endocitose do vírus e do próprio peptídeo (Badani, 2014). Os estudos de fase 1 realizados nos Estados Unidos avaliaram a segurança, a tolerabilidade e a farmacocinética da FF-3 em indivíduos saudáveis (Technologies, A. 2015), enquanto o estudo de fase 2, realizado no Reino Unido, avaliou sua segurança e eficácia em indivíduos saudáveis infectados experimentalmente com o vírus influenza (Technologies, A., 2016). Os resultados desses estudos ainda não foram publicados.

1.4.4 A neuraminidase

A NA do vírus influenza é uma glicoproteína antigênica e participa da liberação de novos vírions da superfície da célula hospedeira. Ela cliva os resíduos terminais do AS presente na superfície das células infectadas e nos novos vírions, facilitando sua liberação e disseminação através do trato respiratório (Von Itzstein, 2007b). Possui 454 aa, é codificada pelo sexto segmento genômico dos vírus influenza e é a segunda proteína mais abundante (aproximadamente 17%) do envelope viral (Nayak *et al.*, 2004).

Esta proteína é um tetrâmero com quatro polipeptídeos idênticos (Figura 1.10 A) e, cada polipeptídeo possui quatro domínios: um domínio citoplasmático N-terminal, seguido de uma âncora transmembranar hidrofóbica, uma haste fina de tamanho variável, que termina em uma cabeça globular na qual está presente o sítio ativo da enzima (Air, 2012). Cada polipeptídeo contém um sítio ativo localizado centralmente (Figura 1.10 A), que é altamente conservado para manter a atividade da molécula (Figura 1.10 B) (Nguyen *et al.*, 2012). Além do sítio ativo, os polipeptídeos possuem um sítio de ligação a íons de cálcio, necessários para a estabilidade e atividade da enzima (Air, 2012).

O sítio ativo da NA possui resíduos de aminoácidos envolvidos na função catalítica da enzima, como Arg118, Asp151, Arg152, Arg224, Glu276, Arg292, Arg371 e Tyr406; e resíduos de aminoácidos estruturais, Glu119, Arg156, Trp178, Ser179, Asp198, Ile222, Glu227, Glu277, Asp293 e Glu425; que estão presentes em todos os subtipos de NA dos vírus influenza A e B (Shtyrya *et al.*, 2009; Jagadesh *et al.*, 2016). Em especial, resíduos de asparagina, que formam o sítio de glicosilação (Asn146); e resíduos de prolina e cisteína, que são requeridos para o enovelamento da cadeia polipeptídica e estabilizam a estrutura tridimensional da molécula; são estritamente conservados. Como exemplo, a figura 1.10 B mostra o sítio ativo da NA e os resíduos de aminoácidos que interagem com a molécula DANA (ácido 2-deoxi-2,3-dehidro-N-acetilneuramínico), um inibidor endógeno específico da NA utilizado para estudar o papel de NAs endógenas no processo no desenvolvimento neural.

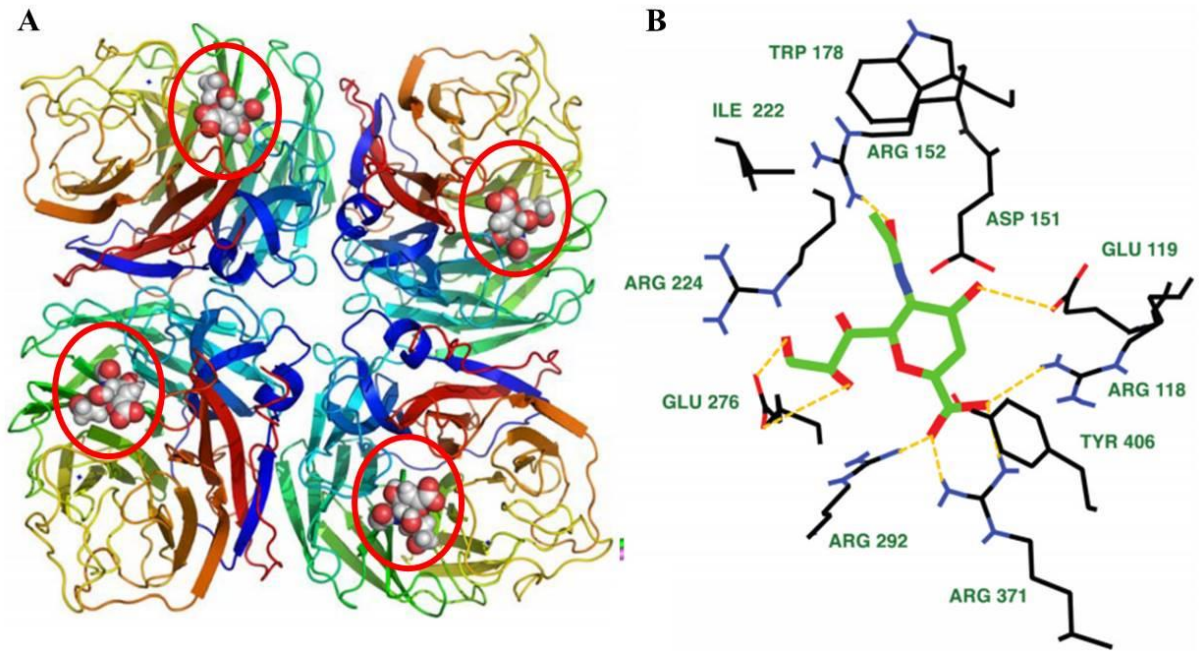

Figura 1.10 - Representação da estrutura da NA do vírus influenza A.
(A) Tetrâmero da NA com uma molécula do inibidor DANA ligada a cada um dos polipeptídeos (átomos de carbono, oxigênio e nitrogênio representados em cinza, vermelho e azul, respectivamente). **(B)** Resíduos de aminoácidos conservados presentes no sítio ativo da NA que interagem com o inibidor DANA (ligações de hidrogênio estão representadas pelas linhas amarelas pontilhadas). Fonte: *Air, G. M.* Influenza Other Respi Viruses, 2012 (Air, 2012).

Devido a importante função da NA durante o ciclo replicativo viral e ao fato do sitio ativo desta enzima ser composto por aminoácidos conservados entre todos os subtipos de NA já descritos na natureza, esta enzima é o principal alvo para antivirais. Atualmente os inibidores de neuraminidase (NAIs) representam a classe de drogas anti-influenza mais importante no tratamento e profilaxia das infecções e existem quatro NAIs aprovados para utilização clínica: oseltamivir (OST), zanamivir (ZAN), peramivir (Cdc, 2016) e laninamivir, sendo o último aprovado somente no Japão (Sankyo, 2010).

Os NAIs passaram a ser estudados após a emergência de vírus resistentes aos bloqueadores de canal M2, primeira classe de drogas anti-influenza utilizada. Estas moléculas são estruturalmente semelhantes ao AS (Figura 1.11) e se ligam ao sítio ativo da NA. Consequentemente, previnem a liberação e espalhamento das novas partículas virais para células não infectadas.

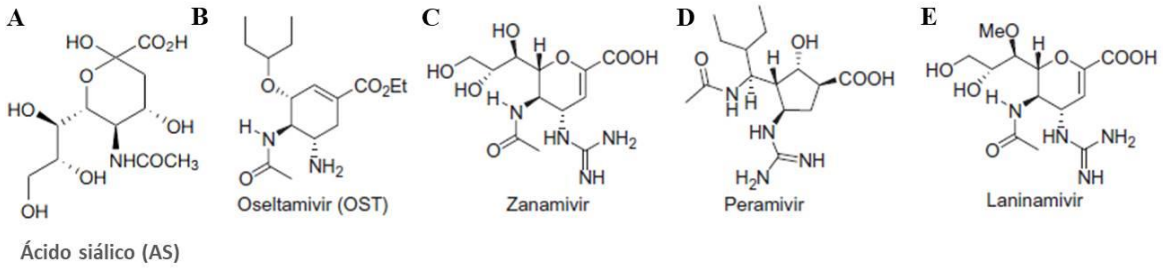

Figura 1.11 - Estruturas químicas do AS e dos NAIs.
Estão representadas as estruturas químicas do ácido siálico (A), oseltamivir (B), zanamivir (C), peramivir (D) e laninamivir (E). Fonte: Adaptado de *Boechat, F. et al* Bioorg Med Chem, 2015 (Boechat *et al.*, 2015).

Os ácidos siálicos são carboidratos presentes nas glicoproteínas e glicolipídeos da membrana plasmática celular, sendo o ácido N-acetilneuramínico o mais abundante nos eucariotos. Como já mencionado, os ácidos siálicos são encontrados ligados a hexoses, como α(2,3)- ou α(2,6)-β-Galactose e ligados a outros ácidos siálicos como α(2,8). Essas moléculas estão envolvidas em diversos processos biológicos no organismo, como as funções de mediadores na adesão célula-célula durante o processo inflamatório, mediadores na comunicação intercelular, renovadores celulares nos eritrócitos, além de serem receptores para bactérias e vírus. Devido à versatilidade de funções dos ácidos siálicos e seu papel durante a infecção pelo vírus influenza, sua estrutura química foi e tem sido utilizada como base para racionalização de novas drogas anti-influenza. A HA e a NA viral te como substrato o AS. A NA liga-se fortemente a resíduos monoméricos de AS terminal das glicoproteínas presentes na célula hospedeira e boa parte dos inibidores desenhados apresentaram alguma atividade inibitória. Diferentemente da NA viral, a HA, tem fraca afinidade por sialosídeos monoméricos (com apenas uma resíduo de AS associado), o que dificulta o desenvolvimento de moléculas derivadas do ácido siálico que atuem de forma eficiente sobre esta enzima (De Fátima *et al.*, 2005).

Durante o desenvolvimento dos NAIs foi proposto que, como os compostos se assemelham com o substrato natural da enzima (AS), seria improvável a emergência de mutantes resistentes aos compostos e, caso emergissem, provavelmente não seriam viáveis (Ives *et al.*, 2002). Porém, durante a temporada de 2007-2008, foi reportado aumento na circulação de cepas do vírus influenza A/H1N1 resistentes ao OST. A resistência foi associada a uma mutação no resíduo 275 da NA viral, que causou a substituição de histidina por tirosina (H275Y) (Cdc, 2015a; b). Embora esta cepa viral tenha parado de circular, a partir da temporada de 2013-2014, o vírus influenza A(H1N1)pdm09 passou a circular de maneira predominante e foram identificados casos esporádicos de cepas resistentes também associadas a mutação H275Y. Atualmente, aproximadamente 1-2 % das cepas de

A(H1N1)pdm09 circulantes apresentam esta mutação de resistência ao OST (Fry e Gubareva, 2012; Cdc, 2015b).

O resíduo 275 – numeração de N1 (ou 274 na numeração de N2) - se encontra em uma região adjacente ao sítio ativo da enzima e não interage diretamente com o substrato (Figura 1.12 A) (Collins *et al.*, 2008). A mutação neste resíduo não altera a atividade enzimática da NA (Collins *et al.*, 2008), porém, reduz significativamente a capacidade inibitória do OST, já que reduz a afinidade da NA pelo composto e altera o sítio de ligação (Collins *et al.*, 2008). O resíduo Glu276, localizado próximo ao sítio de ligação ao OST, possui um grupo carboxil que é deslocado para longe do "bolsão" hidrofóbico durante a interação do OST com a NA selvagem (Figura 1.12 B). Na enzima mutante, a tirosina puxa o grupo carboxil da Glu276 para dentro do sítio de ligação e, a presença deste grupo carregado, desfaz o "bolsão" que acomoda o OST durante a interação (Figura 1.12 B) (Collins *et al.*, 2008; Nguyen *et al.*, 2012).

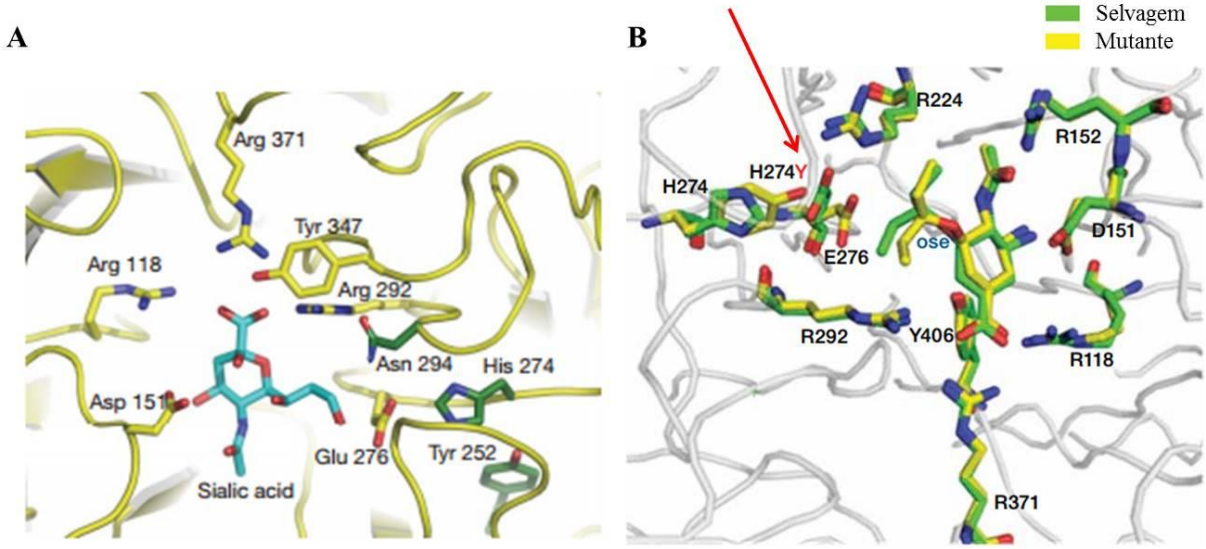

Figura 1.12 - Representação das estruturas das NAs subtipo 1 selvagem e mutante ligadas ao AS e OST.
(A) AS (em azul) docado no sítio ativo da NA subtipo 1 selvagem (em amarelo). Alguns resíduos de aminoácidos importantes na interação da enzima com o composto estão destacados, sendo os átomos de carbono, nitrogênio e oxigênio mostrados em amarelo, azul e vermelho, respectivamente. Entre os resíduos se encontra a His274, com seus átomos de carbono em verde. **(B)** Comparação do sítio ativo da NA subtipo 1 selvagem H274 (verde) e mutante H274Y (amarelo) ligado ao OST. Fonte: Adaptado de *Collins, P. J. et al* Nature, 2008 (Collins *et al.*, 2008) e *Nguyen, H. T. et al* Antivir Ther, 2012 (Nguyen *et al.*, 2012).

Devido à emergência e circulação de cepas resistentes ao OST, muitos grupos seguem buscando novos compostos capazes de inibir a NA viral. Muitos deles focam na modificação e optimização da estrutura química do OST e do ZAN, já que o sítio catalítico da enzima é

extremamente conservado. Outros vêm utilizando como estratégia o desenvolvimento de inibidores irreversíveis, a fim de superar o aparecimento de resistência aos antivirais (Wu *et al.*, 2017). Alguns grupos, também descrevem e resolvem a estrutura de anticorpos específicos contra a NA, sugerindo essa enzima um possível alvo para novas vacinas, já que esses anticorpos poderiam inibir o espalhamento dos vírus e reduzir a severidade da doença (Jagadesh *et al.*, 2016). Além disso, estudos de evolução do gene da NA demonstram que os *drifts* antigênicos (mutações pontuais) e as mutações que levam a substituição de aminoácidos ocorrem em taxas mais baixas na NA que na HA, sugerindo que a evolução da NA ocorre mais lentamente e que anticorpos direcionados a essa enzima poderiam conferir proteção de mais longo prazo (Jagadesh *et al.*, 2016).

1.4.5 A RNA polimerase viral

A polimerase do vírus influenza é uma RNA polimerase RNA dependente (RpRd), constituída por 3 subunidades mencionadas anteriormente: PA, PB1 e PB2 (Figura 1.13 A), responsáveis pela replicação e transcrição do genoma viral (Ruigrok, 1998). As subunidades PB2, PB1 e PA são codificadas pelos segmentos genômicos 1, 2 e 3; e possuem 759, 757 e 716 aa, respectivamente (Figura 1.13 A). As três subunidades interagem formando o complexo polimerase: a subunidade PB1 é o núcleo do complexo, cuja estrutura é N-PA-PB1-PB2-C (Figura 1.13 A e C) e as principais interações são entre os domínios C-terminal de PA e N-terminal de PB1 e entre C-terminal de PB1 e N-terminal de PB2 (Figura 1.13 A).

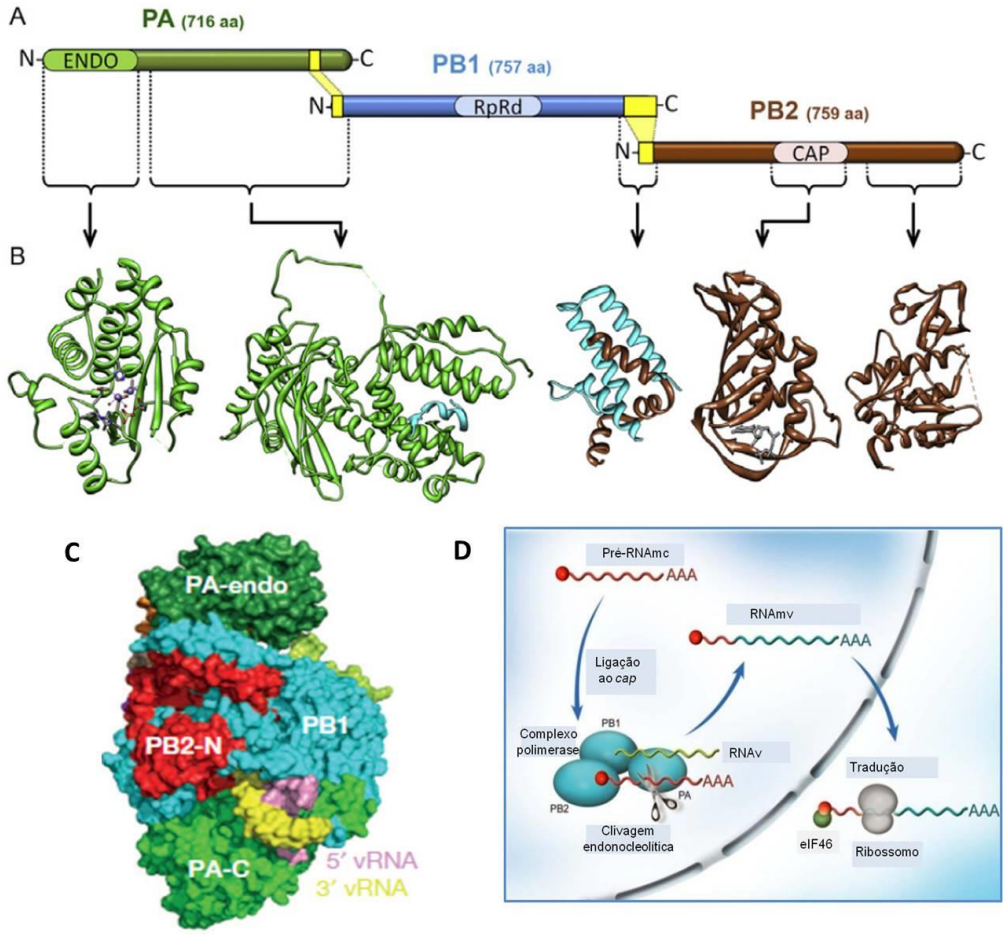

Figura 1.13 - Estrutura e função das três subunidades da RNA polimerase do vírus influenza e estrutura do RNAv promotor.
(A) Estrutura linearizada e **(B)** estruturas terciárias das subunidades PA (verde), PB1 (azul) e PB2 (marrom). Os domínios estruturalmente caracterizados estão representados pelos retângulos de cores mais claras nas três subunidades: verde claro – domínio com função endonuclease de PA (ENDO); azul claro – domínio com função polimerase de PB1 (RpRd); rosa claro – domínio *cap binding* de PB2 (CAP). As regiões em amarelo representam as regiões de interação entre as subunidades. **(C)** Estrutura quaternária mostrando as interfaces de interação entre as subunidades da RNA polimerase: domínio endonuclease de PA (verde escuro), PB1 (azul), domínio N-terminal de PB2 (vermelho), domínio C-terminal de PA; e regiões 5` e 3` do RNAv (lilás e amarelo, respectivamente). **(D)** Representação esquemática da função das subunidades do complexo polimerase. Durante a transcrição do RNAv, a subunidade PB2 da polimerase se liga à extremidade 5`cap do pré-RNAmc (vermelho), que é clivado pelo domínio endonuclease da subunidade PA. O pequeno RNA capeado resultante é utilizado para iniciar a síntese do RNAmv a partir do RNAv molde (verde). O alongamento da nova fita é realizado pela subunidade PB1 e, com isso, é gerado o RNAmv (vermelho e azul), que é exportado para o citoplasma para ser traduzido em proteínas virais. Fonte: Adaptado de *Martín-Benito, J. & Ortín, J.* Adv Virus Res, 2013 (Martín-Benito e Ortín, 2013); *Pflug, A. et al* Nature, 2014 (Pflug *et al.*, 2014); *Boivin et al* J Biol Chem, 2010 (Boivin *et al.*, 2010a).

A estrutura da RNA polimerase do vírus influenza ainda não foi totalmente caracterizada. A estrutura da subunidade PA é a mais conhecida, já que seu domínio C-terminal de interação com a subunidade PB1 foi determinado em 2008 (He *et al.*, 2008;

Obayashi *et al.*, 2008), e, em 2009, foi atribuída ao seu domínio N-terminal a função de endonuclease, responsável pela clivagem do *cap* do pré-RNAmc (Figura 1.13) (Dias *et al.*, 2009; Yuan *et al.*, 2009). A subunidade PB2 possui 3 domínios resolvidos: o domínio C-terminal de interação com PB1, um domínio central cuja função é de ligação ao *cap* do pré-RNAmc chamada de *cap binding*, e o domínio N-terminal de interação com proteínas do hospedeiro (Figura 1.13) (Boivin *et al.*, 2010a). Dentro deste último, estão bem descritos 2 resíduos, o 627, que está relacionado à adaptação do vírus influenza A aos seus diversos hospedeiros, e o de sinal de localização nuclear citado anteriormente (Boivin *et al.*, 2010a). Diferentemente das subunidades PA e PB2, a PB1 permanece pouco caracterizada, sendo conhecidos somente os domínios de interação com as outras 2 subunidades (Figura 1.13 A e B). A estrutura central de PB1 possui motivos conservados característicos de RNA polimerases dependentes de RNA fita simples e, por isso, foi atribuída a função de polimerase propriamente dita a esta subunidade (Poch *et al.*, 1989; Muller *et al.*, 1994).

Os domínios de interação entre PB1 e PA formam uma cavidade central onde se encontra o RNAv, que serve como promotor e molde para os processos de replicação e transcrição. Esta região promotora do RNAv é constituída por 15 e 16 nucleotídeos das extremidades 3` e 5`, respectivamente, que permanecem parcialmente ligados (Tomescu *et al.*, 2014). Quando o RNAv está livre do complexo polimerase, esta região permanece como RNA dupla fita, com seus resíduos parcialmente complementares pareados (Figura 1.14). Se o RNAv está ligado a RNA polimerase, ele se encontra em uma conformação de saca-rolhas, com os resíduos 2 e 3 da extremidade 5` pareados com os resíduos 8 e 9 da extremidade 3` formando dois *loops* (Tomescu *et al.*, 2014). Evidências demonstram que esta estrutura em forma de saca-rolhas é essencial para a atividade endonuclease de PA e que o *loop* formado na extremidade 5`é importante para a poliadenilação do RNAm, já que estas interações dão mais estabilidade a estrutura do complexo polimerase (Tomescu *et al.*, 2014).

Durante o processo de transcrição do RNAv, a síntese do RNAmv se dá pelo complexo polimerase residente nas RNPs, que se encontra ligado ao RNA molde (RNAv) e na conformação *cis* (Figura 1.14) (Jorba *et al.*, 2009). Cada segmento de RNAv contém sequências de 13 e 12 nucleotídeos nas extremidades 5` e 3`, respectivamente, que são conservadas e parcialmente complementares (de 5 a 7 nucleotídeos). Este fato faz com que os nucleotídeos complementares formem uma região pareada, que é reconhecida pelo complexo polimerase (Figura 1.14). O processo de transcrição é dependente de uma sequência iniciadora 5`*cap*, que é obtida através da ligação da subunidade PB2 ao pré-RNAmc e da clivagem pelo domínio endonuclease de PA (Figuras 1.13 D e 1.14). A síntese do RNAmv é preferencialmente iniciada na extremidade 3` do RNA molde, quando esta possui uma

sequencia CA (Martín-Benito e Ortín, 2013). PB1 catalisa o alongamento da nova cadeia formada e a síntese do RNAmv é finalizada com a cópia repetitiva do sinal oligo-U, isto é, uma sequência de 5 a 7 uracilas (U) localizada a 16 nucleotídeos da extremidade 5` do RNA molde. Consequentemente, o RNAmv é poliadenilado levando a ausência da sequencia complementar a extremidade 5` do molde do RNAv (Martín-Benito e Ortín, 2013). Diferentemente do RNAmc, que necessita de uma polimerase específica para a poliadenilação, a própria RNA polimerase viral sintetiza a cadeia poli-A do RNAmv (Fodor, 2013).

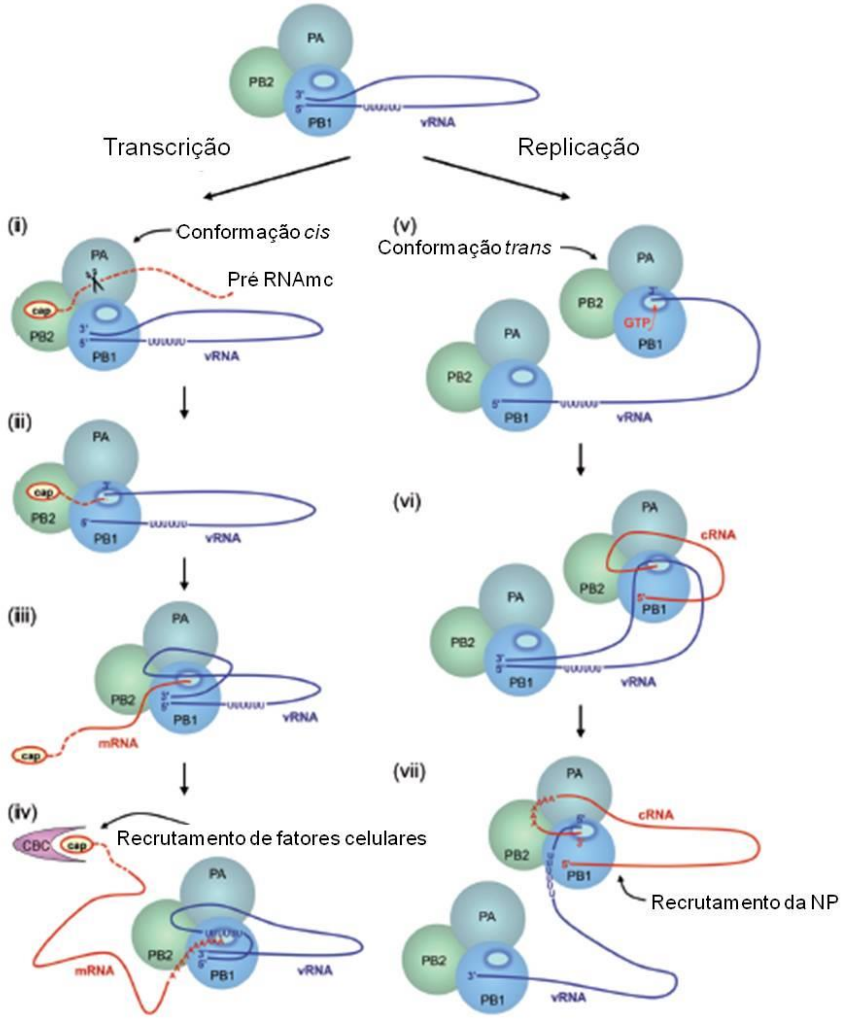

Figura 1.14 - Mecanismos de transcrição e replicação do genoma viral.
O complexo polimerase presente nas RNPs, ou seja, na conformação *cis*, se liga à extremidade parcialmente complementar do RNAv (azul). **(i)** Para o início da transcrição, a subunidade PB2 se liga ao *cap* do pré-RNAmc (vermelho) e PA cliva essa extremidade. **(ii)** Esta extremidade é posicionada no sítio ativo de PB1 junto com a extremidade 3` do RNA molde (RNAv) e a transcrição se inicia. **(iii)** Ocorre o alongamento da fita de RNAmv (vermelho) e a poliadenilação é realizada pela própria RNA polimerase viral através da síntese repetitiva de A a partir da sequência de U presente próxima da extremidade 5` do RNA molde. **(iv)** O RNAmv é então liberado do complexo polimerase e se liga ao complexo de ligação ao cap (CBC) presente no núcleo celular, que auxilia a proteína NEP/NS2 no transporte para o citoplasma celular. **(v)** A replicação do genoma viral é realizada pelo complexo polimerase na conformação *trans*. Para tal, a extremidade 3` do RNA molde (azul) é liberada do complexo polimerase associado às RNPs por mecanismos não conhecidos, permitindo sua ligação ao complexo polimerase na conformação trans. **(vi)** A replicação é iniciada com auxílio de uma molécula de GTP, o que promove o alongamento da fita de RNAc (vermelho). **(vii)** Através da ligação da extremidade 5` do RNA molde ao complexo polimerase na conformação trans, ocorre a síntese completa do RNAc. A proteína NP é então recrutada e ocorre a síntese do novo RNAv (polaridade negativa) a partir do RNAc (não mostrado nesta figura). Fonte: Adaptado de *Fodor, E.* Acta Virologica, 2013 (Fodor, 2013).

A replicação do genoma viral ocorre em um momento mais tardio da infecção pelo complexo polimerase solúvel na conformação *trans* (Figura 1.14) (Jorba *et al.*, 2009). O

processo da replicação é independente de iniciador e o RNAv é sintetizado a partir de um RNAc de polaridade positiva. A extremidade 3` do RNAv (RNA molde) é liberada do complexo polimerase associado as RNPs por mecanismos não conhecidos, permitindo sua ligação ao complexo polimerase solúvel. A replicação é iniciada com auxílio de uma molécula de GTP e necessita altas concentrações de ATP, GTP e CTP, que serão incorporados às posições +2 e +3 da nova cadeia (Martín-Benito e Ortín, 2013). A fita de RNAc é alongada por PB1. A extremidade 3` se desliga deste complexo e permite a ligação da extremidade 5` do RNA molde, para que ocorra a síntese completa do RNAc. A proteína NP é então recrutada e ocorre a síntese do novo RNAv (polaridade negativa) a partir do RNAc (Figura 1.14) (Fodor, 2013), que também necessita altas concentrações de NTPs. O início da síntese se dá na posição +4 do *template* e gera um pppApG, que é então realinhado para a posição +1 para o alongamento da nova cadeia de RNAv (Martín-Benito e Ortín, 2013). Um mecanismo alternativo de síntese do RNAc envolvendo o complexo polimerase na conformação *cis* também já foi proposto. Neste caso, o complexo polimerase residente nas RNPs sintetiza os RNAc, que mesmo em baixos níveis ficam acumulados até que os complexos polimerase recém-sintetizados sejam importados para o núcleo da célula e os utilizem como molde para síntese do novo RNAv de polaridade negativa. Quando o RNAv é formado, a NP é recrutada e são formadas novas RNPs (Fodor, 2013).

O RNAv funciona como molde tanto para a síntese do RNAmv na transcrição quanto para a síntese do RNAc durante a replicação. Embora os mecanismos de síntese sejam distintos, ambos são realizados pelo complexo polimerase do vírus influenza e ainda permanece desconhecido quais são os mecanismos de regulação entre os processos de transcrição e replicação. Uma possível explicação seria que durante a transcrição, o complexo polimerase atuaria em uma conformação distinta quando comparada ao processo de replicação (Jorba *et al.*, 2009).

Diferentemente do RNAmv, os RNAc e RNAv recém sintetizados são encapsidados, isto é, se ligam à NPs solúveis logo após a sua síntese. Este fato sugere que a NP esteja envolvida na regulação da troca entre transcrição e replicação e essa hipótese vem sendo discutida em diversos trabalhos, já que é a NP que interage diretamente tanto com o RNAv quanto com a RNA polimerase (Portela e Digard, 2002; Newcomb *et al.*, 2009). Além da NP, a proteína NEP/NS2 também parece estar envolvida com esse processo de regulação. Alguns artigos demonstraram que o efeito da NEP/NS2 na síntese de RNAv é dependente da sua concentração, já que em grandes quantidades a NEP/NS2 anula completamente a atividade da RNA polimerase (Manz *et al.*, 2012). Este dado ainda é um pouco controverso, já que também foi mostrado que baixas concentrações de NEP/NS2, além de estimularem a replicação,

também estimulam a síntese de RNAmv dependendo do modelo experimental (Robb *et al.*, 2009; Manz *et al.*, 2012).

Diversos outros mecanismos de regulação da troca entre replicação e transcrição vem sendo propostos. Entre eles estão a existência de pequenos RNAs virais que estariam envolvidos na regulação (Perez *et al.*, 2010), além de fatores do hospedeiro, que poderiam interagir com a NP e com a polimerase viral durante estes processos (Momose *et al.*, 2001; Momose *et al.*, 2002), mostrando que ainda são necessários mais estudos estruturais e funcionais sobre as proteínas virais, suas interações e funções.

1.5 Antivirais

Os vírus influenza apresentam grande variabilidade genética, ocasionada basicamente por dois processos mencionados anteriormente, *drift* e *shift* genético. O *drift* genético corresponde ao acúmulo de mutações pontuais nas proteínas mais antigênicas do vírus influenza, HA e NA, devido ao fato da RNA polimerase viral não possuir atividade de correção. As mutações no gene HA constituem o principal obstáculo para o controle da doença através da vacinação, o que demanda a formulação anual das vacinas utilizadas nos hemisférios Norte e Sul (Who, 2009a; 2009b). O outro mecanismo mais drástico que leva ao aumento da diversidade genética, o *shift* genético, corresponde ao rearranjo entre os segmentos genômicos de diferentes linhagens de influenza.

Devido à dificuldade de controle das infecções pelo vírus influenza com a vacinação, outra estratégia empregada para a contenção e tratamento destas infecções durante os surtos sazonais é a utilização de drogas antivirais. Desde 2011, de acordo com o CDC, a utilização de antivirais é recomendada para tratamento de pacientes pertencentes aos grupos de risco e pacientes com infecção severa, complicada, progressiva ou com necessidade de internação; com suspeita ou infecção confirmada pelo vírus influenza, e deve ser iniciado o mais rápido possível (Centers for Disease Control and Prevention, 2011). O tratamento também deve ser utilizado em pacientes fora dos grupos acima mencionados, com suspeita ou infecção confirmada, se for iniciado em até 48h após o aparecimento dos sintomas (Centers for Disease Control and Prevention, 2011).

Além disso, a última atualização do guia para a preparação de uma pandemia ocasionada pelo vírus influenza (publicada pela OMS após a pandemia de 2009), preconiza a estocagem e uso de antivirais para a redução da disseminação viral, já que o tempo para produzir vacinas para novos vírus é geralmente longo e os custos de produção são altos (Who, 2009b).

Existem duas classes de antivirais aprovadas para o uso contra a influenza pela agência reguladora norte americana, *Food and Drug Administration* (FDA) (Fda, 2013). São eles: bloqueadores do canal de prótons M2 e inibidores de neuraminidase (NAIs) (Jackson *et al.*, 2011) (Figura 1.15).

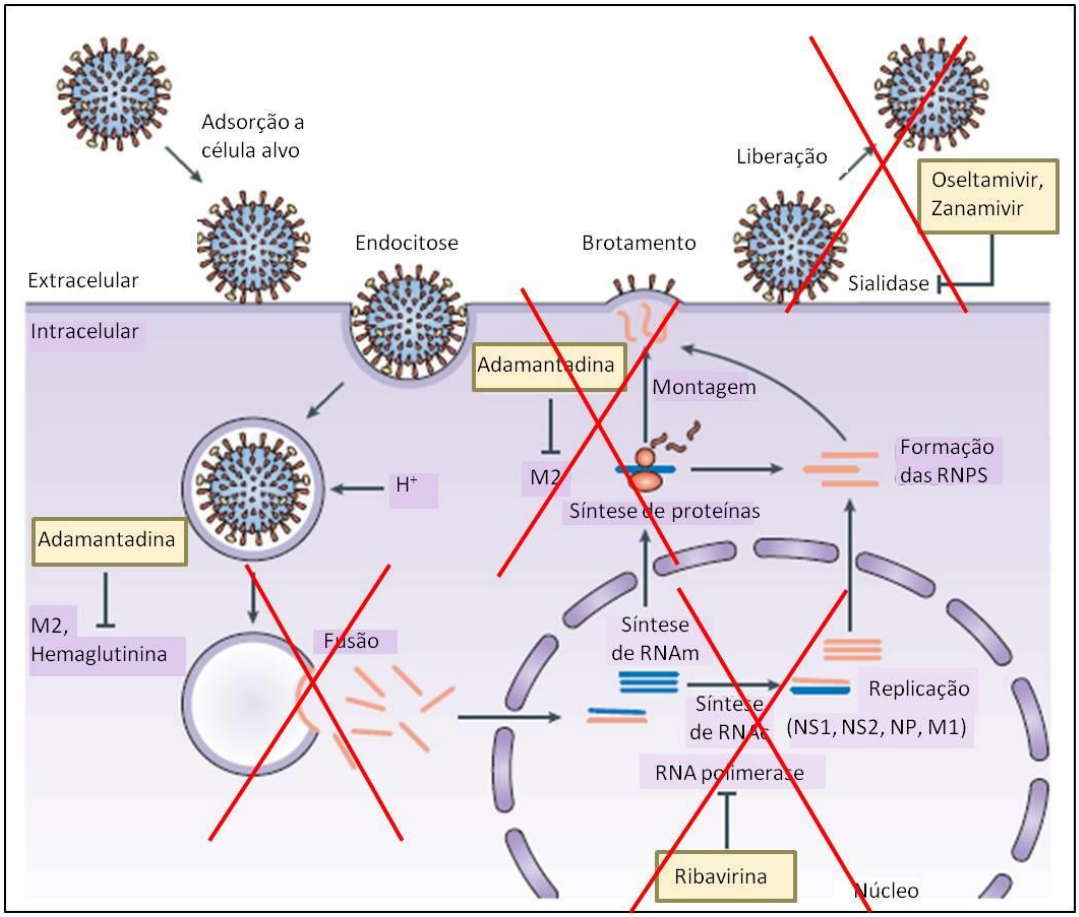

Figura 1.15 - Etapas da replicação do vírus influenza que são alvos dos principais antivirais.
Durante o ciclo replicativo do vírus influenza existem três principais pontos de inibição por drogas antivirais. As adamantanas (amantadina e rimantadina) bloqueiam o canal de prótons M2, não permitindo assim a fusão entre o envelope viral e a membrana do endossoma celular. Os NAIs (oseltamivir e zanamivir) inibem a enzima neuraminidase/sialidase e, consequentemente, inibem a liberação das novas partículas virais formadas. Já a ribavirina, inibe a RNA polimerase viral e, com isso, a replicação e a transcrição do genoma viral. Fonte: Adaptado de *von Itzstein*, Nature, 2007 (Von Itzstein, 2007b).

1.5.1 Bloqueadores do canal M2

Os adamantanos (Figura 1.16), amantadina e rimantadina, foram a primeira classe de drogas anti-influenza utilizada e atua somente contra os vírus influenza A (Couch *et al.*, 1986). Tanto a amantadina quanto a rimantadina possuem o mesmo mecanismo de ação e

podem atuar em dois momentos durante a replicação viral. O primeiro, durante a fusão envelope viral e a membrana do endossoma celular, pois penetram no canal iônico M2 do vírus e bloqueiam o influxo de prótons para o interior do mesmo (Figura 1.15) (Venkataraman *et al.*, 2005). O segundo, durante a síntese de proteínas no complexo de Golgi, que depende do gradiente de pH entre o lúmen desta organela e o citoplasma da célula, para prevenir mudanças conformacionais prematuras na hemaglutinina durante seu transporte para a membrana plasmática (Figura 1.15) (Venkataraman *et al.*, 2005).

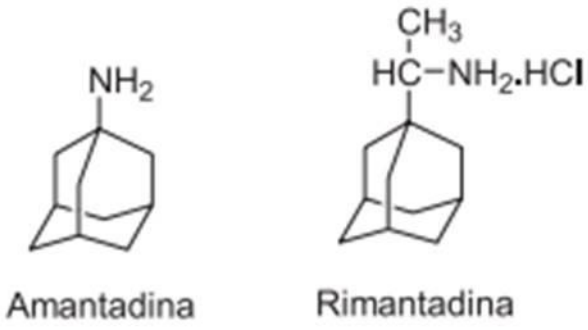

Figura 1.16 - Estrutura química dos adamantanos.
Estão representadas as estruturas químicas da amantadina (à esquerda) e da rimantadina (à direita). Fonte: *de Fátima, A et al.* Quim Nova, 2005 (De Fátima *et al.*, 2005).

Esta classe de drogas não possui atividade contra o vírus influenza B e, além disso, é rápido o desenvolvimento de resistência viral (Fleming, 2001; Saito *et al.*, 2008). O vírus influenza A H1N1 pandêmico de 2009, por exemplo, surgiu naturalmente resistente aos adamantanos, pois adquiriu o gene M de um vírus influenza suíno euro-asiático resistente a esta classe, contendo a mutação de resistência mais frequente, a S31N (troca de serina por asparagina na posição 31 da proteína M2) (Deyde *et al.*, 2010). Esta mutação torna a proteína M2 resistente à ação destas drogas, porém, não perde sua atividade, ou seja, a proteína M2 perde a estabilidade quando fechada mas consegue se abrir e formar o canal de prótons mesmo como a amantadina ligada (Pielak *et al.*, 2009).

1.5.2 Inibidores de neuraminidase (NAIs)

Desde 1999/2000, os NAIs (Oseltamivir - OST; Tamiflu®, Roche e Zanamivir - ZAN; Relenza®, GlaxoSmithKline) (Figura 1.11) têm sido utilizados para o tratamento de infecções pelos vírus influenza dos gêneros A e B (De Clercq, 2006). Atualmente, além do OST e do ZAN, existem mais 2 NAIs, Peramivir (Rapivab®, BioCryst Pharmaceuticals) (Cdc, 2016) e

Laninamivir (Inavir®, Daiichi Sankyo), sendo o último aprovado somente no Japão (Sankyo, 2010) (Figura 1.11).

Como já citado, atualmente, os antivirais são recomendados para o tratamento de suspeita ou infecção confirmada pelo vírus influenza sempre que possível. Entre os compostos recomendados estão o oseltamivir e o zanamivir. O oseltamivir é um medicamento oral, está disponível em cápsulas de 30, 45 e 75 mg e em suspensão líquida. Por ser administrado oralmente, é o medicamento mais utilizado para tratamento e quimioprofilaxia das infecções, podendo ser utilizado, inclusive, ema crianças menores de 1 ano de idade quando indicado (Centers for Disease Control and Prevention, 2011). Já o zanamivir é um medicamento inalatório e possuiu algumas restrições em sua aprovação dependendo da idade do paciente e caso o indivíduo possua outras doenças respiratórias (Centers for Disease Control and Prevention, 2011). As recomendações e posologia para os tratamentos estão resumidos na tabela 1.5.

Tabela 1.5 - Dosagem recomendada e cronograma de tratamento[a] e quimioprofilaxia[b] com antivirais contra o vírus influenza.

		Grupos etários (anos)				
Antiviral	**Recomendação**	**1-6**	**7-9**	**10-12**	**13-64**	**≥65**
Zanamivir	Tratamento, Influenza A e B	NA[*]	10 mg (2 inalações), 2 vezes ao dia	10 mg (2 inalações), 2 vezes ao dia	10 mg (2 inalações), 2 vezes ao dia	10 mg (2 inalações), 2 vezes ao dia
	Quimioprofilaxia, Influenza A e B	NA entre 1-4 anos	5-9 anos, 10 mg (2 inalações), 1 vez ao dia	10 mg (2 inalações), 1 vez ao dia	10 mg (2 inalações), 1 vez ao dia	10 mg (2 inalações), 1 vez ao dia
Oseltamivir	Tratamento, Influenza A e B	Dose varia de acordo com o peso da criança	Dose varia de acordo com o peso da criança	Dose varia de acordo com o peso da criança. Se >40 kg = dose de adulto	75 mg, 2 vezes ao dia	75 mg, 2 vezes ao dia
	Quimioprofilaxia, Influenza A e B	Dose varia de acordo com o peso da criança	Dose varia de acordo com o peso da criança	Dose varia de acordo com o peso da criança. Se >40 kg = dose de adulto	75 mg, 1 vez ao dia	75 mg, 1 vez ao dia

[*] NA: não aprovado. [a] A duração recomendada para tratamento é de 5 dias. Períodos maiores podem ser considerados para indivíduos com doença severa. [b] A duração recomendada para profilaxia é de 7 a 10 dias dependendo da situação de exposição ao vírus. Para controle de surtos em ambientes maiores, como hospitais, é recomendado pelo menos por 2 semanas e até 1 semana depois do caso identificado mais recentemente.

Fonte: Adaptado do Guia de Tratamento e Quimioprofilaxia contra Infecções pelo Vírus Influenza do CDC, 2011 (Centers for Disease Control and Prevention, 2011)

Os NAIs são análogos do AS presente nas células alvo do vírus influenza (Figura 1.11). Portanto, os NAIs ligam-se de forma competitiva ao sítio ativo da NA, impedindo que ocorra a clivagem do ácido siálico e, consequente, a liberação do vírus influenza no trato respiratório, o que acarreta no acúmulo de partículas virais na membrana nas células infectadas e diminui o espalhamento da infecção (Von Itzstein, 2007a).

Até 2007, a circulação mundial de cepas do vírus influenza resistentes aos NAIs era menor que 1% (Monto *et al.*, 2006). Porém, na temporada de 2007-2008 ocorreu a emergência de uma cepa sazonal de influenza A(H1N1) resistente ao OST e, até a temporada de 2008-2009, a prevalência na circulação desta cepa aumentou para mais de 90% mundialmente, chegando a 100% em alguns países (Baranovich *et al.*, 2010; Okomo-Adhiambo *et al.*, 2010). Além da circulação de cepas virais sazonais resistentes do subtipo H1N1, também já foram descritas cepas resistentes do vírus influenza sazonal H3N2 (Okomo-Adhiambo *et al.*, 2010; Cho *et al.*, 2013; Piralla *et al.*, 2013) e do vírus pandêmico de 2009 (Who, 2009a; 2010a), podendo, a última, causar infecções primárias em indivíduos saudáveis (Souza *et al.*, 2013). Estes fatos demonstram a necessidade de vigilância epidemiológica contínua destes vírus.

A sensibilidade da NA aos NAIs é avaliada através de ensaios de inibição enzimática (Potier *et al.*, 1979; Buxton *et al.*, 2000) e, a partir destes ensaios, é definida a concentração de droga capaz de inibir 50% da atividade enzimática (IC_{50}). A diminuição de sensibilidade ou a resistência a uma droga devido a alguma mutação é caracterizada pelo aumento de 100 a 10.000 vezes no valor de IC_{50} (Okomo-Adhiambo *et al.*, 2010). Porém, o valor de IC_{50} depende do tipo de ensaio utilizado, do gênero e subtipo do vírus influenza e da droga avaliada, sendo então necessárias análises adicionais para que a detecção de resistência seja clinicamente relevante. Para tal, é verificada a presença de mutações de resistência ao OST, como a H275Y por pirosequenciamento (Deyde *et al.*, 2009) ou pelo sequenciamento convencional de Sanger (Mckimm-Breschkin *et al.*, 2003). Também vêm sendo descritas mutações consideradas como redutoras da sensibilidade da NA ao OST, como a mutação E119V dos vírus H3N2 e a R152K dos vírus influenza B (Mckimm-Breschkin, 2013).

1.5.3 Ribavirina

A ribavirina (RB) (Figura 1.17) é um antiviral de amplo espectro, que inibe diversos vírus de RNA, como os paramyxovírus (vírus respiratório sincicial – RSV – e vírus parainfluenza), flavivírus (vírus da hepatite C - HCV, vírus da febre amarela e vírus do Oeste do Nilo) e orthomyxovírus (vírus influenza A e B). Este composto também possui atividade

antiviral contra alguns vírus de DNA, como por exemplo os vírus herpes simplex tipos 1 e 2 (HSV-1 e -2) e adenovírus tipo 3. Em modelos animais, o efeito antiviral da RB é mais restrito, inibindo apenas alguns vírus de RNA (Sidwell *et al.*, 1972; Crotty *et al.*, 2002).

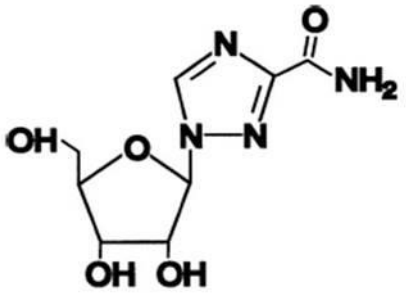

Ribavirina

Figura 1.17 - Estrutura química da Ribavirina.
Fonte: Adaptado de *Lourdes G. Ferreira, M. et al* Med Chem Res, 2013 (Lourdes G. Ferreira *et al.*, 2013)

Em humanos, a RB é utilizada principalmente no tratamento de hepatite C crônica juntamente com o interferon peguilado e no tratamento de infecções severas pelo RSV (Paeshuyse *et al.*, 2011; Razonable, 2011). Embora o RSV e o HCV sejam vírus de RNA, são bastante diferentes entre si. Além disso, o tratamento com a RB requer altas doses e causa muitos efeitos adversos. Desta maneira, compostos alternativos à RB têm sido de grande interesse entre os pesquisadores.

No caso dos vírus influenza, devido ao número limitado de drogas anti-influenza, vários estudos clínicos da eficácia da RB e sua combinação com NAIs vêm sendo realizados. A RB se mostrou um potente inibidor *in vitro* e *in vivo* dos vírus influenza A e B. Em estudos utilizando a tripla combinação de drogas antivirias, amantadina, OST e RB, observou-se um efeito inibitório sinérgico dos três compostos contra os principais subtipos de vírus influenza humanos, H1N1 e H3N2, sensíveis aos compostos ou resistentes à amantadina ou ao OST (Nguyen *et al.*, 2009; Nguyen *et al.*, 2010).

Embora sejam realizados diversos estudos com relação à atividade antiviral da RB, seu mecanismo de ação ainda não foi completamente elucidado. Existem três possíveis mecanismos inibitórios propostos pela literatura (Figura 1.18). O primeiro mecanismo, descrito em 1973, foi o de inibição de enzimas celulares envolvidas na biossíntese de nucleotídeos, mais especificamente, da inosina monofosfato desidrogenase (IMPHD), responsável pela conversão de iosina 5`-monofosfato em xantina 5`-monofosfato e crucial na produção intracelular de guanosina trifosfato (GTP) e na síntese de RNA viral (Figura 1.18 b) (Streeter *et al.*, 1973). O outro mecanismo é o de inibição direta da RNA polimerase viral,

embora acredite-se que este não seja seu principal alvo, já que até hoje não foram descritas mutações de resistência a este composto (Figura 1.18 c). O terceiro mecanismo, proposto mais recentemente, é o de mutagênese letal (Figura 1.18 d) (Crotty *et al.*, 2000; Crotty *et al.*, 2001). Neste caso, a RB é incorporada como sendo análoga de GTP e ATP (adenosina trifosfato) por RNA polimerases dependentes de RNA. Desta maneira, pode ocorrer o aumento do número de mutações geradas durante a replicação viral para uma taxa acima do limite, levando ao acúmulo de erros (catástrofe por erro) e a diminuição da fidelidade genética. Consequentemente, novas partículas virais não funcionais são geradas ou o ciclo replicativo completo é abortado (Crotty *et al.*, 2002).

Além dos mecanismos de inibição da replicação viral, já foi descrita uma possível função imunomodulatória para a RB em modelos de camundongos com hipersensibilidade. Dependendo da linhagem utilizada, a RB inibiu ou aumentou a secreção de interleucina 10 (IL-10) (Tam *et al.*, 1999). Além disso, durante o tratamento de hepatite C crônica com a RB, se observa somente uma pequena redução da carga viral, sendo seu efeito predominante na diminuição dos danos hepáticos, sugerindo que esta droga possui um efeito anti-inflamatório suplementar ao efeito antiviral (Bodenheimer *et al.*, 1997) (Figura 1.18 a).

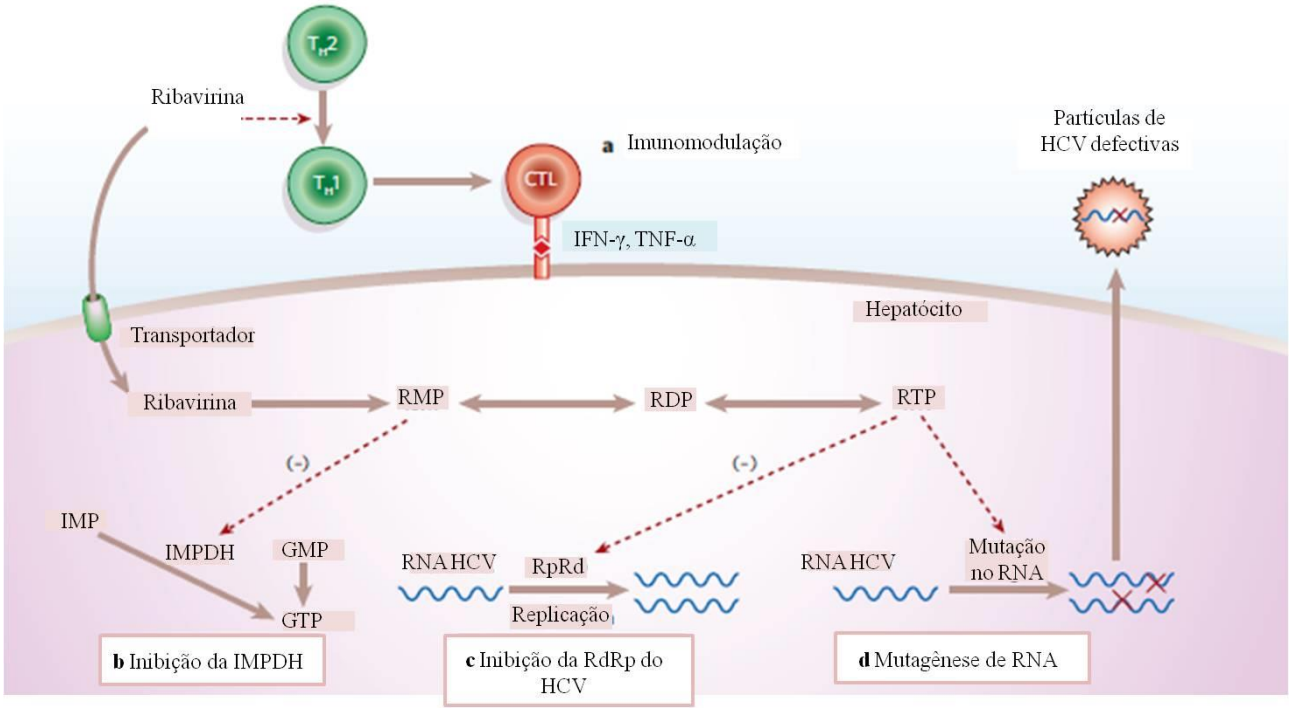

Figura 1.18 - Possíveis mecanismos de ação da ribavirina.
Este esquema demonstra os possíveis mecanismos de ação da RB, tendo como exemplo o tratamento contra hepatite C crônica. (**a**) A RB parece possuir um efeito imunomodulatório, inibindo a resposta Th2 e estimulando Th1. Este estímulo leva à secreção de IFN-γ e TNF-α por células T citotóxicas (CTL). (**b**) Após a entrada da RB na célula, esta é convertida em ribavirina monofosfato (RMP) e é então difosforilada (RDP – ribavirina difosfato) ou trifosforilada (RTP – ribavirina trifosfato) por enzimas celulares. A forma RMP inibe a enzima inosina monofosfato desidrogenase (IMPDH), levando à depleção de GTP intracelular e a inibição indireta da replicação viral. (**c**) A forma RTP é capaz de inibir diretamente a RpRd e, consequentemente, inibe a replicação viral. (**d**) A forma trifosfatada da RB também é capaz de atuar através do mecanismo de catástrofe por erro, que aumenta o número de mutações no RNA viral e os novos vírions formados não são funcionais. Fonte: Adaptado de *Feld & Hoofnagle*, Nature, 2005. (Feld e Hoofnagle, 2005)

1.6 Resposta Imunológica Inata e *Cytokine Storm*

A susceptibilidade ou a resistência a infecções virais dependem de fatores associados ao patógeno, como sua virulência e habilidade de entrar, replicar e lisar as células do epitélio respiratório; e fatores associados ao hospedeiro, como a eficácia da resposta imunológica e agressividade do sistema imune contra o agente infeccioso, que pode melhorar ou exacerbar a infecção e alterar seu desfecho clínico. A resposta imune agressiva contra a infecção pelos vírus influenza já foi correlacionada com maior morbidade e piores desfechos clínicos durante as pandemias de 1918 e 2009, e em humanos infectados com o vírus aviário H5N1 (Teijaro, 2015).

A imunidade inata é a primeira linha de defesa contra as infecções e seus mecanismos são rapidamente ativados pelos microrganismos antes do desenvolvimento de anticorpos específicos. As principais citocinas envolvidas com a resposta antiviral inata são os interferons (IFNs), moléculas que induzem a expressão de proteínas celulares que atuam na resposta antiviral. Os IFNs são classificados em três tipos: tipo I (IFN-α e IFN-β), tipo II (IFN-γ) e tipo III (IFN-λ 1, 2 e 3 ou IL-29, IL-28a e IL-28b, respectivamente). Apesar de suas propriedades antivirais, vários estudos sugerem um papel patogênico dos IFNs durante a infecção pelos vírus influenza, já que a produção de diversas citocinas e quimiocinas pro-inflamatórias se encontra aumentada (Teijaro, 2015). Por exemplo, os IFN tipo I estimulam as células epiteliais infectadas a produzirem IL-6, IL-1, TNF-α, IL-8, MCP-1 e RANTES (também chamados de CCL2 e CCL5, respectivamente), que geram uma resposta tecidual pró-inflamatória e estimulam o recrutamento de monócitos/macrófagos, linfócitos T e B, e células N*atural Killer* (NK) para o local de infecção (Adachi *et al.*, 1997). Essas células, por sua vez, produzem mais citocinas pró-inflamatórias que favorecem a resposta Th1, necessária para a imunidade antiviral específica. Além disso, a resposta celular é de grande importância no combate inicial a infecção pelo vírus influenza, já que as células T $CD8^+$ possuem papel crucial no *clearance* viral. Embora as respostas Th1 e citotóxica sejam essenciais para a eliminação da infecção viral, a grande liberação de citocinas pró-inflamatórias (ou *cytokine storm*) e moléculas citotóxicas resulta em dano no tecido pulmonar e agravo da infecção (Bermejo-Martin *et al.*, 2009; Ramana *et al.*, 2009).

O IFN-γ também possui um papel protetor e patogênico durante a infecção pelo vírus influenza. Para a entrada e fusão do vírus na célula hospedeira, é necessário que proteases intra e extracelulares clivem a HA0 em HA1 e HA2. Os sítios de replicação viral dentro do trato respiratório são repletos destas proteases, que possuem papel na replicação viral e na resposta imune inata já que são mediadores inflamatórios através da ativação dos receptores ativados por proteinase (RAPs). Existem 4 RAPs descritos (RAP 1-4) e, entre eles, os RAP 1 e 2 já foram associados a infecção pelo vírus influenza (Perrone *et al.*, 2010). RAP2, quando ativado, leva a produção de IFN-γ, que foi associada a redução da replicação viral nas células epiteliais, redução dos níveis de RANTES e número de neutrófilos nos fluidos broncoalveolares e a uma resposta anti-influenza protetora (Perrone *et al.*, 2010). Já a ativação do receptor RAP1, contribui para a exacerbação da resposta pró-inflamatória anti-influenza, levando ao aumento da produção de citocinas, aumento na produção viral, aumento da permeabilidade vascular, edema e dano pulmonar, contribuindo, então para patogênese da infecção (Brun-Buisson *et al.*, 2011). Outros trabalhos também demonstraram que o IFN-γ não é necessário para a recuperação da infecção, sugerindo que possíveis alterações na

concentração desta citocina e a presença de outros fatores podem ser necessárias para a definição do papel do IFN-γ durante a infecção (Perrone *et al.*, 2010).

Os IFN-λ também estão envolvidos na resposta anti-influenza. Sua ativação leva a produção de diversas proteínas com propriedades antivirais, antiproliferativas e imunomodulatórias. Os IFN-λ reduzem a produção de citocinas relacionadas à resposta Th2 (IL-4, IL-5, IL-13, IL-14, IL-15), favorecendo, assim, uma resposta Th1 e, também, aumentando a citotoxicidade de células T CD8 (Kelly *et al.*, 2011).

Além dos interferons, outras 3 citocinas estão fortemente ligadas ao *cytokine storm* durante a infecção pelo vírus influenza, IL-1, TNF- α e IL-6. A sinalização desencadeada por IL-1β e altos níveis de TNF-α são frequentemente relacionados com a morbidade consequente da infecção pelo vírus influenza. A presença destas citocinas levou ao aumento da produção de citocinas e quimiocinas pro-inflamatórias, aumento no número de neutrófilos e macrófagos encontrados nos pulmões e aumento na mortalidade em modelos animais (Perrone *et al.*, 2010). Controversamente, outros estudos já viram que camundongos nocaute para os receptores de IL-1 apresentaram demora na resolução da infecção devido à baixa produção de anticorpos anti-influenza e não foi observada diferença na morbidade e mortalidade de camundongos nocaute para o receptor de TNF-α (TNFR) infectados pelo vírus H5N1 (Teijaro, 2015).

Altos níveis de IL-6 são normalmente encontrados em pacientes infectados pelos vírus H5N1 e H1N1pdm09. Apesar da correlação entre esta citocina e a patogênese da infecção, estudos em modelos animais sugerem que a ausência de IL-6 não reduz a mortalidade dos camundongos infectados e a sinalização desencadeada é necessária para o controle da replicação viral nos pulmões, pois leva a geração de células T helper e resposta por células B e anticorpos (Teijaro, 2015).

No caso das principais quimiocinas envolvidas na resposta anti-influenza, como MCP-1, MIP-1α e RANTES, sua produção local e sistêmica e seus efeitos como moléculas quimiotáticas também são associadas à patogênese da infecção. Altos níveis destas moléculas são encontrados no soro de pacientes infectados com cepas mais virulentas do vírus influenza, como H5N1 (Teijaro, 2015). Porém, modelos animais sugerem resultados distintos, já que a presença das quimiocinas também é importante na resolução da infecção (Teijaro, 2015).

Nas infecções mais severas pelos vírus influenza, como H5N1 e H1N1pdm09, o *cytokine storm*, tem sido alvo terapêutico. Nestes casos, drogas imunomodulatórias deveriam apresentar benefícios terapêuticos. A terapia imunomodulatória adjuvante à terapia antiviral é extensamente utilizada através do emprego de corticóides. Porém, os efeitos causados pelo tratamento com estas moléculas são controversos com relação à melhora do paciente, período

de excreção e carga viral (Souza *et al.*, 2010; Brun-Buisson *et al.*, 2011; Lee, 2017). Como exemplo, um trabalho do nosso grupo mostrou que pacientes com câncer, hospitalizados devido à infecção grave pelo vírus influenza, apresentaram longos períodos de excreção viral mesmo sendo tratados com oseltamivir e metilprednisolona (Souza *et al.*, 2010). Outro grupo mostrou que o uso de corticoides para tratar pacientes com síndrome da dificuldade respiratória do adulto (ARDS – do inglês *adult respiratory distress syndrome*) secundária a pneumonia causada pela infecção com o vírus influenza não apresentou benefícios. Inclusive, o tratamento precoce desses pacientes foi associado com casos fatais, casos de pneumonia mais grave e uma tendência para uma maior duração da ventilação mecânica (Brun-Buisson *et al.*, 2011). Já uma revisão publicada recentemente comenta que o uso precoce de imunomoduladores associado a antivirais pode interromper a progressão da pneumonia e induzir recuperação rápida de lesões pulmonares em pacientes infectados pelo vírus influenza e que, durante a pandemia de H1N1 de 2009, pneumônicas que se desenvolveram rapidamente após a infecção viral foram resolvidas drasticamente dentro de 24 h após o tratamento com corticosteroides (Lee, 2017).

Para todas as citocinas e quimiocinas mencionadas anteriormente, tem sido difícil provar uma relação entre as moléculas individualmente e a patogênese da infecção, já que elas também são necessárias para o controle e resolução da infecção pelo vírus influenza. O equilíbrio entre o controle imunológico do vírus influenza e a patologia é bastante delicado. A modulação excessiva da resposta imunológica resulta na perda do controle da infecção viral, enquanto a resposta inflamatória exacerbada que parece contribuir para a redução da replicação viral leva também ao agravo do quadro infeccioso como um todo.

1.7 Justificativa

Os vírus influenza são os principais responsáveis pelas infecções respiratórias agudas que, apesar de geralmente autolimitadas, constituem uma das principais causas e morbidade e mortalidade, apresentando grande impacto na saúde pública. As infecções ocasionadas pelos vírus influenza podem ocorrer na forma de epidemias sazonais e pandemias.

Embora existam vacinas anti-influenza, diversas limitações tornam difícil o controle das infecções causadas pelos vírus influenza através da vacinação. Entre elas, as altas taxas de mutação e recombinação genética (*shift* e *drift* antigênicos) do vírus influenza, sua capacidade de infectar animais, o alto custo e tempo longo para produção de novas vacinas contra novas variantes virais, além da sua indicação somente para indivíduos pertencentes aos grupos de risco de desenvolvimento de doença grave e com outras comorbidades. Por estes motivos, os medicamentos anti-influenza oferecem uma opção importante para o controle das infecções causadas pelos vírus influenza. Também vale ressaltar que, como as características antigênicas de novas variantes virais com potencial pandêmico são imprevisíveis, a estocagem de drogas anti-influenza pode ser uma estratégia viável para o preparo para uma pandemia.

Existem duas classes de drogas anti-influenza aprovadas para uso, os bloqueadores do canal M2 (ou adamantanas) e os NAIs. Virtualmente, todas as cepas circulantes são resistentes as adamantanas e tem sido descritas cepas circulantes resistentes ao oseltamivir, antiviral da classe dos NAIs mais utilizado clinicamente. Desta maneira, torna-se necessária a busca por novas moléculas capazes de inibir essas cepas e/ou atuar sobre outros alvos durante a replicação viral.

2 OBJETIVOS

2.1 Objetivo Geral

O objetivo geral desta tese foi caracterizar compostos naturais e sintéticos com relação a sua capacidade de inibir a replicação do vírus influenza, explorando seus possíveis de mecanismos de ação a fim de encontrarmos novos protótipos para o desenvolvimento de novos compostos anti-influenza.

2.2 Objetivos Específicos

Os objetivos específicos desta tese foram divididos em 5 capítulos, inseridos como artigos ou manuscritos, conforme mostrado a seguir.

2.2.1 Capítulo I - Aureonitol, a Fungi-Derived Tetrahydrofuran, Inhibits Influenza Replication by Targeting Its Surface Glycoprotein Hemagglutinin

Caracterizar os efeitos do composto aureonitol sobre a replicação *in vitro* do vírus influenza.

2.2.2 Capítulo II - 1,2,3-Triazolyl-4-oxoquinolines: a feasible beginning for promising chemical structures to inhibit Oseltamivir-resistant influenza A and B viruses

Caracterizar os efeitos desta nova classe de compostos oxoquinolínicos sobre a replicação *in vitro* do vírus influenza.

2.2.3 Capítulo III – The compound 4-(4-phenyl-1H-1,2,3-triazol-1-yl)-2,2,6,6-tetramethylpiperidine-1-oxyl inhibits influenza replication by targeting the viral neuraminidase

Avaliar efeitos do composto tritempo (4-(4-phenyl-1H-1,2,3-triazol-1-yl)-2,2,6,6-tetramethylpiperidine-1-oxyl) sobre a replicação *in vitro* do vírus influenza.

2.2.4 Capítulo IV – Influenza virus RNA polymerase may be activated inside the virion to enhance diagnostic sensitivity

Avaliar se o vírus influenza possui atividade natural endógena da RNA polimerase e sua aplicabilidade.

2.2.5 Capítulo V – The ribavirin analog methyl 1-benzyl-1H-1,2,3-triazole-4-carboxylate inhibits influenza in vitro and in vivo replication

Caracterizar os efeitos do análogo triazólico da ribavirina, o composto **5b**, sobre a replicação *in vitro* e *in vivo* do vírus influenza.

3 ARTIGO(S) PUBLICADO(S), MANUSCRITO(S) ACEITO(S) OU SUBMETIDOS PARA PUBLICAÇÃO

3.1 CAPITULO I - Aureonitol, a Fungi-Derived Tetrahydrofuran, Inhibits Influenza Replication by Targeting Its Surface Glycoprotein Hemagglutinin

Autores: Carolina Q. Sacramento, Andressa Marttorelli, Natalia Fintelman-Rodrigues, Caroline S. de Freitas, Gabrielle R. de Melo, Marco E. N. Rocha, Carlos R. Kaiser, Katia F. Rodrigues, Gisela L. da Costa, Cristiane M. Alves, Osvaldo Santos-Filho, Jussara P. Barbosa, Thiago Moreno L. Souza

Periódico: Artigo publicado na revista Plos One | DOI:10.1371/journal.pone.0139236 – Outubro de 2015 (Sacramento *et al.*, 2015)

Este estudo foi desenvolvido em colaboração com o grupo da Dra. Gisela da Costa, do Laboratório de Taxonomia, Bioquímica e Bioprospecção de Fungos do Instituto Oswaldo Cruz, FIOCRUZ. O objetivo principal deste trabalho foi investigar e caracterizar a atividade anti-influenza do composto aureonitol, um produto natural derivado do fungo *Chaetomium sp*.

Chaetomium Kuntze ex Fries é um gênero de fungos endofíticos encontrados no interior de organismos terrestres e marinhos, e em solos e substratos que contém celulose. Membros deste gênero são fontes ricas de metabólitos secundários com diferentes estruturas químicas, entre eles, o aureonitol. O aureonitol é um tetrahidrofurano (THF) produzido por diferentes espécies do gênero *Chaetomium* e já foi descrito como um regulador da síntese de outros metabólitos secundários na espécie *Chaetomium globosum*. Embora já tenha sido demonstrado que outros THFs apresentam atividade antiviral, inclusive anti-influenza, os efeitos do aureonitol contra a replicação do vírus influenza ainda não tinham sido caracterizados.

O aureonitol inibe a replicação do vírus influenza A e B em células MDCK de maneira dose-, tempo- e MOI-dependente (MOI representa a relação vírus-célula). Este composto é mais efetivo ao inibir a replicação do vírus influenza A(H3N2), com um valor de EC_{50} igual a 100 nM (concentração da droga que inibe 50 % da replicação viral). A citotoxicidade do aureonitol é muito baixa, valor de CC_{50} igual a 1.426 μM (concentração da droga tóxica para 50 % das células). O alto índice de seletividade do nosso composto (SI - razão entre os valores de CC_{50} e EC_{50} - SI – grau de segurança de uma substância *in vitro*), igual a 14.260,

indica que sua margem de segurança *in vitro* é alta. O aureonitol inibe a hemaglutinina (HA) dos vírus influenza A e B com concentrações na faixa de nano molar, e, consequentemente, bloqueia a adsorção e entrada do vírus na célula hospedeira. Nossos estudos de docking *in silico* demonstraram que o aureonitol se interage com a HA no sítio de ligação ao ácido siálico, formando pontes de hidrogênio com resíduos de aminoácidos altamente conservados.

Produtos naturais são uma fonte ampla de compostos com diferentes estruturas químicas e atividades biológicas. Este trabalho demonstrou a atividade antiviral do aureonitol, um composto natural derivado de fungos gênero *Chaetomium*. Diferentes espécies deste gênero produzem o aureonitol com rendimentos maiores que 70 % e a síntese orgânica deste composto já foi descrita, demonstrando a viabilidade de escalonamento na produção deste composto. Este fato em conjunto com nossos resultados indicam que a estrutura química do aureonitol é bastante promissora para o desenvolvimento de novas drogas anti-influenza.

3.2 CAPITULO II - 1,2,3-Triazolyl-4-oxoquinolines: a feasible beginning for promising chemical structures to inhibit Oseltamivir-resistant influenza A and B viruses

Autores: Fernanda da C. S. Boechat[*], Carolina Q. Sacramento[*], Anna C. Cunha, Fernanda S. Sagrillo, Christiane M. Nogueira, Natalia Fintelman-Rodrigues, Osvaldo Santos-Filho, Cecília S. Riscado, Luana da S. M. Forezi, Letícia V. Faro, Leonardo Brozeguini, Isakelly P. Marques, Vitor F. Ferreira, Thiago Moreno L. Souza[#] and Maria Cecília B. V. de Souza[#]

[*] Estes autores contribuíram igualmente como primeiros autores; [#] Estes autores contribuíram igualmente como últimos autores.

Periódico: Artigo publicado na revista Bioorganic & Medicinal Chemistry | DOI: 10.1016/j.bmc.2015.11.028 – Dezembro de 2015 (Boechat *et al.*, 2015)

Este estudo foi desenvolvido em colaboração com o grupo da Dra. Maria Cecília de Souza do Departamento de Química Orgânica da Universidade Federal Fluminense (UFF). O objetivo geral deste trabalho foi caracterizar os efeitos de uma nova classe de compostos oxoquinolínicos (sintetizada pelo grupo da Dra. Maria Cecília) sobre a replicação *in vitro* do vírus influenza.

Quinolonas e compostos derivados triazólicos tem sido amplamente explorados devido a sua grande variedade de propriedades biológicas. Estes radicais já foram descritos por apresentarem atividade antiviral contra os vírus da imunodeficiência humana (HIV), vírus da hepatite C (HCV), herpes simplex vírus (HSV) e vírus influenza. A estrutura básica das moléculas apresentadas neste trabalho é composta por um motivo 4-oxoquinolínico com um anel triazólico acoplado no carbono 6 ou 7, e diferentes radicais (R1) adicionados ao anel triazólico.

Foram sintetizados 10 compostos oxoquinolínicos (compostos **1a-j**) e todos foram avaliados com relação a sua capacidade de inibir a atividade neuraminidase (NA) do vírus influenza. O composto **1i**, aquele que possui um radical ciclohexenil adicionado ao carbono 6 do anel triazólcio, foi o mais potente entre eles, inibindo em 94,8 % a atividade NA do vírus influenza A(H3N2). Ao investigarmos a potência do composto **1i**, vimos que é capaz de inibir a atividade NA de cepas do vírus influenza A e B, sensíveis e resistentes ao oseltamivir (OST), com valores de IC_{50} (concentração da droga capaz de inibir 50 % da atividade enzimática) na faixa de micro molar. Embora seja menos potente que o composto de

referência ao inibir as cepas sensíveis (os valores de IC_{50} do OST são na faixa de nano molar), nosso composto inibe a atividade NA das cepas de influenza A(H3N2), A(H1N1)pdm09 e B, com as mutações de resistência H275Y, E119V e R152K, respectivamente, nas quais o OST falha em bloquear. Além disso, o composto **1i** é capaz de inibir a replicação do vírus influenza em células MDCK com valor de EC_{50} igual a 0,2 μM. Este composto mostrou baixa citotoxicidade, com CC_{50} igual a 566 μM; e alto SI, 2.830, indicando que é seguro para utilização *in vitro*.

Ensaios de docking *in silico* mostraram que o composto **1i** se liga ao sítio ativo das diferentes isoformas de NA testadas, tanto sensíveis quanto resistentes ao OST (isoformas de NA dos vírus influenza A(H3N2) e A(H1N1)pdm09). Os sítios de ligação do nosso composto e do OST se sobrepõem parcialmente. O radical ciclohexenil, que se mostrou crucial para a atividade antiviral do composto **1i**, se projeta para uma área da NA que não é ocupada pelo OST e interage com resíduos de aminoácidos extremamente conservados entre as 9 NAs do vírus influenza A presentes na natureza. Este fato sugere que mutações neste resíduos poderiam reduzir o fitness viral, tornando difícil o surgimento de cepas virais resistentes ao composto **1i**.

Em conjunto, nossos resultados mostram que a estrutura química desta nova classe de moléculas sintetizadas é um protótipo interessante para o desenvolvimento de novos compostos com atividade anti-influenza.

3.3 CAPITULO III - The compound 4-(4-phenyl-1H-1,2,3-triazol-1-yl)-2,2,6,6-tetramethylpiperidine-1-oxyl inhibits influenza replication by targeting the viral neuraminidase

Autores: Carolina Q. Sacramento, Alessandro Kappel Jordão, Cristiane M. Alves, Andressa Marttorelli, Natalia Fintelman-Rodrigues, Caroline S. de Freitas, Gabrielle R. de Melo, Osvaldo Santos-Filho, Anna Claudia Cunha, Vitor F. Ferreira e Thiago Moreno L. Souza

Periódico: Manuscrito submetido para publicação na revista Bioorganic & Medicinal Chemistry Letters | Aceito com solicitações de revisões (em processo de revisão).

Este estudo foi desenvolvido em colaboração com o grupo do Dr. Vitor Ferreira do Departamento de Química Orgânica da Universidade Federal Fluminense (UFF). O objetivo geral deste trabalho foi caracterizar os efeitos do composto triazólico 4-(4-fenil-1H-1,2,3-triazol-1-il)-2,2,6,6-tetrametilpiperidina-1-oxil (sintetizado pelo grupo do Dr. Vitor e chamado de tritempo) sobre a replicação *in vitro* do vírus influenza.

Como mencionado anteriormente, compostos triazólicos tem sido amplamente estudados devido as suas propriedades medicinais, inclusive antivirais contra os vírus influenza, HIV-1 e os vírus da hepatite A e C. Durante nosso estudo com a nova série de compostos oxoquinolínicos, vimos que o composto mais potente em inibir a atividade da NA dos vírus influenza sensíveis e resistentes ao OST, composto **1i**, possuía como grupos farmacofóricos (grupos funcionais de uma molécula, necessários para seu efeito farmacológico) o radical triazólico e o anel ciclohexenil. Apesar de sua alta potência entre o grupo de moléculas avaliado no trabalho anterior, sua concentração de inibição da replicação viral era na faixa de micro molar. A fim de buscarmos em nossa biblioteca de drogas compostos mais potentes que o **1i**, utilizamos a ontologia química (classificação química baseada em estrutura) para procurar moléculas contendo estruturas semelhantes aos grupos farmacofóricos do composto **1i**. O composto tritempo chamou nossa atenção por possuir um anel triazólico ligado a um radical nitróxido de piperidina-1-oxil. Esse composto já é conhecido por sua atividade anti-inflamatória, característica adicional desejável para novos antivirais.

Primeiramente avaliamos a capacidade do tritempo em inibir a replicação *in vitro* do vírus influenza. Vimos que o tritempo inibe a replicação do vírus influenza em células MDCK com valor de EC_{50} igual a 0,38 μM e é pouco citotóxico (CC_{50} maior que 2.000 μM). Seu alto SI, 5.263, indica que é seguro para utilização *in vitro*.

Esse composto também é capaz de inibir a atividade NA dos vírus influenza A e B. Embora menos potente que o OST em inibir cepas virais sensíveis, se mostrou mais vantajoso ao inibir cepas resistentes ao composto de referência. Tritempo foi igualmente potente em inibir as cepas de influenza A(H1N1)pdm09, A(H3N2) e B que contem as mutações de resistência H275Y, E119V e R152K, respectivamente (valores de IC_{50} iguais a 12, 10 e 18 nM, respectivamente).

Através de ensaios de *docking in silico*, vimos que o composto tritempo se liga a aminoácidos conservados do sítio ativo das diferentes isoformas de NA testadas (NAs dos vírus influenza A(H3N2) e A(H1N1)pdm09), tanto sensíveis quanto com mutações de resistência ao OST, e com baixa energia livre de ligação. Embora o OST se ligue às isoformas de NA através de um número maior de pontes de hidrogênio, o tritempo possuiu maior plasticidade de interação. Além disso, vimos que o anel triazólico e o radical nitróxido de piperidina-1-oxil foram necessários para a interação do composto com as NAs.

Após passagens sequenciais do vírus influenza na presença de concentrações crescentes do tritempo, detectamos uma cepa capaz de crescer mesmo na presença de 2,3 μM do composto (concentração 6 vezes maior que seu EC_{50}). Essa cepa possui a mutação G248P. A seguir, essa cepa resistente ao tritempo foi testada contra o OST e vimos que a mesma permaneceu sensível ao composto de referência, indicando que não há resistência cruzada entre os dois compostos.

Esses resultados demonstram vantagens do composto tritempo em relação às oxoquinolinas, já que é menos citotóxico e mais potente, possuindo, consequentemente, melhor atividade anti-influenza. Esse composto também inibiu a atividade NA de diferentes tipos e subtipos de vírus influenza em concentrações na faixa de nano molar, além de não apresentar resistência cruzada com o OST. Além disso, como já mencionado, o tritempo também apresenta propriedades anti-inflamatórias, atividade complementar desejável em antivirais. Portanto, sua estrutura química é bastante promissora para o desenvolvimento de novos compostos antivirais contra o vírus influenza.

3.4 CAPITULO IV - Influenza virus RNA polymerase may be activated inside the viron to enhance diagnostic sensitivity

Autores: Carolina Q. Sacramento[#], Natalia Fintelman-Rodrigues[#], Milene Miranda, Marilda M. Siqueira, Thiago Moreno L. Souza.

[#] Estes autores contribuíram igualmente como primeiros autores.

Periódico: Manuscrito submetido para publicação na revista *Journal of General Virology* | Em processo de revisão.

Alguns vírus carregam sua própria RNA/DNA polimerase dentro dos vírions. Isso é necessário quando as enzimas virais possuem características diferentes das enzimas celulares. Como exemplo, os vírus HIV-1 carregam a enzima transcriptase reversa (TR) que apresenta atividade RNA polimerase DNA-dependente, atividade essa que não ocorre nas células hospedeiras. Além disso, os vírus HIV são permissivos a entrada de nucleotídeos trifosfatados (NTPs – substratos das polimerases), provavelmente por causa do canal formado pela sua glicoproteína de superfície gp41. Os vírus influenza também possuem sua RNA polimerase dentro dos vírus e essa é uma enzima com atividade RNA polimerase RNA-dependente, também não encontrada em suas células hospedeiras. Como até o momento não existem evidências que a estrutura do vírus influenza é permissível aos NTPs, nós avaliamos funcionalmente essa característica.

Foram realizados ensaios com amostras livres de células dos vírus influenza A(H3N2), A(H1N1)pdm09 e B, a fim de estimularmos a atividade da RNA polimerase viral presente dentro dos vírions. Essas amostras foram incubadas com NTPs e Mg^{++} (substratos e cofator da polimerase, respectivamente) e a atividade enzimática foi determinada através da quantificação dos níveis de RNA viral pela técnica de RT-PCR em tempo real. Com isso, confirmamos que o vírus influenza possui atividade natural endógena da RNA polimerase, chamada de NERP neste trabalho. A atividade NERP poderia ser explorada de duas maneiras. A primeira, para aumentar a sensibilidade do diagnóstico do vírus influenza e, a segunda, para o desenvolvimento de ensaios para triagem de novas drogas antivirais. Neste trabalho, nosso foco foi avaliar a atividade NERP no diagnóstico viral.

As viroses respiratórias humanas podem causar sintomas clínicos muito parecidos, o que dificulta o diagnóstico exato do agente infeccioso. Entre esses agentes, os vírus influenza apresentam grande importância clínica e epidemiológica devido ao seu potencial de causar

epidemias sazonais e pandemias através do surgimento de *drifts* e *shifts* genéticos. Por isso, a o diagnóstico não equivocado e a vigilância laboratorial é crucial. Atualmente, existem diferentes ferramentas para detecção do vírus influenza. Entre elas, o diagnóstico molecular se mostra uma abordagem confiável para o monitoramento e subtipagem das cepas circulantes do vírus influenza. Porém, o período de tempo desde o início da doença até à coleta e testagem das amostras pode comprometer um diagnóstico preciso, já que o RNA viral desaparece rapidamente das amostras do trato respiratório. Desta maneira, ferramentas complementares que possam aumentar a sensibilidade do diagnóstico são de grande ajuda para uma vigilância epidemiológica mais precisa deste vírus. Da mesma maneira mencionada anteriormente, vimos que o estímulo de amostras clínicas com NTPs e Mg^{++} aumenta a atividade NERP dos vírions ali presentes. Consequentemente, ocorre um aumento nos níveis de RNA viral de 1- até 3-$\log_{10}$, permitindo a detecção dos vírus influenza em amostras clínicas anteriormente indetectáveis. Com o aumento da carga viral, a atividade NERP também aumentou nossa capacidade de sequenciar algumas regiões do genoma viral previamente não-sequenciáveis nas amostras clínicas.

Para confirmar que ativamos especificamente a RNA polimerase viral, realizamos o estímulo na presença da ribavirina, antiviral que inibe DNA e RNA polimerases virais. De fato, a atividade NERP do vírus influenza foi inibida na presença da ribavirina. Além de confirmar nossa hipótese, esse resultado mostra que nosso ensaio poderia ser utilizado como ferramenta na triagem de novas drogas antivirais contra a RNA polimerase do vírus influenza.

De maneira geral, esses dados indicam que a atividade da RNA polimerase dos vírus influenza A e B pode ser ativada dentro dos vírions. Além disso, demonstra que essa técnica pode ser útil para aumentar a sensibilidade do diagnóstico laboratorial desses vírus e para o desenvolvimento de ensaios para a triagem de novos antivirais.

3.5 CAPITULO V – The ribavirin analog methyl 1-benzyl-1H-1,2,3-triazole-4-carboxylate inhibits influenza in vitro and in vivo replication

Autores: Carolina Q. Sacramento, Natalia Fintelman-Rodrigues, Andressa Marttorelli, Caroline S. de Freitas, Gabrielle R. de Melo, André C. Ferreira, Cristiana C. Garcia, Alexandre M. V. Machado, Milene Mesquita, Maria de Lourdes G. Ferreira, Luiz C. S. Pinheiro, Nubia Boechat, Thiago Moreno L. Souza

Periódico: Manuscrito submetido para publicação na revista *Journal of General Virology* | Em processo de revisão.

Este estudo foi desenvolvido em colaboração com o grupo dos Drs. Luiz Pinheiro e Nubia Boechat de Farmanguinhos, FIOCRUZ. O objetivo deste trabalho foi caracterizar o mecanismo de ação e os efeitos anti-influenza *in vivo* do composto **5b**, um análogo triazólico da ribavirina sintetizado pelos grupos mencionados acima. A síntese do composto e sua atividade antiviral foi descrita previamente pelo nosso grupo (Lourdes G. Ferreira *et al.*, 2013).

Como mencionado anteriormente, a ribavirina é um antiviral de amplo espectro cuja utilização clínica é limitada devido à sua alta toxicidade. Durante a síntese do seu novo análogo, foram realizadas mudanças estruturais na molécula da ribavirina a fim de deixa-la mais estável, menos tóxica e com melhor atividade antiviral (Silva *et al.*, 2009; Lourdes G. Ferreira *et al.*, 2013). O composto **5b** possui estrutura química semelhante à da ribavirina, contendo a ribose e o anel triazólico, embora o anel 1,2,4-triazol tenha sido substituído pelo 1,2,3-triazol. Foram adicionados radicais benzeno no lugar das hidroxilas e, a principal alteração na estrutura foi o grupo funcional amida da ribavirina, que foi substituído pelo radical metil carboxilato no composto **5b**.

Primeiramente, confirmamos a capacidade do comporto **5b** em inibir a replicação do vírus influenza e encontramos valor de EC_{50} igual a 0,07 µM e CC50 > 1000 µM. Para referência, nosso foi aproximadamente 300 vezes mais potente e 10 vezes menos citotóxico que a ribavirina nas nossas condições experimentais. Esses dados demonstram que nosso composto possui um alto SI e é seguro para utilização *in vitro*.

Por ser um análogo da ribavirina, espera-se que os compostos possuam mecanismos de ação semelhantes. Para verificar se o composto **5b** também inibe a atividade da enzima RNA polimerase viral, utilizamos o método mencionado no artigo anterior, quantificando a atividade endógena da RNA polimerase viral (NERP) na ausência e presença de diferentes

concentrações do nosso composto. Vimos que o composto **5b** de fato inibe a atividade enzimátiza de maneira dose-dependente, independente da quantidade de substrato adicionado.

Durante o ciclo replicativo do vírus influenza, a RNA polimerase viral é responsável pelos processos de duplicação e transcrição do genoma viral e, normalmente, os níveis de RNA viral (genômico e anti-genômico) são maiores que os níveis de RNA mensageiro. Como o alvo do nosso composto é a RNA polimerase, verificamos se esses processos estariam alterados após o tratamento. Observamos que, após o tratamento com o composto **5b**, houve uma redução de aproximadamente 30 % no processo de duplicação do RNA viral enquanto o processo de transcrição aumenta em 10 vezes, sugerindo uma desregulação no balanço entre os dois processos durante o ciclo replicativo viral.

Durante infecções altamente patogênicas pelo vírus influenza (IAPVI) ocorre a produção excessiva de citocinas e quimiocinas inflamatórias, chamada de "cytokine storm". Este fato possui um papel importante na patogênese da infecção pelo vírus influenza e no desfecho clínico de pacientes infectados, já que o "cytokine storm" leva ao agravo da infecção. Seria interessante então se houvesse uma droga anti-influenza com propriedade anti-inflamatórias específicas. Como parte das propriedades antivirais da ribavirina é associada a sua capacidade imunomodulatória, também avaliamos se o composto **5b** é capaz de reduzir a produção de citocinas e quimiocinas pró-inflamatórias induzidas ou não pela infecção com o vírus influenza. Vimos que o nosso composto reduz a produção de IL-8 e CCl2 no sobrenadante de células A549 infectadas com o vírus influenza, além de reduzir TNF-α e IL-6 no sobrenadante de macrófagos estimulados com LPS. Estes resultados sugerem que o composto **5b** possuiu propriedades imunomodulatórias independentes da sua atividade antiviral.

Nosso próximo passo foi avaliar os efeitos antivirais do composto **5b** *in vivo*. Primeiramente, verificamos sua toxicidade em camundongos suíços e observamos que o tratamento oral com altas concentrações do composto **5b** (até 200 mg/kg) não levou a perda de peso, morte ou disfunção motora do animais, sugerindo ausência de toxicidade. A seguir, infectamos camundongos C57Bl/6 com 10^3 PFU do vírus influenza PR8 adaptado a camundongo e tratamos os animais diariamente com 10 mg/kg do composto **5b**. Nosso composto não preveniu a perda de peso dos animais, porém, 5 dias após a infeção, reduziu significativamente o processo inflamatório induzido pela infecção com o vírus influenza, visto pela redução no número total de leucócitos, células mono e polimorfonucleares e na quantidade total de proteínas presentes no lavado broncoalveolar (BAL) e o número total de leucócitos presentes no sangue periférico dos animais. Além disso, houve redução nos níveis das citocinas e quimiocinas pró-inflamatórias TNF-α, IFN-γ, IL-6, KC e CCl2 no BAL dos

animais infectados e tratados com o nosso composto. Ao avaliarmos os pulmões dos animais, observamos intenso infiltrado inflamatório decorrente da infecção pelo vírus influenza. Já as vias aéreas e o parênquima pulmonar dos camundongos infectados e tratados com o composto **5b** estavam semelhantes aos dos animais não infectados. Estes resultados indicam que a atividade antiviral e anti-inflamatória do composto **5b** foram preservadas em modelos *in vivo*.

Em conjunto, os dados demonstram que o composto **5b** possui uma estrutura química bastante promissora para o desenvolvimento de novos compostos anti-influenza.

4 DISCUSSÃO

As infecções causadas pelos vírus influenza são de grande importância para saúde pública, sobretudo em países em desenvolvimento (Who, 2014b). Todo ano ocorrem surtos epidêmicos durante os meses de inverno e, ocasionalmente, novas cepas potencialmente pandêmicas são geradas devido à grande variabilidade genética destes vírus. Embora campanhas de vacinação sejam realizadas anualmente na tentativa primária de controle das infecções causadas pelos vírus influenza, existem diversos casos nos quais a vacinação é ineficaz devido ao escape viral. As estratégias de vacinação custeadas pelos governos são focadas em grupos de pacientes com maior risco de desenvolver infecções mais severas, como crianças, idosos, mulheres grávidas e indivíduos imunossuprimidos. Assim uma porcentagem significativa de indivíduos permanece não imunizada e, portanto, susceptíveis a infecção pelo vírus influenza, podendo servir de hospedeiro de um eventual surto epidêmico. No caso de uma eventual pandemia, é provável que não exista tempo hábil para produção de vacina. Além disso, como o tratamento com antivirais se torna mais efetivo quando administrado nos primeiros dias de infecção, sua estocagem é necessária como estratégia adicional de controle para contornar as lacunas do sistema de vacinação e seu uso pode servir como uma defesa de primeira linha contra novos vírus.

Considerando que atualmente há apenas uma classe de drogas anti-influenza em uso clínico, os NAIs, e levando-se em conta que cepas resistentes e com diminuição de sensibilidade a estes compostos existem (Samson *et al.*, 2013), a busca de novas drogas com diferentes alvos e capazes de inibir estas cepas é de interesse científico e clínico. Neste contexto, esta tese descreve os efeitos anti-influenza e os mecanismos de ação de diferentes compostos naturais e sintéticos.

Produtos naturais são uma fonte rica de compostos quimicamente ativos e nosso grupo vem estudando a atividade antiviral dessas moléculas (Souza *et al.*, 2007; Cirne-Santos *et al.*, 2008; Abrantes *et al.*, 2010). Muitos dos produtos naturais estudados são isolados de bactérias e fungos (Dang e Süssmuth, 2017; Huang *et al.*, 2017), tornando esses microrganismos fundamentais como fontes de novos medicamentos com ênfase em agentes anti-infecciosos. Nesta tese, demos uma atenção especial à atividade antiviral de um produto natural, o aureonitol, derivado de fungo e produzido por de diferentes espécies do gênero *Chaetomium* com mais de 70% de rendimento (Rodríguez *et al.*, 2002). Curiosamente, fungos membros do gênero *Chaetomium* têm sido isolados de plantas medicinais tradicionais da China e da Índia e reconhecidos como organismos que produzem diversos compostos bioativos (Gutiérrez *et al.*,

2008; Wang *et al.*, 2012). Além da produção natural, a síntese orgânica do aureonitol também provou ser bem sucedida (Jervis e Cox, 2008). Essas características indicam a viabilidade de ampliar a produção de aureonitol, demonstrando uma vantagem em comparação a outros produtos naturais.

Durante nosso trabalho, observamos que o aureonitol possui um mecanismo de ação distinto dos NAIs. Os NAIs bloqueiam a liberação e o espalhamento dos vírus influenza inibindo a NA viral, enquanto o aureonitol atua na HA, bloqueando as etapas iniciais do ciclo replicativo. Moléculas capazes de inibir etapas iniciais do ciclo replicativo viral são de interesse de pesquisadores e diversos grupos vêm estudando possíveis inibidores da HA do vírus influenza. A HA possuiu algumas regiões passíveis de bloqueio por novas drogas, como o sítio de ligação ao AS, os sítios de glicosilação, regiões antigênicas alvos de anticorpos neutralizantes, e o peptídeo de fusão. Como mencionado anteriormente, existem dois novos compostos em fase mais avançada de desenvolvimento, o arbidol e a flufirvitida-3. O arbidol possui um anel indol com substituições em quase todas as posições e parece atuar durante a fusão do envelope viral com a membrana da célula infectada (Moss *et al.*, 2012). Embora não aprovado em países ocidentais, é licenciado para utilização clínica como profilaxia e tratamento de influenza na Rússia e na China (Leneva *et al.*, 2009; Liu *et al.*, 2009; Brooks *et al.*, 2012). A flufirvitida-3 está em sendo utilizada nos Estados Unidos e no Reino Unido em estudos clínicos de fase 1 e 2 (Badani, 2014). Esta molécula parece interagir com a membrana celular e/ou envelope viral dentro do endossoma, após a endocitose do vírus e do próprio peptídeo (Badani, 2014).

Embora já tenham sido descritas cepas do vírus influenza circulantes resistentes aos NAIs devido a mutações presentes na NA viral e os *drifts* genéticos ocorram também nessa enzima, a NA continua sendo o principal alvo para o desenvolvimento de antivirais devido à sua importante função durante o ciclo replicativo viral e ao fato do sitio ativo desta enzima ser composto por aminoácidos conservados entre todos os subtipos de NA já descritos na natureza (Shtyrya *et al.*, 2009; Jagadesh *et al.*, 2016). A NA viral é classicamente caracterizada como uma enzima que auxilia a liberação das novas partículas virais formadas. Estudos recentes têm sugerido que a NA também possuiu uma função no início do ciclo replicativo, auxiliando na adsorção e entrada dos vírus na célula hospedeira. A NA parece influenciar na transferência das partículas virais para sítios de endocitose ativa da membrana celular, facilitando a entrada do vírus na célula (Ohuchi *et al.*, 2006). Além disso, a expressão da NA parece ter um impacto direto na fusão viral dependente da HA e na eficiência de infecção, já que a substituição da NA no genoma viral afetou significativamente o início da infecção, a fusão e a liberação dos novos vírus influenza da célula hospedeira (Su

et al., 2009; Chen *et al.*, 2013). Essas características poderiam ser aproveitadas para o desenvolvimento de NAIs como inibidores de entrada e também para reforçar o uso dos NAIs já licenciados como profilaxia para as infecções causadas pelos vírus influenza (Yang *et al.*, 2016).

Considerando a função clássica da NA viral de liberação das novas partículas virais formadas durante o ciclo replicativo, esse trabalho descreve os efeitos e mecanismo de ação de dois compostos, o **1i** e o tritempo. Os dois compostos apresentam grupos farmacofóricos semelhantes, o anel triazózilo em ambos, o radical ciclohexenil no composto **1i** e o radical piperidina-1-oxil no tritempo. Ambos se mostraram capazes de inibir a atividade enzimática da NA de cepas do vírus influenza resistentes ao OST e se ligaram ao sítio ativo da enzima. Os sítios de ligação do composto **1i** e o OST se sobrepõem parcialmente e os dois compostos utilizam aminoácidos extremamente conservados durante a ligação, o que sugere que mutações nestes resíduos poderiam reduzir o fitness viral, tornando difícil o surgimento de cepas virais resistentes ao composto **1i**. É curioso notar que, da mesma maneira, o tritempo interage com aminoácidos conversados do sítio ativo da NA, porém, após passagens sequenciais do vírus na presença de concentrações crescentes do composto, foi possível gerar um cepa do vírus influenza com uma mutação de resistência ao tritempo. O aminoácido mutado, uma glicina na posição 248, está localizado próximo ao sítio ativo da enzima e não é utilizado para a ligação do tritempo nem do OST à NA viral. Esse fato pode justificar o porquê essa mutação não reduziu o fitness viral e essa cepa permaneceu sensível ao composto de referência OST, o que indica ausência de resistência cruzada entre os compostos. Essa característica é interessante pois a maioria dos NAIs utilizados clinicamente possuem resistência cruzada, o que impede seu uso para o tratamento de infecções causadas por vírus resistentes ao OST (Nitsch-Osuch e Brydak, 2014; Takashita *et al.*, 2015).

Na busca por novas moléculas com atuação em alvos alternativos durante o ciclo replicativo do vírus influenza, a RNA polimease viral surge com um alvo promissor. A RNA polimerase do vírus influenza possui múltiplas funções essenciais para duplicação e transcrição do genoma viral (Boivin *et al.*, 2010b), além de ser altamente conservada entre todos os subtipos do vírus influenza presente na natureza (Wu *et al.*, 2017). Por não possuir atividade de correção durante a replicação do genoma viral, a RNA polimerase também se torna crucial para a evolução do vírus influenza já que é responsável pelos *drifts* genéticos que podem levar ao escape vacinal, resistência antiviral e melhor adaptação do vírus a novas espécies de hospedeiros (Boivin *et al.*, 2010b). Recentemente, diversos grupos vêm buscando moléculas capazes de inibir o complexo polimerase. Como exemplo temos moléculas que inibem a subunidade PA e sua atividade endonuclease (Dubois *et al.*, 2012; Yamada *et al.*,

2012); moléculas que inibem a interação entre as subunidades da polimerase, como a ligação PA-PB1 (Muratore *et al.*, 2012); e moléculas que, além de inibirem essa enzima, induzem indiretamente citocinas ligadas à resposta antiviral como o IFN (Ortigoza *et al.*, 2012). Entre estes compostos, o que se mostrou mais promissor foi o favipiravir (T-705), inibindo a replicação *in vitro* e *in vivo* dos vírus influenza A, B e C cujo alvo é diretamente na RNA polimerase viral (Furuta *et al.*, 2005). Este composto teve estudos clínicos de fase II (Estados Unidos) e fase III (Japão) sobre eficácia e segurança contra infecção não complicada por influenza em adultos concluídos recentemente, (dados não publicados – www.clinicaltrials.gov) e seu licenciamento para uso contra influenza é esperado para um futuro próximo.

O composto **5b** descrito nessa tese é extremamente interessante já que possui como alvo a RNA polimerase viral. Desta maneira, o composto **5b** atua em uma etapa diferente do ciclo replicativo, desregulando o balanço entre duplicação e transcrição do genoma viral. Observamos uma redução na transcrição viral pelo composto **5b** e acreditamos que, como a transcrição foi bloqueada, o genoma viral foi preferencialmente usado por outros processos, como a síntese de RNA viral genômico e antigenômico.

Na infecção pelo vírus influenza, as principais citocinas envolvidas com a resposta imunológica inata são os IFN tipo I. Estes estimulam as células epiteliais infectadas a produzirem citocinas como IL-6, IL-1 e TNF-α, e quimiocinas IL-8, CCL2 e CCL5 (Adachi *et al.*, 1997). Essas citocinas levam a uma resposta tecidual pró-inflamatória que favorecem a resposta Th1, necessária para a imunidade antiviral específica. Além disso, a resposta de células T $CD8^+$ possui papel crucial *clearance* viral. Embora as respostas Th1 e citotóxica sejam essenciais para a eliminação da infecção viral, a grande liberação de citocinas pró-inflamatórias e moléculas citotóxicas resulta em dano no tecido pulmonar e agravo da infecção (Bermejo-Martin *et al.*, 2009; Ramana *et al.*, 2009). O *cytokine storm* foi descrito pela primeira vez em infecções pelo vírus altamente patogênico H5N1(Yuen e Wong, 2005). Infecções altamente patogênicas podem ser causadas por outros tipos de vírus influenza além do H5N1, e também estão relacionadas ao *cytokine storm*. Injúria pulmonar aguda e sua forma severa, síndrome da insuficiência respiratória aguda, podem ocorrer durante infecções altamente patogênicas causadas pelos vírus influenza como consequência do *cytokine storm* e da intensa resposta inflamatória causada por células mononucleares e neutrófilos no ambiente pulmonar (Tisoncik *et al.*, 2012). Desta maneira, a redução no recrutamento de células inflamatórias para o sítio de infecção e a regulação na secreção de citocinas pró- e anti-inflamatória é crucial para manter a homeostase desse ambiente. Um mecanismo para diminuir a inflamação pulmonar é regular a ativação dos macrófagos pulmonares e estimular a

produção de citocinas reguladoras, principalmente IL-10, pelas células Th2 e T reguladoras e células B (Snelgrove *et al.*, 2008). Nestes casos, drogas imunomodulatórias deveriam apresentar benefícios terapêuticos. A terapia imunomodulatória com corticoides adjuvantes à terapia antiviral é utilizada, porém, os efeitos causados pelo tratamento com estas moléculas são controversos com relação à melhora do paciente, período de excreção e carga viral (Souza *et al.*, 2010; Brun-Buisson *et al.*, 2011). Seria interessante então, se uma droga anti-influenza também possuísse propriedades anti-inflamatórias específicas.

Além de antiviral, o composto **5b** se mostrou um potente imunomodulador *in vitro* e *in vivo*. *In vitro*, foi capaz de reduzir a secreção de citocinas e quimiocinas pró-inflamatórias IL-6, TNF-α, IL-8 e CCL2, induzidas ou não pela infecção pelo vírus influenza. No modelo *in vivo* utilizado, camundongos infectados com o vírus influenza e tratados diariamente com nosso composto, é interessante notar que o composto **5b** reduziu o processo inflamatório causado pelo vírus influenza, observado através da diminuição do número de células (leucócitos totais e células mono e polimorfonucleares), citocinas (TNF-α, IFN-γ e IL-6) e quimiocinas (KC e CCl2) pró-inflamatórias no BAL desses animais. Além disso, observamos também uma diminuição significativa do infiltrado inflamatório nos pulmões de camundongos infectados e tratados com o nosso composto. As vias aéreas e o parênquima pulmonar desses animais é bastante semelhante aos dos animais utilizados como controle e não infectados pelo vírus influenza. Estes dados são de grande importância uma vez que se espera que a imunomodulação controle a gravidade das complicações inflamatórias induzidas pelo vírus influenza durante a infecção.

Além do estudo de diferentes moléculas com propriedades antivirais, verificamos neste trabalho que a RNA polimerase do vírus influenza possui atividade natural endógena dentro do vírion (chamada de NERP – do inglês *natural endogenous RNA polymerase activity*). Sabe-se que a pré-existência de uma polimerase funcional dentro da partícula viral de vírus com genoma de RNA é necessária para o início da replicação e transcrição, já que o RNA viral de polaridade negativa não pode ser diretamente traduzido para proteína (Boivin *et al.*, 2010b). Por exemplo, o vírus HIV carrega sua própria transcriptase reversa e sua atividade pode ser ativada dentro da partícula viral com a adição do substrato e co-fator da enzima (deoxinucleotídeos e Mg^{++}, respectivamente) (Aguiar *et al.*, 2007). Vimos que o mesmo acontece com o vírus influenza: ao adicionarmos nucleotídeos trifosfatados e Mg^{++} à amostras virais livres de células, ocorre um aumento nos níveis de RNA dentro da partícula viral. A atividade NERP pode ter diferentes aplicações, como melhorar a sensibilidade do diagnóstico do vírus influenza e ser utilizada como uma ferramenta para triagem de novas drogas com

alvo na RNA polimerase viral. Ambas as aplicações foram avaliadas de forma bem sucedidas durante esse trabalho.

Devido à importância clínica e epidemiológica dos vírus influenza e do fato das viroses respiratórias causarem sintomas clínicos muito parecidos, crítico o diagnóstico não equivocado desses vírus. Desta maneira, ferramentas complementares que possam aumentar a sensibilidade do diagnóstico são de grande ajuda para uma vigilância epidemiológica mais precisa do vírus influenza. Vimos que ao estimular amostras clínicas aparentemente negativas para o vírus influenza com NTPs e Mg^{++}, ocorre o aumento da atividade NERP dos vírions ali presentes. Consequentemente, aumenta os níveis de RNA viral permitindo a detecção dos vírus influenza em amostras clínicas previamente indetectáveis. Com o aumento da carga viral, a atividade NERP também aumentou nossa capacidade de sequenciar algumas regiões do genoma viral previamente não-sequenciáveis nas amostras clínicas. Esses fatos demonstram que essa técnica pode ser útil para aumentar a sensibilidade do diagnóstico laboratorial do vírus influenza.

Além disso, testamos a atividade NERP na presença da ribavirina, antiviral inibidor de DNA e RNA polimerases virais. Ao adicionarmos a ribavirina, a atividade NERP foi inibida, confirmando a hipótese de que este ensaio poderia ser utilizado como ferramenta na triagem de novas drogas antivirais contra a RNA polimerase do vírus influenza. Assim, utilizamos essa técnica para investigar a atividade anti-influenza do composto **5b** e confirmamos a habilidade do composto em inibir a RNA polimerase viral.

5 CONCLUSÕES

Sabemos que o vírus influenza A infecta milhares de pessoas anualmente, especialmente durante períodos de epidemia, promovendo, desta forma, expressivo impacto no sistema de saúde, principalmente, em países em desenvolvimento, como é o caso do Brasil. Como discutido anteriormente, existem falhas no sistema atual de vacinação e, devido a variabilidade genética do vírus, ocorre o escape vacinal e a resistência aos tratamentos antivirais disponíveis atualmente. Logo, entender a biologia deste vírus e buscar novos alvos de inibição e compostos que possam ser utilizados como protótipos para novos tratamentos não é apenas um desafio, mas uma necessidade em saúde pública. Assim, a presente tese desenvolveu estudos relacionados a este vírus e a busca por novas moléculas.

Através do uso de técnicas de biologia celular, molecular e computacional, farmacologia, imunologia e experimentação animal; e do estudo de conceitos multidisciplinares como química medicinal, relação estrutura-função de novas moléculas, biologia do vírus influenza e fisiopatologia da infecção viral, visamos construir uma plataforma pré-clínica para desenvolvimento de novos antivirais. Essas abordagens e as colaborações iniciadas nesse trabalho seguem permitindo ao nosso grupo estudar não só o vírus influenza e novas drogas anti-influenza, mas também outros alvos e moléculas promissoras contra o vírus HIV, Zika vírus (Sacramento *et al.*, 2017), Chikungunya e o vírus da dengue.

Desta forma, essa tese contribui com aspectos aplicados no escopo da virologia humana, da patogênese de doenças infecciosas, de mecanismos da imunidade inata e da química medicinal.

6 OUTRAS PRODUÇÕES DURANTE O DOUTORADO

6.1 The clinically approved antiviral drug sofosbuvir inhibits Zika virus replication.

Autores: Carolina Q. Sacramento[*], Gabrielle R. de Melo[*], Natasha Rocha[*], Lucas Villas Bôas Hoelz, Milene Mesquita, Caroline S. de Freitas, Natalia Fintelman- Rodrigues, Andressa Marttorelli, André C. Ferreira, Giselle Barbosa-Lima, Mônica M. Bastos, Eduardo de Mello Volotão, Diogo A. Tschoeke, Luciana Leomil, Fernando A. Bozza, Patrícia T. Bozza, Nubia Boechat, Fabiano L. Thompson, Ana M. B. de Filippis, Karin Brüning e Thiago Moreno L. Souza

[*] Estes autores contribuíram igualmente para esse trabalho.

Periódico: *Scientific Reports* | DOI: 10.1038/srep40920 – Janeiro de 2017 (Sacramento *et al*., 2017)

6.2 Sofosbuvir protects Zika virus-infected mice from mortality, preventing short- and long-term sequelae.

Autores: André C. Ferreira[*], Camila Zaverucha-do-Valle[*], Patrícia A. Reis[*], Giselle Barbosa-Lima, Yasmine Rangel Vieira, Mayara Mattos, Priscila de Paiva Silva, Carolina Sacramento, Hugo C. de Castro Faria Neto, Loraine Campanati, Amilcar Tanuri, Karin Brüning, Fernando A. Bozza, Patrícia T. Bozza & Thiago Moreno L. Souza

[*] Estes autores contribuíram igualmente para esse trabalho.

Periódico: *Scientific Reports* | DOI: 10.1038/s41598-017-09797-8 – Agosto de 2017 (Ferreira *et al.*, 2017)

7 REFERÊNCIAS BIBLIOGRÁFICAS

ABRANTES, J. L. et al. The effects of the diterpenes isolated from the Brazilian brown algae Dictyota pfaffii and Dictyota menstrualis against the herpes simplex type-1 replicative cycle. **Planta Med,** v. 76, n. 4, p. 339-44, Mar 2010. ISSN 1439-0221. Disponível em: < http://www.ncbi.nlm.nih.gov/pubmed/19764012 >.

ADACHI, M. et al. Expression of cytokines on human bronchial epithelial cells induced by influenza virus A. **Int Arch Allergy Immunol,** v. 113, n. 1-3, p. 307-11, May-Jul 1997. ISSN 1018-2438 (Print)
1018-2438 (Linking). Disponível em: < http://www.ncbi.nlm.nih.gov/entrez/query.fcgi?cmd=Retrieve&db=PubMed&dopt=Citation&list_uids=9130560 >.

AGUIAR, R. S. et al. Development of a new methodology for screening of human immunodeficiency virus type 1 microbicides based on real-time PCR quantification. **Antimicrob Agents Chemother,** v. 51, n. 2, p. 638-44, Feb 2007. ISSN 0066-4804. Disponível em: < http://www.ncbi.nlm.nih.gov/pubmed/17116672 >.

AIR, G. M. Influenza neuraminidase. **Influenza Other Respir Viruses,** v. 6, n. 4, p. 245-56, Jul 2012. ISSN 1750-2659. Disponível em: < http://www.ncbi.nlm.nih.gov/pubmed/22085243 >.

BADANI, H. **Understanding The Mechanism Of Action Of Flufirvitide-3 A Peptide Based Inhibitor Of Influenza Virus.** 2014. 182 (PhD). Department of Biomedical Sciences, Tulane University, Tulane University Theses and Dissertations Archive.

BARANOVICH, T. et al. Emergence of H274Y oseltamivir-resistant A(H1N1) influenza viruses in Japan during the 2008-2009 season. **J Clin Virol,** v. 47, n. 1, p. 23-8, Jan 2010. ISSN 1873-5967 (Electronic)
1386-6532 (Linking). Disponível em: < http://www.ncbi.nlm.nih.gov/entrez/query.fcgi?cmd=Retrieve&db=PubMed&dopt=Citation&list_uids=19962344 >.

BEIGEL, J. H. et al. Avian influenza A (H5N1) infection in humans. **N Engl J Med,** v. 353, n. 13, p. 1374-85, Sep 2005. ISSN 1533-4406. Disponível em: < http://www.ncbi.nlm.nih.gov/pubmed/16192482 >.

BELSHE, R. B. Implications of the emergence of a novel H1 influenza virus. **N Engl J Med,** v. 360, n. 25, p. 2667-8, Jun 2009. ISSN 1533-4406. Disponível em: < http://www.ncbi.nlm.nih.gov/pubmed/19423870 >.

BERMEJO-MARTIN, J. F. et al. Th1 and Th17 hypercytokinemia as early host response signature in severe pandemic influenza. **Crit Care,** v. 13, n. 6, p. R201, 2009. ISSN 1466-609X (Electronic)
1364-8535 (Linking). Disponível em: < http://www.ncbi.nlm.nih.gov/entrez/query.fcgi?cmd=Retrieve&db=PubMed&dopt=Citation&list_uids=20003352 >.

BLACHERE, F. M. et al. Bioaerosol sampling for the detection of aerosolized influenza virus. **Influenza Other Respi Viruses,** v. 1, n. 3, p. 113-20, May 2007. ISSN 1750-2659 (Electronic) 1750-2640 (Linking). Disponível em: < http://www.ncbi.nlm.nih.gov/entrez/query.fcgi?cmd=Retrieve&db=PubMed&dopt=Citation&list_uids=19453416 >.

BODENHEIMER, H. C., JR. et al. Tolerance and efficacy of oral ribavirin treatment of chronic hepatitis C: a multicenter trial. **Hepatology,** v. 26, n. 2, p. 473-7, Aug 1997. ISSN 0270-9139 (Print)
0270-9139 (Linking). Disponível em: < http://www.ncbi.nlm.nih.gov/entrez/query.fcgi?cmd=Retrieve&db=PubMed&dopt=Citation&list_uids=9252161 >.

BOECHAT, F. A. C. et al. 1,2,3-Triazolyl-4-oxoquinolines: A feasible beginning for promising chemical structures to inhibit oseltamivir-resistant influenza A and B viruses. **Bioorg Med Chem,** v. 23, n. 24, p. 7777-84, Dec 2015. ISSN 1464-3391. Disponível em: < http://www.ncbi.nlm.nih.gov/pubmed/26643220 >.

BOIVIN, S. et al. Influenza A virus polymerase: structural insights into replication and host adaptation mechanisms. **J Biol Chem,** v. 285, n. 37, p. 28411-7, Sep 10 2010a. ISSN 1083-351X (Electronic)
0021-9258 (Linking). Disponível em: < http://www.ncbi.nlm.nih.gov/entrez/query.fcgi?cmd=Retrieve&db=PubMed&dopt=Citation&list_uids=20538599 >.

_____. Influenza A Virus Polymerase: Structural Insights into Replication and Host Adaptation Mechanisms. **J Biol Chem,** v. 285, n. 37, p. 28411–28417, 2010b.

BROOKS, M. J. et al. Antiviral activity of arbidol, a broad-spectrum drug for use against respiratory viruses, varies according to test conditions. **J Med Virol,** v. 84, n. 1, p. 170-81, Jan 2012. ISSN 1096-9071 (Electronic) 0146-6615 (Linking). Disponível em: < http://www.ncbi.nlm.nih.gov/entrez/query.fcgi?cmd=Retrieve&db=PubMed&dopt=Citation&list_uids=22028179 >.

BRUN-BUISSON, C. et al. Early Corticosteroids in Severe Influenza A/H1N1 Pneumonia and Acute Respiratory Distress Syndrome. **J Respir Crit Care Med,** v. 183, p. 1200–1206, 2011.

BUXTON, R. C. et al. Development of a sensitive chemiluminescent neuraminidase assay for the determination of influenza virus susceptibility to zanamivir. **Anal Biochem,** v. 280, n. 2, p. 291-300, May 1 2000. ISSN 0003-2697 (Print)
0003-2697 (Linking). Disponível em: < http://www.ncbi.nlm.nih.gov/entrez/query.fcgi?cmd=Retrieve&db=PubMed&dopt=Citation&list_uids=10790313 >.

CARDONA, C. J. et al. Avian influenza in birds and mammals. **Comp Immunol Microbiol Infect Dis,** v. 32, n. 4, p. 255-73, Jul 2009. ISSN 1878-1667. Disponível em: < http://www.ncbi.nlm.nih.gov/pubmed/18485480 >.

CARRAT, F.; FLAHAULT, A. Influenza vaccine: the challenge of antigenic drift. **Vaccine,** v. 25, n. 39-40, p. 6852-62, Sep 2007. ISSN 0264-410X. Disponível em: < http://www.ncbi.nlm.nih.gov/pubmed/17719149 >.

CASPER, C.; ENGLUND, J.; BOECKH, M. How I treat influenza in patients with hematologic malignancies. **Blood,** v. 115, n. 7, p. 1331-42, Feb 2010. ISSN 1528-0020. Disponível em: < https://www.ncbi.nlm.nih.gov/pubmed/20009037 >.

CDC. The 2009 H1N1 Pandemic: Summary Highlights, April 2009-April 2010., 2010. Disponível em: < http://www.cdc.gov/h1n1flu/cdcresponse.htm >.

CDC. Antiviral Drug Resistance among Influenza Viruses. 2015a. Disponível em: < http://www.cdc.gov/flu/professionals/antivirals/antiviral-drug-resistance.htm >. Acesso em: July 06.

CDC. Influenza Antiviral Drug Resistance. 2015b. Disponível em: < http://www.cdc.gov/flu/about/qa/antiviralresistance.htm >. Acesso em: July 06.

CDC. Influenza Antiviral Medications: Summary for Clinicians. 2016. Disponível em: < http://www.cdc.gov/flu/professionals/antivirals/summary-clinicians.htm >. Acesso em: 06 de julho.

CENTERS FOR DISEASE CONTROL AND PREVENTION, C. **Antiviral Agents for the Treatment and Chemoprophylaxis of Influenza. Recommendations of the Advisory Committee on Immunization Practices (ACIP)** 2011

CHEN, Q. et al. NA proteins of influenza A viruses H1N1/2009, H5N1, and H9N2 show differential effects on infection initiation, virus release, and cell-cell fusion. **PLoS One,** v. 8, n. 1, p. e54334, 2013. ISSN 1932-6203. Disponível em: < https://www.ncbi.nlm.nih.gov/pubmed/23349854 >.

CHO, H. G. et al. Oseltamivir-resistant influenza viruses isolated in South Korea from 2005 to 2010. **Arch Virol**, May 21 2013. ISSN 1432-8798 (Electronic)
0304-8608 (Linking). Disponível em: < http://www.ncbi.nlm.nih.gov/entrez/query.fcgi?cmd=Retrieve&db=PubMed&dopt=Citation&list_uids=23690054 >.

CIRNE-SANTOS, C. C. et al. The dolabellane diterpene Dolabelladienetriol is a typical noncompetitive inhibitor of HIV-1 reverse transcriptase enzyme. **Antiviral Res,** v. 77, n. 1, p. 64-71, Jan 2008. ISSN 0166-3542. Disponível em: < https://www.ncbi.nlm.nih.gov/pubmed/17888523 >.

COLLINS, P. J. et al. Crystal structures of oseltamivir-resistant influenza virus neuraminidase mutants. **Nature,** v. 453, n. 7199, p. 1258-61, Jun 2008. ISSN 1476-4687. Disponível em: < http://www.ncbi.nlm.nih.gov/pubmed/18480754 >.

COUCH, R. B. et al. Influenza: its control in persons and populations. **J Infect Dis,** v. 153, n. 3, p. 431-40, Mar 1986. ISSN 0022-1899 (Print)
0022-1899 (Linking). Disponível em: < http://www.ncbi.nlm.nih.gov/entrez/query.fcgi?cmd=Retrieve&db=PubMed&dopt=Citation&list_uids=3950437 >.

CROTTY, S.; CAMERON, C.; ANDINO, R. Ribavirin's antiviral mechanism of action: lethal mutagenesis? **J Mol Med (Berl),** v. 80, n. 2, p. 86-95, Feb 2002. ISSN 0946-2716 (Print)

0946-2716 (Linking). Disponível em: < http://www.ncbi.nlm.nih.gov/entrez/query.fcgi?cmd=Retrieve&db=PubMed&dopt=Citation&list_uids=11907645 >.

CROTTY, S.; CAMERON, C. E.; ANDINO, R. RNA virus error catastrophe: direct molecular test by using ribavirin. **Proc Natl Acad Sci U S A,** v. 98, n. 12, p. 6895-900, Jun 5 2001. ISSN 0027-8424 (Print)
0027-8424 (Linking). Disponível em: < http://www.ncbi.nlm.nih.gov/entrez/query.fcgi?cmd=Retrieve&db=PubMed&dopt=Citation&list_uids=11371613 >.

CROTTY, S. et al. The broad-spectrum antiviral ribonucleoside ribavirin is an RNA virus mutagen. **Nat Med,** v. 6, n. 12, p. 1375-9, Dec 2000. ISSN 1078-8956 (Print)
1078-8956 (Linking). Disponível em: < http://www.ncbi.nlm.nih.gov/entrez/query.fcgi?cmd=Retrieve&db=PubMed&dopt=Citation&list_uids=11100123 >.

DANG, T.; SÜSSMUTH, R. D. Bioactive Peptide Natural Products as Lead Structures for Medicinal Use. **Acc Chem Res**, Jun 2017. ISSN 1520-4898. Disponível em: < https://www.ncbi.nlm.nih.gov/pubmed/28650175 >.

DAS, K. et al. Structures of influenza A proteins and insights into antiviral drug targets. **Nat Struct Mol Biol,** v. 17, n. 5, p. 530-8, May 2010. ISSN 1545-9985 (Electronic)
1545-9985 (Linking). Disponível em: < http://www.ncbi.nlm.nih.gov/entrez/query.fcgi?cmd=Retrieve&db=PubMed&dopt=Citation&list_uids=20383144 >.

DE CLERCQ, E. Antiviral agents active against influenza A viruses. **Nat Rev Drug Discov,** v. 5, n. 12, p. 1015-25, Dec 2006. ISSN 1474-1776 (Print)
1474-1776 (Linking). Disponível em: < http://www.ncbi.nlm.nih.gov/entrez/query.fcgi?cmd=Retrieve&db=PubMed&dopt=Citation&list_uids=17139286 >.

DE FÁTIMA, A. et al. Ácidos Siálicos. Da compreensão do seu envolvimento em processos biológicos ao desenvolvimento de fármacos contra o agente etiológico da gripe. **Química Nova,** v. 28, n. 2, p. 306-316, 2005. Disponível em: < http://www.scielo.br/pdf/qn/v28n2/23654.pdf >.

DEYDE, V. M. et al. Pyrosequencing as a tool to detect molecular markers of resistance to neuraminidase inhibitors in seasonal influenza A viruses. **Antiviral Res,** v. 81, n. 1, p. 16-24, Jan 2009. ISSN 1872-9096 (Electronic)
0166-3542 (Linking). Disponível em: < http://www.ncbi.nlm.nih.gov/entrez/query.fcgi?cmd=Retrieve&db=PubMed&dopt=Citation&list_uids=18835410 >.

DEYDE, V. M.. Detection of molecular markers of drug resistance in 2009 pandemic influenza A (H1N1) viruses by pyrosequencing. **Antimicrob Agents Chemother,** v. 54, n. 3, p. 1102-10, Mar 2010. ISSN 1098-6596 (Electronic)
0066-4804 (Linking). Disponível em: < http://www.ncbi.nlm.nih.gov/entrez/query.fcgi?cmd=Retrieve&db=PubMed&dopt=Citation&list_uids=20028826 >.

DIAS, A. et al. The cap-snatching endonuclease of influenza virus polymerase resides in the PA subunit. **Nature,** v. 458, n. 7240, p. 914-8, Apr 16 2009. ISSN 1476-4687 (Electronic) 0028-0836 (Linking). Disponível em: < http://www.ncbi.nlm.nih.gov/entrez/query.fcgi?cmd=Retrieve&db=PubMed&dopt=Citation&list_uids=19194459 >.

DUBOIS, R. M. et al. Structural and biochemical basis for development of influenza virus inhibitors targeting the PA endonuclease. **PLoS Pathog,** v. 8, n. 8, p. e1002830, 2012. ISSN 1553-7374 (Electronic) 1553-7366 (Linking). Disponível em: < http://www.ncbi.nlm.nih.gov/entrez/query.fcgi?cmd=Retrieve&db=PubMed&dopt=Citation&list_uids=22876176 >.

EDINGER, T. O.; POHL, M. O.; STERTZ, S. Entry of influenza A virus: host factors and antiviral targets. **J Gen Virol,** v. 95, n. Pt 2, p. 263-77, Feb 2014. ISSN 1465-2099. Disponível em: < http://www.ncbi.nlm.nih.gov/pubmed/24225499 >.

FAUQUET, C. M.; FARGETTE, D. International Committee on Taxonomy of Viruses and the 3,142 unassigned species. **Virol J,** v. 2, p. 64, 2005. ISSN 1743-422X (Electronic) 1743-422X (Linking). Disponível em: < http://www.ncbi.nlm.nih.gov/entrez/query.fcgi?cmd=Retrieve&db=PubMed&dopt=Citation&list_uids=16105179 >.

FDA. Food and Drug administration. 2013. Disponível em: < http://www.fda.gov/ForConsumers/byAudience/ForPatientAdvocates/HIVandAIDSActivities/ucm118915.htm >.

FELD, J. J.; HOOFNAGLE, J. H. Mechanism of action of interferon and ribavirin in treatment of hepatitis C. **Nature,** v. 436, n. 18, p. 967-972, 2005.

FERREIRA, A. C. et al. Sofosbuvir protects Zika virus-infected mice from mortality, preventing short- and long-term sequelae. **Sci Rep,** v. 7, n. 1, p. 9409, Aug 2017. ISSN 2045-2322. Disponível em: < https://www.ncbi.nlm.nih.gov/pubmed/28842610 >.

FLEMING, D. M. Managing influenza: amantadine, rimantadine and beyond. **Int J Clin Pract,** v. 55, n. 3, p. 189-95, Apr 2001. ISSN 1368-5031 (Print) 1368-5031 (Linking). Disponível em: < http://www.ncbi.nlm.nih.gov/entrez/query.fcgi?cmd=Retrieve&db=PubMed&dopt=Citation&list_uids=11351773 >.

FLU.GOV. Pandemic Flu History. 2011. Disponível em: < http://www.flu.gov/pandemic/history/ >. Acesso em: 19 de maio.

FODOR, E. The RNA polymerase of influenza A virus: mechanisms of viral transcription and replication. **Acta Virol,** v. 57, n. 2, p. 113-22, 2013. ISSN 0001-723X (Print) 0001-723X (Linking). Disponível em: < http://www.ncbi.nlm.nih.gov/entrez/query.fcgi?cmd=Retrieve&db=PubMed&dopt=Citation&list_uids=23600869 >.

FRY, A. M.; GUBAREVA, L. V. Understanding influenza virus resistance to antiviral agents; early warning signs for wider community circulation. **J Infect Dis,** v. 206, n. 2, p. 145-7, Jul 15 2012. ISSN 1537-6613 (Electronic) 0022-1899 (Linking). Disponível em: <

http://www.ncbi.nlm.nih.gov/entrez/query.fcgi?cmd=Retrieve&db=PubMed&dopt=Citation&list_uids=22561368 >.

FURUTA, Y. et al. Mechanism of action of T-705 against influenza virus. **Antimicrob Agents Chemother,** v. 49, n. 3, p. 981-6, Mar 2005. ISSN 0066-4804 (Print)
0066-4804 (Linking). Disponível em: < http://www.ncbi.nlm.nih.gov/entrez/query.fcgi?cmd=Retrieve&db=PubMed&dopt=Citation&list_uids=15728892 >.

GAO, R. et al. Human infection with a novel avian-origin influenza A (H7N9) virus. **N Engl J Med,** v. 368, n. 20, p. 1888-97, May 2013. ISSN 1533-4406. Disponível em: < http://www.ncbi.nlm.nih.gov/pubmed/23577628 >.

GOLDSMITH, C. S.; A., B. **Negative stained transmission electron micrograph of A/CA/4/09 swine flu virus.** CDC website**:** This colorized negative stained transmission electron micrograph (TEM) depicted some of the ultrastructural morphology of the A/CA/4/09 swine flu virus. p. 2009.

GOMEZ-PUERTAS, P. et al. Influenza virus matrix protein is the major driving force in virus budding. **J Virol,** v. 74, n. 24, p. 11538-47, Dec 2000. ISSN 0022-538X (Print)
0022-538X (Linking). Disponível em: < http://www.ncbi.nlm.nih.gov/entrez/query.fcgi?cmd=Retrieve&db=PubMed&dopt=Citation&list_uids=11090151 >.

GUTIÉRREZ, R. M.; MITCHELL, S.; SOLIS, R. V. Psidium guajava: a review of its traditional uses, phytochemistry and pharmacology. **J Ethnopharmacol,** v. 117, n. 1, p. 1-27, Apr 2008. ISSN 0378-8741. Disponível em: < http://www.ncbi.nlm.nih.gov/pubmed/18353572 >.

HA, J. W.; SCHWAHN, A. B.; DOWNARD, K. M. Proteotyping to establish gene origin within reassortant influenza viruses. **PLoS One,** v. 6, n. 1, p. e15771, 2011. ISSN 1932-6203 (Electronic)
1932-6203 (Linking). Disponível em: < http://www.ncbi.nlm.nih.gov/entrez/query.fcgi?cmd=Retrieve&db=PubMed&dopt=Citation&list_uids=21305059 >.

HALE, B. G. et al. The multifunctional NS1 protein of influenza A viruses. **J Gen Virol,** v. 89, n. Pt 10, p. 2359-76, Oct 2008. ISSN 0022-1317 (Print)
0022-1317 (Linking). Disponível em: < http://www.ncbi.nlm.nih.gov/entrez/query.fcgi?cmd=Retrieve&db=PubMed&dopt=Citation&list_uids=18796704 >.

HE, X. et al. Crystal structure of the polymerase PA(C)-PB1(N) complex from an avian influenza H5N1 virus. **Nature,** v. 454, n. 7208, p. 1123-6, Aug 28 2008. ISSN 1476-4687 (Electronic)
0028-0836 (Linking). Disponível em: < http://www.ncbi.nlm.nih.gov/entrez/query.fcgi?cmd=Retrieve&db=PubMed&dopt=Citation&list_uids=18615018 >.

HUANG, Z. et al. Anti-HSV-1, antioxidant and antifouling phenolic compounds from the deep-sea-derived fungus Aspergillus versicolor SCSIO 41502. **Bioorg Med Chem Lett,** v.

27, n. 4, p. 787-791, Feb 2017. ISSN 1464-3405. Disponível em: < https://www.ncbi.nlm.nih.gov/pubmed/28129981 >.

ICTVDB. **Influenzavirus B**. ICTVdB - The Universal Virus Database. BÜCHEN-OSMOND, C. New York, USA: Columbia University. 4 2006.

IVES, J. A. et al. The H274Y mutation in the influenza A/H1N1 neuraminidase active site following oseltamivir phosphate treatment leave virus severely compromised both in vitro and in vivo. **Antiviral Res,** v. 55, n. 2, p. 307-17, Aug 2002. ISSN 0166-3542. Disponível em: < http://www.ncbi.nlm.nih.gov/pubmed/12103431 >.

JACKSON, R. J. et al. Oseltamivir, zanamivir and amantadine in the prevention of influenza: a systematic review. **J Infect,** v. 62, n. 1, p. 14-25, Jan 2011. ISSN 1532-2742 (Electronic) 0163-4453 (Linking). Disponível em: < http://www.ncbi.nlm.nih.gov/entrez/query.fcgi?cmd=Retrieve&db=PubMed&dopt=Citation&list_uids=20950645 >.

JAGADESH, A. et al. Influenza virus neuraminidase (NA): a target for antivirals and vaccines. **Arch Virol**, Jun 2016. ISSN 1432-8798. Disponível em: < http://www.ncbi.nlm.nih.gov/pubmed/27255748 >.

JERVIS, P. J.; COX, L. R. Total synthesis and proof of relative stereochemistry of (-)-aureonitol. **J Org Chem,** v. 73, n. 19, p. 7616-24, Oct 3 2008. ISSN 1520-6904 (Electronic) 0022-3263 (Linking). Disponível em: < http://www.ncbi.nlm.nih.gov/entrez/query.fcgi?cmd=Retrieve&db=PubMed&dopt=Citation&list_uids=18774862 >.

JORBA, N.; COLOMA, R.; ORTIN, J. Genetic trans-complementation establishes a new model for influenza virus RNA transcription and replication. **PLoS Pathog,** v. 5, n. 5, p. e1000462, May 2009. ISSN 1553-7374 (Electronic) 1553-7366 (Linking). Disponível em: < http://www.ncbi.nlm.nih.gov/entrez/query.fcgi?cmd=Retrieve&db=PubMed&dopt=Citation&list_uids=19478885 >.

KAISER, J. A one-size-fits-all flu vaccine? **Science,** v. 312, n. 5772, p. 380-2, Apr 21 2006. ISSN 1095-9203 (Electronic) 0036-8075 (Linking). Disponível em: < http://www.ncbi.nlm.nih.gov/entrez/query.fcgi?cmd=Retrieve&db=PubMed&dopt=Citation&list_uids=16627732 >.

KELLY, C.; KLENERMAN, P.; BARNES, E. Interferon lambdas: the next cytokine storm. **Gut,** v. 60, n. 9, p. 1284-93, Sep 2011. ISSN 1468-3288. Disponível em: < https://www.ncbi.nlm.nih.gov/pubmed/21303914 >.

KOLLEROVA, E.; BETAKOVA, T. Influenza viruses and their ion channels. **Acta Virol,** v. 50, n. 1, p. 7-16, 2006. ISSN 0001-723X (Print) 0001-723X (Linking). Disponível em: < http://www.ncbi.nlm.nih.gov/entrez/query.fcgi?cmd=Retrieve&db=PubMed&dopt=Citation&list_uids=16599180 >.

LAMB, R. A.; KRUG, R. M. **Orthomyxoviridae: The viruses and their replication.** 3rd Vol.1. Philadelphia: Lippincott-Raven, 1996.

LAMB, R. A. ***Orthomyxoviridae*: the viruses and their replication.** 4th ed. Lippincott Williams & Wilkins, 2001.

LAURSEN, N. S.; WILSON, I. A. Broadly neutralizing antibodies against influenza viruses. **Antiviral Res,** v. 98, n. 3, p. 476-83, Jun 2013. ISSN 1872-9096. Disponível em: < http://www.ncbi.nlm.nih.gov/pubmed/23583287 >.

LEE, K. Y. Pneumonia, Acute Respiratory Distress Syndrome, and Early Immune-Modulator Therapy. **Int J Mol Sci,** v. 18, n. 2, Feb 2017. ISSN 1422-0067. Disponível em: < https://www.ncbi.nlm.nih.gov/pubmed/28208675 >.

LENEVA, I. A. et al. Characteristics of arbidol-resistant mutants of influenza virus: implications for the mechanism of anti-influenza action of arbidol. **Antiviral Res,** v. 81, n. 2, p. 132-40, Feb 2009. ISSN 1872-9096 (Electronic) 0166-3542 (Linking). Disponível em: < http://www.ncbi.nlm.nih.gov/entrez/query.fcgi?cmd=Retrieve&db=PubMed&dopt=Citation&list_uids=19028526 >.

LI, F.; MA, C.; WANG, J. Inhibitors targeting the influenza virus hemagglutinin. **Curr Med Chem,** v. 22, n. 11, p. 1361-82, 2015. ISSN 1875-533X. Disponível em: < http://www.ncbi.nlm.nih.gov/pubmed/25723505 >.

LIU, M. Y. et al. Pharmacokinetic properties and bioequivalence of two formulations of arbidol: an open-label, single-dose, randomized-sequence, two-period crossover study in healthy Chinese male volunteers. **Clin Ther,** v. 31, n. 4, p. 784-92, Apr 2009. ISSN 0149-2918 (Print) 0149-2918 (Linking). Disponível em: < http://www.ncbi.nlm.nih.gov/entrez/query.fcgi?cmd=Retrieve&db=PubMed&dopt=Citation&list_uids=19446151 >.

LIU, Y. et al. Altered receptor specificity and cell tropism of D222G hemagglutinin mutants isolated from fatal cases of pandemic A(H1N1) 2009 influenza virus. **J Virol,** v. 84, n. 22, p. 12069-74, Nov 2010. ISSN 1098-5514 (Electronic)
0022-538X (Linking). Disponível em: < http://www.ncbi.nlm.nih.gov/entrez/query.fcgi?cmd=Retrieve&db=PubMed&dopt=Citation&list_uids=20826688 >.

LOURDES G. FERREIRA, M. et al. Design, synthesis, and antiviral activity of new 1H-1,2,3-triazole nucleoside ribavirin analogs. **Medicinal Chemistry Research,** v. 23, p. 1501-1511, 2013.

MANZ, B. et al. Adaptive mutations in NEP compensate for defective H5N1 RNA replication in cultured human cells. **Nat Commun,** v. 3, p. 802, 2012. ISSN 2041-1723 (Electronic)
2041-1723 (Linking). Disponível em: < http://www.ncbi.nlm.nih.gov/entrez/query.fcgi?cmd=Retrieve&db=PubMed&dopt=Citation&list_uids=22549831 >.

MANZ, B.; SCHWEMMLE, M.; BRUNOTTE, L. Adaptation of avian influenza a virus polymerase in mammals to overcome the host species barrier. **J Virol,** v. 87, n. 13, p. 7200-9, Jul 2013. ISSN 1098-5514 (Electronic)

0022-538X (Linking). Disponível em: < http://www.ncbi.nlm.nih.gov/entrez/query.fcgi?cmd=Retrieve&db=PubMed&dopt=Citation&list_uids=23616660 >.

MARTÍN-BENITO, J.; ORTÍN, J. Influenza virus transcription and replication. **Adv Virus Res,** v. 87, p. 113-37, 2013. ISSN 1557-8399. Disponível em: < https://www.ncbi.nlm.nih.gov/pubmed/23809922 >.

MCAULEY, J. L.; ZHANG, K.; MCCULLERS, J. A. The effects of influenza A virus PB1-F2 protein on polymerase activity are strain specific and do not impact pathogenesis. **J Virol,** v. 84, n. 1, p. 558-64, Jan 2010. ISSN 1098-5514 (Electronic)
0022-538X (Linking). Disponível em: < http://www.ncbi.nlm.nih.gov/entrez/query.fcgi?cmd=Retrieve&db=PubMed&dopt=Citation&list_uids=19828614 >.

MCKIMM-BRESCHKIN, J. et al. Neuraminidase sequence analysis and susceptibilities of influenza virus clinical isolates to zanamivir and oseltamivir. **Antimicrob Agents Chemother,** v. 47, n. 7, p. 2264-72, Jul 2003. ISSN 0066-4804 (Print)
0066-4804 (Linking). Disponível em: < http://www.ncbi.nlm.nih.gov/entrez/query.fcgi?cmd=Retrieve&db=PubMed&dopt=Citation&list_uids=12821478 >.

MCKIMM-BRESCHKIN, J. L. Influenza neuraminidase inhibitors: antiviral action and mechanisms of resistence. **Influenza and other respiratory viruses,** v. 7, p. 25-36, 2013.

MEMOLI, M. J. et al. The natural history of influenza infection in the severely immunocompromised vs nonimmunocompromised hosts. **Clin Infect Dis,** v. 58, n. 2, p. 214-24, Jan 2014. ISSN 1537-6591. Disponível em: < https://www.ncbi.nlm.nih.gov/pubmed/24186906 >.

MIKULÁSOVÁ, A.; VERECKOVÁ, E.; FONDOR, E. Transcription and replication of the influenza A viruses genome. **Acta. Virologica,** v. 44, p. 273-282, 2000.

MOMOSE, F. et al. Cellular splicing factor RAF-2p48/NPI-5/BAT1/UAP56 interacts with the influenza virus nucleoprotein and enhances viral RNA synthesis. **J Virol,** v. 75, n. 4, p. 1899-908, Feb 2001. ISSN 0022-538X (Print)
0022-538X (Linking). Disponível em: < http://www.ncbi.nlm.nih.gov/entrez/query.fcgi?cmd=Retrieve&db=PubMed&dopt=Citation&list_uids=11160689 >.

MOMOSE, F. Identification of Hsp90 as a stimulatory host factor involved in influenza virus RNA synthesis. **J Biol Chem,** v. 277, n. 47, p. 45306-14, Nov 22 2002. ISSN 0021-9258 (Print)
0021-9258 (Linking). Disponível em: < http://www.ncbi.nlm.nih.gov/entrez/query.fcgi?cmd=Retrieve&db=PubMed&dopt=Citation&list_uids=12226087 >.

MONTO, A. S. et al. Detection of influenza viruses resistant to neuraminidase inhibitors in global surveillance during the first 3 years of their use. **Antimicrob Agents Chemother,** v. 50, n. 7, p. 2395-402, Jul 2006. ISSN 0066-4804 (Print)

0066-4804 (Linking). Disponível em: < http://www.ncbi.nlm.nih.gov/entrez/query.fcgi?cmd=Retrieve&db=PubMed&dopt=Citation&list_uids=16801417 >.

MOSS, R. B. et al. A phase II study of DAS181, a novel host directed antiviral for the treatment of influenza infection. **J Infect Dis,** v. 206, n. 12, p. 1844-51, Dec 2012. ISSN 1537-6613. Disponível em: < https://www.ncbi.nlm.nih.gov/pubmed/23045618 >.

MULLER, R. et al. Rift Valley fever virus L segment: correction of the sequence and possible functional role of newly identified regions conserved in RNA-dependent polymerases. **J Gen Virol,** v. 75 (Pt 6), p. 1345-52, Jun 1994. ISSN 0022-1317 (Print) 0022-1317 (Linking). Disponível em: < http://www.ncbi.nlm.nih.gov/entrez/query.fcgi?cmd=Retrieve&db=PubMed&dopt=Citation&list_uids=7515937 >.

MURATORE, G. et al. Small molecule inhibitors of influenza A and B viruses that act by disrupting subunit interactions of the viral polymerase. **Proc Natl Acad Sci U S A,** v. 109, n. 16, p. 6247-52, Apr 17 2012. ISSN 1091-6490 (Electronic) 0027-8424 (Linking). Disponível em: < http://www.ncbi.nlm.nih.gov/entrez/query.fcgi?cmd=Retrieve&db=PubMed&dopt=Citation&list_uids=22474359 >.

MURPHY, B. R.; WEBSTER, R. G. **Orthomyxoviruses.** 3rd. Philadelphia: Lappincott-Raven Publishers, 1996.

NAKADA, S. et al. Influenza C virus hemagglutinin: comparison with influenza A and B virus hemagglutinins. **J Virol,** v. 50, n. 1, p. 118-24, Apr 1984. ISSN 0022-538X (Print) 0022-538X (Linking). Disponível em: < http://www.ncbi.nlm.nih.gov/entrez/query.fcgi?cmd=Retrieve&db=PubMed&dopt=Citation&list_uids=6699942 >.

NAYAK, D. P.; HUI, E. K.; BARMAN, S. Assembly and budding of influenza virus. **Virus Res,** v. 106, n. 2, p. 147-65, Dec 2004. ISSN 0168-1702 (Print) 0168-1702 (Linking). Disponível em: < http://www.ncbi.nlm.nih.gov/entrez/query.fcgi?cmd=Retrieve&db=PubMed&dopt=Citation&list_uids=15567494 >.

NEWCOMB, L. L. et al. Interaction of the influenza a virus nucleocapsid protein with the viral RNA polymerase potentiates unprimed viral RNA replication. **J Virol,** v. 83, n. 1, p. 29-36, Jan 2009. ISSN 1098-5514 (Electronic) 0022-538X (Linking). Disponível em: < http://www.ncbi.nlm.nih.gov/entrez/query.fcgi?cmd=Retrieve&db=PubMed&dopt=Citation&list_uids=18945782 >.

NGUYEN, H. T.; FRY, A. M.; GUBAREVA, L. V. Neuraminidase inhibitor resistance in influenza viruses and laboratory testing methods. **Antivir Ther,** v. 17, n. 1 Pt B, p. 159-73, 2012. ISSN 2040-2058 (Electronic) 1359-6535 (Linking). Disponível em: < http://www.ncbi.nlm.nih.gov/entrez/query.fcgi?cmd=Retrieve&db=PubMed&dopt=Citation&list_uids=22311680 >.

NGUYEN, J. T. et al. Triple combination of amantadine, ribavirin, and oseltamivir is highly active and synergistic against drug resistant influenza virus strains in vitro. **PLoS One,** v. 5, n. 2, p. e9332, 2010. ISSN 1932-6203 (Electronic)
1932-6203 (Linking). Disponível em: < http://www.ncbi.nlm.nih.gov/entrez/query.fcgi?cmd=Retrieve&db=PubMed&dopt=Citation&list_uids=20179772 >.

NGUYEN, J. T. Triple combination of oseltamivir, amantadine, and ribavirin displays synergistic activity against multiple influenza virus strains in vitro. **Antimicrob Agents Chemother,** v. 53, n. 10, p. 4115-26, Oct 2009. ISSN 1098-6596 (Electronic)
0066-4804 (Linking). Disponível em: < http://www.ncbi.nlm.nih.gov/entrez/query.fcgi?cmd=Retrieve&db=PubMed&dopt=Citation&list_uids=19620324 >.

NICHOLSON, K. G. **Human influenza.** . London: Blackwell Science, 1998.

NITSCH-OSUCH, A.; BRYDAK, L. B. Influenza viruses resistant to neuraminidase inhibitors. **Acta Biochim Pol,** v. 61, n. 3, p. 505-8, 2014. ISSN 1734-154X. Disponível em: < http://www.ncbi.nlm.nih.gov/pubmed/25195142 >.

OBAYASHI, E. et al. The structural basis for an essential subunit interaction in influenza virus RNA polymerase. **Nature,** v. 454, n. 7208, p. 1127-31, Aug 28 2008. ISSN 1476-4687 (Electronic)
0028-0836 (Linking). Disponível em: < http://www.ncbi.nlm.nih.gov/entrez/query.fcgi?cmd=Retrieve&db=PubMed&dopt=Citation&list_uids=18660801 >.

OHUCHI, M. et al. Roles of neuraminidase in the initial stage of influenza virus infection. **Microbes Infect,** v. 8, n. 5, p. 1287-93, Apr 2006. ISSN 1286-4579. Disponível em: < https://www.ncbi.nlm.nih.gov/pubmed/16682242 >.

OKOMO-ADHIAMBO, M. et al. Neuraminidase inhibitor susceptibility testing in human influenza viruses: a laboratory surveillance perspective. **Viruses,** v. 2, n. 10, p. 2269-89, Oct 2010. ISSN 1999-4915 (Electronic)
1999-4915 (Linking). Disponível em: < http://www.ncbi.nlm.nih.gov/entrez/query.fcgi?cmd=Retrieve&db=PubMed&dopt=Citation&list_uids=21994620 >.

ORTIGOZA, M. B. et al. A novel small molecule inhibitor of influenza A viruses that targets polymerase function and indirectly induces interferon. **PLoS Pathog,** v. 8, n. 4, p. e1002668, 2012. ISSN 1553-7374 (Electronic)
1553-7366 (Linking). Disponível em: < http://www.ncbi.nlm.nih.gov/entrez/query.fcgi?cmd=Retrieve&db=PubMed&dopt=Citation&list_uids=22577360 >.

PAESHUYSE, J.; DALLMEIER, K.; NEYTS, J. Ribavirin for the treatment of chronic hepatitis C virus infection: a review of the proposed mechanisms of action. **Curr Opin Virol,** v. 1, n. 6, p. 590-8, Dec 2011. ISSN 1879-6265 (Electronic). Disponível em: < http://www.ncbi.nlm.nih.gov/entrez/query.fcgi?cmd=Retrieve&db=PubMed&dopt=Citation&list_uids=22440916 >.

PALESE, P.; SHAW, M. L. **Orthomyxoviridae: The viruses and their replication**. Philadelphia: Lippincott, Williams & Wilkins, 2007.

PALESE, P. **Orthomyxoviridae: The viruses and their replication.** Philadelphia: Lippincott, Williams & Wilkins, 2007.

PEREZ, J. T. et al. Influenza A virus-generated small RNAs regulate the switch from transcription to replication. **Proc Natl Acad Sci U S A,** v. 107, n. 25, p. 11525-30, Jun 22 2010. ISSN 1091-6490 (Electronic)
0027-8424 (Linking). Disponível em: < http://www.ncbi.nlm.nih.gov/entrez/query.fcgi?cmd=Retrieve&db=PubMed&dopt=Citation&list_uids=20534471 >.

PERRONE, L. A. et al. Mice lacking both TNF and IL-1 receptors exhibit reduced lung inflammation and delay in onset of death following infection with a highly virulent H5N1 virus. **J Infect Dis,** v. 202, n. 8, p. 1161-70, Oct 2010. ISSN 1537-6613. Disponível em: < https://www.ncbi.nlm.nih.gov/pubmed/20815704 >.

PFLUG, A. et al. Structure of influenza A polymerase bound to the viral RNA promoter. **Nature,** v. 516, n. 7531, p. 355-60, Dec 2014. ISSN 1476-4687. Disponível em: < https://www.ncbi.nlm.nih.gov/pubmed/25409142 >.

PIELAK, R. M.; SCHNELL, J. R.; CHOU, J. J. Mechanism of drug inhibition and drug resistance of influenza A M2 channel. **Proc Natl Acad Sci U S A,** v. 106, n. 18, p. 7379-84, May 2009. ISSN 1091-6490. Disponível em: < https://www.ncbi.nlm.nih.gov/pubmed/19383794 >.

PIRALLA, A. et al. Different drug-resistant influenza A(H3N2) variants in two immunocompromised patients treated with oseltamivir during the 2011-2012 influenza season in Italy. **J Clin Virol**, Jun 27 2013. ISSN 1873-5967 (Electronic)
1386-6532 (Linking). Disponível em: < http://www.ncbi.nlm.nih.gov/entrez/query.fcgi?cmd=Retrieve&db=PubMed&dopt=Citation&list_uids=23810646 >.

POCH, O. et al. Identification of four conserved motifs among the RNA-dependent polymerase encoding elements. **EMBO J,** v. 8, n. 12, p. 3867-74, Dec 1 1989. ISSN 0261-4189 (Print) 0261-4189 (Linking). Disponível em: < http://www.ncbi.nlm.nih.gov/entrez/query.fcgi?cmd=Retrieve&db=PubMed&dopt=Citation&list_uids=2555175 >.

PORTELA, A.; DIGARD, P. The influenza virus nucleoprotein: a multifunctional RNA-binding protein pivotal to virus replication. **J Gen Virol,** v. 83, n. Pt 4, p. 723-34, Apr 2002. ISSN 0022-1317 (Print) 0022-1317 (Linking). Disponível em: < http://www.ncbi.nlm.nih.gov/entrez/query.fcgi?cmd=Retrieve&db=PubMed&dopt=Citation&list_uids=11907320 >.

POTIER, M. et al. Fluorometric assay of neuraminidase with a sodium (4-methylumbelliferyl-alpha-D-N-acetylneuraminate) substrate. **Anal Biochem,** v. 94, n. 2, p. 287-96, Apr 15 1979. ISSN 0003-2697 (Print)
0003-2697 (Linking). Disponível em: < http://www.ncbi.nlm.nih.gov/entrez/query.fcgi?cmd=Retrieve&db=PubMed&dopt=Citation&list_uids=464297 >.

RAMANA, C. V. et al. Role of alveolar epithelial early growth response-1 (Egr-1) in CD8+ T cell-mediated lung injury. **Mol Immunol,** v. 47, n. 2-3, p. 623-31, Dec 2009. ISSN 1872-9142 (Electronic) 0161-5890 (Linking). Disponível em: < http://www.ncbi.nlm.nih.gov/entrez/query.fcgi?cmd=Retrieve&db=PubMed&dopt=Citation&list_uids=19786304 >.

RAZONABLE, R. R. Antiviral drugs for viruses other than human immunodeficiency virus. **Mayo Clin Proc,** v. 86, n. 10, p. 1009-26, Oct 2011. ISSN 1942-5546 (Electronic) 0025-6196 (Linking). Disponível em: < http://www.ncbi.nlm.nih.gov/entrez/query.fcgi?cmd=Retrieve&db=PubMed&dopt=Citation&list_uids=21964179 >.

ROBB, N. C. et al. NS2/NEP protein regulates transcription and replication of the influenza virus RNA genome. **J Gen Virol,** v. 90, n. Pt 6, p. 1398-407, Jun 2009. ISSN 0022-1317 (Print) 0022-1317 (Linking). Disponível em: < http://www.ncbi.nlm.nih.gov/entrez/query.fcgi?cmd=Retrieve&db=PubMed&dopt=Citation&list_uids=19264657 >.

RODRÍGUEZ, K.; STCHIGEL, A.; GUARRO, J. Three new species of Chaetomium from soil. **Mycologia,** v. 94, n. 1, p. 116-26, 2002 Jan-Feb 2002. ISSN 0027-5514. Disponível em: < http://www.ncbi.nlm.nih.gov/pubmed/21156483 >.

RUIGROK, R. W. H. **Structure of Influenza A, B and C viruses.** London: Blackwell Science, 1998.

SACRAMENTO, C. Q. et al. The clinically approved antiviral drug sofosbuvir inhibits Zika virus replication. **Sci Rep,** v. 7, p. 40920, Jan 2017. ISSN 2045-2322. Disponível em: < https://www.ncbi.nlm.nih.gov/pubmed/28098253 >.

SACRAMENTO, C. Q. et al. Aureonitol, a Fungi-Derived Tetrahydrofuran, Inhibits Influenza Replication by Targeting Its Surface Glycoprotein Hemagglutinin. **PLoS One,** v. 10, n. 10, p. e0139236, 2015. ISSN 1932-6203. Disponível em: < http://www.ncbi.nlm.nih.gov/pubmed/26462111 >.

SAITO, R. et al. Increased incidence of adamantane-resistant influenza A(H1N1) and A(H3N2) viruses during the 2006-2007 influenza season in Japan. **J Infect Dis,** v. 197, n. 4, p. 630-2; author reply 632-3, Feb 15 2008. ISSN 0022-1899 (Print) 0022-1899 (Linking). Disponível em: < http://www.ncbi.nlm.nih.gov/entrez/query.fcgi?cmd=Retrieve&db=PubMed&dopt=Citation&list_uids=18275281 >.

SAMSON, M. et al. Influenza virus resistance to neuraminidase inhibitors. **Antiviral Res,** v. 98, n. 2, p. 174-85, May 2013. ISSN 1872-9096 (Electronic) 0166-3542 (Linking). Disponível em: < http://www.ncbi.nlm.nih.gov/entrez/query.fcgi?cmd=Retrieve&db=PubMed&dopt=Citation&list_uids=23523943 >.

SANKYO, M. I.-D. **Daiichi Sankyo Receives Approval to Manufacture and Market Inavir(R) Influenza Antiviral Inhalant for Treatment in Japan**: Daiichi Sankyo 2010.

SAÚDE, M. D. **Protocolo de tratamento de influenza 2015.** Biblioteca Virtual em Saúde

do Ministério da Saúde: www.saúde.gov.br/bvs: Ministério da Saúde 2015.

SAÚDE, M. D. Informe Epidemiológico Influenza: Monitoramento até a Semana Epidemiológica 52 de 2016., 2017a. Disponível em: < http://portalarquivos.saude.gov.br/images/pdf/2017/janeiro/05/Informe-Epidemiologico-Influenza-2016-SE-52.pdf >. Acesso em: 25 de maio.

SAÚDE, M. D. Nota informativa e recomendações sobre a sazonalidade da influenza 2017., 2017b. Disponível em: < http://portalsaude.saude.gov.br/index.php/o-ministerio/principal/leia-mais-o-ministerio/414-secretaria-svs/vigilancia-de-a-a-z/influenza/22873-informacoes-sobre-gripe >. Acesso em: 01 de junho.

SAÚDE, M. D. Informe Epidemiológico Influenza: Monitoramento até a Semana Epidemiológica 19 de 2017., 2017a. Disponível em: < http://portalarquivos.saude.gov.br/images/pdf/2017/maio/19/Informe%20Epidemiolgico_Influenza%202017-SE-19.pdf >. Acesso em: 25 de maio.

SAÚDE, M. D. Informe Epidemiológico Influenza: Monitoramento até a Semana Epidemiológica 52 de 2016., 2017b. Disponível em: < http://portalarquivos.saude.gov.br/images/pdf/2017/janeiro/05/Informe-Epidemiologico-Influenza-2016-SE-52.pdf >. Acesso em: 25 de maio.

SCHRAUWEN, E. J. et al. Determinants of virulence of influenza A virus. **Eur J Clin Microbiol Infect Dis,** v. 33, n. 4, p. 479-90, Apr 2014. ISSN 1435-4373. Disponível em: < http://www.ncbi.nlm.nih.gov/pubmed/24078062 >.

SHEN, H. Q. et al. Isolation and phylogenetic analysis of hemagglutinin gene of H9N2 influenza viruses from chickens in South China from 2012 to 2013. **J Vet Sci,** v. 16, n. 3, p. 317-24, 2015. ISSN 1976-555X. Disponível em: < http://www.ncbi.nlm.nih.gov/pubmed/25643797 >.

SHEN, X.; ZHANG, X.; LIU, S. Novel hemagglutinin-based influenza virus inhibitors. **J Thorac Dis,** v. 5 Suppl 2, p. S149-59, Aug 2013. ISSN 2072-1439. Disponível em: < http://www.ncbi.nlm.nih.gov/pubmed/23977436 >.

SHTYRYA, Y. A.; MOCHALOVA, L. V.; BOVIN, N. V. Influenza virus neuraminidase: structure and function. **Acta Naturae,** v. 1, n. 2, p. 26-32, Jul 2009. ISSN 2075-8251. Disponível em: < http://www.ncbi.nlm.nih.gov/pubmed/22649600 >.

SIDWELL, R. W. et al. Broad-spectrum antiviral activity of Virazole: 1-beta-D-ribofuranosyl-1,2,4-triazole-3-carboxamide. **Science,** v. 177, n. 4050, p. 705-6, Aug 25 1972. ISSN 0036-8075 (Print) 0036-8075 (Linking). Disponível em: < http://www.ncbi.nlm.nih.gov/entrez/query.fcgi?cmd=Retrieve&db=PubMed&dopt=Citation&list_uids=4340949 >.

SILVA, F. C. et al. Synthesis, HIV-RT inhibitory activity and SAR of 1-benzyl-1H-1,2,3-triazole derivatives of carbohydrates. **Eur J Med Chem,** v. 44, n. 1, p. 373-83, Jan 2009. ISSN 1768-3254 (Electronic) 0223-5234 (Linking). Disponível em: < http://www.ncbi.nlm.nih.gov/entrez/query.fcgi?cmd=Retrieve&db=PubMed&dopt=Citation&list_uids=18486994 >.

SNELGROVE, R. J. et al. A critical function for CD200 in lung immune homeostasis and the severity of influenza infection. **Nat Immunol,** v. 9, n. 9, p. 1074-83, Sep 2008. ISSN 1529-2916. Disponível em: < https://www.ncbi.nlm.nih.gov/pubmed/18660812 >.

SOUZA, T. M. et al. The alkaloid 4-methylaaptamine isolated from the sponge Aaptos aaptos impairs Herpes simplex virus type 1 penetration and immediate-early protein synthesis. **Planta Med,** v. 73, n. 3, p. 200-5, Mar 2007. ISSN 0032-0943 (Print) 0032-0943 (Linking). Disponível em: < http://www.ncbi.nlm.nih.gov/entrez/query.fcgi?cmd=Retrieve&db=PubMed&dopt=Citation&list_uids=17285480 >.

SOUZA, T. M. et al. Detection of Oseltamivir-Resistant Pandemic Influenza A(H1N1)pdm2009 in Brazil: Can Community Transmission Be Ruled Out? **PLoS One,** v. 8, n. 11, p. e80081, 2013. ISSN 1932-6203 (Electronic) 1932-6203 (Linking). Disponível em: < http://www.ncbi.nlm.nih.gov/entrez/query.fcgi?cmd=Retrieve&db=PubMed&dopt=Citation&list_uids=24244615 >.

SOUZA, T. M. et al. H1N1pdm influenza infection in hospitalized cancer patients: clinical evolution and viral analysis. **PLoS One,** v. 5, n. 11, p. e14158, 2010. ISSN 1932-6203 (Electronic) 1932-6203 (Linking). Disponível em: < http://www.ncbi.nlm.nih.gov/entrez/query.fcgi?cmd=Retrieve&db=PubMed&dopt=Citation&list_uids=21152402 >.

SRIWILAIJAROEN, N.; SUZUKI, Y. Molecular basis of the structure and function of H1 hemagglutinin of influenza virus. **Proc Jpn Acad Ser B Phys Biol Sci,** v. 88, n. 6, p. 226-49, 2012. ISSN 1349-2896. Disponível em: < http://www.ncbi.nlm.nih.gov/pubmed/22728439 >.

STREETER, D. G. et al. Mechanism of action of 1- -D-ribofuranosyl-1,2,4-triazole-3-carboxamide (Virazole), a new broad-spectrum antiviral agent. **Proc Natl Acad Sci U S A,** v. 70, n. 4, p. 1174-8, Apr 1973. ISSN 0027-8424 (Print) 0027-8424 (Linking). Disponível em: <http://www.ncbi.nlm.nih.gov/entrez/query.fcgi?cmd=Retrieve&db=PubMed&dopt=Citation&list_uids=4197928 >.

SU, B. et al. Enhancement of the influenza A hemagglutinin (HA)-mediated cell-cell fusion and virus entry by the viral neuraminidase (NA). **PLoS One,** v. 4, n. 12, p. e8495, Dec 2009. ISSN 1932-6203. Disponível em: < https://www.ncbi.nlm.nih.gov/pubmed/20041119 >.

TAKASHITA, E. et al. Characterization of a large cluster of influenza A(H1N1)pdm09 viruses cross-resistant to oseltamivir and peramivir during the 2013-2014 influenza season in Japan. **Antimicrob Agents Chemother,** v. 59, n. 5, p. 2607-17, May 2015. ISSN 1098-6596. Disponível em: < http://www.ncbi.nlm.nih.gov/pubmed/25691635 >.

TAM, R. C. et al. Contact hypersensitivity responses following ribavirin treatment in vivo are influenced by type 1 cytokine polarization, regulation of IL-10 expression, and costimulatory signaling. **J Immunol,** v. 163, n. 7, p. 3709-17, Oct 1 1999. ISSN 0022-1767 (Print) 0022-1767 (Linking). Disponível em: < http://www.ncbi.nlm.nih.gov/entrez/query.fcgi?cmd=Retrieve&db=PubMed&dopt=Citation&list_uids=10490966 >.

TAUBENBERGER, J. K.; MORENS, D. M. The Pathology of Influenza. **Annu Rev Pathol,** v. 3, p. 499-522, 2008.

TECHNOLOGIES, A. A Phase 1, Randomized, Double-blind, Placebo-controlled Assessment of the Safety, Tolerability and Pharmacokinetics of Escalating Single and Repeat Doses of Flufirvitide-3 Dry Powder for Inhalation in Healthy Subjects., 2015. Disponível em: < https://clinicaltrials.gov/ct2/show/NCT01990846?term=Flufirvitide-3&rank=2 >. Acesso em: 01 de junho.

TECHNOLOGIES, A. A Phase 2a, Randomized, Double-blind, Placebo-controlled Assessment of the Safety and Protective Efficacy of FF-3 Dry Powder Administered by Nasal Inhalation for 5 Days to Healthy Adult Subjects Who Are Experimentally Infected With a Challenge Strain of Influenza A Virus., 2016. Disponível em: < https://clinicaltrials.gov/ct2/show/NCT02423577?term=NCT02423577&rank=1 >. Acesso em: 01 de junho.

TEIJARO, J. R. The role of cytokine responses during influenza virus pathogenesis and potential therapeutic options. **Curr Top Microbiol Immunol,** v. 386, p. 3-22, 2015. ISSN 0070-217X. Disponível em: < https://www.ncbi.nlm.nih.gov/pubmed/25267464 >.

TISONCIK, J. R. et al. Into the eye of the cytokine storm. **Microbiol Mol Biol Rev,** v. 76, n. 1, p. 16-32, Mar 2012. ISSN 1098-5557 (Electronic) 1092-2172 (Linking). Disponível em: < http://www.ncbi.nlm.nih.gov/entrez/query.fcgi?cmd=Retrieve&db=PubMed&dopt=Citation&list_uids=22390970 >.

TOMESCU, A. I. et al. Single-molecule FRET reveals a corkscrew RNA structure for the polymerase-bound influenza virus promoter. **Proc Natl Acad Sci U S A,** v. 111, n. 32, p. E3335-42, Aug 2014. ISSN 1091-6490. Disponível em: < https://www.ncbi.nlm.nih.gov/pubmed/25071209 >.

VENKATARAMAN, P.; LAMB, R. A.; PINTO, L. H. Chemical rescue of histidine selectivity filter mutants of the M2 ion channel of influenza A virus. **J Biol Chem,** v. 280, n. 22, p. 21463-72, Jun 2005. ISSN 0021-9258. Disponível em: < https://www.ncbi.nlm.nih.gov/pubmed/15784624 >.

VON ITZSTEIN, M. The war against influenza: discovery and development of sialidase inhibitors. **Nat. Rev. Drug. Discov.,** v. 6, n. 12, p. 967-74, 2007a.

WANG, G. et al. H6 influenza viruses pose a potential threat to human health. **J Virol,** v. 88, n. 8, p. 3953-64, Apr 2014. ISSN 1098-5514. Disponível em: < http://www.ncbi.nlm.nih.gov/pubmed/24501418 >.

WANG, Y. et al. Bioactive metabolites from Chaetomium globosum L18, an endophytic fungus in the medicinal plant Curcuma wenyujin. **Phytomedicine,** v. 19, n. 3-4, p. 364-8, Feb 2012. ISSN 1618-095X. Disponível em: < http://www.ncbi.nlm.nih.gov/pubmed/22112725 >.

WEBSTER, R. G. et al. Evolution and ecology of influenza A viruses. **Microbiol. Rev.,** v. 56, p. 152–79, 1992.

WEBSTER, R. G.; GOVORKOVA, E. A. Continuing challenges in influenza. **Ann N Y Acad Sci,** v. 1323, n. 1, p. 115-39, Sep 2014. ISSN 1749-6632. Disponível em: < http://www.ncbi.nlm.nih.gov/pubmed/24891213 >.

WHO. Influenza Pandemic Plan. The Role of WHO and Guidelines for National and Regional Planning. Geneva, Switzerland., 1999. Disponível em: < http://www.who.int/csr/resources/publications/influenza/whocdscsredc991.pdf >.

WHO. Influenza. **Fact sheet** v. 211, 2003.

WHO. Pandemic (H1N1) 2009 briefing note 1 Viruses resistant to oseltamivir (Tamiflu) identified. **Wkly. Epidemiol. Rec.,** v. 84, n. 29, p. 299-399, 2009a.

WHO. **Pandemic influenza preparedness and response. A WHO guidance document.** 2009b

WHO. Recommended composition of influenza virus vaccines for use in the 2010 influenza season (southern hemisphere winter). **Wkly Epidemiol Rec.,** v. 84, p. 421-31, 2009a.

WHO. Recommended composition of influenza virus vaccines for use in the 2009-2010 influenza season (northern hemisphere winter). **Wkly Epidemiol Rec.,** v. 84, p. 65-72, 2009b.

WHO. Recommended viruses for influenza vaccines for use in the 2011 southern hemisphere influenza season., 2010a. Disponível em: < http://www.who.int/influenza/vaccines/virus/recommendations/201009_Recommendation.pdf >.

WHO. WHO reccomendations for the post-pandemic period. 2010b. Disponível em: < http://www.who.int/csr/disease/swineflu/notes/briefing_20100810/en/ >. Acesso em: 19 de maio.

WHO. Weekly update on oseltamivir resistance to pandemic influenza A (H1N1) 2009 viruses. . 2010a. Disponível em: < http://www.who.int/csr/disease/influenza/weeklyupdateoseltamivirresistant20101108.pdf >.

WHO. Recommended composition of influenza virus vaccines for use in the 2012 southern hemisphere influenza season., 2011. Disponível em: < http://www.who.int/influenza/vaccines/virus/recommendations/2011_09_recommendation.pdf >.

WHO. Standardization of terminology of the pandemic A(H1N1)2009 virus. . 2011a. Disponível em: < http://www.who.int/influenza/gisrs_laboratory/terminology_ah1n1pdm09/en/ >. Acesso em: 28 de junho.

WHO. Recommended composition of influenza virus vaccines for use in the 2013 southern hemisphere influenza season., 2012a. Disponível em: < http://www.who.int/influenza/vaccines/virus/recommendations/201209_recommendation.pdf >.

WHO. Recommended composition of influenza virus vaccines for use in the 2014 southern hemisphere influenza season. 2013a. Disponível em: < http://www.who.int/influenza/vaccines/virus/recommendations/2014_south/en/ >. Acesso em: 19 de maio.

WHO. WHO Risk Assessement: Human infections with avian influenza A(H7N9) virus., 2013b. Disponível em: < http://www.who.int/influenza/human_animal_interface/influenza_h7n9/RiskAssessment_H7N9_07Jun13.pdf >.

WHO. **Influenza (seasonal) Fact Sheet N°211**. http://www.who.int/mediacentre/factsheets/fs211/en/: World Health Organization [online] 2014a.

WHO. **Recommended composition of influenza virus vaccines for use in the 2015 southern hemisphere influenza season** 2014b.

WHO. Recommended composition of influenza virus vaccines for use in the 2015 southern hemisphere influenza season. 2014c. Disponível em: < http://www.who.int/influenza/vaccines/virus/recommendations/2015_south/en/ >. Acesso em: 19 de maio.

WHO. Recommended composition of influenza virus vaccines for use in the 2016 southern hemisphere influenza season. 2015a. Disponível em: < http://www.who.int/influenza/vaccines/virus/recommendations/201509_recommendation.pdf >. Acesso em: 19 de maio.

WHO. Warning signals from the volatile world of influenza viruses., 2015b. Disponível em: < http://www.who.int/influenza/publications/warningsignals201502/en/ >. Acesso em: 01 de junho.

WHO. Influenza at the human-animal interface. Summary and assessment, 21 April to 16 May 2017., 2017a. Disponível em: < http://www.who.int/influenza/human_animal_interface/Influenza_Summary_IRA_HA_interface_05_16_2017.pdf?ua=1 >. Acesso em: 01 de junho.

WHO. Influenza virus detections. FluNet - Charts., 2017b. Disponível em: < http://www.who.int/influenza/gisrs_laboratory/flunet/charts/en/ >. Acesso em: 25 de maio.

WILEY, D. C.; SKEHEL, J. J. The structure and function of the hemagglutinin membrane glycoprotein of influenza virus. **Annu Rev Biochem,** v. 56, p. 365-94, 1987. ISSN 0066-4154. Disponível em: < http://www.ncbi.nlm.nih.gov/pubmed/3304138 >.

WRIGHT, P. F.; NEUMANN, G.; KAWAOKA, Y. **Orthomyxoviruses**. Philadelphia: Lippincott Williams & Wilkins, 2007.

WS, H. **Medical Meanings: a Glossary of Word Origins.** Philadelphia, Pennsylvania: American College of Physicians 1997.

WU, X. et al. Progress of small molecular inhibitors in the development of anti-influenza virus agents. **Theranostics,** v. 7, n. 4, p. 826-845, 2017. ISSN 1838-7640. Disponível em: < https://www.ncbi.nlm.nih.gov/pubmed/28382157 >.

YAMADA, K. et al. Identification of a novel compound with antiviral activity against influenza A virus depending on PA subunit of viral RNA polymerase. **Microbes Infect,** v. 14, n. 9, p. 740-7, Aug 2012. ISSN 1769-714X (Electronic) 1286-4579 (Linking). Disponível em: <

http://www.ncbi.nlm.nih.gov/entrez/query.fcgi?cmd=Retrieve&db=PubMed&dopt=Citation&list_uids=22441116 >.

YANG, J. et al. Influenza A virus entry inhibitors targeting the hemagglutinin. **Viruses,** v. 5, n. 1, p. 352-73, Jan 2013. ISSN 1999-4915. Disponível em: < http://www.ncbi.nlm.nih.gov/pubmed/23340380 >.

YANG, J, et al. A new role of neuraminidase (NA) in the influenza virus life cycle: implication for developing NA inhibitors with novel mechanism of action. **Rev Med Virol,** v. 26, n. 4, p. 242-50, Jul 2016. ISSN 1099-1654. Disponível em: < https://www.ncbi.nlm.nih.gov/pubmed/27061123 >.

YUAN, P. et al. Crystal structure of an avian influenza polymerase PA(N) reveals an endonuclease active site. **Nature,** v. 458, n. 7240, p. 909-13, Apr 16 2009. ISSN 1476-4687 (Electronic) 0028-0836 (Linking). Disponível em: < http://www.ncbi.nlm.nih.gov/entrez/query.fcgi?cmd=Retrieve&db=PubMed&dopt=Citation&list_uids=19194458 >.

YUEN, K. Y.; WONG, S. S. Human infection by avian influenza A H5N1. **Hong Kong Med J,** v. 11, n. 3, p. 189-99, Jun 2005. ISSN 1024-2708 (Print) 1024-2708 (Linking). Disponível em: < http://www.ncbi.nlm.nih.gov/entrez/query.fcgi?cmd=Retrieve&db=PubMed&dopt=Citation&list_uids=15951584 >.

PLOS ONE

RESEARCH ARTICLE

Aureonitol, a Fungi-Derived Tetrahydrofuran, Inhibits Influenza Replication by Targeting Its Surface Glycoprotein Hemagglutinin

Carolina Q. Sacramento[1,2,3], Andressa Marttorelli[1,2,3], Natalia Fintelman-Rodrigues[1,2,3], Caroline S. de Freitas[1,2,3], Gabrielle R. de Melo[1,2,3], Marco E. N. Rocha[1,2,3,4], Carlos R. Kaiser[5], Katia F. Rodrigues[6], Gisela L. da Costa[6], Cristiane M. Alves[1], Osvaldo Santos-Filho[1], Jussara P. Barbosa[6], Thiago Moreno L. Souza[1,2,3]*

1 Laboratório de Vírus Respiratórios, Instituto Oswaldo Cruz, Fundação Oswaldo Cruz, Rio de Janeiro, Rio de Janeiro, Brazil, **2** Laboratório de Imunofarmacologia, Instituto Oswaldo Cruz, Fundação Oswaldo Cruz, Rio de Janeiro, Rio de Janeiro, Brazil, **3** Centro de Desenvolvimento Tecnológico em Saúde, Fundação Oswaldo Cruz, Rio de Janeiro, Rio de Janeiro, Brazil, **4** Laboratório de Química de Produtos Naturais 5, Farmanguinhos, Fundação Oswaldo Cruz, Rio de Janeiro, Rio de Janeiro, Brazil, **5** Instituto de Química, Universidade Federal do Rio de Janeiro, Rio de Janeiro, Rio de Janeiro, Brazil, **6** Laboratório de Taxonomia, Bioquímica e Bioprospecção de Fungos, Instituto Oswaldo Cruz, Fundação Oswaldo Cruz, Rio de Janeiro, Rio de Janeiro, Brazil

* tmoreno@ioc.fiocruz.br

OPEN ACCESS

Citation: Sacramento CQ, Marttorelli A, Fintelman-Rodrigues N, de Freitas CS, de Melo GR, Rocha MEN, et al. (2015) Aureonitol, a Fungi-Derived Tetrahydrofuran, Inhibits Influenza Replication by Targeting Its Surface Glycoprotein Hemagglutinin. PLoS ONE 10(10): e0139236. doi:10.1371/journal.pone.0139236

Editor: Balaji Manicassamy, The University of Chicago, UNITED STATES

Received: March 10, 2015

Accepted: September 10, 2015

Published: October 13, 2015

Data Availability Statement: All relevant data are within the paper and Supporting Information file.

Funding: This study was supported by grants from CNPq (www.cnpq.br), and Faperj (www.faperj.br). The funders had no role in study design, data collection and analysis, decision to publish, or preparation of the manuscript.

Competing Interests: The authors have declared that no competing interests exist.

Abstract

The influenza virus causes acute respiratory infections, leading to high morbidity and mortality in groups of patients at higher risk. Antiviral drugs represent the first line of defense against influenza, both for seasonal infections and pandemic outbreaks. Two main classes of drugs against influenza are in clinical use: M2-channel blockers and neuraminidase inhibitors. Nevertheless, because influenza strains that are resistant to these antivirals have been described, the search for novel compounds with different mechanisms of action is necessary. Here, we investigated the anti-influenza activity of a fungi-derived natural product, aureonitol. This compound inhibited influenza A and B virus replication. This compound was more effective against influenza A(H3N2), with an EC_{50} of 100 nM. Aureonitol cytoxicity was also very low, with a CC_{50} value of 1426 μM. Aureonitol inhibited influenza hemagglutination and, consequently, significantly impaired virus adsorption. Molecular modeling studies revealed that aureonitol docked in the sialic acid binding site of hemagglutinin, forming hydrogen bonds with highly conserved residues. Altogether, our results indicate that the chemical structure of aureonitol is promising for future anti-influenza drug design.

Introduction

Acute respiratory infections are a major cause of morbidity and mortality and, therefore, have a great impact on public health [1]. Episodes of severe acute respiratory infections (SARI) are likely to be triggered by the influenza virus [2, 3]. Influenza is a zoonotic agent that can cause seasonal infections and pandemic outbreaks in humans [3]. The influenza virus has a negative-

sense segmented RNA, a characteristic of members of the orthomyxovirus family [2]. To enter host cells, the influenza surface glycoprotein hemagglutinin (HA) binds to sialic acid residues on proteins localized in the cellular plasma membrane. Subsequently, virions are endocytosed, and the viral envelope and endocytic membrane are fused due to influenza protein M2 proton channel activity [4]. Viral ribonucleoproteins (RNP) are then released into the cytoplasm and transported to the cell nucleus, where transcription and replication of the viral genome occur. Following replication assembled virus particles bud through the cellular plasma membrane and are released via viral neuraminidase (NA) activity [5].

Although anti-influenza vaccines exist, several limitations make eradication through vaccination a difficult strategy. First, influenza has multiple zoonotic hosts [6]. The time frame to produce vaccines against novel influenza viruses is also generally very long [7]. The high cost of vaccine production and the fact that vaccines are only recommended for patient groups who are at high risk for serious illnesses are additional limitations [7].

Due to the limitations of vaccination, antiviral drugs are an important option for controlling influenza virus replication [8, 9]. Because the antigenic characteristics of viral strains that might cause future pandemic outbreaks are unpredictable, the stockpiling of anti-influenza drugs is a key step in pandemic preparedness [8, 9]. However, antiviral resistance to the adamantanes, M2-channel blockers, is very common. Neuraminidase inhibitors (NAIs) are the main class of antiviral drugs currently in clinical use [10], but mutants that are resistant and have decreased sensitivity to oseltamivir (OST) have been described [11, 12]. Therefore, the identification of molecules that can inhibit influenza strains resistant to these antivirals and/or block another step in the virus life cycle is necessary.

Chaetomium Kuntze ex Fries (*Chaetomiaceae*) is a cosmopolitan fungus found in soil and cellulose-containing substrates [13]. Members of this genus are rich sources of bioactive secondary metabolites with different chemical structures [14–16], such as alkaloids [17, 18], esters [19] and polyketides [20]. Among the secondary metabolites produced by this genus, aureonitol, a tetrahydrofuran (THF) derivative [21], is an abundant metabolite. Using the fungus *Chaetomium globosum* as a model organism, it has been shown that aureonitol acts as a transcriptional regulator for the synthesis of other secondary metabolites in this species [22]. Aureonitol has been isolated from different species of the genus *Chaetomium*, from pure cultures *in vitro* and in association with the plant *Helichrysum aureonitens* in nature [21]. Although it has been demonstrated that other THF derivatives are endowed with antiviral activity [23–25], including against influenza [26], the effects of aureonitol on influenza replication have not been characterized. We show here that aureonitol inhibits influenza replication by targeting conserved residues on HA.

Materials and Methods

Compound

The THF derivative aureonitol (Fig 1) was isolated from mycelium plugs obtained from *in vitro* cultures of the fungus *Chaetomium coarctatum* and identified as previously described [21, 27–30]. A voucher of the specimen was deposited on the Filamentous fungal collection (IOC--FIOCRUZ; CCFF/IOC-4613). Aureonitol, at over 99% purity, was diluted in 100% dimethyl sulfoxide (DMSO) and stored at– 20°C. The resulting DMSO concentrations during the assays were below 0.1%, a level that is not significantly cytotoxic.

Cells and viruses

Madin-Darby Canine Kidney cells (MDCK), donated by Influenza Reagent Resource (IRR; http://www.influenzareagentresource.org/) to the Brazilian National Influenza Center (NIC), were cultured with Minimum Essential Eagle's Medium (MEM; LGC Biotecnologia, São Paulo,

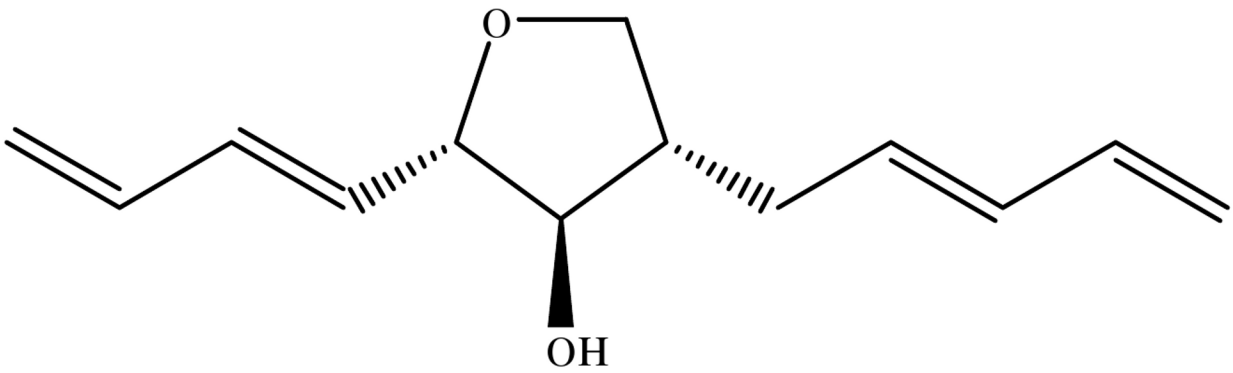

Fig 1. Chemical structure of aureonitol.

doi:10.1371/journal.pone.0139236.g001

Brazil). Human embryonic kidney 293 cells (HEK293) were cultured with Minimum Dulbecco ´s Modified Eagle Medium (DMEM; LGC Biotecnologia, São Paulo, Brazil) and used in transfection assays. These culture were supplemented with 10% fetal bovine serum (FBS; HyClone, Logan, UT, USA), 100 U/mL penicillin and 100 mg/mL streptomycin (Sigma-Aldrich). The cells were cultured at 37°C in a 5% CO_2 atmosphere. A list of all the influenza A and B strains used in this study is presented in the supporting information file (Table A in S1 File). Experiments were conducted using either a laboratory-adapted strain or clinical isolates (Table A in S1 File). These viruses were grown in MDCK cells [31]. Viral stocks were aliquoted and stored at -70°C for further studies.

Cell viability

Confluent (2 x 10^4 cell/well) or semi-confluent (2 x 10^3 cell/well) monolayers of MDCKs in 96-well culture plates were incubated with the compounds at different concentrations for 72 h. Then, 2,3-Bis-(2-Methoxy-4-Nitro-5-Sulfophenyl)-2*H*-Tetrazolium-5-Carboxanilide (XTT) at 5 mg/ml was added to the DMEM in the presence of 0.01% N-methyl-dibenzopirazina methyl sulfate (PMS). After incubation for 4 h at 37°C, the plates were read in a spectrophotometer at 492 nm and 620 nm [32]. The 50% cytotoxic concentration (CC_{50}) was calculated by performing a linear regression analysis on the dose—response curves generated from the data.

Yield reduction assay

Monolayers of MDCK cells (2 x 10^5 cell/well) in 24-well plates were infected with influenza at different MOIs for 1 h at 37°C. The cells were then washed to remove residual viruses and varying concentrations of the compounds were added. At different time points after infection, viruses in the supernatant were harvested and titrated by end-point 50% cell culture infective dose ($TCID_{50}$/mL) using MDCK cells (5x10^4 cells/well in 96-well plates) [33, 34]. For comparison, the reference compound oseltamivir carboxylate (OST; kindly donated by Hoffman-La Roche Inc., Basel, Switzerland) was used as a control. Non-linear regression of the dose-response curves was performed to determine the 50%, 90% and 99% inhibitory effects on viral replication (EC_{50}, EC_{90} and EC_{99}, respectively) for the tested and reference compounds.

Measurements of influenza attachment/entry

Monolayers of 2 x 10^6 cells in 6-well plates were incubated with different concentrations of aureonitol in the presence of influenza (MOI = 1) for 1 h at 4°C, a condition that allows only virus adsorption. Then, the cultures were washed with PBS, lysed with buffer A (10 mM HEPES, 1.5

mM $MgCl_2$, 10 mMKCl, 0.5% NP-40, 1 mM DTT, 0.5 mM PMSF) and centrifuged (10 min. at 1000 x *g*). The resulting supernatant, which contained the plasma membrane, was submitted for quantitative RT-PCR to detect virus genome from particles that were able to adsorb onto the cells [35]. Quantitative RT-PCR to detect influenza A was performed based on the standard curve method described elsewhere [35]. A plasmid containing the influenza gene M1 was used as the reference. Notably, controls to verify the purity of the RNA preparations were performed to detect the housekeeping transcripts GAPDH, RNAse P, β-actin and long non-coding RNA (lncRNA). As expected, the supernatants were free of the nuclear exclusive transcript lncRNA (Fig A in S1 File) [35, 36].

Alternatively, HEK293 were transfected using lipofectamine 2000® with pCDNA 3.1 (+) containing the influenza HA insert between HindIII and XhohI sites (encoding for either HA types H1, H3 or B of the viruses shown in Table A in S1 File). These cells were also co-transfected with a retrovirus expressing the vector plasmid pNL4-3.Luc.R-.E- (NIH AIDS Reagent Program; https://www.aidsreagent.org/index.cfm). This last plasmid encodes for luciferase and HIV-1 proteins, except for those associated in the envelope, and Vpr. At 24 h after co-transfection, the cells were treated with 50 U/mL of NA from *Clostridium perfinges* (Sigma-Aldrich) to release tethered pseudotyped viruses. Next, pseudotyped viruses were concentrated under centrifugation with Centricon membranes to remove particles $<$ 100 kDa. These viruses were quantified by ELISA against the retroviral antigen (Ag) p24 (Zeptometrix). Infection assays with pseudotyped viruses were performed with doses equivalent to 10 ng/ml of p24 Ag.

To evaluate the effects of aureonitol on influenza attachment/entry, we tested the following three different approaches with pseudotyped viruses: cells and pseudotyped viruses were treated simultaneously (a), cells were treated prior to infection with a pseudotyped virus (b), or pseudotyped viruses were treated with the compound prior to cellular infection (c). In protocol (a), MDCKs (10^5 cell/well) in 24-well plates were exposed to the pseudotypes virus (10 ng/ml of p24 Ag) and simultaneously treated with different concentrations of aureonitol for 1 h at 4°C; under these conditions, viruses bind but are not able to enter the cells. Next, the cells were washed with PBS, covered with DMEM containing 5% FBS, and the temperature was raised to 37°C for 3 h [8]. After this period, the cells were lysed and luciferase activity was measured with Promega's kit, according to manufacturer's instructions. When we raised the temperature to 37°C, only the bound virus particles were able to penetrate and replicate; however, if aureonitol blocked influenza attachment/entry, less virus would enter, and consequently the luciferase activity would be reduced at 3 h after infection. In protocol (b), the same number of cells were pre-treated for 1 h at 37°C with aureonitol at different concentrations and then washed with PBS. The cells were subsequently exposed to pseudotyped virus for 1 h at 4°C, washed with PBS again, and then incubated in DMEM with 5% FBS for 3 h. Finally, the cells were lysed, and luciferase activity was measured, as described above. In protocol (c), different concentrations of aureonitol were prepared, and these solutions were diluted in PBS containing pseudotyped viruses. These solutions were incubated for 1 h at room temperature, after which the appropriate dilutions were added to monolayers of MDCKs for 1 h to infect the cells with virus. After infection, the cells were washed with PBS and incubated in DMEM with 5% FBS for 3 h. The cells were then lysed and the virus was tittered, as in protocol (a). For comparison, we also employed protocols (a), (b) and (c) to analyze the effects of OST and specific anti-sera as negative and positive controls, respectively.

NA inhibition assay

To evaluate the ability of the compound to inhibit influenza NA activity, we performed cell-free assays using the NA-Star kit (Life Technologies, CA) according to the manufacturer's

instructions. Briefly, influenza NA activity was titrated and then measured in the presence of different concentrations of the compound to quantify enzyme inhibition. The concentration able to inhibit 50% of influenza`s NA activity (IC_{50}) was calculated using a non-linear regression. For comparison, every assay was performed with OST carboxylate as a positive control.

HA inhibition assay

Hemagglutination inhibition assays (HAI) were performed according to the protocol recommended by the World Health Organization (WHO) [37,38]. Briefly, aureonitol or the reference sera against the influenza virus (CDC/Atlanta; WHO Collaborating Center for influenza), were treated with receptor destroying enzyme (RDE; Denka-Seiken, Japan) to inhibit nonspecific hemagglutination inhibitors. These sera were then incubated with 4 HAU of influenza HA along with guinea pig red blood cells (RBC) at a concentration of 0.5% for 1 h. After this incubation, HAI was read. The results are expressed as the reciprocal of the highest dilution that inhibited hemagglutination for the control sera and as the minimal inhibitory concentration (MIC) for aureonitol.

Molecular studies of aureonitol`s docking site

To perform *in silico* studies, the structure of aureonitol was designed using Accelrys Draw 4.1 software (Accelrys, Inc), hydrogens were added and the geometry was optimized. Aureonitol was docked into different regions of HA, encompassing the entire protein structure. Alternatively, aureonitol was docked only in predetermined active sites of HA. To perform these experiments, we used the "Dock a Ligand" option in Arguslab 4.0.1 (Planaria Software LLC) [39]. The crystal structures of HA proteins representative of the strains used in this study were also analyzed (Table B in S1 File). These structures are available from the Protein Data Bank (PDB; http://www.rcsb.org) [40]. A spacing of 0.4 Å between the grid points was used. The ligand was assumed to be flexible while the protein was assumed to be rigid. A maximum of 150 poses were analyzed, and each docking run was repeated three times to obtain the best results. The binding site box was set to 25 × 25 × 25 Å to encompass the entire active site of the enzyme. The results were analyzed using PoseView software[41,42].

Statistical analysis

The dose-response curves used to calculate the pharmacological parameter values were generated using Excel for Windows [42]. When appropriate, Student`s-t-test was used to evaluate significant differences, with $P < 0.05$ set as the threshold for significance. All of the experiments were performed at least three times, and the results are displayed as the mean ± standard error of the mean (SEM).

Results

Aureonitol inhibits influenza replication in a dose-, MOI- and time-dependent fashion

Because aureonitol is a THF derivative, and other compounds with this basic chemical structure may possess antiviral activity, we evaluated aureonitol's ability to inhibit influenza replication. Aureonitol inhibited influenza replication 24 h after infection with the A(H3N2) subtype in a dose-dependent fashion, with EC_{50} values of 30, 100 and 183 nM at MOIs of 0.01, 0.05 and 0.01, respectively (Table 1, Figs B-D in S1 File). At 48 h after infection, aureonitol's potency was slightly reduced, as the obtained EC_{50} values were 48, 121 and 201 nM for MOIs of 0.01, 0.05 and 0.1, respectively (Table 1, Figs B-D in S1 File). For comparison, at 24 post-infection

Table 1. MOI- and time-dependent inhibition of influenza replication by aureonitol.

	EC_{50} (nM)			
	24 h		48 h	
MOIs	Aureonitol	OST	Aureonitol	OST
0.1	183 ± 21	49 ± 2.6	201 ± 13	56 ± 3.1
0.05	100 ± 16	30 ± 2.3	121 ± 18	38 ± 2.8
0.01	30 ± 3.4	12 ± 0.9	42 ± 3.9	28 ± 1.1

doi:10.1371/journal.pone.0139236.t001

OST presented EC_{50} values of 12, 30 and 49 nM for MOIs of 0.01, 0.05 and 0.1, respectively (Table 1, Figs B-D in S1 File). At 48 h after infection, the EC_{50} concentration for OST also increased slightly to 28, 38 and 56 nM for MOIs of 0.01, 0.05 and 0.1, respectively (Table 1, Figs B-D in S1 File). Similar observations were also made based on the pharmacological parameters of antiviral effect 90 and 99% (Table C in S1 File). Together, these results indicate that, although OST is more potent than aureonitol, both compounds act at nanomolar concentrations and are potent against influenza replication *in vitro*.

Next, we evaluated aureonitol's efficacy against circulating strains of influenza A and B. Aureonitol inhibited the replication of the laboratory-adapted and clinically isolated strains of influenza A(H3N2) with similar efficiencies, although it was three times more potent against the laboratory-adapted virus (Table 2, Table D and Fig E-H in S1 File). Similarly, aureonitol also inhibited Influenza A(H1N1)pdm09 replication with an efficiency that was not significantly different than that observed for the influenza A(H3N2) viral strains (Table 2, Table D and Figs E-H in S1 File). Again, the doses to inhibit replication of the clinical isolates by 50% were four-times higher than the EC_{50} for the laboratory-adapted strain (Table 2, Table D and Figs E-H in S1 File). Although inhibition of influenza B replication was achieved with aureonitol, the pharmacological parameters for potency and efficiency were higher than those observed for the influenza A subtypes (Table 2, Table D and Figs E-H in S1 File). As a control, OST was used in all experiments (Table 2, Table D and Figs E-H in S1 File). The reference compound was more potent and efficient than aureonitol by 10- and 100-times, respectively. Nevertheless, our data indicate that aureonitol's chemical structure is promising for the future development of novel influenza antivirals.

Aureonitol is safe to be used *in vitro*

Aureonitol had very low cytotoxicity, similar to OST; these compounds had CC_{50} values of 1426 ± 13 μM and 2132 ± 26 μM, respectively (Fig 2A) when tested in cell cultures that were 100% confluent. When the cytotoxicity was tested at 60% confluency, the CC_{50} values

Table 2. Antiviral activity of Aureonitol against influenza A and B viruses.

Influenza Type (subtypes)	EC_{50} (nM)		EC_{90} (nM)		EC_{99} (nM)	
	Aureonitol	OST	Aureonitol	OST	Aureonitol	OST
A(H3N2)*	100 ± 16	30 ± 2.3	3000 ± 236	90 ± 14	3091 ± 168	98 ± 8
A(H3N2)	312 ± 23	32 ± 2.1	2801 ± 123	92 ± 16	2912 ± 322	112 ± 13
A(H1N1)pdm09	417 ± 30	12 ± 1.9	2008 ± 212	78 ± 9	2023 ± 113	92 ± 7
B	2012 ± 87	52 ± 7.1	15876 ± 432	132 ± 25	16789 ± 455	155 ± 18

*Laboratory-adapted influenza A(H3N2).

doi:10.1371/journal.pone.0139236.t002

A

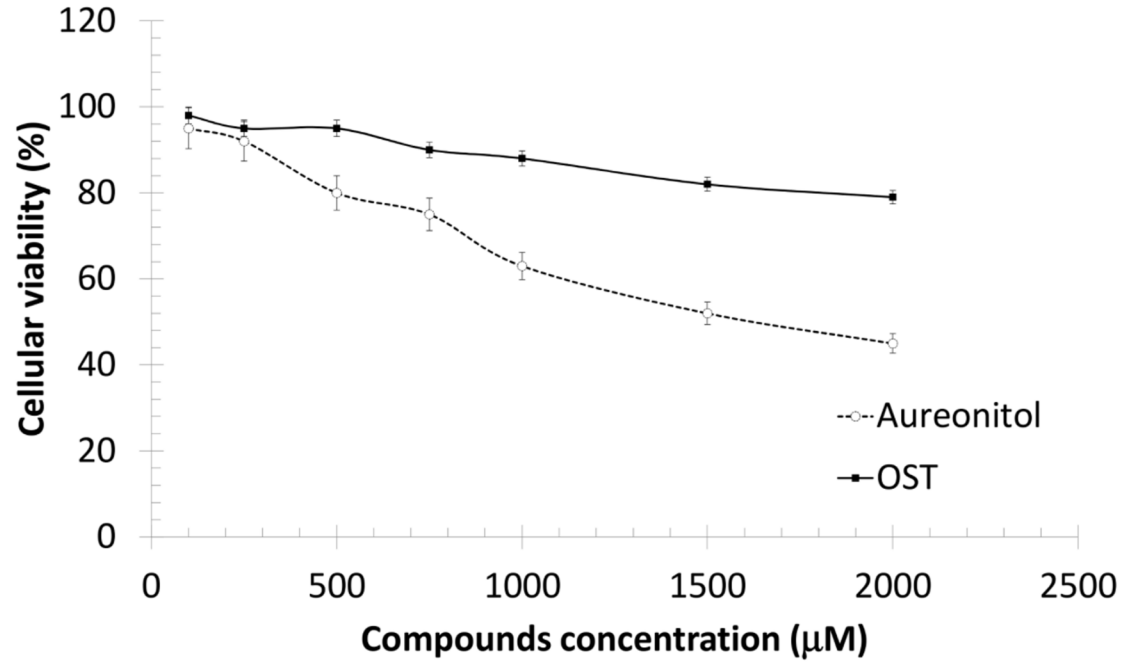

B

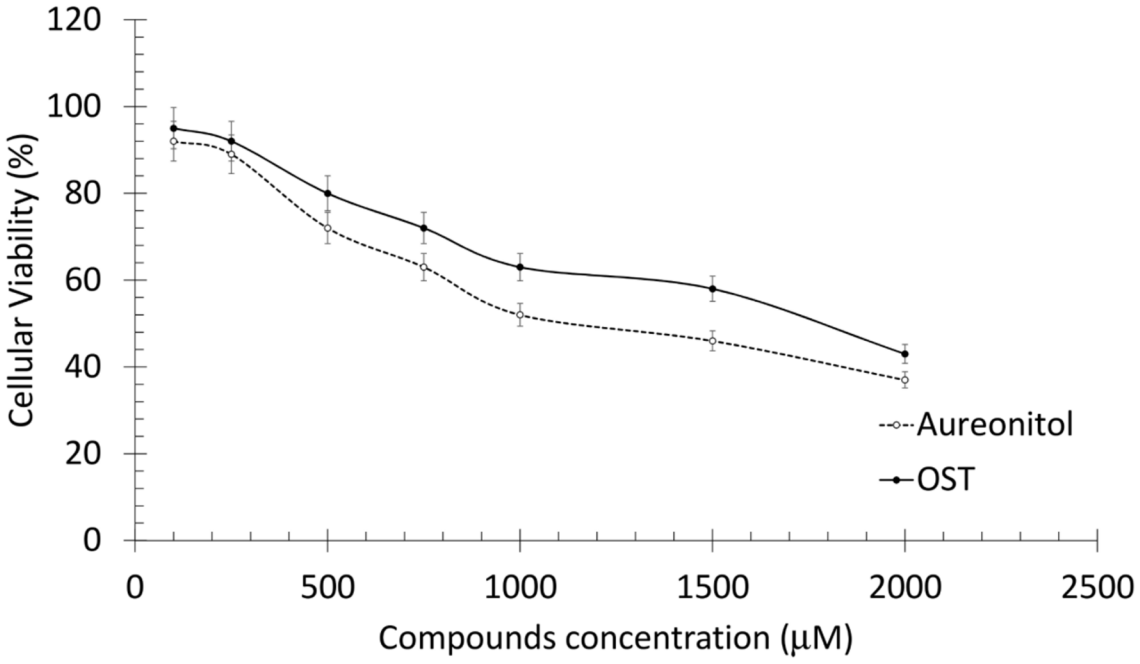

Fig 2. Cytotoxicity of aureonitol. MDCKs were seeded at full confluence (2 x 10^4 cells) (A) or semi-confluence (2 x 10^3 cells) (B) in 96-well plates. The cells were then incubated with the indicated concentrations of the compound for 72 h, after which XTT (5 mg/ml) and PMS (0.01%) were added. After 4 h of incubation, the plates were read at 492 nm and 620 nm. Experiments from both panels were performed 5 times in triplicate.

doi:10.1371/journal.pone.0139236.g002

decreased to 1357 ± 19 μM for aureonitol and 1683 ± 32 μM for OST (Fig 2B). The selectivity index (SI), which is the ratio between the CC_{50} and EC_{50} values, for aureonitol and OST varied due to the different potencies of these drugs against the influenza viruses used (Table 3). Although OST's SI value was higher than that observed for aureonitol, our molecule's SI value indicates that it is still very safe to be used *in vitro*, as the threshold of cytotoxicity is thousands of times higher than the antiviral potency (Table 3).

Aureonitol inhibits hemagglutination, but not NA activity, and consequently impairs influenza entry

Influenza surface glycoproteins HA and NA are responsible for viral entry and release, respectively [43]. Moreover, these proteins are validated anti-influenza targets [44, 45]. Aureonitol inhibited hemagglutination with MICs ranging from 60 to 200 nM (Table 4) for the various influenza A and B strains used. As a control, standard serum raised in sheep against the different influenza types and subtypes were tested and inhibited hemagglutination with appropriate dilution (Table 4). The correlation between aureonitol's potency over hemagglutination and viral replication inhibition was comparable (i.e., both pharmacological parameters revealed potencies in the nanomolar range). This good correlation could indicate that hemagglutination inhibition is aureonitol's target on the influenza life cycle [46, 47].

To monitor the anti-hemagglutination activity of aureonitol in a functional way, we performed a series of adsorption inhibition assays. From the results, it is apparent that aureonitol inhibited influenza attachment/entry either when the viruses were pretreated with the compound or when the viruses and cells were treated simultaneously (Fig 3A). On the other hand, pre-treatment of the cells had no effect on the inhibition of influenza attachment/entry (Fig 3B). These results suggest that aureonitol targets a viral, rather than a cellular structure, with primary importance to attachment/entry. This finding is consistent with the hemagglutination inhibition promoted by our compound. As a positive control, specific sera against the influenza A(H3N2) pseudotyped virus displayed the same results as aureonitol (Fig 3A). The negative control, OST had no relevant effect on influenza attachment/entry (Fig 3A). Aureonitol is able to inhibit influenza attachment/entry for different subtypes of influenza A and influenza B to different degrees (Fig 3B). Finally, we evaluated whether our compound could decrease influenza attachment onto cells, using virus infectivity assays with real rather than chimeric viruses. Indeed, aureonitol significantly blocked influenza adsorption at both suboptimal and optimal concentrations (Fig 3C). These results confirm that aureonitol is endowed with a mechanism of action that is different from most anti-influenza drugs in clinical use.

Nevertheless, we tested whether aureonitol inhibits influenza NA activity because another THF derivative is known to have such an activity [26]. Aureonitol had no effect on this enzyme activity (Fig 4), even when tested at 1000 nM (10 times its EC_{50}). As a control, OST inhibited NA activity with an IC_{50} value of 0.1 ± 0.012 nM (Fig 4).

Aureonitol docked on conserved amino acid residues on HA

To gain insight on the aureonitol docking site, we performed *in silico* studies. We evaluated the entire influenza HA structure by docking aureonitol at each of the 19 amino acid residues to better comprehend the most likely binding site. We observed that the free binding energies were lower in the sialic acid binding site, also known as the receptor binding site (RBS) in the three-dimensional receptor binding domain (Fig 5A). Surprisingly, aureonitol binding was versatile, showing higher free energies for other areas of the influenza HA (Fig 5A). To confirm aureonitol docking in the RBS, its binding was specifically evaluated in the binding sites of 2-O-methyl-5-N-acetyl-α-D-neuraminic acid (MNA), β-D-manose (BMA), and N-acetyl-D-

Table 3. Selectivity index of Aureonitol for Influenza A and B viruses.

Influenza types (subtypes)	EC50 (μM)		CC50 (μM)		SI	
	Aureonitol	OST	Aureonitol	OST	Aureonitol	OST
A(H3N2)*	0.100	0.030	1426	2132	14260	71067
A(H3N2)	0.312	0.032	1426	2132	4571	66625
A(H1N1)	0.417	0.012	1426	2132	3420	177667
B	2.012	0.052	1426	2132	709	41000

*Laboratory-adapted influenza A(H3N2).

doi:10.1371/journal.pone.0139236.t003

glucosamine (NGA). MNA is docked in the RBS, whereas BMA and NGA were used as negative controls. As shown in Fig 5B, the free binding energy was lower for aureonitol`s docking at the MNA binding site, indicating that our compound nestled most spontaneously in this site (Fig 5C). Aureonitol`s docking site is located in HA`s globular head in an area that is rich in amino acid residues that are conserved for most of influenza strains[48, 49]. Aureonitol interacted by hydrogen bonding with the amino acids Tyr98, His183, Glu190 and Ser228 (Fig 5D and Table E in S1 File), which are critical for HA-cellular receptor interactions during influenza entry [49].

Because the HA structure used to bind aureonitol is derived from the laboratory-adapted strain of influenza A(H3N2) used in our study, we also evaluated aureonitol docking in the HA structures of other influenza viruses. Interestingly, aureonitol docked in the influenza A (H3N2) HA, a viral structure that is closer to the clinically isolated strain used in our investigation, with the polymorphism E190D (Fig 5E and Table E in S1 File) and used the amino acid residues mentioned in the paragraph above, except for the Glu190. For influenza A(H1N1) pdm09, aureonitol formed hydrogen bonds with the polymorphic residue Asp190 and Gln226, in addition to the residues mentioned in the first structure (Fig 5F and Table E in S1 File). With influenza B HA, aureonitol formed fewer hydrogen bonds, targeting the Arg202 and Thr139 residues (Fig 5G and Table E in S1 File). In addition to hydrogen bonds, other weak interactions were also observed between aureonitol and the HAs analyzed (Table E in S1 File). The free binding energies to dock aureonitol in the different HAs were proportional to the number of hydrogen bonds formed (Fig 5H and Table E in S1 File), indicating that aureonitol binds more spontaneously to influenza A(H3N2) and A(H1N1)pdm09 than to influenza B. These results predict the most likely binding site of aureonitol in the HA structure and highlight that this molecule is a promising candidate for the development of novel anti-influenza drugs.

Table 4. Anti-hemagglutination activity of Aureonitol against influenza A and B.

Influenza types (subtypes)	Minimal inhibitory concentration or reverse dilution	
	Aureonitol (nM)	Specific anti-sera
A(H3N2)*	100	1024
A(H3N2)	120	512
A(H1N1)	60	1024
B	400	512

*Laboratory-adapted influenza A(H3N2).

doi:10.1371/journal.pone.0139236.t004

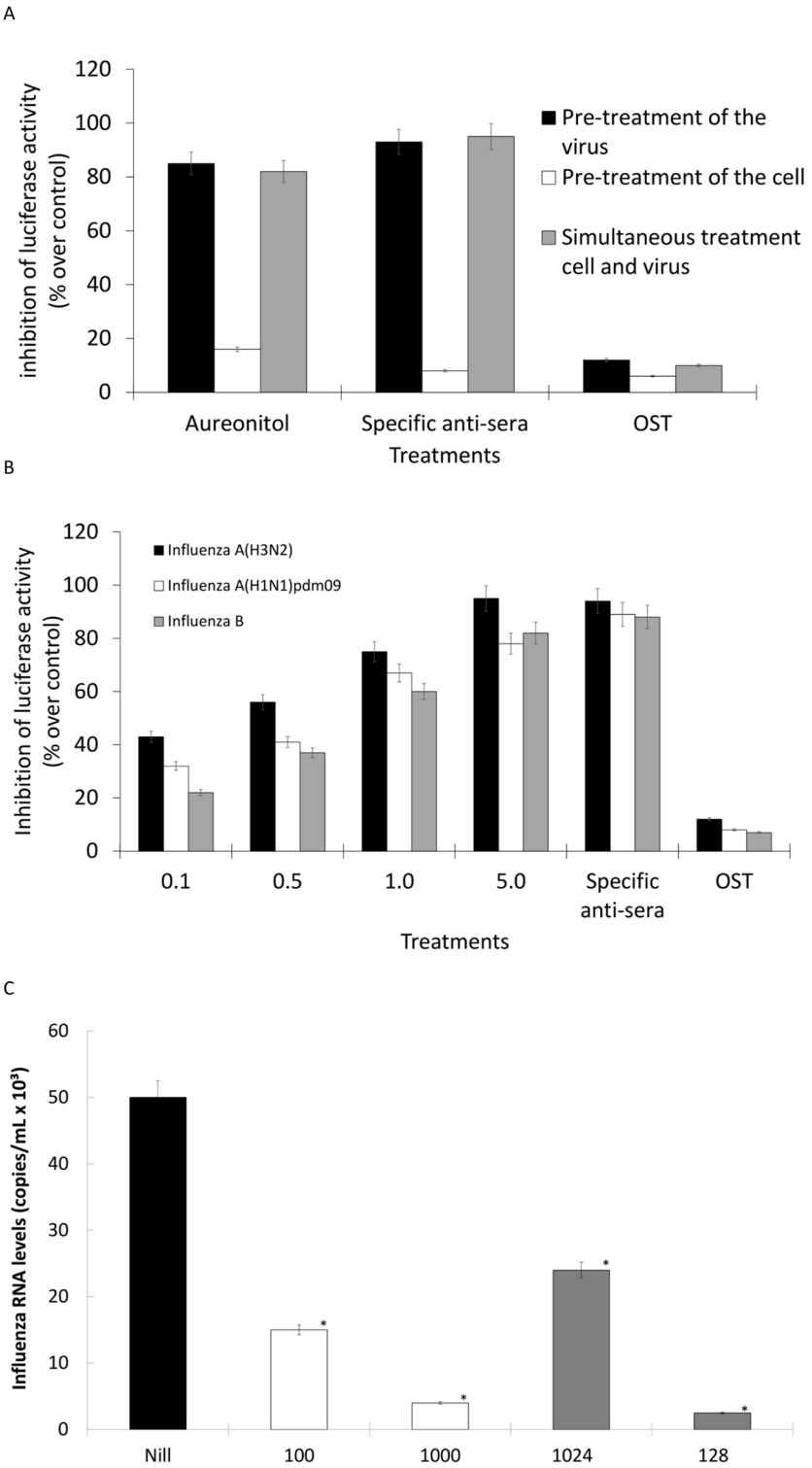

Fig 3. Effects of aureonitol on influenza attachment/entry. (A) Virus particles were pre-treated for 1 h at room temperature. This mixture was diluted and incubated with MDCK cells for 1 h at 37°C (black bar). MDCK cells were pre-treated for 1 h at 37°C and washed. The cells were then exposed to pseudotyped influenza for 1 h at 4°C, washed again, and the temperature was shifted to 37°C (white bar). MDCK cells were exposed to the indicated influenza pseudotyped virus and treated for 1 h at 4°C. The cells were then washed with PBS and the temperature was raised to 37°C (gray bars). (B) Using the last treatment approach, pseudotyped

influenza viruses representative of the indicated strains were used, and different concentrations of aureonitol were evaluated. (C) MDCKs (2 x 10^6 cells) were infected with influenza at a MOI of 1.0 for 1 h at 4°C in the presence of the indicated treatments. After that, the cells were washed, lysed with buffer A and centrifuged (10 min. at 1000 x *g*). RNA was extract from the supernatant fraction, and quantitative RT-PCR to detect influenza A genome was performed. In panels A and B, luciferase activity was measured with a commercial kit (Promega). In panel C, the standard curve method was employed using a plasmid containing the influenza M1 gene as a reference. The experiments were performed 4 times. *$P < 0.01$.

doi:10.1371/journal.pone.0139236.g003

Discussion

Influenza viruses cause a recurrent public health problem for populations who are at higher risk for serious illness, such as newborns, the elderly, pregnant women and immunocompromised individuals [1–3], and constantly impose threats of pandemic outbreaks[1–3]. Antiviral drugs against influenza are essential to fight both seasonal and pandemic infections[1–3]. Because influenza antivirals are more effective when administered within the first days after the onset of illness[50], stockpiling of anti-influenza drugs that can be used as the first line of

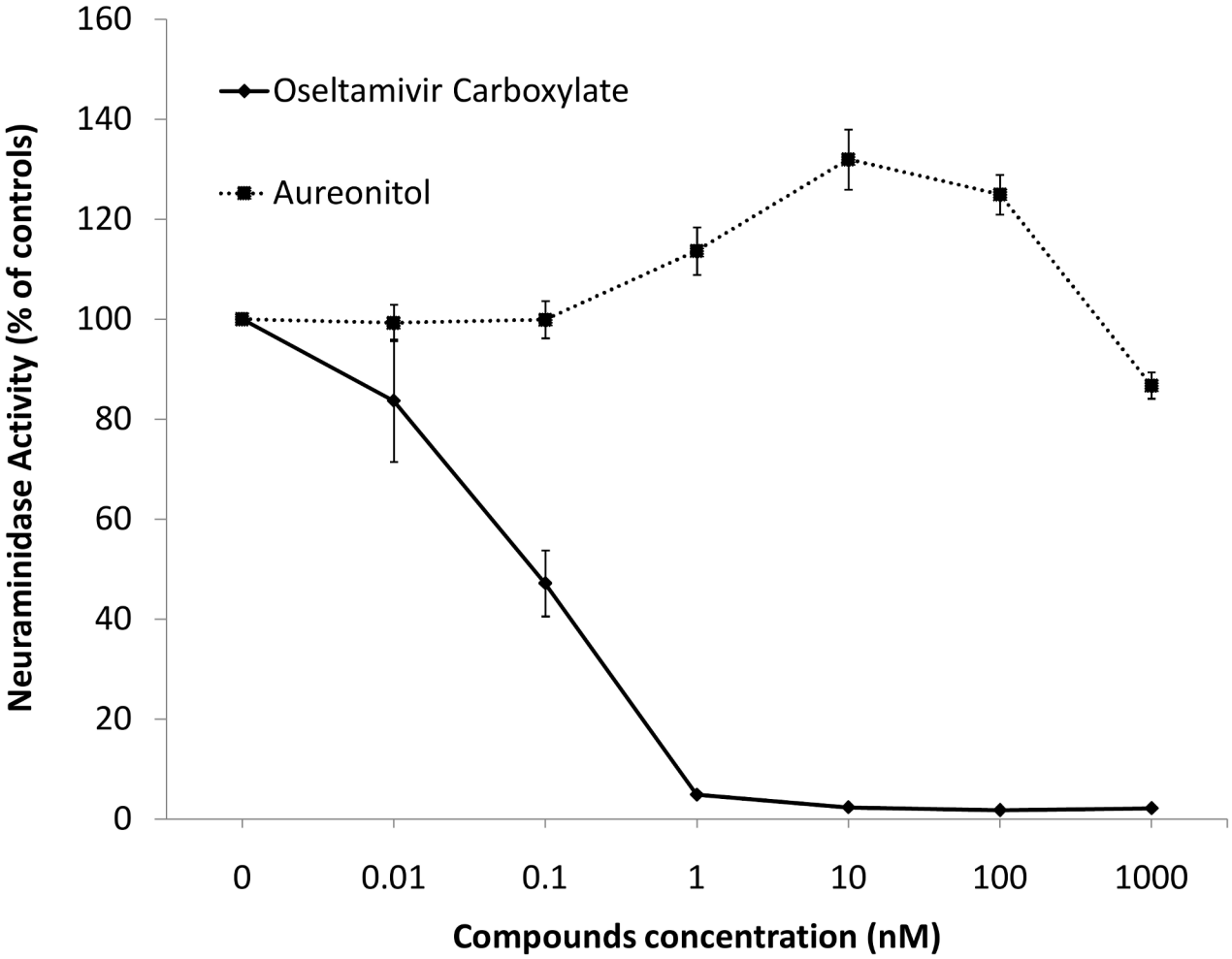

Fig 4. Aureonitol does not inhibit influenza NA activity. The NA activity of the influenza A H3N2 virus was measured in the presence of the indicated concentrations of aureonitol or the reference compound OST-c using a chemiluminescent substrate, NA-star kit (Applied Biosystems, CA). The results were obtained in relative luminescence units (RLU) but were converted to a percentage of the control for normalization of the data displayed. This experiment was performed 4 times.

doi:10.1371/journal.pone.0139236.g004

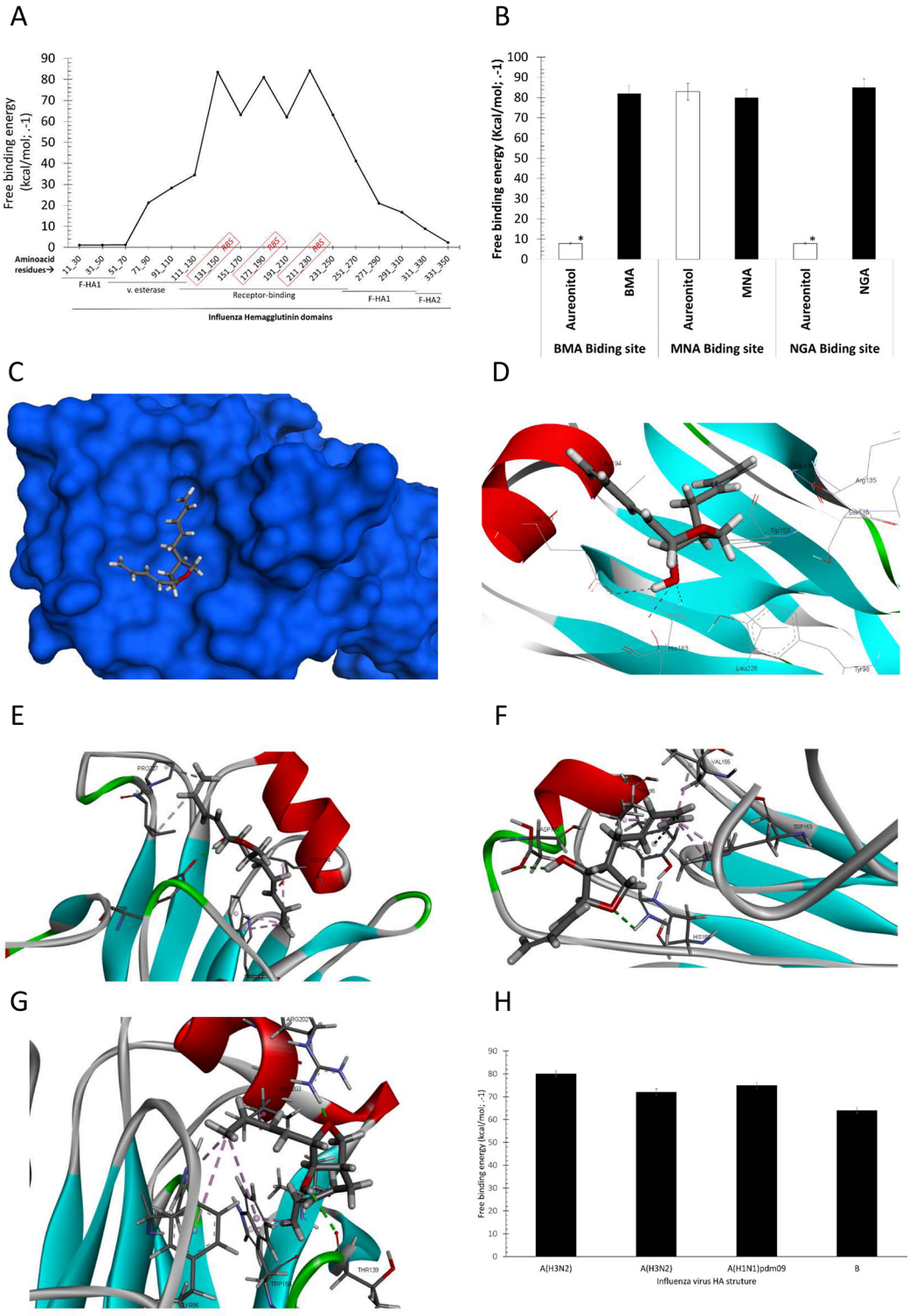

Fig 5. *In silico* analysis of aureonitol docked to influenza HA. (A) Aureonitol was docked over all 19 amino acid residues of influenza A(H3N2) HA (pdb #1HGE). (B) Aureonitol was docked on the BMA, MNA and NGA binding sites, using these molecules as a reference. (C) Crystal structure of the H3 isoform mentioned above (blue) and aureonitol (gray) docked in the globular head of HA, the sialic acid binding site. Aureonitol interacts with conserved amino acid residues by hydrogen and Pi-Alkalyl bonds with HAs representative of laboratory-adapted influenza A(H3N2) (D) and clinically isolated influenza A(H3N2) (E), influenza A(H1N1)pdm09 (F) and Influenza B (G). Free binding energies were calculated for the interactions between aureonitol and each HA structure used in panels D through G (H). Docking was performed three times. *$P < 0.01$ indicates significant differences.

doi:10.1371/journal.pone.0139236.g005

defense against a novel virus is a key step in pandemic preparedness. Moreover, considering the emergence of drug-resistant strains of influenza, the search for molecules that are able to inhibit the influenza life cycle at different steps than molecules currently in clinical use is pivotal. Here, we show that aureonitol, a fungi-derived natural product, inhibits influenza attachment/entry by targeting conserved amino acid residues on the viral surface glycoprotein HA.

Aureonitol inhibited influenza replication at nanomolar concentrations and with very low cytotoxicity. Consequently, aureonitol presented a very safe range to be used *in vitro*. Our compound was approximately 100-times more potent than other fungi-derived natural products previously studied against influenza[51, 52]. Aureonitol's chemical structure has a THF ring, and other molecules with this same ring have shown antiviral activity [23–26], including against influenza NA. Notably, under our experimental conditions, no anti-NA activity of aureonitol was been observed.

When compared to other influenza inhibitors that are in clinical use, such as OST, aureonitol was slightly less potent. Nevertheless, OST and aureonitol possess different mechanisms of action. Whereas OST blocks the spread of influenza by inhibiting the viral enzyme NA, aureonitol impairs influenza entry by targeting the viral HA. Importantly, circulating strains of influenza are resistant to adamantanes, and approximately 2% are resistant to OST [11, 12]. Thus, the effect of aureonitol on a different step of the virus life cycle may be of great interest. Other investigators have previously attempted to block virus entry by targeting influenza HA. An example is the promising new compound Flufirvitide-3, which is currently being tested in clinical trials [53]. Another molecule, arbidol, which is an indole ring with substituents in almost all positions, also inhibits influenza replication by targeting the viral HA [54]. Although arbidol is not approved for clinical use in western countries, it is being used clinically in Russia and China [45, 54, 55].

Aureonitol binds in versatile ways to influenza HA at the sialic acid binding site in the RBD. This pocket in the HA structure is responsible for binding the sialic acid residues on cell surfaces for influenza entry [56]. Therefore, the sialic acids binding site is extremely conserved in HA, even in influenza strains carrying mutated HA that escapes the host immune response. In HA's sialic acid binding site, the conserved amino acid residues His183, Tyr98 and Glu190 have polar side chains and interact with the receptor by hydrogen bonding, while Trp153, Leu194 and Leu226 have non-polar side chains that facilitate receptor binding through Van Der Waals interactions [56]. Our results suggest that aureonitol disrupts these interactions between influenza HA and sialic acid, which could result in a much weaker interface between the virus and cell surface, thereby preventing viral entry. Considering that the conserved amino acid residues in influenza HA are responsible for viral entry along with the molecular modeling results for aureonitol, it is possible that influenza strains resistant to our compound might lose fitness/virulence. This possibility is currently under investigation in our laboratories.

Since natural products are a fruitful source of chemically rich compounds, our laboratory has been studying the antiviral activity of these molecules [28, 57–60]. In this article, we pay special attention to the antiviral activity of fungi-derived natural products, which may have been overlooked in the literature. Interestingly, fungi members of the genus *Chaetomium* have been isolated from traditional medicinal plants from China and India and are recognized to be the organisms producing the bioactive compounds [61, 62]. Aureonitol is produced by different species of the genus *Chaetomium* [63]. When compared to other natural products, aureonitol possesses some advantageous features. Different species of *Chaetomium* produce aureonitol with over 70% yield[63], and organic synthesis of aureonitol has be proven to be successful [21]. Because these characteristics indicate the feasibility of scaling up aureonitol production and our result show that this molecule inhibits influenza replication by targeting viral entry via

conserved residues on HA, aureonitol's chemical structure may be of interest for further development of anti-influenza drugs.

Supporting Information

S1 File. Includes all the supporting Information, Tables A-E and Figs A-H and their legends.
(RAR)

Acknowledgments

Thanks are due to the Influenza Reagent Resource (IRR; http://www.influenzareagentresource.org/), the Centers for Disease Control (CDC/Atlanta; WHO Collaborating Center for influenza) and Hoffman-La Roche Inc., Basel, Switzerland for donating materials to conduct this investigation.

Author Contributions

Conceived and designed the experiments: CQS AM MENR CRK KFR GLC CMA OSF JPB TMLS. Performed the experiments: CQS NFR CSF GRM AM MENR CMA OSF. Analyzed the data: CQS AM MENR CRK KFR GLC CMA OSF JPB TMLS. Wrote the paper: CQS MENR TMLS.

References

1. Damjanovic D, Small CL, Jeyanathan M, Jeyananthan M, McCormick S, Xing Z. Immunopathology in influenza virus infection: uncoupling the friend from foe. Clin Immunol. 2012; 144(1):57–69. doi: 10.1016/j.clim.2012.05.005 PMID: 22673491.
2. Murphy BR, Webster RG. Orthomyxoviruses. 3rd ed. Fields BNKDMHIPMCRMMJLMTPRBSSE, editor. Philadelphia: Lappincott-Raven Publishers; 1996.
3. Tang JW, Shetty N, Lam TT, Hon KL. Emerging, novel, and known influenza virus infections in humans. Infect Dis Clin North Am. 2010; 24(3):603–17. doi: 10.1016/j.idc.2010.04.001 PMID: 20674794.
4. Kollerova E, Betakova T. Influenza viruses and their ion channels. Acta Virol. 2006; 50(1):7–16. Epub 2006/04/08. PMID: 16599180.
5. Das K, Aramini JM, Ma LC, Krug RM, Arnold E. Structures of influenza A proteins and insights into antiviral drug targets. Nat Struct Mol Biol. 2010; 17(5):530–8. Epub 2010/04/13. nsmb.1779 [pii] doi: 10.1038/nsmb.1779 PMID: 20383144.
6. Manz B, Schwemmle M, Brunotte L. Adaptation of avian influenza a virus polymerase in mammals to overcome the host species barrier. J Virol. 2013; 87(13):7200–9. Epub 2013/04/26. JVI.00980-13 [pii] doi: 10.1128/JVI.00980-13 PMID: 23616660.
7. WHO. Recommended composition of influenza virus vaccines for use in the 2014 southern hemisphere influenza season. Wkly Epidemiol Rec. 2013; 88(41):437–48. PMID: 24159667.
8. Balicer RD, Huerta M, Davidovitch N, Grotto I. Cost-benefit of stockpiling drugs for influenza pandemic. Emerg Infect Dis. 2005; 11(8):1280–2. Epub 2005/08/17. doi: 10.3201/eid1108.041156 PMID: 16102319.
9. Patel A, Gorman SE. Stockpiling antiviral drugs for the next influenza pandemic. Clin Pharmacol Ther. 2009; 86(3):241–3. Epub 2009/08/27. clpt2009142 [pii] doi: 10.1038/clpt.2009.142 PMID: 19707215.
10. Hurt AC. The epidemiology and spread of drug resistant human influenza viruses. Curr Opin Virol. 2014; 8C:22–9. doi: 10.1016/j.coviro.2014.04.009 PMID: 24866471.
11. Fry AM, Gubareva LV. Understanding influenza virus resistance to antiviral agents; early warning signs for wider community circulation. J Infect Dis. 2012; 206(2):145–7. Epub 2012/05/09. jis338 [pii] doi: 10.1093/infdis/jis338 PMID: 22561368.
12. Hurt AC, Hardie K, Wilson NJ, Deng YM, Osbourn M, Leang SK, et al. Characteristics of a widespread community cluster of H275Y oseltamivir-resistant A(H1N1)pdm09 influenza in Australia. J Infect Dis. 2012; 206(2):148–57. Epub 2012/05/09. jis337 [pii] doi: 10.1093/infdis/jis337 PMID: 22561367.

13. Ellis D, Alexiou H, Handke R, Bartley R. *Chaetomium* Kunze ex Fries. Description of Medical Fungi. 2ª ed. Adelaide2007. p. 41.
14. Zhang Q, Li HQ, Zong SC, Gao JM, Zhang AL. Chemical and bioactive diversities of the genus Chaetomium secondary metabolites. Mini Rev Med Chem. 2012; 12(2):127–48. PMID: 22372603.
15. Park JH, Choi GJ, Jang KS, Lim HK, Kim HT, Cho KY, et al. Antifungal activity against plant pathogenic fungi of chaetoviridins isolated from Chaetomium globosum. FEMS Microbiol Lett. 2005; 252(2):309–13. Epub 2005/10/08. S0378-1097(05)00628-2 [pii] doi: 10.1016/j.femsle.2005.09.013 PMID: 16209910.
16. Phonkerd N, Kanokmedhakul S, Kanokmedhakul K, Soytong K, Prabpai S, Kongsearee P. Bis-spiro-azaphilones and azaphilones from the fungi Chaetomium cochliodes VTh01 and C. cochliodes CTh05. Tetrahedron. 2008; 64:9636–45.
17. Jiao RH, Xu S, Liu JY, Ge HM, Ding H, Xu C, et al. Chaetominine, a cytotoxic alkaloid produced by endophytic Chaetomium sp. IFB-E015. Org Lett. 2006; 8(25):5709–12. Epub 2006/12/01. doi: 10.1021/ol062257t PMID: 17134253.
18. Ding G, Song YC, Chen JR, Xu C, Ge HM, Wang XT, et al. Chaetoglobosin U, a cytochalasan alkaloid from endophytic Chaetomium globosum IFB-E019. J Nat Prod. 2006; 69(2):302–4. Epub 2006/02/28. doi: 10.1021/np050515+ PMID: 16499339.
19. Schlörke O, Zeek A. Orsellides A-E: an example for 6-deoxyhexose derivatives produced by fungi. Eur J Org Chem. 2006:1043–9.
20. Marwah RG, Fatope MO, Deadman ML, Al-Maqbali YM, Husband J. Musanahol: a new aureonitol-related metabolite from a Chaetomium sp. Tetrahedron. 2007; 63(34):8174–80.
21. Jervis PJ, Cox LR. Total synthesis and proof of relative stereochemistry of (-)-aureonitol. J Org Chem. 2008; 73(19):7616–24. doi: 10.1021/jo801338t PMID: 18774862.
22. Nakazawa T, Ishiuchi K, Sato M, Tsunematsu Y, Sugimoto S, Gotanda Y, et al. Targeted disruption of transcriptional regulators in Chaetomium globosum activates biosynthetic pathways and reveals transcriptional regulator-like behavior of aureonitol. J Am Chem Soc. 2013; 135(36):13446–55. doi: 10.1021/ja405128k PMID: 23941144.
23. Bedard J, May S, Lis M, Tryphonas L, Drach J, Huffman J, et al. Comparative study of the anti-human cytomegalovirus activities and toxicities of a tetrahydrofuran phosphonate analogue of guanosine and cidofovir. Antimicrob Agents Chemother. 1999; 43(3):557–67. Epub 1999/02/27. PMID: 10049267; PubMed Central PMCID: PMC89160.
24. Yedidi RS, Garimella H, Aoki M, Aoki-Ogata H, Desai DV, Chang SB, et al. A conserved hydrogen-bonding network of P2 bis-tetrahydrofuran-containing HIV-1 protease inhibitors (PIs) with a protease active-site amino acid backbone aids in their activity against PI-resistant HIV. Antimicrob Agents Chemother. 2014; 58(7):3679–88. doi: 10.1128/AAC.00107-14 PMID: 24752271; PubMed Central PMCID: PMCPMC4068604.
25. Zhang H, Wang YF, Shen CH, Agniswamy J, Rao KV, Xu CX, et al. Novel P2 tris-tetrahydrofuran group in antiviral compound 1 (GRL-0519) fills the S2 binding pocket of selected mutants of HIV-1 protease. J Med Chem. 2013; 56(3):1074–83. doi: 10.1021/jm301519z PMID: 23298236; PubMed Central PMCID: PMCPMC3574189.
26. Wang GT, Wang S, Gentles R, Sowin T, Maring CJ, Kempf DJ, et al. Design, synthesis, and structural analysis of inhibitors of influenza neuraminidase containing a 2,3-disubstituted tetrahydrofuran-5-carboxylic acid core. Bioorg Med Chem Lett. 2005; 15(1):125–8. doi: 10.1016/j.bmcl.2004.10.022 PMID: 15582424.
27. Rodrigues KF, Samuels GJ. Fungal endophytes of Spondias mombin leaves in Brazil. Journal of Basic Microbiology. 1999; 39:131–5.
28. Abrantes JL, Barbosa J, Cavalcanti D, Pereira RC, Fontes CFL, Teixeira VL, et al. The Effects of the Diterpenes Isolated from the Brazilian Brown Algae Dictyota pfaffii and Dictyota menstrualis against the Herpes Simplex Type-1 Replicative Cycle. Planta Medica. 2010; 76(4):339–44. doi: 10.1055/s-0029-1186144 WOS:000275033200005. PMID: 19764012
29. Barbosa JP, Pereira RC, Abrantes JL, dos Santos CCC, Rebello MA, Frugulhetti I, et al. In vitro antiviral diterpenes from the Brazilian brown alga Dictyota pfaffii. Planta Medica. 2004; 70(9):856–60. doi: 10.1055/s-2004-827235 WOS:000224440700014. PMID: 15503355
30. Barbosa JP, Teixeira VL, Villaca R, Pereira RC, Abrantes JL, Frugulhetti I. A dolabellane diterpene from the Brazilian brown alga Dictyota pfaffii. Biochemical Systematics and Ecology. 2003; 31 (12):1451–3. doi: 10.1016/s0305-1978(03)00120-0 WOS:000186644800007.
31. Szretter KJ, Balish AL, Katz JM. Influenza: propagation, quantification, and storage. Curr Protoc Microbiol. 2006;Chapter 15:Unit 15G.1. Epub 2008/09/05. doi: 10.1002/0471729256.mc15g01s3 PMID: 18770580.

32. Scudiero DA, Shoemaker RH, Paull KD, Monks A, Tierney S, Nofziger TH, et al. Evaluation of a soluble tetrazolium/formazan assay for cell growth and drug sensitivity in culture using human and other tumor cell lines. Cancer Res. 1988; 48(17):4827–33. Epub 1988/09/01. PMID: 3409223.

33. Reed LJ, Muench H. A simple method of estimating fifty per cent endpoints. Am J Epidemiol. 1938; 27 (3):493–7.

34. WHO, CDC. Serological Diagnosis of Influenza by Microneutralization Assay. 2010.

35. Mesquita M, Fintelman-Rodrigues N, Sacramento CQ, Abrantes JL, Costa E, Temerozo JR, et al. HIV-1 and Its gp120 Inhibits the Influenza A(H1N1)pdm09 Life Cycle in an IFITM3-Dependent Fashion. PLoS One. 2014; 9(6):e101056. doi: 10.1371/journal.pone.0101056 PMID: 24978204; PubMed Central PMCID: PMCPMC4076258.

36. Bergmann JH, Spector DL. Long non-coding RNAs: modulators of nuclear structure and function. Curr Opin Cell Biol. 2014; 26:10–8. doi: 10.1016/j.ceb.2013.08.005 PMID: 24529241; PubMed Central PMCID: PMCPMC3927160.

37. Rowe T, Abernathy RA, Hu-Primmer J, Thompson WW, Lu X, Lim W, et al. Detection of antibody to avian influenza A (H5N1) virus in human serum by using a combination of serologic assays. J Clin Microbiol. 1999; 37(4):937–43. Epub 1999/03/13. PMID: 10074505.

38. Souza TM, Salluh JI, Bozza FA, Mesquita M, Soares M, Motta FC, et al. H1N1pdm influenza infection in hospitalized cancer patients: clinical evolution and viral analysis. PLoS One. 2010; 5(11):e14158. Epub 2010/12/15. doi: 10.1371/journal.pone.0014158 PMID: 21152402.

39. Joy S, Nair PS, Hariharan R, Pillai MR. Detailed comparison of the protein-ligand docking efficiencies of GOLD, a commercial package and ArgusLab, a licensable freeware. In Silico Biol. 2006; 6(6):601–5. PMID: 17518767.

40. Bernstein FC, Koetzle TF, Williams GJ, Meyer EF, Brice MD, Rodgers JR, et al. The Protein Data Bank: a computer-based archival file for macromolecular structures. Arch Biochem Biophys. 1978; 185 (2):584–91. PMID: 626512.

41. Hussain Basha S, Prasad RN. In-Silico screening of Pleconaril and its novel substituted derivatives with Neuraminidase of H1N1 Influenza strain. BMC Res Notes. 2012; 5:105. doi: 10.1186/1756-0500-5-105 PMID: 22340192; PubMed Central PMCID: PMCPMC3369820.

42. Souza TM, Abrantes JL, de AER, Leite Fontes CF, Frugulhetti IC. The alkaloid 4-methylaaptamine isolated from the sponge Aaptos aaptos impairs Herpes simplex virus type 1 penetration and immediate-early protein synthesis. Planta Med. 2007; 73(3):200–5. Epub 2007/02/08. doi: 10.1055/s-2007-967109 PMID: 17285480.

43. Palese P, Shaw ML. Orthomyxoviridae: The viruses and their replication. Knipe DMH, P. M., editors, editor. Philadelphia: Lippincott, Williams & Wilkins; 2007.

44. Moscona A. Neuraminidase inhibitors for influenza. N Engl J Med. 2005; 353(13):1363–73. Epub 2005/09/30. 353/13/1363 [pii] doi: 10.1056/NEJMra050740 PMID: 16192481.

45. Brooks MJ, Burtseva EI, Ellery PJ, Marsh GA, Lew AM, Slepushkin AN, et al. Antiviral activity of arbidol, a broad-spectrum drug for use against respiratory viruses, varies according to test conditions. J Med Virol. 2012; 84(1):170–81. Epub 2011/10/27. doi: 10.1002/jmv.22234 PMID: 22028179.

46. Auwerx J, Stevens M, Van Rompay AR, Bird LE, Ren J, De Clercq E, et al. The phenylmethylthiazolylthiourea nonnucleoside reverse transcriptase (RT) inhibitor MSK-076 selects for a resistance mutation in the active site of human immunodeficiency virus type 2 RT. J Virol. 2004; 78(14):7427–37. Epub 2004/06/29. doi: 10.1128/JVI.78.14.7427-7437.2004 78/14/7427 [pii]. PMID: 15220416.

47. Schinazi RF, Hernandez-Santiago BI, Hurwitz SJ. Pharmacology of current and promising nucleosides for the treatment of human immunodeficiency viruses. Antiviral Res. 2006; 71(2–3):322–34. Epub 2006/05/24. S0166-3542(06)00091-X [pii] doi: 10.1016/j.antiviral.2006.03.012 PMID: 16716415.

48. Austin FJ, Kawaoka Y, Webster RG. Molecular analysis of the haemagglutinin gene of an avian H1N1 influenza virus. J Gen Virol. 1990; 71 (Pt 10):2471–4. PMID: 2230742.

49. Al-Majhdi FN. Structure of the Sialic Acid Binding Site in Influenza A Virus: Hemagglutinin. Journal of Biological Sciences2007. p. 113–22.

50. Muthuri SG, Venkatesan S, Myles PR, Leonardi-Bee J, Al Khuwaitir TS, Al Mamun A, et al. Effectiveness of neuraminidase inhibitors in reducing mortality in patients admitted to hospital with influenza A H1N1pdm09 virus infection: a meta-analysis of individual participant data. Lancet Respir Med. 2014; 2 (5):395–404. doi: 10.1016/S2213-2600(14)70041-4 PMID: 24815805.

51. Nishihara Y, Tsujii E, Yamagishi Y, Kino T, Hino M, Yamashita M, et al. FR191512, a Novel Anti-influenza Agent Isolated from a Fungus Strain No.17415. II. Biological Properties. J Antibiotics. 2000; 53 1341–5.

52. Jing L, Dingmei Z, Xun Z, Zhenjian H, Shu L, Mengfeng L, et al. Studies on Synthesis and Structure-Activity Relationship (SAR) of Derivatives of a New Natural Product from Marine Fungi as Inhibitors of

Influenza Virus Neuraminidase. Mar Drugs. 2011; 9(10):1887–901. doi: 10.3390/md9101887 PMID: 22073001

53. Hopkins S. Safety Study of Flufirvitide-3 Nasal Spray in Healthy Subjects 2012 [cited 2012 February 3]. Available from: http://clinicaltrials.gov/ct2/show/NCT01313962?term=Flufirvitide-3&rank=1.

54. Leneva IA, Russell RJ, Boriskin YS, Hay AJ. Characteristics of arbidol-resistant mutants of influenza virus: implications for the mechanism of anti-influenza action of arbidol. Antiviral Res. 2009; 81(2):132–40. doi: 10.1016/j.antiviral.2008.10.009 PMID: 19028526.

55. Liu MY, Wang S, Yao WF, Wu HZ, Meng SN, Wei MJ. Pharmacokinetic properties and bioequivalence of two formulations of arbidol: an open-label, single-dose, randomized-sequence, two-period crossover study in healthy Chinese male volunteers. Clin Ther. 2009; 31(4):784–92. Epub 2009/05/19. S0149-2918(09)00125-8 [pii] doi: 10.1016/j.clinthera.2009.04.016 PMID: 19446151.

56. Sauter NK, Hanson JE, Glick GD, Brown JH, Crowther RL, Park SJ, et al. Binding of influenza virus hemagglutinin to analogs of its cell-surface receptor, sialic acid: analysis by proton nuclear magnetic resonance spectroscopy and X-ray crystallography. Biochemistry. 1992; 31(40):9609–21. PMID: 1327122.

57. Cirne-Santos CC, Souza TML, Teixeira VL, Fontes CFL, Rebello MA, Castello-Branco LRR, et al. The dolabellane diterpene Dolabelladienetriol is a typical noncompetitive inhibitor of HIV-1 reverse transcriptase enzyme. Antiviral Research. 2008; 77(1):64–71. doi: 10.1016/j.antiviral.2007.08.006 WOS:000253021500009. PMID: 17888523

58. Soares AR, Abrantes JL, Lopes Souza TM, Leite Fontes CF, Pereira RC, de Palmer Paixao Frugulhetti IC, et al. In vitro antiviral effect of meroditerpenes isolated from the Brazilian seaweed Stypopodium zonale (Dictyotales). Planta Medica. 2007; 73(11):1221–4. doi: 10.1055/s-2007-981589 WOS:000250143800016. PMID: 17713872

59. Souza TML, Abrantes JL, Epifanio RdA, Fontes CFL, Frugulhetti ICPP. The alkaloid 4-methylaaptamine isolated from the sponge Aaptos aaptos impairs herpes simplex virus type 1 penetration and immediate-early protein synthesis. Planta Medica. 2007; 73(3):200–5. doi: 10.1055/s-2007-967109 WOS:000245588700002. PMID: 17285480

60. de Souza Pereira H, Leão-Ferreira LR, Moussatché N, Teixeira VL, Cavalcanti DN, da Costa LJ, et al. Effects of diterpenes isolated from the Brazilian marine alga Dictyota menstrualis on HIV-1 reverse transcriptase. Planta Med. 2005; 71(11):1019–24. doi: 10.1055/s-2005-873113 PMID: 16320202.

61. Wang Y, Xu L, Ren W, Zhao D, Zhu Y, Wu X. Bioactive metabolites from Chaetomium globosum L18, an endophytic fungus in the medicinal plant Curcuma wenyujin. Phytomedicine. 2012; 19(3–4):364–8. doi: 10.1016/j.phymed.2011.10.011 PMID: 22112725.

62. Gutiérrez RM, Mitchell S, Solis RV. Psidium guajava: a review of its traditional uses, phytochemistry and pharmacology. J Ethnopharmacol. 2008; 117(1):1–27. doi: 10.1016/j.jep.2008.01.025 PMID: 18353572.

63. Rodríguez K, Stchigel A, Guarro J. Three new species of Chaetomium from soil. Mycologia. 2002; 94 (1):116–26. PMID: 21156483.

Supplementary Information

Aureonitol, a Fungi-Derived Tetrahydrofuran, Inhibits Influenza Replication by Targeting Its Surface Glycoprotein Hemagglutinin

Figures

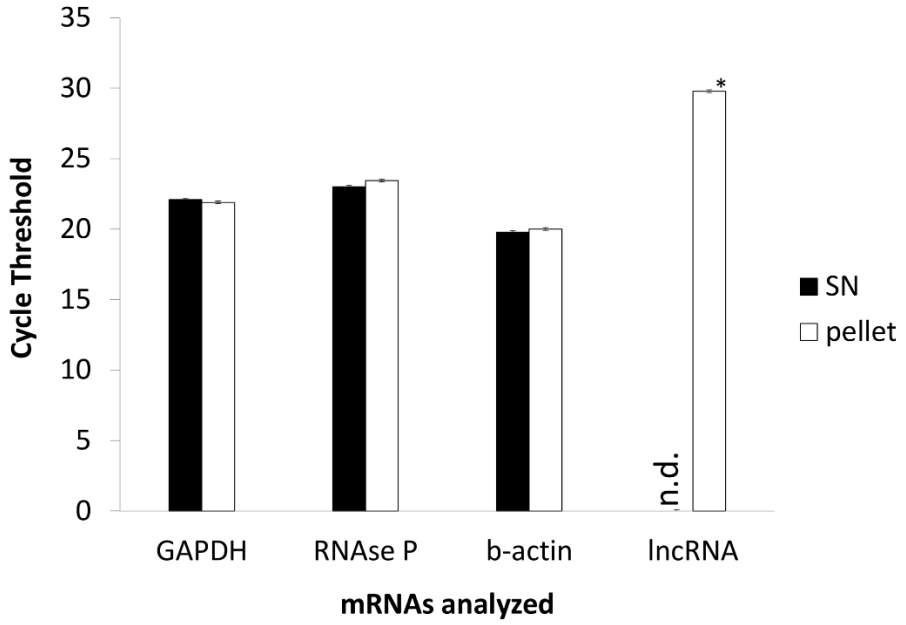

Figure S1. Purity of the RNA preparation. MDCKs (2 x 10^6 cells) were lysed with buffer A and centrifuged. The pellet and supernatant (SN) contained the nuclear and non-nuclear fractions, respectively. RNA from each of these fractions was extracted and used to perform cDNA synthesis and real time. * $P<0.001$ for comparisons between corresponding white and black bars. Amplicon was not detected (n.d.) within 45 cycles, as indicated (n = 6).

A

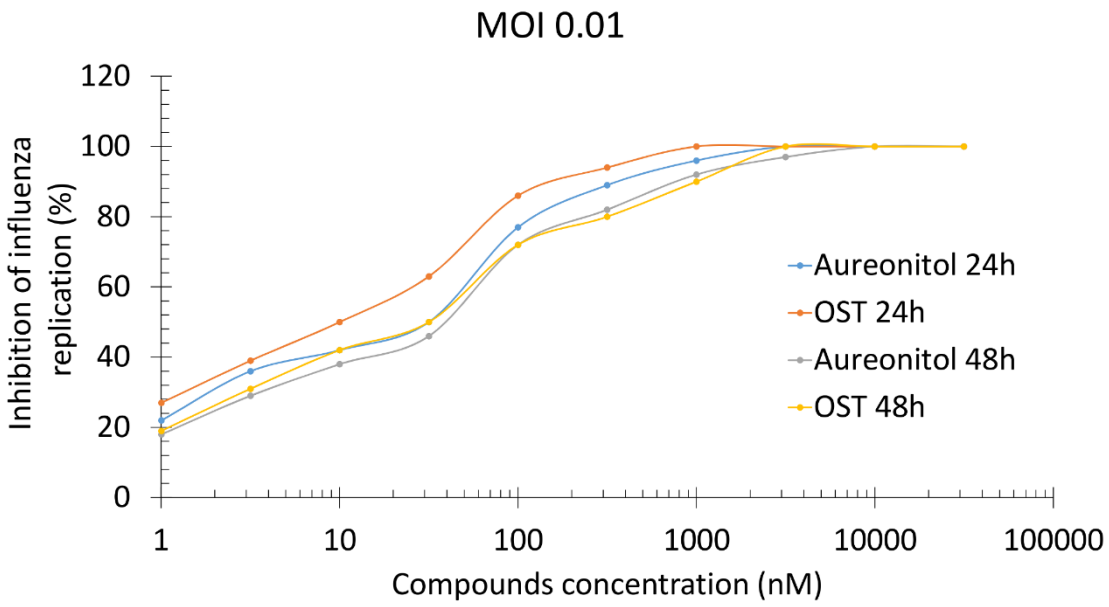
MOI 0.01
Inhibition of influenza replication (%)
120
100
80
60
40
20
0
1
10
100
1000
10000
100000
Compounds concentration (nM)
Aureonitol 24h
OST 24h
Aureonitol 48h
OST 48h

B

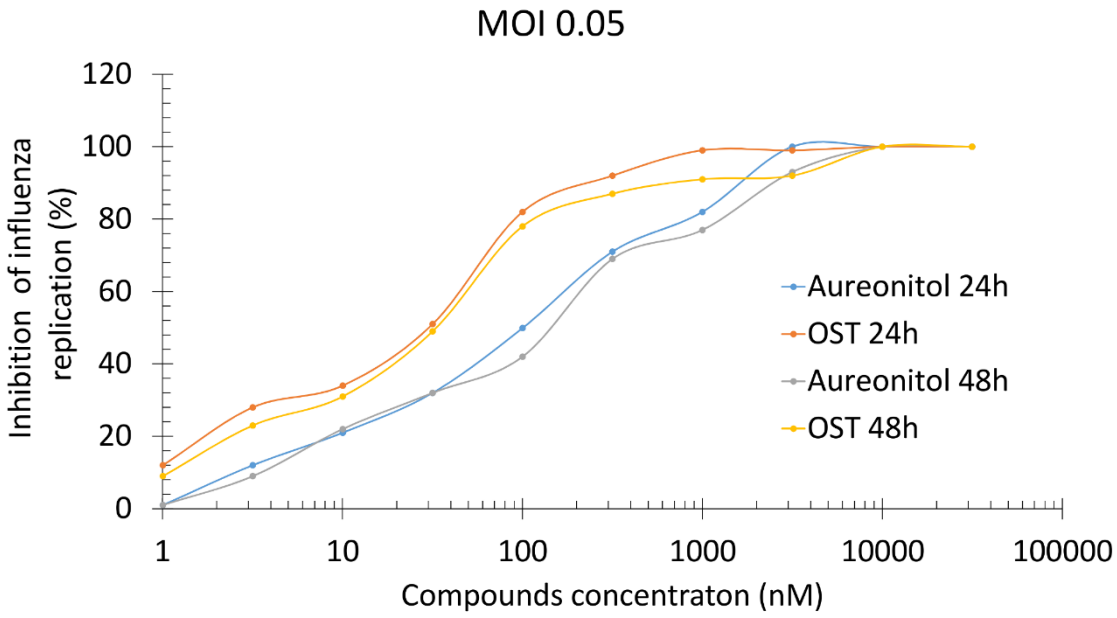
MOI 0.05
Inhibition of influenza replication (%)
120
100
80
60
40
20
0
1
10
100
1000
10000
100000
Compounds concentraton (nM)
Aureonitol 24h
OST 24h
Aureonitol 48h
OST 48h

C

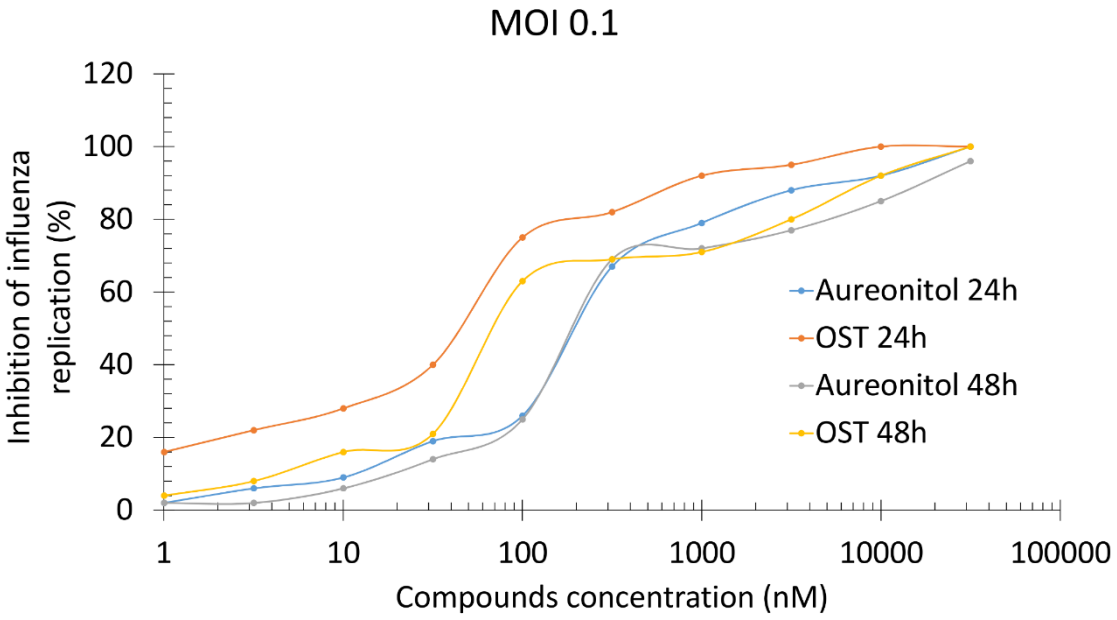

Figure S2. MOI- and time-dependent inhibition of aureonitol against influenza. MDCKs (2 x 10^5 cells) were infected with influenza at MOIs of 0.01 (A), 0.05 (B), and 0.1 (C) for 1 h at 37 ^{0}C. The cells were washed and treated with indicated concentrations of the compounds. After 24 and 48 h, viruses in the supernatant were titrated. The experiments were performed 5 times in triplicate.

A

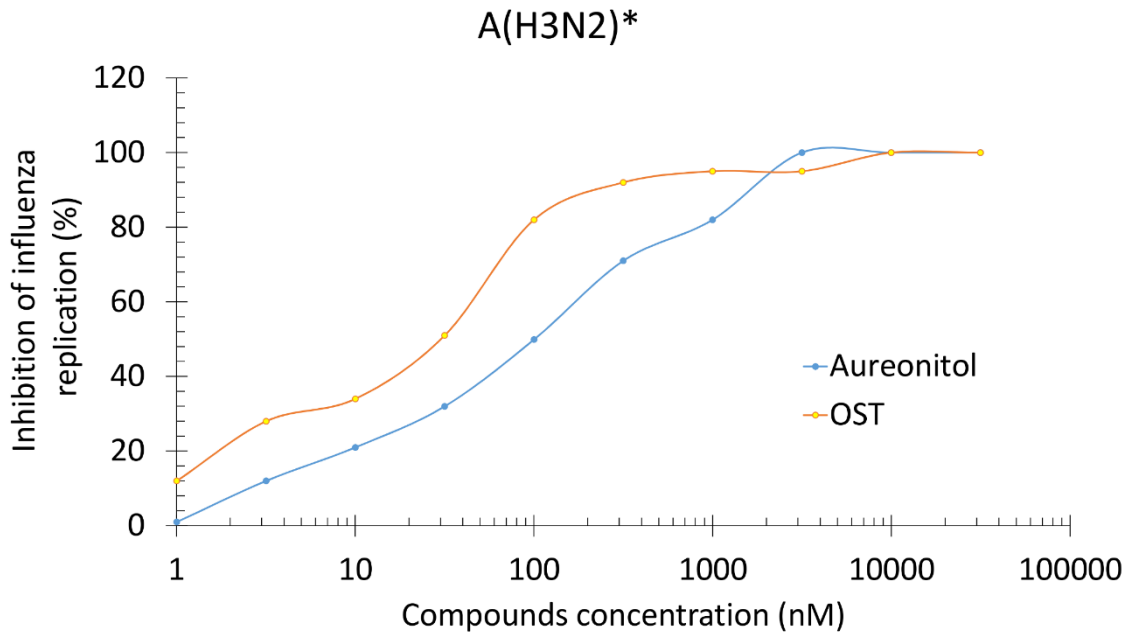
A(H3N2)*
Inhibition of influenza replication (%)
120
100
80
60
40
20
0
1
10
100
1000
10000
100000
Compounds concentration (nM)
Aureonitol
OST

B

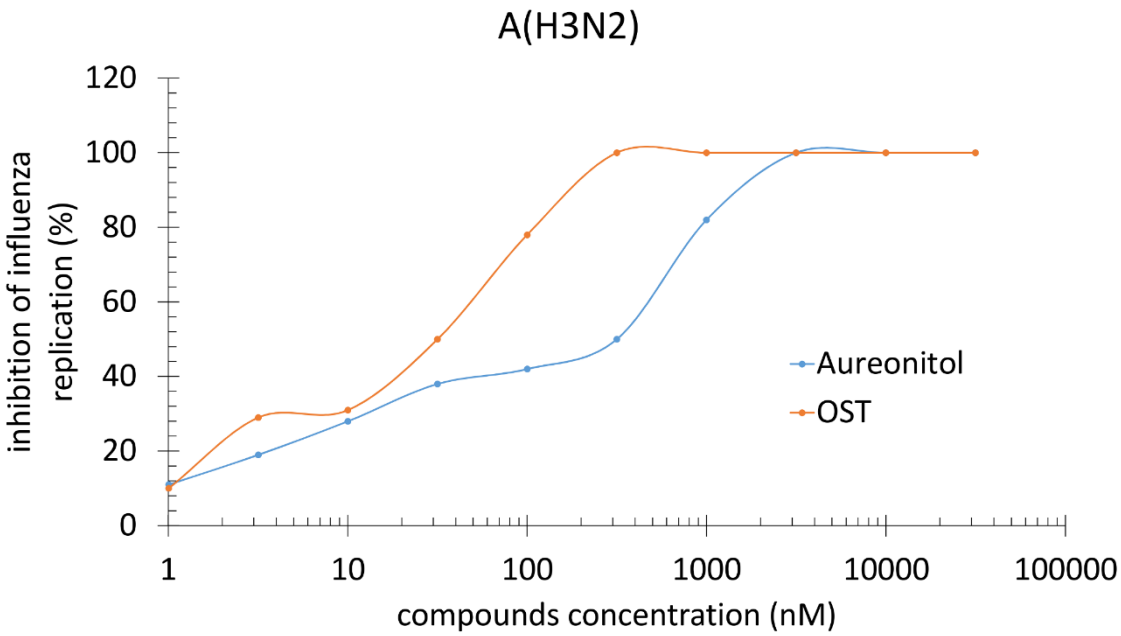
A(H3N2)
inhibition of influenza replication (%)
120
100
80
60
40
20
0
1
10
100
1000
10000
100000
compounds concentration (nM)
Aureonitol
OST

C

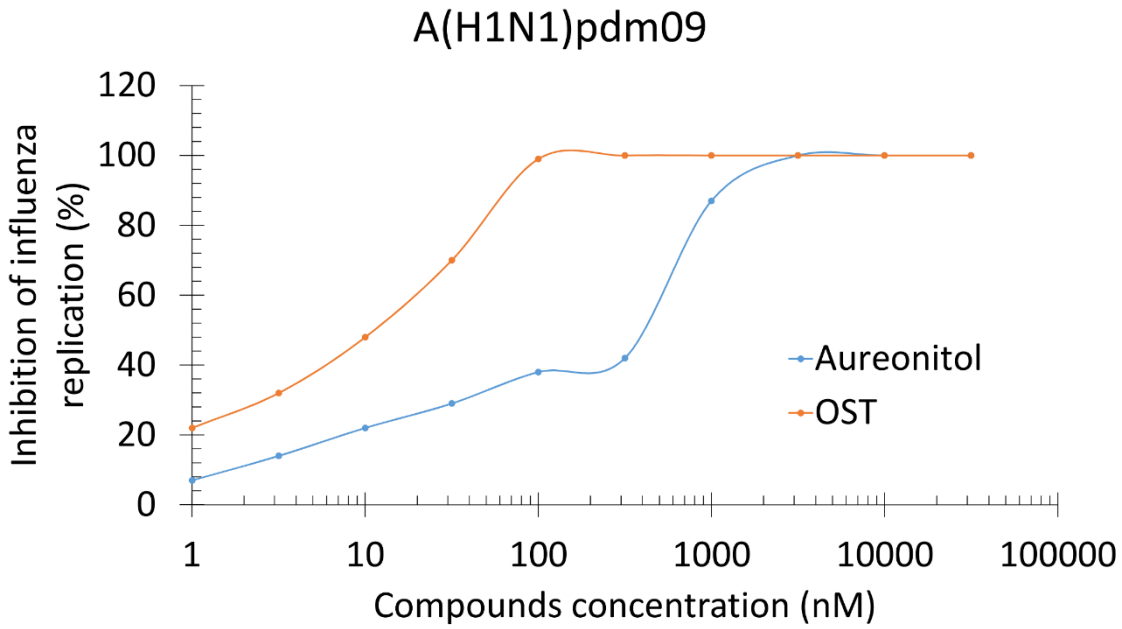

D

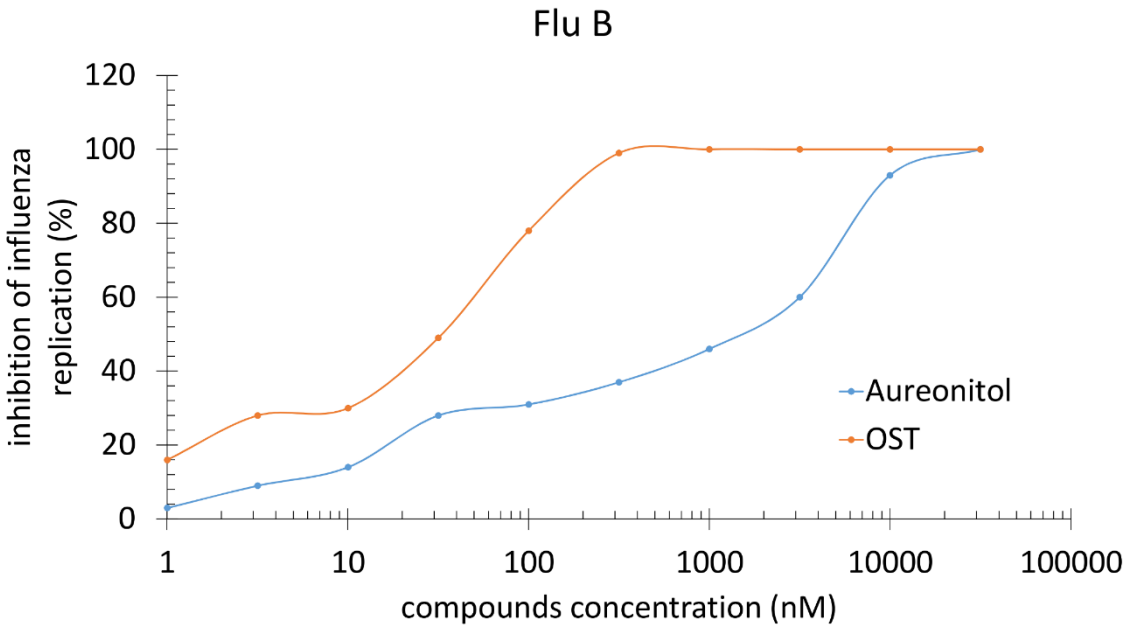

Figure S3. Aureonitol antiviral activity against influenza A and B viruses. MDCKs (2 x 10^5 cells) were infected with laboratory-adapted influenza A(H3N2)* (A) or clinical isolates of influenza A(H3N2) (B), Influenza A(H1N1)pdm09 (C) and influenza B (D) at a MOI of 0.05 for 1 h at 37 ^{0}C. The cells were washed and treated with the indicated concentrations of the compounds. After 24 h, viruses in the supernatant were

titrated. The experiments were performed 5 times in triplicate.

Tables

Table S1: Influenza A and B viruses used in the study

Strains	Type/Subtype	Laboratory-adapted or clinical isolate
A/RJ/512/2009	A(H1N1)pdm09	Clinical Isolate
A/WA/01/2007	A(H3N2)	Clinical Isolate
A/ENG/42/1972	A(H3N2)	Laboratory-adapted
B/MEMPHIS/20/1996	B	Clinical Isolate

Table S2: Hemagglutinin protein structures used for molecular modeling

Strains	Type/Subtype	PDB accession codes for HAs closer to the strain used in the study
A/RJ/512/2009	A(H1N1)pdm09	3UBE
A/WA/01/2007	A(H3N2)	2YP4
A/ENG/42/1972	A(H3N2)	1HGE
B/MEMPHIS/20/1996	B	4NRL

Table S3 – Pharmacological parameters of virus growth inhibition by aureonitol in different MOIs and time-points.

MOI	**0.01**				**0.05**				**0.1**			
Time points after infection (h)	**24**		**48**		**24**		**48**		**24**		**48**	
Compound (nM)	**Aureonitol**	**OST**	**Aureonitol**	**OST**	**Aureonitol**	**OST**	**Aureonitol**	**OST**	**Aureonitol**	**OST**	**Aureonitol**	**OST**
EC_{50}	30 ± 3.4	12 ± 0.9	42 ± 3.9	28 ± 1.1	100 ± 16	30 ± 2.3	121 ± 18	38 ± 2.8	183 ± 21	49 ± 2.6	201 ± 13	56 ± 3.1
EC_{90}	319 ± 13	38 ± 1.2	976 ± 14	67 ± 2.8	3000 ± 236	90 ± 14	3053 ± 331	97 ± 8.7	3227 ± 187	101 ± 23	10557 ± 321	121 ± 31
EC_{99}	1029 ± 43	44 ± 3.3	1074 ± 24	75 ± 3.4	3091 ± 245	98 ± 8	3359 ± 287	113 ± 12	3549 ± 246	115 ± 32	11613 ± 289	134 ± 26

Table S4 – Antiviral activity of aureonitol agasint influenza A and B virus at 48 h after infection

	EC_{50} (nM)		EC_{90} (nM)		EC_{99} (nM)	
Influenza Type (subtypes)	**Aureonitol**	**OST**	**Aureonitol**	**OST**	**Aureonitol**	**OST**
A(H3N2)*	121	38	3053	97	3359	113
A(H3N2)	389	40	3245	101	3345	129
A(H1N1)pdm09	523	26	2765	98	2845	105
B	2543	97	18905	234	19087	245

Table S5 – Molecular interactions between Aureonitol and the hemagglutinin of Influenza A and B viruses

Influenza Type (subtype)	PDB accession number	Aureonitol free binding energy (kcal/mol)	hydrogen bonds	P-Alkalyl bonds
A(H3N2)	1HGE	- 80	Tyr98, His183, Glu190, Ser228	Gly134, Trp153, Thr155, Ser186, Leu194, Tyr195, Trp222, Gly225, Leu226, Ser227
A(H3N2)	2YP4	- 72	Tyr98, His183, Ser228	Gly134, Ser136, Trp153, Thr155, Leu194, Arg222, Asp225, Ile226, Pro227
A(H1N1)pdm09	3UBE	- 75	Tyr98, His183, Pro185, Asp190, Gln226	Asn133, Gly134, Val135, Trp153, Leu154, Val155, Ser186, Leu194, Tyr195, Lys222, Asp225, Glu227, Gly228
B	4NRL	- 64	Thr139, Arg202	Tyr95, Gly138, Ser140, Trp158, Val159, Ile160, His193, Asp195, Gln199, Leu203, Ser242, Gly243

Bioorganic & Medicinal Chemistry 23 (2015) 7777–7784

Contents lists available at ScienceDirect

Bioorganic & Medicinal Chemistry

journal homepage: www.elsevier.com/locate/bmc

1,2,3-Triazolyl-4-oxoquinolines: A feasible beginning for promising chemical structures to inhibit oseltamivir-resistant influenza A and B viruses

Fernanda da C. S. Boechat [a,†], Carolina Q. Sacramento [b,c,d,†], Anna C. Cunha [a], Fernanda S. Sagrillo [a], Christiane M. Nogueira [a], Natalia Fintelman-Rodrigues [b,c,d], Osvaldo Santos-Filho [b], Cecília S. Riscado [a], Luana da S. M. Forezi [a], Letícia V. Faro [a], Leonardo Brozeguini [a], Isakelly P. Marques [a], Vitor F. Ferreira [a], Thiago Moreno L. Souza [b,c,d,*,‡], Maria Cecília B. V. de Souza [a,*,‡]

[a] Universidade Federal Fluminense, Instituto de Química—Outeiro de São João Batista, s/n°.Campus do Valonguinho, Centro, Niterói, RJ CEP 24020-150, Brazil
[b] Fundação Oswaldo Cruz, Instituto Oswaldo Cruz, Laboratório de Vírus Respiratórios, NIC-WHO, Rio de Janeiro, RJ CEP 21041-360, Brazil
[c] Fundação Oswaldo Cruz, Instituto Oswaldo Cruz, Laboratório de Imunofarmacologia, Rio de Janeiro, RJ CEP 21041-360, Brazil
[d] Fundação Oswaldo Cruz, Centro de Desenvolvimento Tecnológico em Saúde, Rio de Janeiro, RJ CEP 21041-360, Brazil

ARTICLE INFO

Article history:
Received 11 September 2015
Revised 11 November 2015
Accepted 21 November 2015
Available online 26 November 2015

Keywords:
1,2,3-Triazole
4-Oxoquinoline
Influenza viruses
Neuraminidase inhibitors
Oseltamivir carboxylate
Antiviral resistance

ABSTRACT

We described the synthesis of a new congener series of 1,2,3-triazolyl-4-oxoquinolines and evaluated their ability to inhibit oseltamivir (OST)-resistant influenza strains. Oxoquinoline derivative **1i** was the most potent compound within this series, inhibiting 94% of wild-type (WT) influenza neuraminidase (NA) activity. Compound **1i** inhibited influenza virus replication with an EC_{50} of 0.2 μM with less cytotoxicity than OST, and also inhibited different OST-resistant NAs. These results suggest that 1,2,3-triazolyl-4-oxoquinolines represent promising lead molecules for further anti-influenza drug design.

Published by Elsevier Ltd.

1. Introduction

Acute respiratory infections have a great impact on public health because they are a major cause of morbidity and mortality.[1] Influenza virus, a negative-sense-RNA orthomixovirus,[2] is the most important etiologic agent of severe acute respiratory infections (SARI). Influenza virus causes both seasonal infections and pandemic outbreaks.[3] To enter host cells, influenza binds to sialic acid residues on glycoproteins localized in the cellular plasma membrane. This is followed by endocytosis and the fusion of the viral envelope with the endocytic membrane in a manner that is dependent on the viral protein M2.[4] Next, viral ribonucleoproteins (RNP) composed of the RNA polymerase complex, viral RNA, nucleoprotein (NP) and nuclear export proteins (NEP) are released into the cytoplasm and transported to the cell nucleus, where transcription and replication of the viral genome occur. Then, viral proteins are trafficked to the host cell plasma membrane for the assembly of new viruses. These particles bud through the cellular plasma membrane and are released via viral neuraminidase (NA) activity.[5]

Strategies to control influenza virus infections include vaccination and antiviral drugs.[6,7] The existence of multiple zoonotic hosts,[8] the time required to produce vaccines against novel viruses, the costs of vaccine production and its recommendation only for groups of patients at high risk for serious influenza-related illnesses represent major limitations for the use of vaccines.[9] In contrast, anti-influenza drugs are now recommended for clinical use whenever possible because the most effective time frame for treatment is approximately 2.5 days after the onset of illness.[10] Moreover, because the antigenic characteristics of viral strains that might cause future pandemic outbreaks are unpredictable, the stockpiling of anti-influenza drugs is a key issue in pandemic preparedness.[11,12]

Virtually all circulating strains of influenza are resistant to the adamantanes (M2-channel blockers). Thus, neuraminidase inhibitors (NAIs) such as oseltamivir (OST), zanamivir, peramivir and

* Corresponding authors. Tel.: +55 21 26292148.
E-mail address: mceciliabvs@gmail.com (M.C.B.V. de Souza).
† These authors contributed equally as first authors.
‡ These authors contributed equally as last authors.

http://dx.doi.org/10.1016/j.bmc.2015.11.028
0968-0896/Published by Elsevier Ltd.

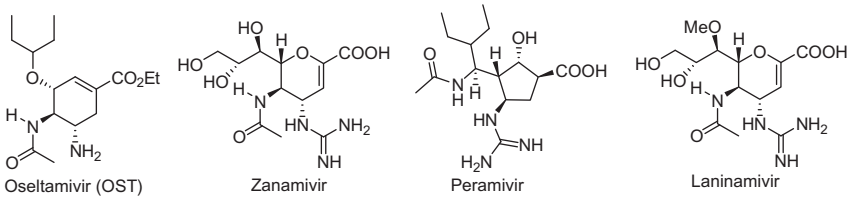

Figure 1. Structures of neuraminidase inhibitors (NAIs) approved for clinical use.

laninamivir constitute the only licensed class of drugs available for clinical use against influenza (Fig. 1).[13] OST is the most used anti-influenza drug because it is orally administered and is licensed to more countries than the other drugs.[14] However, approximately 1–2% of the circulating strains of influenza A(H1N1)pdm09 virus are resistant to OST, and OST-resistant viruses may also cause primary infections.[15,16] Therefore, the identification of novel molecules endowed with the ability to inhibit OST-resistant strains of influenza is pivotal because it may increase the number of options available to fight this virus infection in the future.

Quinolones and triazolic derivatives have been largely explored due to multiple biological properties. With respect to these radicals as antivirals, they have been proven to be active against HIV,[17,18] HSV,[19] HCV[20,21] and influenza.[22,23]

In this work, we synthesized new 4-oxoquinoline derivatives **1a–j** in which the core quinolone was connected to a 1,2,3-triazole nucleus and investigated their ability to inhibit influenza virus replication and the NA activity of OST-resistant strains of influenza. Importantly, our most effective compound inhibited multi-resistant strains of influenza. The triazolic ring and the cyclohexenyl radical were found to be critical for anti-influenza activity and allowed the compound to bind to conserved amino acid residues of both WT and OST-resistant NAs. Our results suggest that the chemical structure of 1,2,3-triazolyl-4-oxoquinolines is promising for the development of novel anti-influenza drugs.

2. Chemistry

The synthesis of 1,2,3-triazolyl-4-oxoquinoline derivatives **1a–j** was initiated with the treatment of *meta*- or *para*-nitroaniline with diethyl ethoxymethylenemalonate (EMME) to obtain enamine-type derivatives that were then cyclized in refluxing diphenyl ether.[19]

The corresponding 1,4-dihydro-4-oxo-quinolines **2** were submitted to an alkylation reaction with ethyl bromide, thereby affording the desired *N*-ethyl 4-oxoquinolines **3**.[24] After the chemical reduction of these compounds with iron and aqueous ammonium chloride solution, the diazonium salts of the amino-4-oxoquinolines were reacted with sodium azide, leading to desired azidoquinolones **4a–b** in quantitative yield (Scheme 1).[25] The azido-4-oxoquinolines **2a** and **2b** allowed us to study their application in the Huisgen 'click-chemistry' reaction using copper sulfate and ascorbic acid as the catalysts and dimethylformamide as the solvent at 50 °C[25] (Table 1).

Table 1
Scheme summarizing the synthesis of 4-oxoquinoline **1a–j** moiety, R^1 substituents coupled to triazole ring located in positions C-6 or C-7 of the 4-oxoquinolines, the yield of each derivative after purification and their anti-influenza NA activity

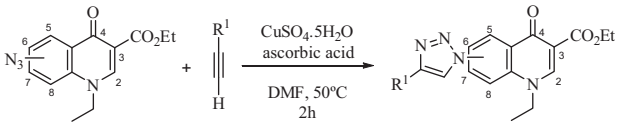

(**4a**) 6-N_3
(**4b**) 7-N_3

(**1**)

#	R^1	Triazole position	Yield (%)	Influenza H3N2 NA inhibition at 50 μM (%)
1a		C-6	88	59.1 ± 3.2
1b		C-7	85	62.3 ± 1.1
1c		C-6	83	56.5 ± 1.4
1d		C-7	79	57.4 ± 2.2
1e		C-6	97	89.0 ± 1.2
1f		C-7	93	56.3 ± 3.3
1g		C-6	95	0
1h		C-7	90	0
1i		C-6	98	94.8 ± 2.1
1j		C-7	95	44.5 ± 2.3

Their reactions with different alkynes resulted in the coupled inedited 4-oxoquinolines **1a–j**, with 79–98% yields after purification (Table 1).

All the structures of the new compounds **1a–j** were confirmed by spectral data (^{1}H and ^{13}C NMR spectra) and by high resolution mass spectrometry analysis.

3. Results and discussion

3.1. Anti-influenza NA activity of 1,2,3-triazolyl-4-oxoquinoline derivatives

As mentioned above, NAIs are the only class of anti-influenza drug in clinical use. Although this class is effective against all NA types, drug-resistant influenza viruses have been described.[15,16]

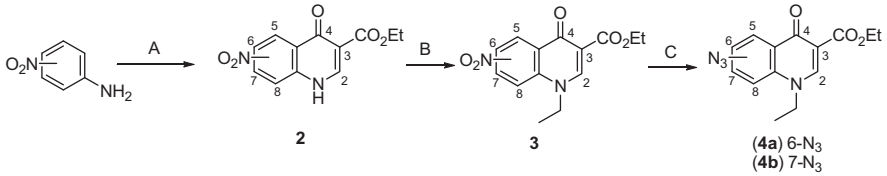

Scheme 1. General synthetic route to obtain azidoquinolones **4a–b**: (A) (1) EMME, EtOH, reflux, 24 h; (2) diphenyl ether, 250 °C, 6 h; (B) K_2CO_3, DMF, EtBr, 80 °C, 24 h; (C) (1) iron, NH_4Cl 0.05 M; (2) $NaNO_3$, HCl, 30 min; (3) NaN_3, 15 min.

We initially performed NA inhibition assays with a single dose of 320 triazolic compounds. The molecules were tested against different NA types (or isoforms), either WT or OST-resistant enzymes. Ideally, high values for the ratio between the inhibitory activities against the OST-resistant and WT enzymes would indicate promising hits. We identified 8 promising compounds with ratios above 0.8. Among these, two 1,2,3-triazolyl-4-oxoquinoline derivatives showed ratios above 1.0 (Table S1), suggesting that they are more effective against the OST-resistant NA than the WT. Therefore, in this work we will further examine the mechanism of inhibition of these 1,2,3-triazolyl-4-oxoquinoline derivatives (hits 3 and 6 from Table S1), while the other hits will be studied in future works. All 1,2,3-triazolyl-4-oxoquinoline derivatives analyzed in this study are shown in Table 1 and named henceforth as compounds **1a–j**. Compounds **1e** and **1i** were the most potent against the NA activity, reaching inhibitions equal to 89.0% and 94.8%, respectively (Table 1).

For comparison, OST inhibits the NA activity at the same concentration of the tested compounds by 100%. Interestingly, **1e** and **1i** have similar R^1 substituents including a phenyl or cyclohexenyl ring, respectively; which is bound to the triazolic moiety at carbon 6 on the 4-oxoquinoline ring (Table 1). The change of the triaolic moiety position compromised the anti-influenza activity, probably because it interferes with the pattern by which our compound interacts with its targets. More interestingly, changes in R^1 radical, which led to a decrease in the steric space occupied by our compounds, could even abolish their antiinfluenza activity (Table 1). Considering that these compounds are very similar, being molecule **1i** is slightly more potent than **1e**, subsequent experiments were performed with the former compound.

3.2. Potency of 1,2,3-triazolyl-4-oxoquinoline derivative 1i against NA

To evaluate the potency of compound **1i**, we measured its ability to inhibit WT and OST-resistant NAs from circulating strains of influenza A and B. We can see, Table 2, that compound **1i** showed some advantages over OST in the inhibition of resistant strains of influenza. Although OST was more potent than compound **1i** in the inhibition of WT strains, compound **1i** IC_{50} values suffered only marginal changes in the presence of resistance mutations to OST (Table 2). That is, the ratios of **1i**'s IC_{50} values for OST-resistant NAs over the WT counterpartners were 3.0, 0.13 and 1.4 for influenza A(H1N1)pdm09, A/H3N2 and B, respectively (Table 2). This indicates a marginal effect of OST-related resistance mutations towards compound **1i**'s ability to inhibit influenza A and B NAs (Table 2). The reference compound, OST, inhibited the NA activity of the antiviral resistant mutants of Influenza A(H1N1) [H275Y], A(H3N2) [E119V] and B [R152K] with higher IC_{50} values when compared to WT enzymes, these values increased by 27-, 380- and 5.3-fold, respectively (Table 2). Therefore, our data indicate that compound **1i** chemical structure may be a promising one to develop novel broad spectrum anti-influenza compounds able to impair the NA activity of OST-resistant strains.

Table 2
Potency of the compound **1i** and the reference compound OST on WT and OST-resistant influenza strains

Influenza strains	IC_{50}		IC_{50} change (times)	
	1i (μM)	OST (nM)	**1i**	OST
A/H3N2 WT	19.90 ± 1.3	0.15 ± 0.032	NA	NA
A/H3N2 E119V	2.60 ± 0.8	4.19 ± 0.16	0.13	27.00
A/H1N1 WT	3.50 ± 0.9	0.21 ± 0.011	NA	NA
A/H1N1 H275Y	10.60 ± 0.9	79.94 ± 3.2	3.00	380.00
B WT	22.00 ± 1.1	16.00 ± 2.9	NA	NA
B R152 K	30.00 ± 1.6	85.00 ± 5.4	1.40	5.30

3.3. Insights into the docking site of compound 1i and its pharmacophore group

We showed above that the presence of the phenyl or cyclohexenyl ring linked to triazolic moiety bound to carbon C-6 of the 4-oxoquinoline derivatives was critical to inhibit influenza NA activity (Table 1) and compound **1i** (cyclohexenyl substituent) was able to inhibit OST-resistant influenza A and B NAs (Table 2). Thus, we next performed in silico docking studies of compound **1i** with WT and OST-resistant NAs (Table S2) to get insight on the pharmacophore group of this molecule and its predicted binding sites. Compound **1i** docked in the active site cleft of all tested isoforms of NA, either WT or resistant to OST (Fig. 2). The docking sites of compound **1i** and OST partially overlapped (Fig. 2A). The cyclohexenyl substituent shown above to be critical for the anti-influenza activity had a singular projection towards an area of the NA not occupied by OST (Fig. 2A and B), suggesting a possible mechanism on the inhibition of OST-resistant strains. Fig. 1C–G reveal multiple points of interaction between our compound and the amino acids in the active site of the NA. Moreover, the critical groups for biological activity (i.e., the triazolic moiety at position 6 and the cyclohexenyl ring) were nestled by very conserved amino acid residues among various influenza NA types (Figs. 2C–G and S1). These conserved amino acid residues are found in influenza viruses infecting either humans or animals (Figs. 2 and S1).[26] Because the pharmacophore group of compound **1i** docked in conserved areas of the NA in versatile ways, it is difficult to elicit specific amino acids to perform site-direct mutagenesis assays to further evaluate the particular contribution of amino acid residues to the interaction between compound **1i** and the influenza A and B NAs. Nevertheless, subsequent passages of the influenza virus in the presence of the compound **1i** are ongoing to evaluate whether influenza mutants resistant to compound **1i** may emerge.

For comparisons, all the interactions of compound **1i** and OST with their targets are displayed in Table 3. Compound **1i** bound to the different NAs with free energies comparable to those observed for OST (Table 3). Nevertheless, compound **1i** is endowed with the ability to inhibit isoforms of NA that OST binds without achieving any antiviral effects (Table 2).

OST interacts with the different NAs using more hydrogen bonds than compound **1i** (Table 3). However, compound **1i** was more versatile in interacting with the different NAs than OST, as judged by multiple steric hindrances with different amino acids residues (Table 3). Altogether, our data suggest that the 4-oxoquinolines moiety is important for compound **1i** docking, while the triazole ring and the cyclohexenyl radical are required for antiviral activity. It is important to note that our computational prediction (Table 3) revealed that OST interacted with the NAS as described in the literature.[27,28]

3.4. Potency of compound 1i against influenza replication and its cytotoxicity

Next, we evaluated the anti-influenza activity and cytotoxicity of compound **1i** cell-based assays. The EC_{50} for compounds **1i** was 0.2 ± 0.01 μM, while for OST it was 0.03 ± 0.0023 μM (Table 4). Compound **1i** was less cytotoxic than OST, CC_{50} values of 566 ± 89.5 μM and 321 ± 26 μM, respectively, were obtained (Table 4). Selective index (SI) values were calculated based on the ratio between the CC_{50} and the EC_{50} values. SI values for OST and compound **1i** were 10,700 and 2830, respectively (Table 4). Although OST' SI value is higher than the one observed for compound **1i**, our molecule is still very safe to be used in vitro. For

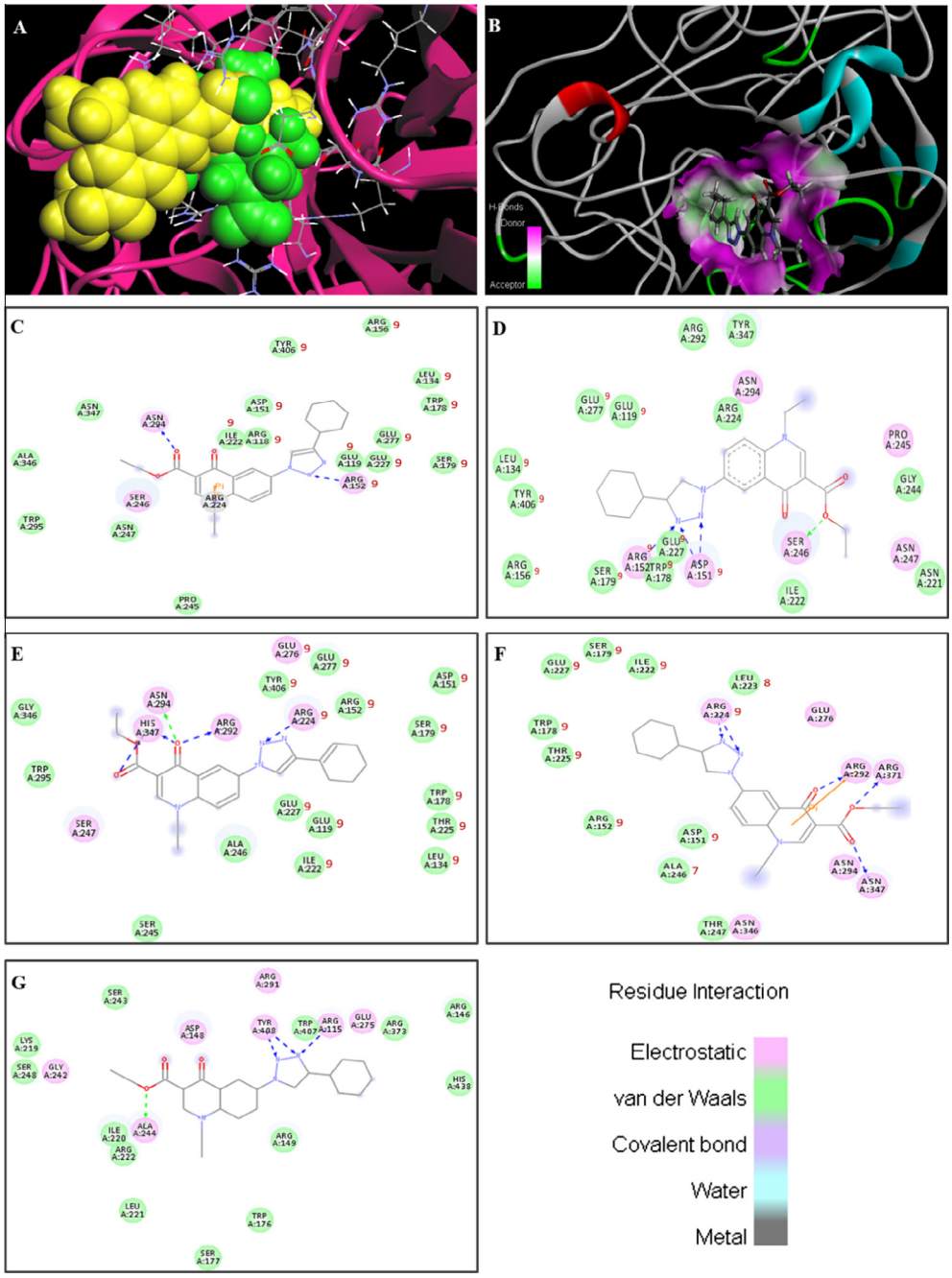

Figure 2. In silico analysis of compound **1i** bound to different isoforms of influenza NA enzyme. The crystal structure of WT N1 isoform with the compound **1i** (yellow) and OST (green) docked in the active site cleft (A). The cyclehexenyl radical of compound **1i** is projected to an area of NA enzyme which is not occupied by OST (B). 2D schematic figures showing compound **1i** docking to different NA isoforms are displayed as following: WT N1 (C), OST-resistant N1 (D), WT N2 (E), OST-resistant N2 (F) and WT influenza B NA (G). The types of interaction between compound **1i** and the NAs are indicated, hydrogen bounds are represented by doted lines. The red numbers, next the amino acid residues surrounding the triazolic ring and the cyclehexenyl moiety, represent in how many different types of influenza NA these residues are conserved (please see also Fig. S1).

comparisons, compound **1i** was more potent than other triazolic derivatives described in the literature using cell-based assays, including the zanamivir analogues.[22] These results indicate that compound **1i** is endowed with a very important margin between anti-influenza activity and cytotoxicity. These information, together with the anti-influenza activity over OST-resistant strains and the apparent ability to bind into conserved amino acid residues on NA, indicate that the chemical structure of compound **1i** is promising and may be of interest for further development of novel anti-influenza drugs.

4. Conclusions

Novel 4-oxoquinoline derivatives containing 1,2,3-triazolyl substituents **1a–j** were successfully synthesized and fully characterized. Compounds **1e** and **1i** were the most potent in inhibiting influenza virus NA enzymes. In addition to the inhibition of susceptible strains of influenza A and B, they also inhibited OST-resistant strains. Compound **1i** binds to the cleft of the active site in all WT and OST-resistant NA isoforms. The cyclohexenyl radical projects into an area of the NA that is not occupied by OST and is critical

Table 3
Compound **1i** and OST with WT and OST interactions during docking

Neuraminidase types	Compound **1i**					OST				
	Binding energy (kcal/mol)	No. of hydrogen bonds	Amino acid residues involved in H-bounding	No. of bumps	Amino acid residues involved in bumps	Binding energy (kcal/mol)	No. of hydrogen bonds	Amino acid residues involved in H-bounding	No. of bumps	Amino acid residues involved in bumps
N1 WT	−6.44	2	Arg 152, Asn 294	18	Arg 118, 153, 224; Glu 119, 227, 277; Leu 134; Asp 151; Trp 178, 295; Ser 179, 246; Ile 222; Pro 245; Asn 247, 347; Ala 346; Tyr 406	−7.44	6	Arg 118, 152, 292, 371; Glu 119; Asp 151	8	Trp 178; Ile 222; Arg 224; Ser 246; Glu 276, 277; Asn 294; Tyr 406
N1 H275Y	−7.49	4	Asp 151; Arg 152; Ser 246	17	Glu 119, 227, 277; Leu 134; Arg 156, 224, 292; Trp 178; Ser 179; Asn 221, 247, 294; Ile 222; Gly 244; Pro 245; Tyr 347, 406	−7.98	7	Arg 118, 152, 292, 371; Glu 119; Tyr 347	9	Asp 151; Trp 178; Ile 222; Arg 224; Ser 246; Glu 276, 277; Asn 294; Tyr 406
N2 WT	−7.59	5	Arg 224, 292; Asn 294; His 347	17	Glu 119, 227, 276, 277; Leu 134; Asp 151; Arg 152; Trp 178, 295; Ser 179, 245, 247; Ile 222; Thr 225; Ala 246; Gly 346; Tyr 406	−8.57	6	Glu 119; Asp 151; Arg 152, 282, 371	10	Arg 118, 224; Trp 178; Ile 222; Ala 246; Glu 276, 277; Asn 294; His 347; Tyr 406
N2 E119V	−7.65	5	Arg 224, 292, 371; Asn 347	13	Asp 151; Arg 152; Trp 179; Ser 179; Ile 222; Leu 223; Glu 227, 276; Ala 246; Thr 247; Asn 294, 346	−8.20	10	Arg 118, 152, 292, 371; Asp 151; Trp 178; Glu 227; Tyr 406	6	Leu 134; Arg 156, 224; Ile 222; Glu 276, 277
N B	−7.60	4	Arg 115; Ala 244; Tyr 408	17	Arg 146, 149, 222, 291, 373; Asp 148; Trp 176, 407; Ser 177, 247, 248; Lys 219; Ile 220; Leu 221; Gly 242; Glu 275; His 438	−7.99	7	Arg 115, 149, 291, 373; Glu 116; Asp 148	7	Trp 176; Ile 220; Arg 222; Ala 244; Glu 274; Asn 293; Tyr 408

Table 4
Potency against influenza replication and cytotoxicity of compound **1i**

Compound	EC_{50} (μM)	CC_{50} (μM)	SI[a]
1i	0.20 ± 0.01	566 ± 89.5	2,830
Oseltamivir	0.03 ± 0.0023	321 ± 26	10,700

[a] SI, selective index is determined by the ratio between CC_{50} and EC_{50} values.

for compound **1i** antiviral activity. Some of the amino acid residues required for the docking of compound **1i** are conserved, and changes in these residues could reduce virus fitness. These results indicate that the chemical structure of our synthesized oxoquinoline analogues are interesting prototypes for further development of novel anti-influenza drugs.

5. Experimental

5.1. Chemistry

5.1.1. Synthesis of ethyl-1-ethyl-7-azido-4-oxo-1,4-dihydroquinoline-3-carboxylate (4b)

The new compound **4b** was synthesized as described previously by us to obtain the derivative **4a**.[25] Reaction of 1-ethyl-3-carbethoxy-7-amino-4-oxo-1,4-dihydroquinoline with nitrous acid (generated in situ from $NaNO_3$ and HCl) followed by the addition of sodium azide afforded the new compound **4b** at a yield of 84%. **4b**: 1-ethyl-3-carbethoxy-7-azido-4-oxo-1,4-dihydroquinoline (84%) mp 143–145 °C; ^{1}H NMR (300.00 MHz, DMSO-d_6, internal standard: Me_4Si), δ 8.55 (s, 1H, H-2), 8.53 (d, 1H, J = 8.5 Hz, H-5), 7.15 (dd, 1H, J = 8.5; 1.8 Hz, H-6), 6.96 (d, 1H, J = 1.8 Hz, H-8), 4.40 (q, 2H, J = 7.1 Hz, NCH_2CH_3), 4.22 (q, 2H, J = 7.1 Hz, OCH_2CH_3), 1.54 (t, 3H, J = 7.1 Hz, NCH_2CH_3), and 1.42 (t, 3H, J = 7.1 Hz, OCH_2CH_3); ^{13}C NMR (75.0 MHz, DMSO-d_6) δ 172.0 (C-4), 164.4 ($CO_2CH_2CH_3$), 149.2 (C-2), 144.1 (C-8a), 139.7 (C-6), 128.7 (C-4a), 125.3 (C-7), 116.2 (C-8), 110.4 (C-5), 106.6 (C-3), 59.7 (OCH_2CH_3), 47.8 (NCH_2CH_3), 14.2 (OCH_2CH_3), and 14.1 (NCH_2CH_3); HRMS (ESI) m/z: calcd for $C_{14}H_{14}N_4O_3$ [M+H+] 287.1144, and found 287.1143.

5.1.2. Synthesis of ethyl 1-ethyl-(1,2,3-triazol-1′-yl)-4-oxo-1,4-dihydroquinoline-3-carboxylates (1a–j)

$CuSO_4{\cdot}5H_2O$ (17.5 mg, 0.07 mmol) and ascorbic acid (29.6 mg, 0.15 mmol) were added to a solution of azidoquinolone (**10a** or **10b**, 100 mg, 0.37 mmol) and the desired alkyne (0.55 mmol) in DMF (10.0 mL).

The resulting solution was stirred for 2 h (monitored by TLC) at 50 °C. After this time, the reaction mixture was poured into ice, leading to a yellow solid that was purified by flash column chromatography (CH_2Cl_2/EtOH as the gradient). **1a**: ethyl 1-ethyl-6-[4′-(2″-hydroxypropan-2″-yl)-*1H* -1,2,3-triazol-1′-yl]-4-oxo-1,4-dihydroquinoline3-carboxylate (88%), mp 175–177°C; ^{1}H NMR (300.00 MHz, DMSO-d_6, internal standard: Me_4Si), δ 8.77 (s, 1H, H-5′), 8.75 (s, 1H, H-2), 8.66 (d, 1H, J = 2.4 Hz, H-5), 8.33 (dd, 1H, J = 9.1; 2.4; H-7), 8.06 (d, 1H, J = 9.1; H-8), 5.26 (s, 1H, $C(CH_3)_2OH$), 4.48 (q, 2H, J = 6.8 Hz, OCH_2CH_3), 4.25 (q, 2H, J = 7.0 Hz, NCH_2CH_3), 1.56 (s, 6H, $C(CH_3)_2OH$), 1.40 (t, 3H, J = 6.8 Hz, OCH_2CH_3), and 1.30 (t, 3H, J = 7.0 Hz, NCH_2CH_3); ^{13}C NMR (75.0 MHz, DMSO-d_6) δ 172.2 (C-4), 164.3 ($CO_2CH_2CH_3$), 157.0 (C-4′), 149.2 (C-2), 137.9 (C-8a), 133.4 (C-6), 129.0 (C-4a), 124.2 (C-7), 119.0 (C-5′), 119.3 (C-8), 116.6 (C-5), 110.3 (C-3), 66.9 ($C(CH_3)_2OH$), 59.8 (NCH_2CH_3), 48.1 (OCH_2CH_3), 30.4 ($C(CH_3)_2OH$), 14.3 (OCH_2CH_3), and 14.2 (NCH_2CH_3); ESI-FTICRMS: m/z calcd for $C_{19}H_{22}N_4O_4$ [M+H] 371.1873, found 371.1870; **1b**: ethyl 1-ethyl-7-[4′-(2″-hydroxypropan-2″-yl)-*1H* -1,2,3-triazol-1′-yl]-4-oxo-1,4-dihydroquinoline-3-carboxylatye (85%), mp 179–181 °C; ^{1}H NMR (300.00 MHz, DMSO-d_6, internal standard:Me_4Si) δ 8.92 (s, 1H, H-5′), 8.75

(s, 1H, H-2), 8.40 (d, 1H, J = 8.8 Hz, H-5), 8.07 (dd, 1H, J = 8.8; 1.7; H-6), 8.20 (d, 1H, J = 1.7; H-8), 4.52 (q, 2H, J = 7.1 Hz, OCH_2CH$_3$), 4.24 (q, 2H, J = 7.1 Hz, NCH_2CH$_3$), 1.56 (s, 6H, C(CH_3)$_2$OH), 1.41 (t, 3H, J = 7.1 Hz, OCH$_2$CH_3), and 1.30 (t, 3H, J = 7.1 Hz, NCH$_2$CH_3); ^{13}C NMR (75.0 MHz, DMSO-d_6) δ 172.2 (C-4), 164.3 (CO_2CH$_2$CH$_3$), 157.3 (C-4′), 149.7 (C-2), 139.7 (C-8a), 139.5 (C-7), 127.4 (C-4a), 128.7 (C-5), 119.4 (C-5′), 116.3 (C-6), 110.8 (C-3), 107.3 (C-8), 67.0 (C(CH$_3$)$_2$OH), 59.8 (NCH$_2$CH$_3$), 48.0 (OCH$_2$CH$_3$), 30.5 (C(CH$_3$)$_2$OH), 14.3 (OCH$_2$CH$_3$), and 14,2 (NCH$_2$CH$_3$); ESI-FTICRMS: m/z calcd for $C_{19}H_{22}N_4O_4$ [M+H] 371.1873, found 371.1876; **1c**: ethyl 1-ethyl-6-[4′-(1″-hydroxycyclohexyl)-*1H* -1,2,3-triazol-1′-yl]-4-oxo-1,4-dihydroquinoline-3-carboxylate (83%), mp 228–230 °C; ^{1}H NMR (300.00 MHz, DMSO-d_6) δ 8.77 (s, 1H, H-5′), 8.74 (s, 1H, H-2), 8.66 (d, 1H, J = 2.4 Hz, H-5), 8.32 (dd, 1H, J = 9.2; 2.4 Hz, H-7), 8.05 (d, 1H, J = 9.2 Hz, H-8), 4.48 (q, 2H, J = 6.8 Hz, OCH_2CH$_3$), 4.25 (q, 2H, J = 7.1 Hz, NCH_2CH$_3$), 2.03–1.48 (m, 10H, H-2″ to H-6″), 1.40 (t, 3H, J = 6.8 Hz, OCH$_2$CH_3), and 1.30 (t, 3H, J = 7.1 Hz, NCH$_2$CH_3); ^{13}C NMR (75.0 MHz, DMSO-d_6) δ 172.1 (C-4), 164.3 (CO_2CH$_2$CH$_3$), 156.8 (C-4′), 149.1 (C-2), 137.9 (C-8a), 133.4 (C-6), 124.1 (C-7), 120.0 (C-4a), 119.4 (C-5′), 119.3 (C-8), 116.6 (C-5), 110.3 (C-3), 67.8 (C-1″), 59.7 (NCH$_2$CH$_3$), 48.1 (OCH$_2$CH$_3$), 37.5 (C-2″ and C-6″), 25.1 (C-4″), 21.6 (C-3″ and C-5″), 14.3 (OCH$_2$CH$_3$), and 14.2 (NCH$_2$CH$_3$); ESI-FTICRMS: m/z calcd for $C_{22}H_{26}N_4O_4$ [M+H] 411.2227, found 411.2222; **1d**: ethyl 1-ethyl-7-[4′-(1″-hydroxycyclohexyl)-*1H* -1,2,3-triazol-1′-yl]-4-oxo-1,4-dihydroquinoline-3-carboxylate (79%) mp 105–107 °C; ^{1}H NMR (300.00 MHz, DMSO-d_6, internal standard: Me$_4$Si) δ 8.93 (s, 1H, H-5′), 8.74 (s, 1H, H-2), 8.41 (d, 1H, J = 8.8 Hz, H-5), 8.07 (dd, 1H, J = 8.8; 1.8 Hz, H-6), 8.20 (d, 1H, J = 1.8 Hz, H-8), 4.52 (q, 2H, J = 7.1 Hz, OCH_2CH$_3$), 4.25 (q, 2H, J = 7.0 Hz, NCH_2CH$_3$), 2.02–1.49 (m, 10H, H-2″ to H-6″), 1.46 (t, 3H, J = 7.1 Hz, OCH$_2$CH_3), and 1.30 (t, 3H, J = 7.1 Hz, NCH$_2$CH_3); ^{13}C NMR (75.0 MHz, DMSO-d_6) δ 172.0 (C-4), 164.2 (CO_2CH$_2$CH$_3$), 157.1 (C-4′), 149.4 (C-2), 139.6 (C-7), 139.4 (C-8a), 128.5 (C-5), 127.2 (C-4a), 119.6 (C-5′), 116.0 (C-6), 110.1 (C-3), 107.1 (C-8), 67.9 (C-1″), 59.5 (NCH$_2$CH$_3$), 47.7 (OCH$_2$CH$_3$), 37.3 (C-2″ and C-6″), 24.8 (C-4″), 21.2 (C-3″ and C-5″), 14.0 (OCH$_2$CH$_3$), and 13.9 (NCH$_2$CH$_3$); ESI-FTICRMS: m/z calcd for $C_{22}H_{26}N_4O_4$ [M+H] 411.2227, found 411.2226; **1e**: ethyl 1-ethyl-6-(4′-phenyl-*1H* -1,2,3-triazol-1′-yl)-4-oxo-1,4-dihydroquinoline-3-carboxylate (97%), mp 237–239 °C; ^{1}H NMR (300.00 MHz, DMSO-d_6, internal standard: Me$_4$Si) δ 9.46 (s, 1H, H-5′), 8.74 (s, 1H, H-2), 8.73 (d, 1H, J = 2.7 Hz, H-5), 8.37 (dd, 1H, J = 9.1; 2.7 Hz, H-7), 8.10 (d, 1H, J = 9.1 Hz, H-8), 7.99 (d, 2H, J = 7.1 Hz, H-2″ and H-6″), 7.51 (t, 2H, J = 7.3 Hz, H-3″ and H-5″), 7.40 (t, 1H, J = 7.1 Hz, H-4″), 4.48 (q, 2H, J = 7.1 Hz, OCH_2CH$_3$), 4.27 (q, 2H, J = 7.1 Hz, NCH_2CH$_3$), 1.44 (t, 3H, J = 7.1 Hz, OCH$_2$CH_3), and 1.32 (t, 3H, J = 7.1 Hz, NCH$_2$CH_3); ^{13}C NMR (75.0 MHz, DMSO-d_6) δ 172.1 (C-4), 164.2 (CO_2CH$_2$CH$_3$), 149.0 (C-2), 147.4 (C-4′), 138.1 (C-8a), 133.1 (C-6), 131.5 (C-1″), 130.0 (C-4a), 128.7 (C-3″ and C-5″), 128.1 (C-4″), 125.2 (C-2″ and C-6″), 124.1 (C-7), 119.3 (C-8), 116.7 (C-5), 115.0 (C-5′), 110.4 (C-3), 59.6 (NCH$_2$CH$_3$), 48.0 (OCH$_2$CH$_3$), 14.2 (OCH$_2$CH$_3$), and 14.1 (NCH$_2$CH$_3$); ESI-FTICRMS: m/z calcd for $C_{22}H_{20}N_4O_3$ [M+H] 389.1535, found 389.1532; **1f**: ethyl 1-ethyl-7-(4′-phenyl-*1H*-1,2,3-triazol-1′-yl)-4-oxo-1,4-dihydroquinoline-3-carboxylate (93%) mp 127–129 °C; ^{1}H NMR (300.00 MHz, DMSO-d_6, internal standard: Me$_4$Si) δ 9.52 (s, 1H, H-5′), 8.76 (s, 1H, H-2), 8.46 (d, 1H, J = 8.7 Hz, H-5), 8.09 (dd, 1H, J = 8.7; 1.6 Hz, H-6), 8.26 (d, 1H, J = 1.6 Hz, H-8), 7.97 (dd, 2H, J = 8.2; 1.2 Hz, H-2″ and H-6″), 7.54 (t, 2H, J = 7.2 Hz, H-3″ and H-5″), 7.43 (t, 1H, J = 7.2 Hz, H-4″), 4.52 (q, 2H, J = 7.0 Hz, OCH_2CH$_3$), 4.25 (q, 2H, J = 7.0 Hz, NCH_2CH$_3$), 1.46 (t, 3H, J = 7.0 Hz, OCH$_2$CH_3), and 1.31 (t, 3H, J = 7.0 Hz, NCH$_2$CH_3); ^{13}C NMR (75.0 MHz, DMSO-d_6) δ 171.9 (C-4), 164.0 (CO_2CH$_2$CH$_3$), 149.4 (C-2), 147.3 (C-4′), 139.2 (C-8a and C-7), 129.3 (C-1″), 128.8 (C-3″ and C-5″), 128.3 (C-4″), 127.4 (C-4a), 125.1 (C-2″ and C-6″), 128.7 (C-5), 119.9 (C-5′), 116.2 (C-6), 108.1 (C-3), 107.5 (C-8), 59.6 (NCH$_2$CH$_3$), 47.8 (OCH$_2$CH$_3$), 14.0 (OCH$_2$CH$_3$), and 13.9 (NCH$_2$CH$_3$); ESI-FTICRMS: m/z calcd for $C_{22}H_{20}N_4O_3$ [M+H] 389.1535, found 389.1538; **1g**: ethyl 1-ethyl-6-[4′-(hydroxymethyl)-*1H* -1,2,3-triazol-1′-yl]-4-oxo-1,4-dihydroquinoline-3-carboxylate (95%) mp 220–221 °C; ^{1}H NMR (300.00 MHz, DMSO-d_6, internal standard: Me$_4$Si) δ 8.85 (s, 1H, H-5′), 8.75 (s, 1H, H-2), 8.66 (d, 1H, J = 2.7 Hz, H-5), 8.32 (dd, 1H, J = 9.3; 2.7, H-7), 8.07 (d, 1H, J = 9.3; H-8), 5.35 (t, 1H, J = 5.5 Hz, CH$_2$OH), 4.63 (d, 2H, J = 5.5 Hz, CH_2OH), 4.48 (q, 2H, J = 7.1 Hz, OCH_2CH$_3$), 4.25 (q, 2H, J = 7.3 Hz, NCH_2CH$_3$), 1.40 (t, 3H, J = 7.1 Hz, OCH$_2$CH_3), and 1.30 (t, 3H, J = 7.3 Hz, NCH$_2$CH_3); ^{13}C NMR (75.0 MHz, DMSO-d_6) δ 172.2 (C-4), 164.4 (CO_2CH$_2$CH$_3$), 149.3 (C-4′), 149.2 (C-2), 138.0 (C-8a), 133.4 (C-6), 129.0 (C-4a), 124.3 (C-7), 121.2 (C-5′), 119.4 (C-8), 116.8 (C-5), 110.3 (C-3), 59.8 (NCH$_2$CH$_3$), 54.9 (CH$_2$OH), 48.2 (OCH$_2$CH$_3$), 14.4 (OCH$_2$CH$_3$), and 14.3 (NCH$_2$CH$_3$); ESI-FTICRMS: m/z calcd for $C_{17}H_{18}N_4O_4$ [M+H] 343.1328, found 343.1324; **1h**: ethyl 1-ethyl-7-[4′-(hydroxymethyl)-*1H* -1,2,3-triazol-1′-yl]-4-oxo-1,4-dihydroquinoline-3-carboxylate (90%) mp 223–225 °C; ^{1}H NMR (300.00 MHz, DMSO-d_6, internal standard: Me$_4$Si) δ 9.00 (s, 1H, H-5′), 8.75 (s, 1H, H-2), 8.41 (d, 1H, J = 8.6 Hz, H-5), 8.21 (d, 1H, J = 1.7; H-8), 8.07 (dd, 1H, J = 8.6; 1.7, H-6), 4.66 (s, 1H, CH$_2$OH), 4.51 (q, 2H, J = 7.1 Hz, OCH_2CH$_3$), 4.25 (q, 2H, J = 7.1 Hz, NCH_2CH$_3$), 1.42 (t, 3H, J = 7.1 Hz, OCH$_2$CH_3), and 1.30 (t, 3H, J = 7.1 Hz, NCH$_2$CH_3); ^{13}C NMR (75.0 MHz, DMSO-d_6) δ 172.0 (C-4), 164.4 (CO_2CH$_2$CH$_3$), 149.5 (C-4′), 149.7 (C-2), 139.5 (C-8a), 128.8 (C-5), 127.4 (C-4a), 124.3 (C-7), 121.6 (C-5′), 116.3 (C-6), 110.8 (C-3), 107.5 (C-8), 59.8 (NCH$_2$CH$_3$), 54.9 (CH$_2$OH), 48.0 (OCH$_2$CH$_3$), 14.3 (OCH$_2$CH$_3$), and 14.2 (NCH$_2$CH$_3$); ESI-FTICRMS: m/z calcd for $C_{17}H_{18}N_4O_4$ [M+H] 343.1328, found 343.1326; **1i**: ethyl 1-ethyl-6-(4′-cyclohexenyl-*1H* -1,2,3-triazol-1′-yl)-4-oxo-1,4-dihydroquinoline-3-carboxylate (98%) mp 230–231 °C; ^{1}H NMR (300.00 MHz, DMSO-d_6, internal standard: Me$_4$Si) δ 8.94 (s, 1H, H-5′), 8.73 (s, 1H, H-2), 8.67 (d, 1H, J = 2.5 Hz, H-5), 8.30 (dd, 1H, J = 9.1; 2.5 Hz, H-7), 8.06 (d, 1H, J = 9.1 Hz, H-8), 6.58 (t, 1H, J = 3.6 Hz, H-2″), 4.47 (q, 2H, J = 7.0 Hz, OCH_2CH$_3$), 4.26 (q, 2H, J = 7.1 Hz, NCH_2CH$_3$), 1.96–1.74 (m, 8H, H-3″ to H-6″), 1.42 (t, 3H, J = 7.0 Hz, OCH$_2$CH_3), and 1.31 (t, 3H, J = 7.1 Hz, NCH$_2$CH_3); ^{13}C NMR (75.0 MHz, DMSO-d_6) δ 172.2 (C-4), 164.2 (CO_2CH$_2$CH$_3$), 149.0 (C-2), 149.1 (C-4′), 137.9 (C-8a), 133.3 (C-6), 129.0 (C-4a), 127.0 (C-1″), 124.5 (C-2″), 124.0 (C-7), 119.3 (C-8), 118.0 (C-5′), 116.5 (C-5), 110.3 (C-3), 59.7 (NCH$_2$CH$_3$), 48.1 (OCH$_2$CH$_3$), 24.6 (C-6″), 25.7 (C-3″), 21.9 (C-4″), 21.7 (C-5″),14.3 (OCH$_2$CH$_3$), and 14.2 (NCH$_2$CH$_3$); ESI-FTICRMS: m/z calcd for $C_{22}H_{24}N_4O_3$ [M+H] 393.1758, found 393.1754; **1j**: ethyl 1-ethyl-7-(4′-cyclohexenyl-*1H* -1,2,3-triazol-1′-yl)-4-oxo-1,4-dihydroquinoline-3-carboxylate (95%), mp 235–237 °C; ^{1}H NMR (300.00 MHz, DMSO-d_6, internal standard: Me$_4$Si) δ 9.02 (s, 1H, H-5′), 8.75 (s, 1H, H-2), 8.41 (d, 1H, J = 8.7 Hz, H-5), 8.17 (d, 1H, J = 1.6 Hz, H-8), 8.05 (dd, 1H, J = 8.7; 1.6 Hz, H-6), 6.59 (t, 1H, J = 3.6 Hz, H-2″), 4.48 (q, 2H, J = 6.8 Hz, NCH_2CH$_3$), 4.25 (q, 2H, J = 7.0 Hz, OCH_2CH$_3$), 2.44–2.42 (m, 2H, H-3″ or H-6″), 2.22–2.10 (m, 2H, H-3″ or H-6″), 1.80–1.72 (m, 2H, H-4″ or H-5″), 1.67–1.64 (m, 2H, H-4″ or H-5″), 1.40 (t, 3H, J = 6.8 Hz, NCH$_2$CH_3), and 1.30 (t, 3H, J = 7.0 Hz, NCH$_2$CH_3); ^{13}C NMR (75.0 MHz, DMSO-d_6) δ 172.3 (C-4), 164.5 (CO_2CH$_2$CH$_3$), 149.6 (C-4′), 149.4 (C-2), 139.8 (C-7 and C-8a), 128.6 (C-5), 127.8 (C-4a), 127.2 (C-1″), 124.7 (C-2″), 117.7 (C-5′), 116.0 (C-6), 110.2 (C-3), 107.1 (C-8), 59.7 (NCH$_2$CH$_3$), 47.8 (OCH$_2$CH$_3$), 25.5 (C-6″), 24.4 (C-3″), 21.6 (C-4″), 21.5 (C-5″), 14.1 (OCH$_2$CH$_3$), and 14.0 (NCH$_2$CH$_3$); ESI-FTICRMS: m/z calcd for C22H24N4O3 [M+H] 393.1758, found 393.1755.

5.2. Cells and viruses

Madin-Darby canine kidney epithelial cells (MDCKs) were cultured in Dulbecco's Modified Eagle Medium (DMEM; Life Technologies, Grand Island, NY) supplemented with 10% fetal bovine serum and antibiotics (100 U/mL penicillin and 100 μg/mL

streptomycin) at 37 °C and 5% CO_2. Both wild-type and NAI-resistant influenza A and B virus strains (Table S3) were propagated in MDCKs and stored at −70 °C. The influenza strains displayed in Table S3 were kindly donated by Dr. Larisa V. Gubareva and Dr. Alexander I. Klimov from the Centers for Disease Control (CDC), Atlanta, to the Brazilian National Influenza Center (NIC) at FIOCRUZ, Rio de Janeiro. These viruses are reference strains used for laboratory-based surveillance to monitor the antiviral susceptibility of circulating influenza viruses to NAIs.

5.2.1. Cytotoxicity assay

Monolayers of 2×10^4 MDCKs in 96-well culture plates were incubated with the compounds at different concentrations for 72 h. Then, 2,3-bis-(2-methoxy-4-nitro-5-sulfophenyl)-2*H*-tetrazolium-5-carboxanilide (XTT) at 5 mg/mL was added to the DMEM in the presence of 0.01% *N*-methyl-dibenzopirazin methyl sulfate (PMS). After incubation for 4 h at 37 °C, the plates were read in a spectrophotometer at 492 nm and 620 nm.[29] The 50% cytotoxic concentration (CC_{50}) was calculated by linear regression analysis of the dose–response curves generated from the data.

5.2.2. Yield reduction assay

Monolayers of MDCK cells (2×10^5 cell/well) in 24-well plates were infected with influenza at an MOI of 0.05 for 1 h at 37 °C. Cells were washed to remove residual viruses and various concentrations of the compounds were added. After 24 h, viruses in the supernatant were harvested and titrated by end-point 50% cell culture infective dose ($TCID_{50}$/mL) using MDCK cells. For compression, the reference compound OST carboxylate (kindly donated by Hoffman-La Roche Inc., Basel, Switzerland) was used as a positive control. Linear regression of the dose-response curve was performed to determine the 50% inhibitory effect on viral replication (EC_{50}) for the tested and reference compounds.

5.2.3. Influenza titration

MDCKs plated in 96-well plates (5×10^4 cells/well) were infected with serial 10-fold dilutions of the supernatants from the yield-reduction assays described above for 1 h at 37 °C and 5% CO_2. Then, viruses were washed out and the cells were incubated for 72 h. After this period of time, influenza-induced cytopathic effects (CPE) were scored by $TCID_{50}$.[30,31]

5.2.4. NA inhibition assay

To evaluate the ability of the compounds to inhibit the NA activity of the influenza strains described in Table S1, we performed cell-free based assays using the NA-Starkit (Life Technologies, CA) according to the manufacturer's instructions. Briefly, the NA activity of the different influenza virus strains was tittered. Next, the NA activity was measured in the presence of different concentrations of the compounds to determine the enzyme inhibition. The concentration able to inhibit 50% of influenza's NA activity (IC_{50}) was calculated using non-linear regression. For comparison, every assay was performed with OST carboxylate as a positive control.

5.3. In silico docking

Docking of the compound **1i** or OST with different NAs (Table S4) was performed using the ArgusLab 4.0.1 software (Planaria Software LLC).[32] The crystal structures of WT and OST-resistant NAs were obtained from the Protein Data Bank (PDB, www.rcsb.org).[33] PDB accession numbers and the degree of resolution of the X-ray crystals are shown in Table S2. We selected these files because they already have an OST molecule bound in the crystal structure of the NA. To our knowledge, no OST-resistant influenza B NA structure is deposited in the PDB. Before docking, the structures of the proteins were cleaned by removing the water molecules and external ligands, with the exception of OST. The modified structure was saved in the .pdb format to be used in all docking studies. The structure of compound **1i** was designed using Accelrys Draw 4.1 software (Accelrys, Inc.) and improved using Accelrys® Discovery Studio 3.5 software to add hydrogens and optimize the compound geometry (UFF Molecular Mechanics method).[34] The optimized **1i** molecule file was saved in .mol format for further docking studies. The docking between the ligand **1i** and each NA enzyme isoform was performed using the 'Dock a Ligand' option in the Arguslab software. The area occupied by amino acid residues involved in the docking of OST was considered to be the center of the actual **1i** bind site (Table S2). A spacing of 0.4 Å between the grid points was used and the ligand was assumed to be flexible and the protein rigid. A maximum of 150 poses were allowed in the analysis, and each docking run was repeated three times to obtain the best results. 'ArgusDock' and 'Dock' were chosen as the docking engine for the simulations and calculation type, respectively. Displays of the 2D interactions between compound **1i** and different NAs were obtained with Accelrys® Discovery Studio 3.5 software.[35] OST was docked over the original reference compound found in these protein X-ray structures as a control. Poses with lower free-energy and with differences smaller than 3 Å between the two docked OST structures were considered to be reliable.

5.3.1. Alignment of genetically diverse neuraminidases

To compare the relevant residues found in the docking analysis with their equivalents on the sequenced NA isoforms found in nature, we created alignments using Mega 6.06 software. DNA sequences were aligned by Clustal W (1.6), and amino acid residues were predicted. We have chosen to align the complete genome segment of influenza A NA isoforms N1–N9 (NCBI codes and influenza strains are listed in Table S4) and analyzed specific regions containing the amino acid residues involved in the **1i** and NA interactions.

5.4. Statistical analyses

The dose-response curves used to calculate the IC_{50}, EC_{50} and CC_{50} values were generated by Excel for Windows. All of the experiments were performed at least three times, and the results are displayed as mean ± standard error of the mean (SEM).

Acknowledgments

We thank the Conselho Nacional de Desenvolvimento Científico e Tecnológico (CNPq), Coordenação de Aperfeiçoamento de Pessoal Docente (CAPES) and Fundação de Amparo à Pesquisa do Estado do Rio de Janeiro (FAPERJ) for financial support and fellowships.

Supplementary data

Supplementary data associated with this article can be found, in the online version, at http://dx.doi.org/10.1016/j.bmc.2015.11.028.

References and notes

1. Damjanovic, D.; Small, C. L.; Jeyanathan, M.; Jeyananthan, M.; McCormick, S.; Xing, Z. *Clin. Immunol.* **2012**, *144*, 57.
2. Murphy, B. R.; Webster, R. G. *Orthomyxoviruses*, 3rd ed.; Lappincott-Raven: Philadelphia, 1996.
3. Tang, J. W.; Shetty, N.; Lam, T. T.; Hon, K. L. *Infect. Dis. Clin. North Am.* **2010**, *24*, 603.
4. Kollerova, E.; Betakova, T. *Acta Virol.* **2006**, *50*, 7.
5. Das, K.; Aramini, J. M.; Ma, L. C.; Krug, R. M.; Arnold, E. *Nat. Struct. Mol. Biol.* **2010**, *17*, 530.

6. Grohskopf, L. A.; Olsen, S. J.; Sokolow, L. Z.; Bresee, J. S.; Cox, N. J.; Broder, K. R.; Karron, R. A.; Walter, E. B.C. f. D. C. a Prevention *MMWR Morb. Mortal. Wkly. Rep.* **2014**, *63*, 691.
7. Fiore, A. E.; Fry, A.; Shay, D.; Gubareva, L.; Bresee, J. S.; Uyeki, T. M. *MMWR Recomm. Rep.* **2011**, *60*, 1.
8. Manz, B.; Schwemmle, M.; Brunotte, L. *J. Virol.* **2013**, *87*, 7200.
9. WHO *Wkly. Epidemiol. Rec.* **2013**, *88*, 437.
10. Muthuri, S. G.; Myles, P. R.; Venkatesan, S.; Leonardi-Bee, J.; Nguyen-Van-Tam, J. S. *J. Infect. Dis.* **2013**, *207*, 553.
11. Balicer, R. D.; Huerta, M.; Davidovitch, N.; Grotto, I. *Emerg. Infect. Dis.* **2005**, *11*, 1280.
12. Patel, A.; Gorman, S. E. *Clin. Pharmacol. Ther.* **2009**, *86*, 241.
13. Hurt, A. C. *Curr. Opin. Virol.* **2014**, *8C*, 22.
14. Jefferson, T.; Jones, M.; Doshi, P.; Spencer, E. A.; Onakpoya, I.; Heneghan, C. J. *BMJ* **2014**, *348*, g2545.
15. Fry, A. M.; Gubareva, L. V. *J. Infect. Dis.* **2012**, *206*, 145.
16. Hurt, A. C.; Hardie, K.; Wilson, N. J.; Deng, Y. M.; Osbourn, M.; Leang, S. K.; Lee, R. T.; Iannello, P.; Gehrig, N.; Shaw, R.; Wark, P.; Caldwell, N.; Givney, R. C.; Xue, L.; Maurer-Stroh, S.; Dwyer, D. E.; Wang, B.; Smith, D. W.; Levy, A.; Booy, R.; Dixit, R.; Merritt, T.; Kelso, A.; Dalton, C.; Durrheim, D.; Barr, I. G. *J. Infect. Dis.* **2012**, *206*, 148.
17. Souza, T. M. L.; Rodrigues, D. Q.; Ferreira, V. F.; Marques, I. P.; Santos, F. C.; Cunha, A. C.; Souza, M. C. B. V.; Frugulhetti, I. C. P. P.; Bou-Habib, D. C.; Fontes, C. F. L. *Curr. HIV Res.* **2009**, *7*, 327.
18. Wang, Z.; Wu, B.; Kuhen, K. L.; Bursulaya, B.; Nguyen, T. N.; Nguyen, D. G.; He, Y. *Bioorg. Med. Chem. Lett.* **2006**, *16*, 4174.
19. Duffin, G. F.; Kendall, J. D. *J. Chem. Soc.* **1948**, *70*, 893.
20. Kumar, D. V.; Rai, R.; Brameld, K. A.; Somoza, J. R.; Rajagopalan, R.; Janc, J. W.; Xia, Y. M.; Ton, T. L.; Shaghafi, M. B.; Hu, H.; Lehoux, I.; To, N.; Young, W. B.; Green, M. J. *Bioorg. Med. Chem. Lett.* **2011**, *21*, 82.
21. Wittine, K.; Stipković Babić, M.; Makuc, D.; Plavec, J.; Kraljević Pavelić, S.; Sedić, M.; Pavelić, K.; Leyssen, P.; Neyts, J.; Balzarini, J.; Mintas, M. *Bioorg. Med. Chem.* **2012**, *20*, 3675.
22. Li, J.; Zheng, M.; Tang, W.; He, P. L.; Zhu, W.; Li, T.; Zuo, J. P.; Liu, H.; Jiang, H. *Bioorg. Med. Chem. Lett.* **2006**, *16*, 5009.
23. Głowacka, I. E.; Balzarini, J.; Andrei, G.; Snoeck, R.; Schols, D.; Piotrowska, D. G. *Bioorg. Med. Chem.* **2014**, *22*, 3629.
24. Ruxer, J. M.; Lachoux, C.; Ousset, J. B.; Torregrosa, J. L.; Mattioda, G. *J. Heterocycl. Chem.* **1994**, *31*, 409.
25. Abreu, P. A.; da Silva, V. A. G. G.; Santos, F. C.; Castro, H. C.; Riscado, C. S.; Souza, M. T.; Ribeiro, C. P.; Barbosa, J. E.; dos Santos, C. C. C.; Rodrigues, C. R.; Lione, V.; Correa, B. A. M.; Cunha, A. C.; Ferreira, V. F.; Souza, M. C. B. V.; Paixão, I. C. N. P. *Curr. Microbiol.* **2011**, *62*, 1349.
26. Webster, R. G.; Govorkova, E. A. *Ann. N. Y. Acad. Sci.* **2014**, *1323*, 115.
27. von Itzstein, M.; Wu, W. Y.; Kok, G. B.; Pegg, M. S.; Dyason, J. C.; Jin, B.; Van Phan, T.; Smythe, M. L.; White, H. F.; Oliver, S. W. *Nature* **1993**, *363*, 418.
28. Aoki, F. Y.; Boivin, G.; Roberts, N. *Antiviral Ther.* **2007**, *12*, 603.
29. Scudiero, D. A.; Shoemaker, R. H.; Paull, K. D.; Monks, A.; Tierney, S.; Nofziger, T. H.; Currens, M. J.; Seniff, D.; Boyd, M. R. *Cancer Res.* **1988**, *48*, 4827.
30. Reed, L. J.; Muench, H. *Am. J. Epidemiol.* **1938**, *27*, 493.
31. WHO; CDC. Serological Diagnosis of Influenza by Microneutralization Assay; 2010.
32. Joy, S.; Nair, P. S.; Hariharan, R.; Pillai, M. R. *In Silico Biol.* **2006**, *6*, 601.
33. Bernstein, F. C.; Koetzle, T. F.; Williams, G. J.; Meyer, E. F.; Brice, M. D.; Rodgers, J. R.; Kennard, O.; Shimanouchi, T.; Tasumi, M. *Arch. Biochem. Biophys.* **1978**, *185*, 584.
34. Rappe, A. K.; Casewit, C. J.; Colwell, K. S.; Goddard, W. A. I.; Skiff, W. M. *J. Am. Chem. Soc.* **1992**, *114*, 10024.
35. Hussain Basha, S.; Prasad, R. N. *BMC Res. Notes* **2012**, *5*, 105.

Supplementary Information

1,2,3-Triazolyl-4-oxoquinolines: a feasible beginning for inhibitor prototypes of Oseltamivir-resistant influenza A and B viruses

Fernanda da C. S. Boechat[1,#], Carolina Q. Sacramento[2,3,4,#], Anna C. Cunha[1], Fernanda S. Sagrillo[1], Christiane M. Nogueira[1], Natalia Fintelman-Rodrigues[2,3,4], Osvaldo Santos-Filho[2], Cecília S. Riscado[1], Luana da S. M. Forezi[1], , Leonardo Brozeguini[1], Isakelly P. Marques[1], Vitor F. Ferreira[1], Thiago Moreno L. Souza[2,3,4,] and Maria Cecília B. V. de Souza[1,*]*

[1] Universidade Federal Fluminense, Instituto de Química - Outeiro de São João Batista, s/nº.Campus do Valonguinho - Centro - Niterói – RJ, CEP: 24020-150, Brazil

[2] Fundação Oswaldo Cruz, Instituto Oswaldo Cruz, Laboratório de Vírus Respiratórios, NIC-WHO, Rio de Janeiro, RJ, CEP 21041-360, Brazil

[3] Fundação Oswaldo Cruz, Instituto Oswaldo Cruz, Laboratório de Imunofarmacologia, Rio de Janeiro, RJ, CEP 21041-360, Brazil

[4] Fundação Oswaldo Cruz, Centro de Desenvolvimento Tecnológico em Saúde, Rio de Janeiro, RJ, CEP 21041-360, Brazil

# These authors contributed equally as first authors

* These authors contributed equally as last authors

Contents:

Table S1. Percentage of inhibition of WT and OST-resistant NA activity by triazolic compounds.

Representative numbers of the best hits	Inhibition of NA (%) OST-R[a]	WT[a]	Ratio[b]
1	79	96	0.82
2	70	87	0.80
3	99	95	1.04
4	77	90	0.86
5	72	89	0.81
6	98	89	1.10
7	75	86	0.87
8	68	80	0.85

[a] Influenza NA from H3N2 virus was used. The resistant strain carries the mutation E119V.
[b] Ratio between inhibitory activities against OST-resistant and WT enzymes.

Table S2. Protein Data Bank (PDB) accession numbers of the proteins used for *in silico* docking of compound 1i.

Influenza strain	Sensitivity to OST	PDB ID	Resolution factor (Å) of the crystal structures from PDB	Grid Dimension (x, y, z) (Å) used for compound **1i** docking
H1N1pdm09	WT	3TI6	1.69	68 x 45 x 75
H1N1	Resistant: H274Y mutation	3CL0	2.20	54 x 62 x 38
H3N2	WT	4GZP	2.30	53 x 63 x 38
H3N2	Resistant: E119G mutation	1L7G	1.85	50 x 61 x 39
B	WT	4CPM	2.75	59 x 50 x 52

Table S3: Influenza A and B viruses, WT and OST-resistant strains, used in the study.

Strains	Type/Subtype	NA mutation
A/WA/10/2008	A (H1N1)	WT
A/FL/21/2008	A (H1N1)	H275Y
A/RJ/512/2009	A(H1N1pdm09)	WT
A/WA/01/2007	A (H3N2)	WT
A/ENG/42/72	A (H3N2)*	WT
A/TX/12/2007	A (H3N2)	E119V
B/MEMPHIS/20/1996	B	WT
B/MEMPHIS/20/1996	B	R152K

Table S4: Accession numbers of NCBI sequences of NA from different influenza strains used in the alignment analysis.

Influenza Strains	Accession Numbers
A/California/04/2009 (H1N1)	FJ966084.1
A/Wisconsin/13/2008 (H3N2)	FJ549063.1
A/equine/New Market/79 (H3N3)	L06581
A/mallard/Alberta/283/1977 (H8N4)	K01023.1
A/chicken/Texas/9686-3/2014 (H6N5)	KM244094.1
A/sanderling/Delaware/1258/86 (H6N6)	AY207557.1
A/FPV/Weybridge (H7N7)	M38330.1
A/duck/Memohis/928/74 (H3N8)	L06575
A/tern/Australia/G70C/1975 (H11N9)	M11445.1

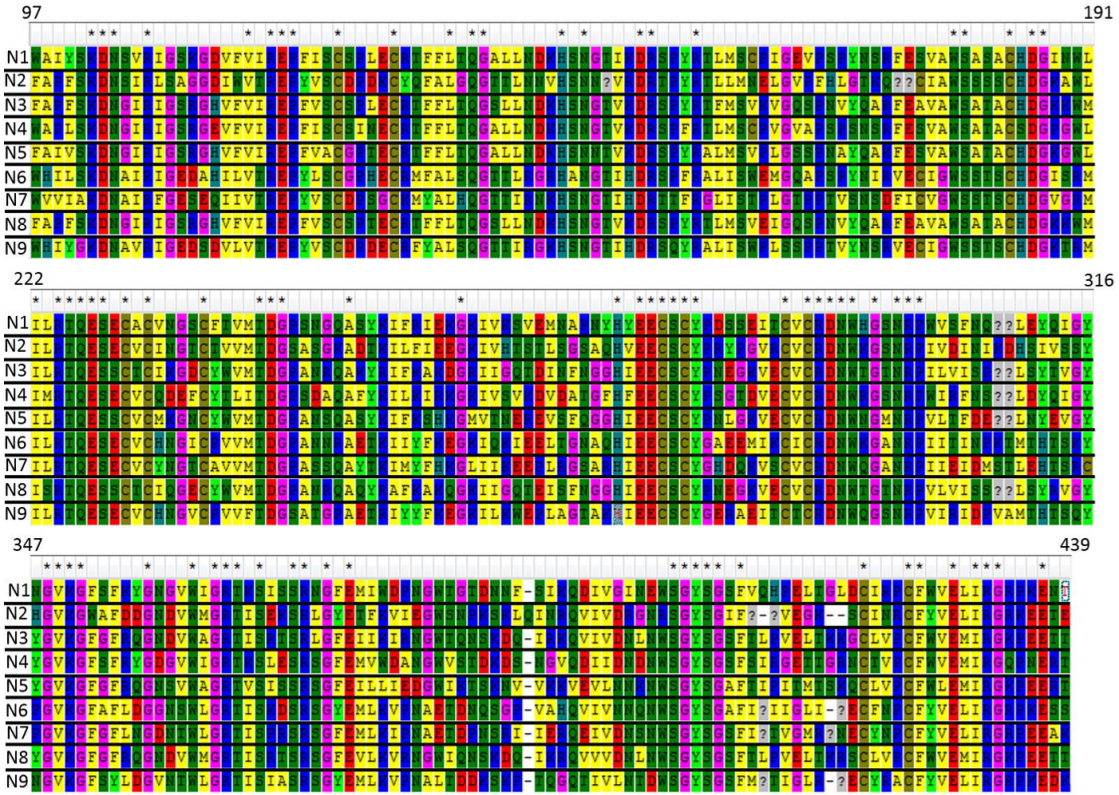

Figure S1: Alignment NA types from human and animal influenza viruses. Nucleotide sequences from the viral strains displayed in Table S3 were retrieved from GenBank, aligned by ClustalW (Mega software 6.0) and predicted amino acid sequenced compared. Although there are reports in the literature of 11 isoforms of influenza A NA, the NA types 10 and 11 did not have available sequences for alignment. Types of NA are indicated. Conserved amino acid residues among these representative NA types are indicated by the asterisks.

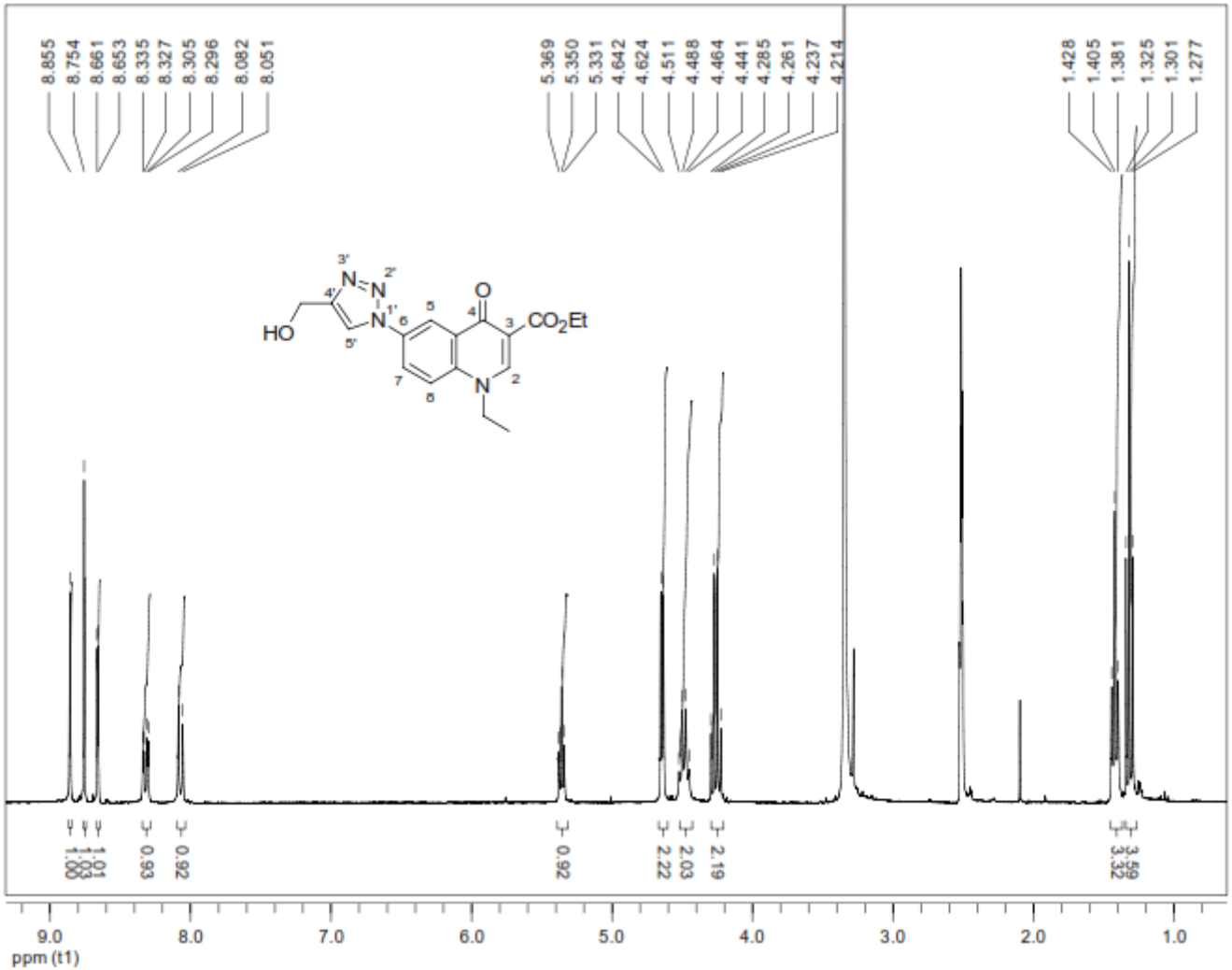

Figure S2: ^{1}H NMR Spectra of compound **1a** (300,00 MHz, DMSO-d_6)

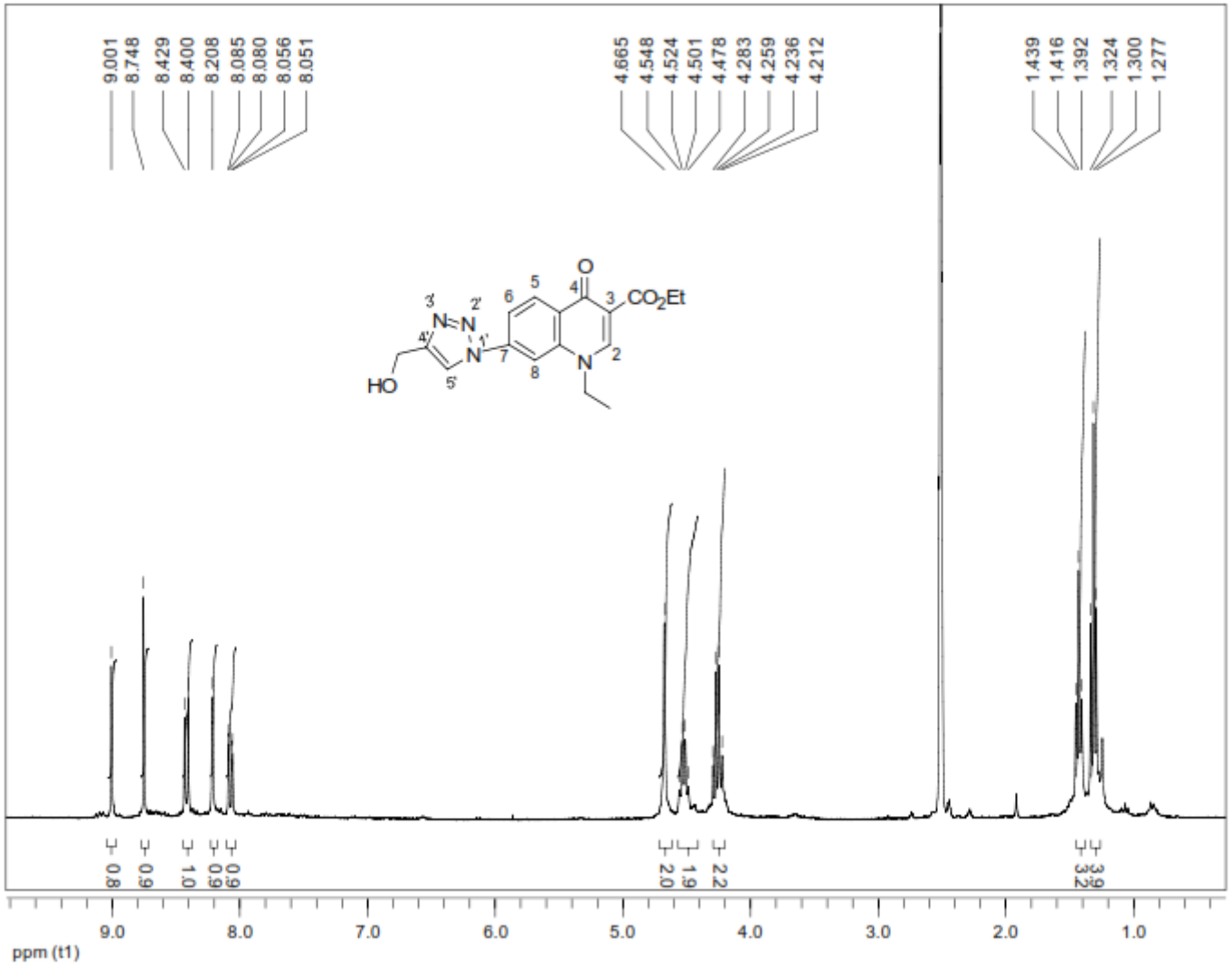

Figure S3: ^{1}H NMR Spectra of compound **1b** (300,00 MHz, DMSO-d_6)

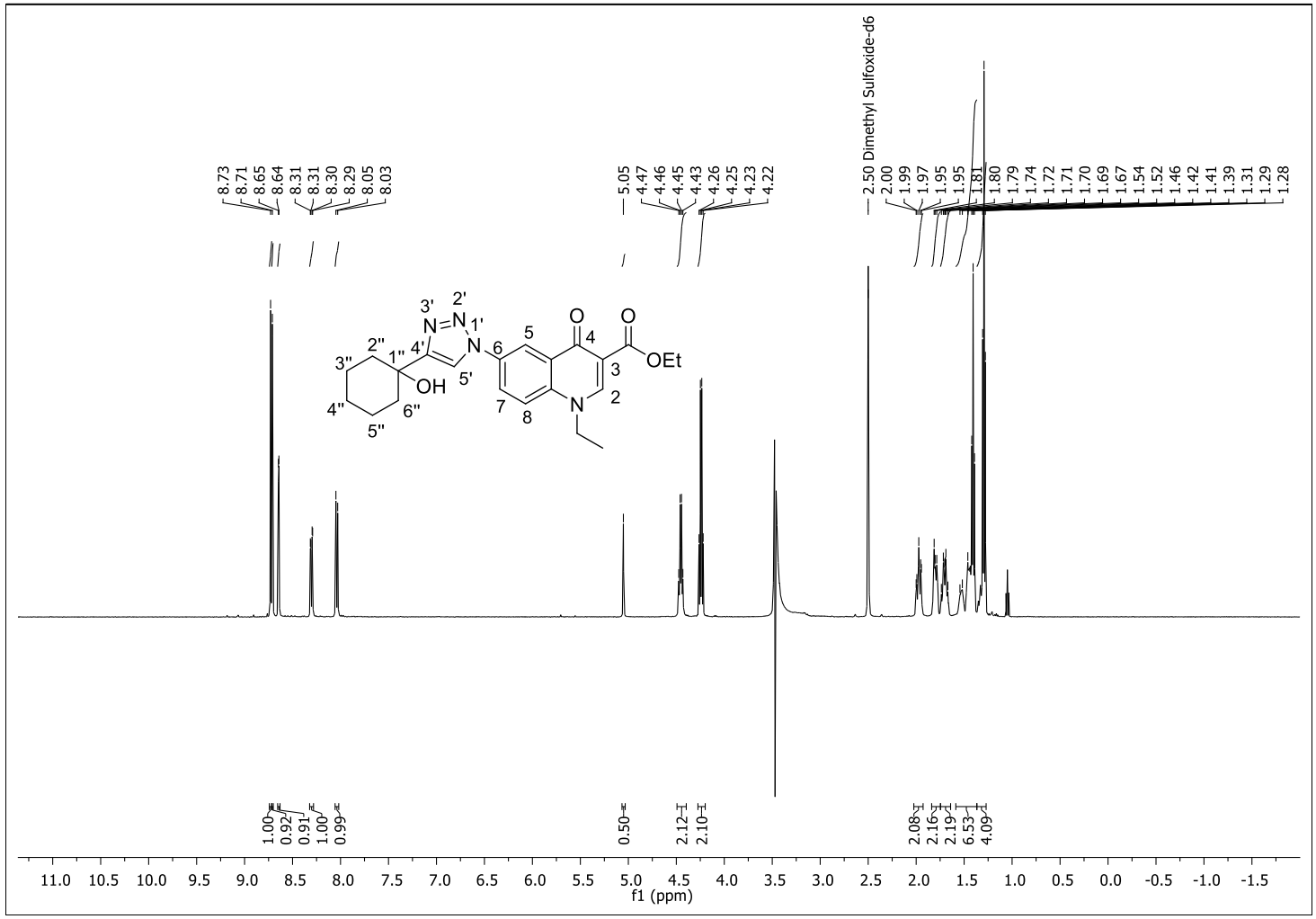

Figure S4: ^{1}H NMR Spectra of compound **1c** (500,00 MHz, DMSO-d_6)

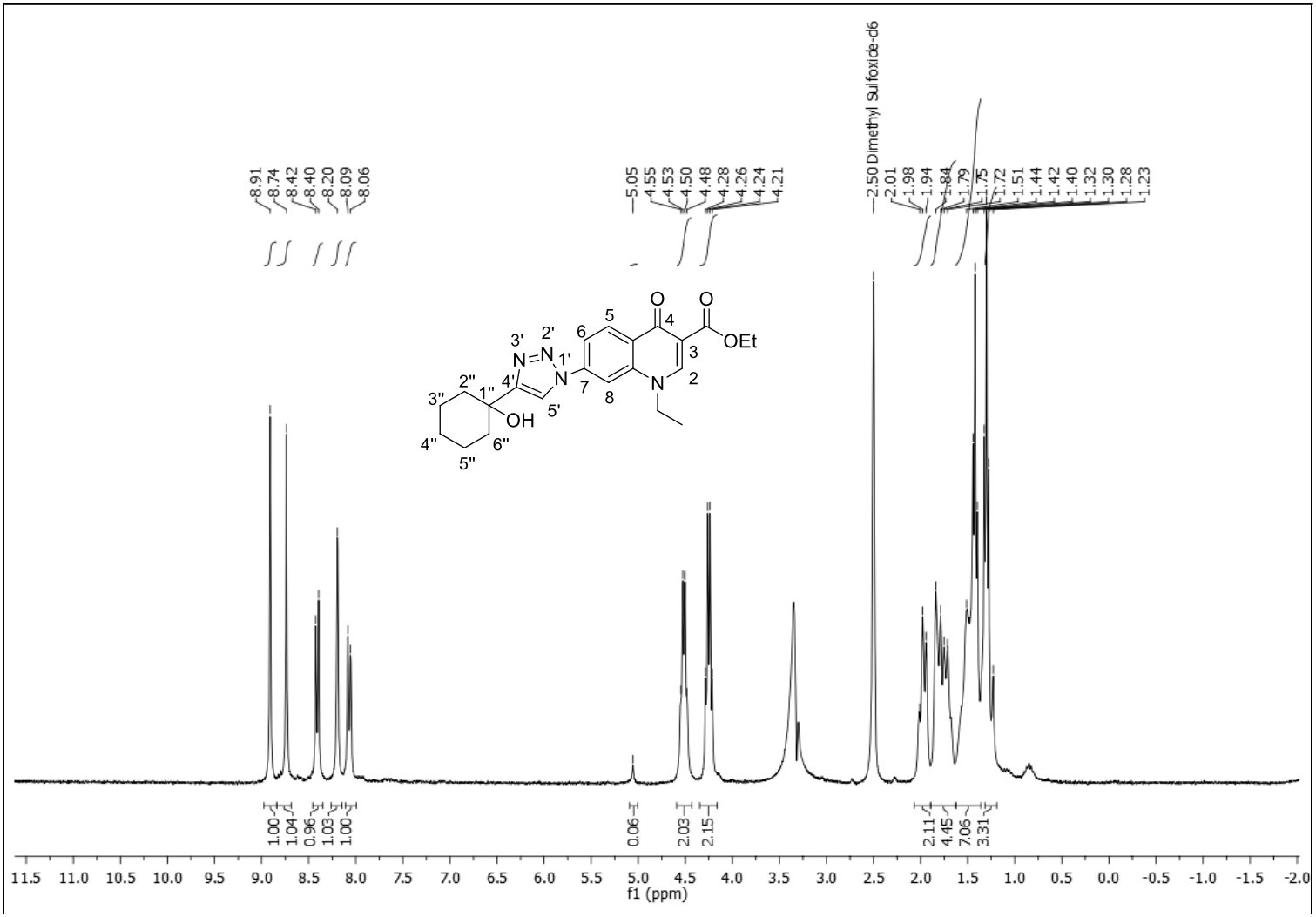

Figure S5: ^{1}H NMR Spectra of compound **1d** (300,00 MHz, DMSO-d_6)

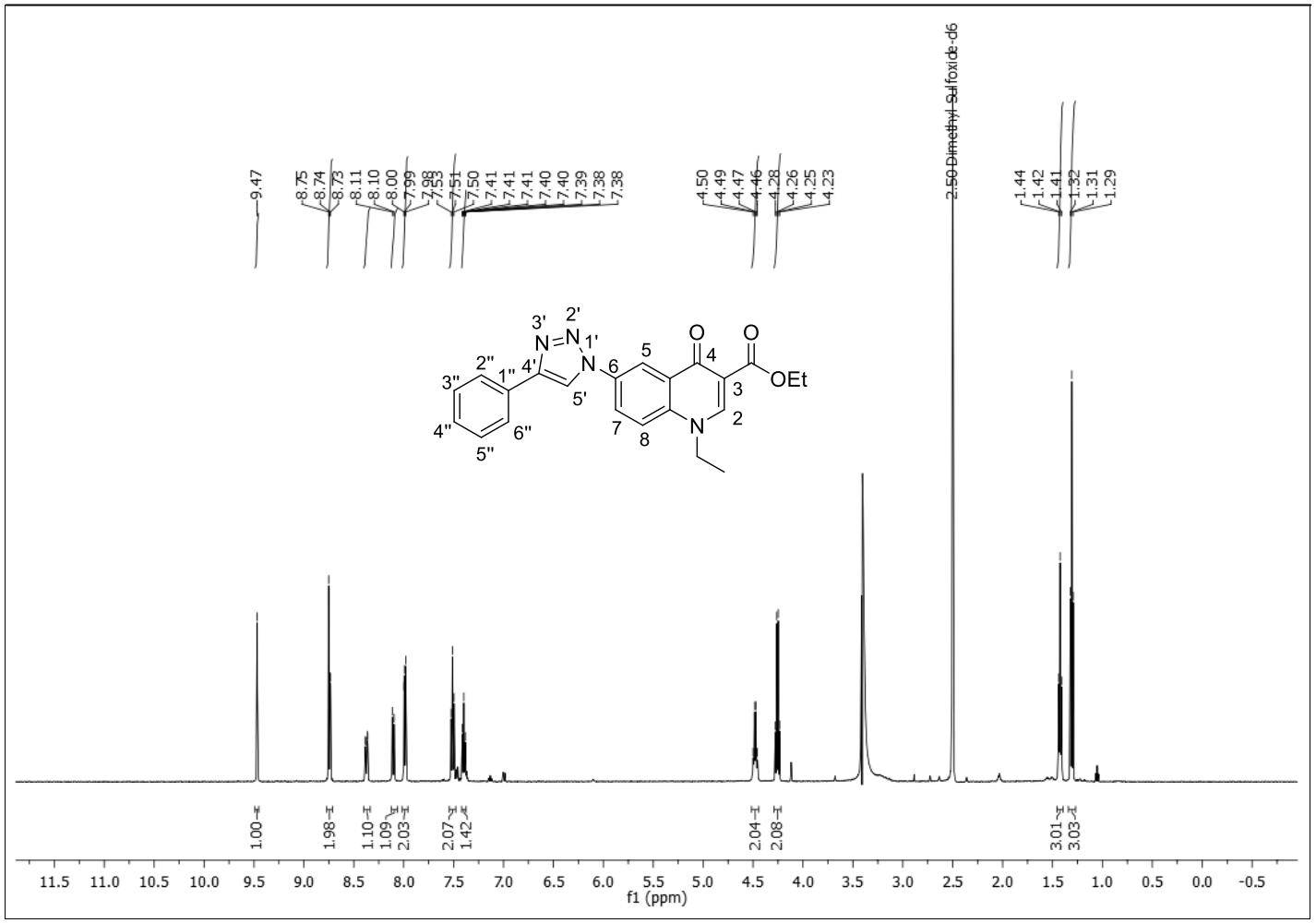

Figure S6: ^{1}H NMR Spectra of compound **1e** (500,00 MHz, DMSO-d_6)

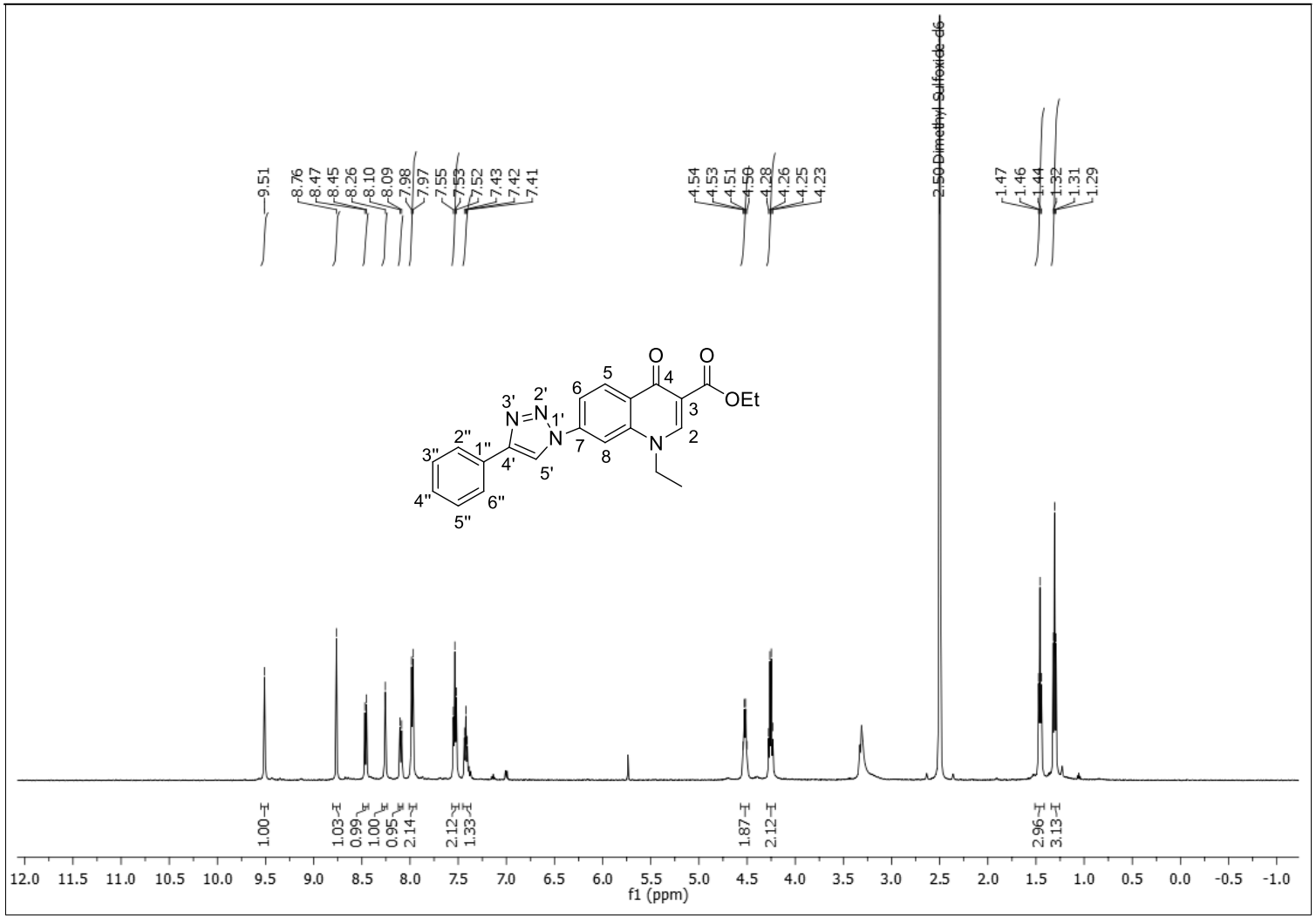

Figure S7: ^{1}H NMR Spectra of compound **1f** (500,00 MHz, DMSO-d_6)

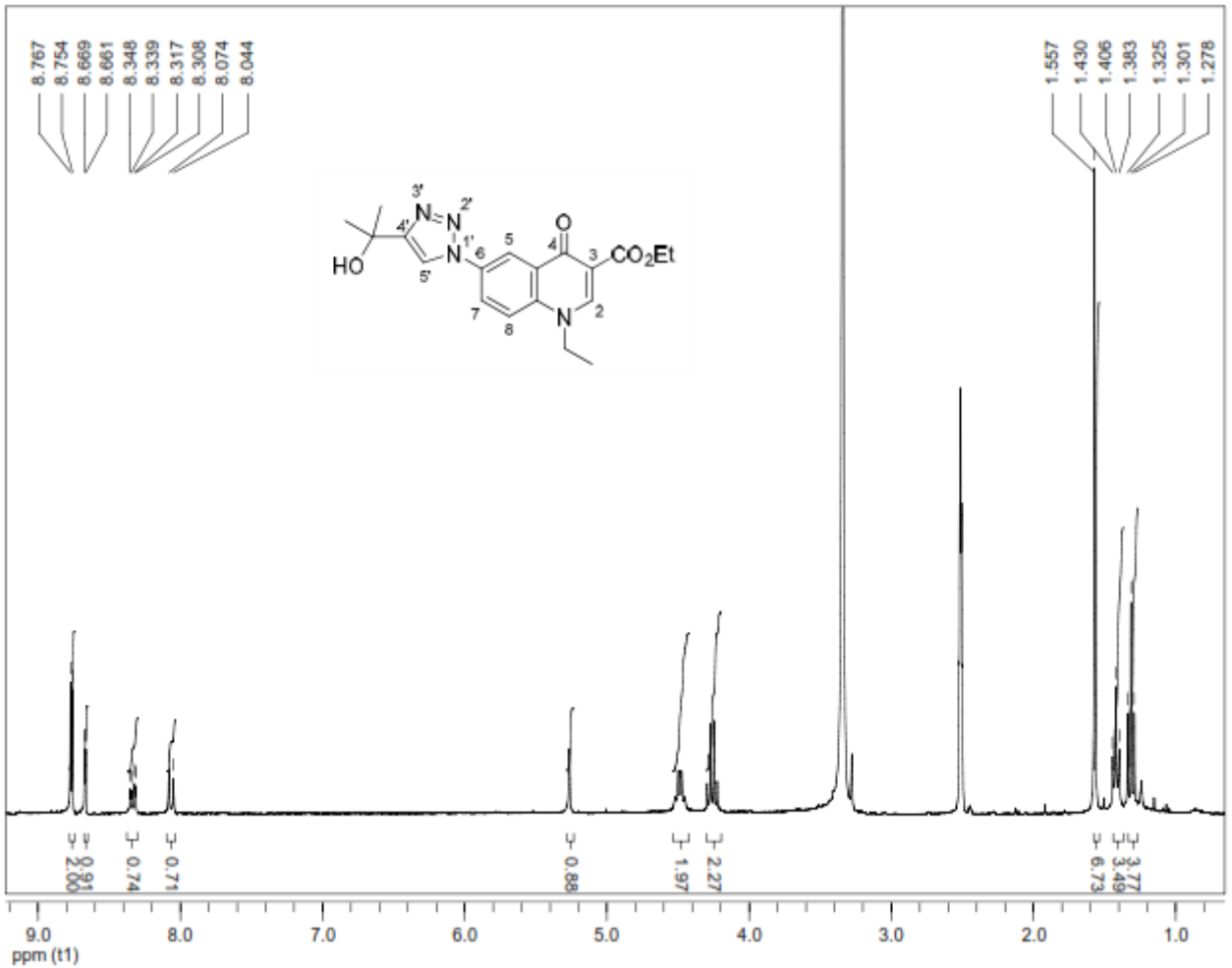

Figure S8: ^{1}H NMR Spectra of compound **1g** (300,00 MHz, DMSO-d_6)

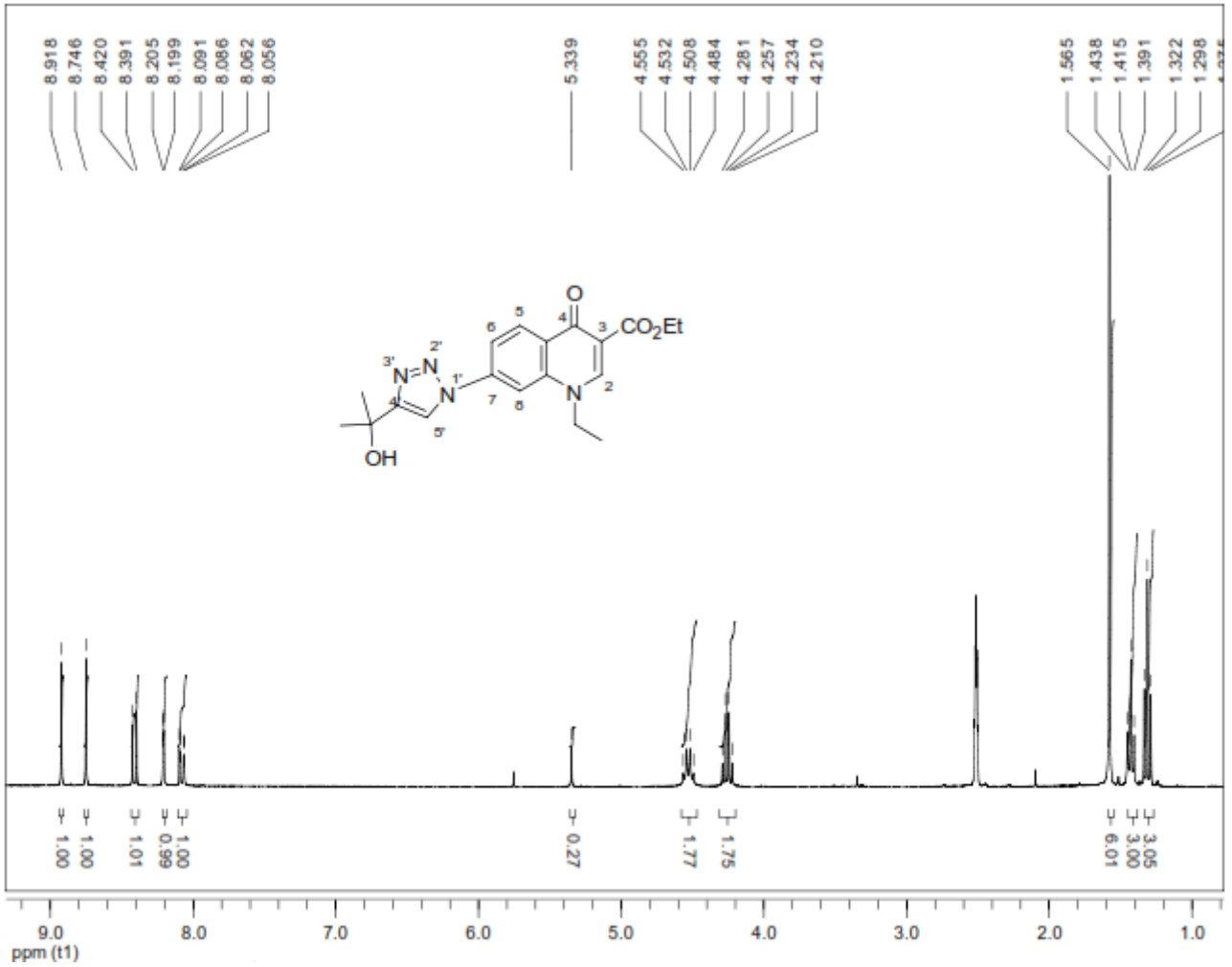

Figure S9: ^{1}H NMR Spectra of compound **1h** (300,00 MHz, DMSO-d_6)

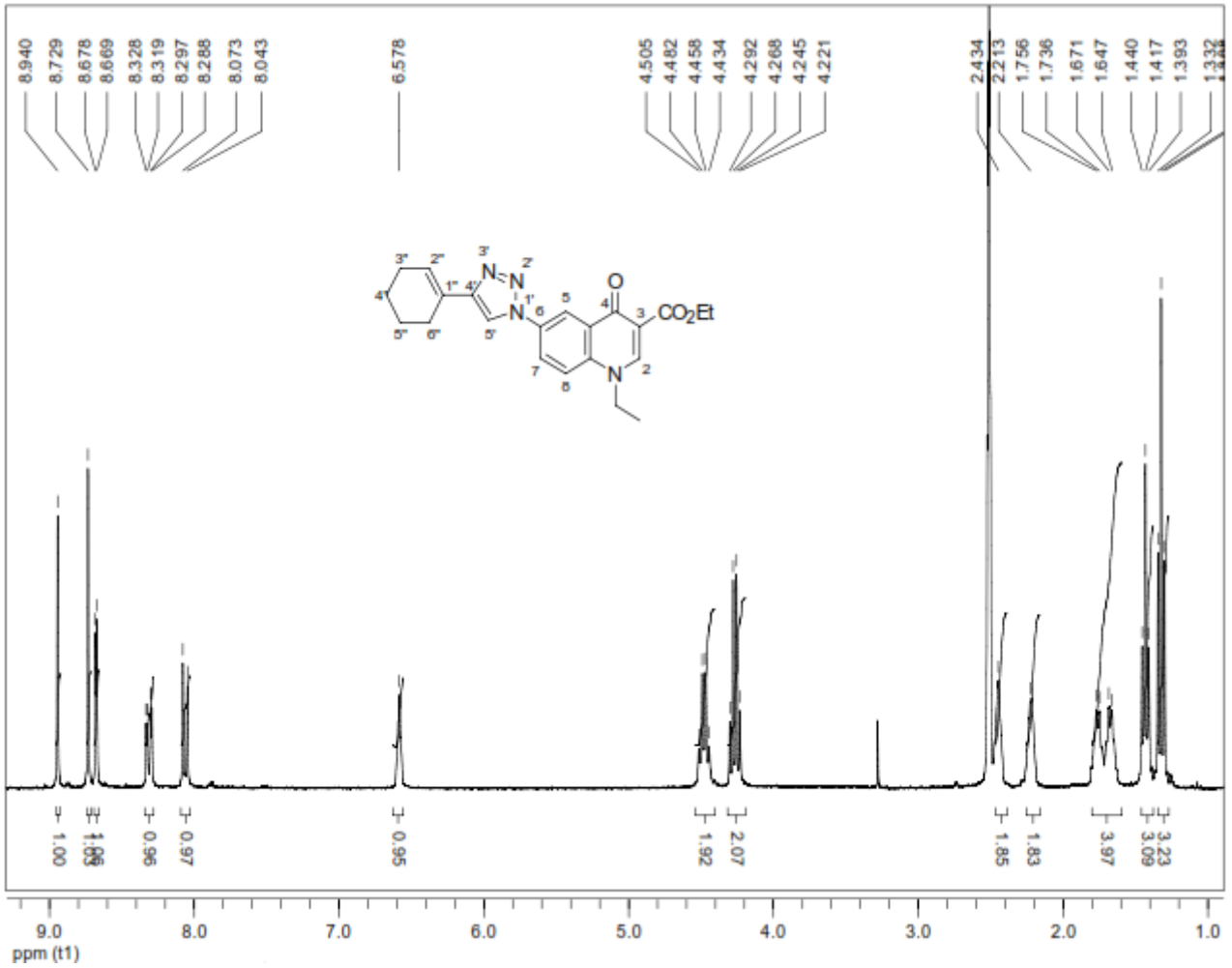

Figure S10: ^{1}H NMR Spectra of compound **1i** (300,00 MHz, DMSO-d_6)

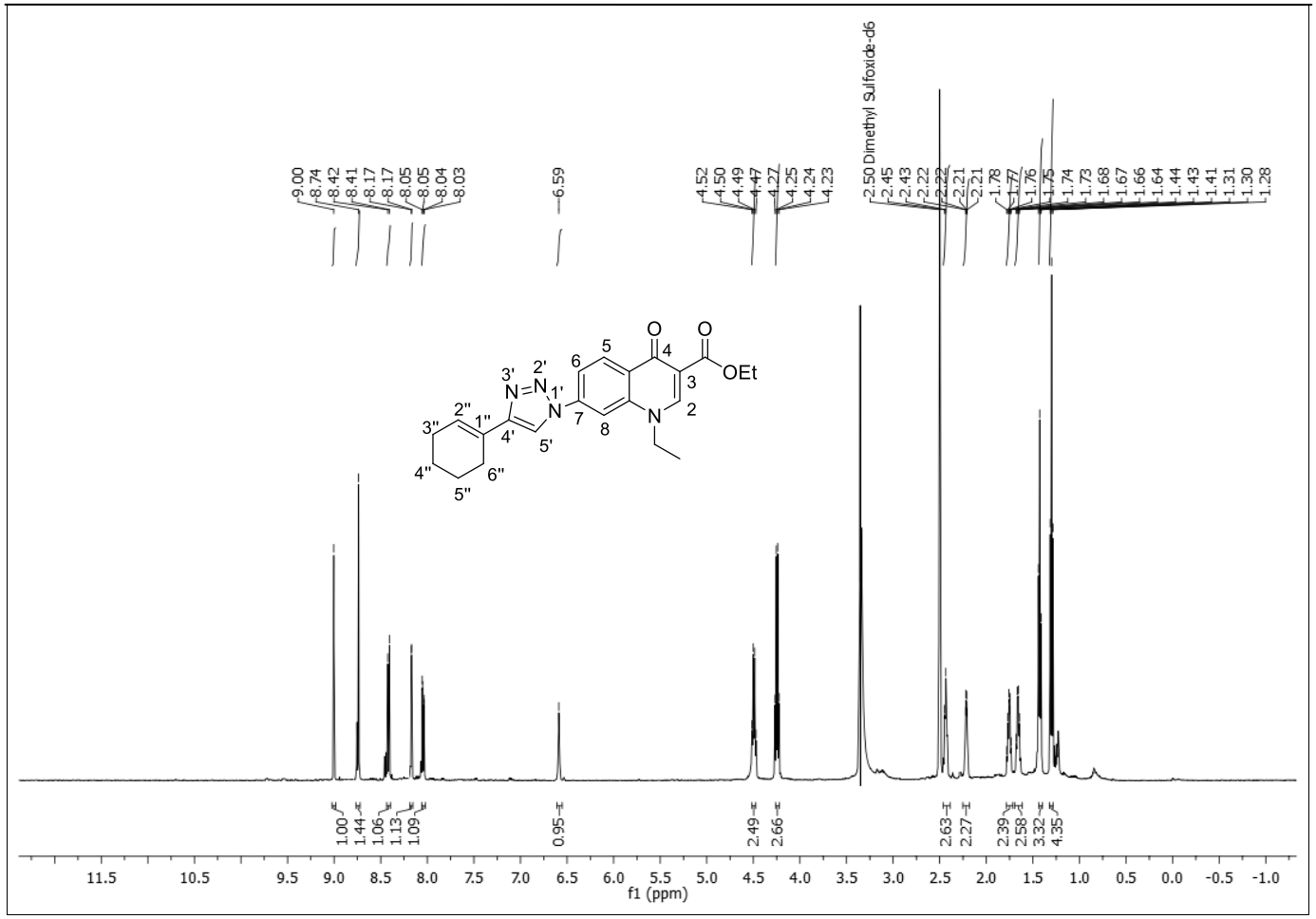

Figure S11: ^{1}H NMR Spectra of compound **1j** (500,00 MHz, DMSO-d_6)

The compound 4-(4-phenyl-1*H*-1,2,3-triazol-1-yl)-2,2,6,6-tetramethylpiperidine-1-oxyl inhibits influenza replication by targeting the viral neuraminidase

Carolina Q. Sacramento[a,b,e], Alessandro Kappel Jordão[c,d], Cristiane M. Alves[a], Andressa Marttorelli[a,b,e], Natalia Fintelman-Rodrigues [a,b,e], Caroline S. de Freitas [a,b,e], Gabrielle R. de Melo [a,b,e], Osvaldo Santos-Filho[a], Anna Claudia Cunha[c], Vitor F. Ferreira[c] and Thiago Moreno L. Souza [a,b,e,*]

[a] Laboratório de Vírus Respiratórios, Instituto Oswaldo Cruz, Fundação Oswaldo Cruz, Rio de Janeiro, Rio de Janeiro, Brazil

[b] Laboratório de Imunofarmacologia, Instituto Oswaldo Cruz, Fundação Oswaldo Cruz, Rio de Janeiro, Rio de Janeiro, Brazil

[c] Laboratório de Síntese Orgânica, Programa de pós-Graduação em Química, Departamento de Química Orgânica, Instituto de Química, Universidade Federal Fluminense, Niterói, Rio de Janeiro, Brazil

[d] Unidade Universitária de Farmácia, Fundação Centro Universitário Estadual da Zona Oeste, Rio de Janeiro, Rio de Janeiro, Brazil

[e] National Institute for Science and Technology on Innovation on Neglected Diseases (INCT/IDN), Center for Technological Development in Health (CDTS), Oswaldo Cruz Foundation, Rio de Janeiro, Rio de Janeiro, Brazil.

* Corresponding Author

E-mail: tmoreno@cdts.fiocruz.br

Abstract

Since influenza virus is the main cause of seasonal acute respiratory infections, and pandemic outbreaks, antiviral drugs are critical to mitigate infections and impair chain of transmission. Despite that, influenza strains resistant to oseltamivir (OST), to the most used anti-influenza drug, have been emerging. Therefore, novel compounds with anti-influenza activity are necessary. We show that the compound 4-(4-phenyl-1*H*-1,2,3-triazol-1-yl)-2,2,6,6-tetramethylpiperidine-1-oxyl (Tritempo), a triazolic ring bound to piperidine-1-oxyl nitroxide radical inhibited influenza A replication, with an EC_{50} of 0.38 µM, and with very low cytotoxicity, CC_{50} > 2,000 µM. Interestingly, Tritempo inhibited the neuraminidase (NA) activity of OST-resistant strains of influenza A and B at the nanomolar range. After several passages, we generated an influenza A strain resistant to Tritempo (NA G248P mutant), which continued to be sensitive to OST – indicating no cross-resistance between Tritempo and the reference molecule. Tritempo bound to WT and OST-resistant influenza NA isoforms at the sialic acid binding site with low free binding energies. Altogether, our results suggest that Tritempo chemical structure is a promising one to the development of novel antivirals.

Keywords: Influenza virus, neuraminidase, oseltamivir-resistant, triazolic compounds**,** nitroxide radical

Influenza is a negative-sense-RNA virus, belonging to the *Orthomixoviridae* family (1). Clinically relevant influenza A and B viruses provoke acute respiratory tract infections and lead to high morbidity, mortality and public health burden (2). Influenza A subtypes may be distinguished among each other by viral surface glycoproteins, hemagglutinin (HA) and neuraminidase (NA) (3), and cause seasonal infections and even pandemics outbreaks (4). NA is the target of the main class of anti-influenza drugs available to clinical use, the NA inhibitors (NAIs), such as oseltamivir (OST), zanamivir, peramivir and laninamivir (5). OST is the most used anti-influenza drug, because it is orally administered and licensed in more countries than the other drugs (6). However, around 2 % of the circulating strains of influenza A(H1N1)pdm09 virus are resistant to OST (7, 8). Remarkably, detection of OST-resistant strains have been made in untreated individuals (9), meaning that the prevalence of OST-resistant strains of influenza may scale up. Altogether, these data motivated the search for novel molecules able to inhibit OST-resistant strains of influenza.

Triazolic compounds have been largely explored due to its application as medicines. The antiviral activity of triazolic compounds has been observed for influenza (10), as well as for a variety of other clinically relevant viruses, such as human immunodeficiency virus 1 (HIV-1) (11), hepatitis A and C (12, 13). We have recently published that molecules within the series of 1,2,3-Triazolyl-4-oxoquinolines are endowed with anti-influenza activity, by targeting the NA from wild-type (WT) and OST-resistant strains (10). Whereas the 4-oxoquinoline moiety was important for docking, the pharmacophoric groups of these derivatives were the triazolic radical and the cyclohexyl ring (10). Despite that anti-influenza activity of 1,2,3-Triazolyl-4-oxoquinolines, they were active against viral NA at micromolar range (10). In order to rationalize the search for more potent inhibitors of influenza viruses NA, we performed

a chemical ontology search in our database (14), for molecules containing structures like the triazolic radical and the cyclohexyl ring of the 1,2,3-Triazolyl-4-oxoquinolines derivatives. One particular compound caught our attention, 4-(4-phenyl-1*H*-1,2,3-triazol-1-yl)-2,2,6,6-tetramethylpiperidine-1-oxyl (Tritempo – Fig. 1). Tritempo possesses a triazolic ring bound to piperidine-1-oxyl nitroxide radical, these structures are closely related to the pharmacophoric groups of 1,2,3-Triazolyl-4-oxoquinolines derivatives, without the 4-oxoquinoline moiety (10). Besides, Tritempo has been shown to endowed with anti-inflamatory activity (15), a desirable additional pharmacological activity for a potential antiviral.

Figure 1. The chemical structure of the compound 4-(4-phenyl-1*H*-1,2,3-triazol-1-yl)-2,2,6,6-tetramethylpiperidine-1-oxyl (Tritempo).

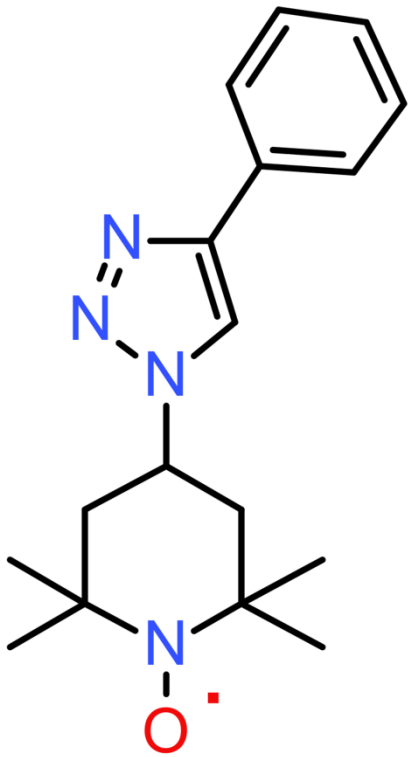

By means of functional assays against influenza A/H3N2 replication (10), We confirmed that Tritempo is endowed with antiviral activity. Tritempo presented an EC_{50}

value of 0.38 ± 0.051 µM (Table 1). For reference, this pharmacological parameter for oseltamivir carboxylate (OST-c), its bioactive form, was 0.03 ± 0.023 µM (Table 1). We also evaluated Tritempo`s cytotoxicity by quantifying cellular viability (10, 16). Our compound`s cytotoxicity was very low, comparable to the reference molecule OST-c, both molecules had CC_{50} values higher than 2,000 µM (Table 1). Based on the ratio between CC_{50} and EC_{50}, the selective index (SI) values were calculated. Although the SI value for OST-c and Tritempo are 66,667 and 5,263, respectively (Table 1), our compound`s SI value is very high – indicating its safety *in vitro*. Altogether, the results confirmed our scientific premise that this novel molecule inhibit influenza replication.

Table 1: Tritempo`s cytotoxicity and antiviral potency against laboratory-adapted influenza A/H3N2/ENG/42/72 virus strain.

Compounds	CC_{50} (µM)	EC_{50} (µM)	SI (CC_{50}/EC_{50})
Tritempo	> 2,000	0.38 ± 0.051	>5,263
OST-c	> 2,000	0.03 ± 0.023	>66,667

Tritempo's ability to inhibit the NA activity of influenza A and B viruses, either WT and OST-resistant strains, was measured, as previously described (10). Tritempo inhibited influenza NA activity in a nanomolar range (Table 2), being more potent than its anti-influenza analogs 1,2,3-Triazolyl-4-oxoquinolines, previously studied by us (10) Although Tritempo was less potent than OST-c in inhibiting WT strains, its advantage over the reference molecule is clear against OST-resistant strains of influenza (Table 2). IC_{50}`s values for Tritempo were relatively similar independently whether NA was carrying OST-associated resistance mutation (H275Y, E119V or R152K) [fold increase of 1.2, 1.25 and 1.2 for influenza A(H1N1)pdm09, A/H3N2 and B, respectively] (Table 2). On the other hand, OST-c`s IC_{50} values increase by 107-, 80- and 27-fold for mutant

viruses A(H1N1)pdm09 (H275Y), A/H3N2 (E119V) and influenza B (R152K), respectively (Table 2). Our results demonstrate that Tritempo blocks the NA activity of influenza strains that the reference compound in use clinically, OST, fails to inhibit.

Table 2: Tritempo's potency towards WT and OST-resistant NAs from strains of influenza A and B.

			IC_{50} (nM)	
Strains	**Type/Subtype**	**NA mutation**	**Tritempo**	**OST-c**
A/WA/10/2008	A (H1N1)	WT	10 ± 2.0	0.9 ± 0.03
A/RJ/512/2009	A(H1N1pdm09)	WT	9 ± 2.1	0.7 ± 0.04
A/FL/21/2008	A (H1N1)	H275Y	12 ± 1.7 (1.2)*	97 ± 23 (107)
A/WA/01/2007	A (H3N2)	WT	10 ± 2.5	0.2 ± 0.02
A/ENG/42/72	A (H3N2)	WT	8 ± 1.6	0.1 ± 0.02
A/TX/12/2007	A (H3N2)	E119V	10 ± 1.9 (1.25)	8 ± 0.09 (80)
B/MEMPHIS/20/1996	B	WT	15 ± 3.0	1.9 ± 0.5
B/MEMPHIS/20/1996	B	R152K	18 ± 3.2 (1.2)	52 ± 0.9 (27)

* The numbers in parentheses represent the fold change of IC_{50}´s values for OST-resistant over WT strains.

Tritempo was then docked into the NA structure of WT and OST-resistant strains of influenza A and B, as previously described (10). Tritempo docked to the different isoforms of NA, either WT or resistant to OST, with low free binding energies, comparable to OST (Table 3). Our compound docked in the active site of all isoforms of NA, and conserved amino acid residues are predicted to be required for binding (Fig. 2) (10). Although OST binds to the NAs by more hydrogen bonds than Tritempo, our molecule interacted with the NA with more plasticity than the reference compound (Fig. 2 and Table 3). Our data suggest that triazolic and the 2,2,6,6-tetramethylpiperidine-1-oxyl (TEMPO) moieties are required for binding.

Table 3: Comparisons between Tritempo and OST interaction with WT and OSt-resistant NAs.

	Tritempo					OST				
Neuraminidase Types (PDB accession numbers)	Binding energy (kcal/mol)	No. of hydrogen bonds	Amino acid residues involved in H-bounding	No. of bumps	Amino acid residues involved in bumps	Binding energy (kcal/mol)	No. of hydrogen bonds	Amino acid residues involved in H-bounding	No. of bumps	Amino acid residues involved in bumps
N2 WT (4GZP)	- 6.99	4	Arg 292, Asn 294	7	Ile 222; Arg 224; Ala 246; Ser 247; Glu 276, 277; His 347	- 8.57	6	Glu 119; Asp 151; Arg 152, 282, 371	10	Arg 118, 224; Trp 178; Ile 222; Ala 246; Glu 276, 277; Asn 294; His 347; Tyr 406
N2 E119G (1L7G)	- 7.62	7	Asp 151; Arg 152, 292	9	Leu 134; Arg 156, 371; Trp 178; Ser 179; Ala 246; Asn 294, 347; Tyr 406	- 8.20	10	Arg 118, 152, 292, 371; Asp 151; Trp 178; Glu 227; Tyr 406	6	Leu 134; Arg 156, 224; Ile 222; Glu 276, 277
N1 WT (3TI6)	- 8.39	5	Asp 151; Arg 152, 292	14	Arg 118, 224, 371; Trp 178; Ser 179; Ile 222; Leu 223; Glu 227, 277; Ser 246; Asn 294, 347; Gly 348; Tyr 406	- 7.44	6	Arg 118, 152, 292, 371; Glu 119; Asp 151	8	Trp 178; Ile 222; Arg 224; Ser 246; Glu 276, 277; Asn 294; Tyr 406
N1 H275Y (3CL0)	- 8.00	3	Arg 152; Tyr 406	15	Arg 118, 224, 292; Glu 119, 227, 276, 277; Asp 151; Trp 178; Ser 179, 246; Asn 221; Ile 222; Gly 244; Pro 245	- 7.98	7	Arg 118, 152, 292, 371; Glu 119; Tyr 347	9	Asp 151; Trp 178; Ile 222; Arg 224; Ser 246; Glu 276, 277; Asn 294; Tyr 406
N B (4CPM)	- 7.21	2	Arg 149	17	Glu 116, 225, 275; Leu 131; Asp 148; Arg 153, 222, 291; Trp 176; Ser 177, 243; Lys 219; Ile 220; Thr 223; Gly 242; Ala 244; Tyr 408	- 7.99	7	Arg 115, 149, 291, 373; Glu 116; Asp 148	7	Trp 176; Ile 220; Arg 222; Ala 244; Glu 274; Asn 293; Tyr 408

Figure 2. *In silico* analysis of Tritempo docked to influenza NA. Tritempo was docked over the amino acid residues of WT and OST-resistant influenza NAs. Crystal structures of influenza WT N2 (A), OST-resistant N2 (C), WT N1 (E), OST-resistant N1 (G) and WT influenza B NA (I) with Tritempo docked in the active site cleft. 2D schematic figures showing Tritempo docked to the different NA isoforms displayed as following: WT N2 (B), OST-resistant N2 (D), WT N1 (F), OST-resistant N1 (H) and WT influenza B NA (J). The types of interaction between Tritempo and the NAs are indicated and hydrogen bounds are represented by dotted lines. The red numbers, next to the amino acid residues interacting with Tritempo, represent in how many different types of influenza NA these residues are conserved.

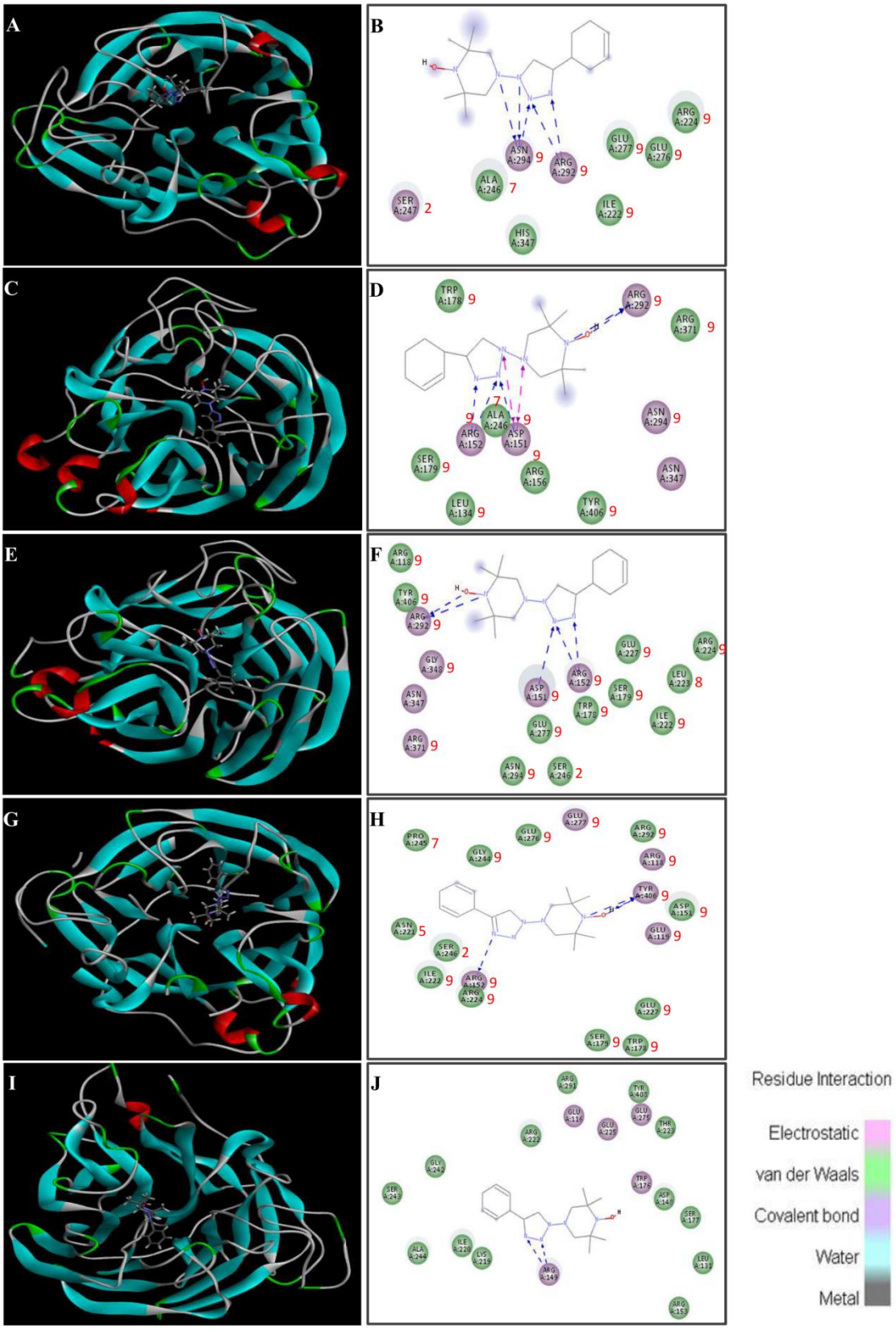
A
B
C
D
E
F
G
H
I
J
Residue Interaction
Electrostatic
van der Waals
Covalent bond
Water
Metal

12

13

Tritempo is able to inhibit influenza replication, by targeting conserved amino acid residues on NA structure, with potencies at the nanomolar range against WT and OST-resistant strains. Subsequently, we addressed whether OST could inhibit a Tritempo-resistant strain of influenza. To generate a Tritempo-resistant strain, influenza A/H3N2 was propagated with increasing concentrations of this drug. As a control, in parallel, the same viral strain was passaged in the absence of any drug. We raised a strain able to be grow even in the presence of Tritempo at 2.3 µM, an concentration 6-times higher than it's EC_{50} value, carrying the mutation G248P (G742C, G743C) in the NA (Fig. 3A). Subsequently, we evaluated whether Tritempo's resistant mutant would be susceptible to the reference compound, OST-c. Indeed, the Tritempo-resistant strain remained sensitive to OST-c (Fig. 3B) – indicating the lack of cross-resistance between Tritempo and OST.

Figure 3. Susceptibility to OST is maintained in influenza mutant resistant to Tritempo. Influenza was passaged in MDCK cells with or without increasing concentrations of Tritempo (up to 2.3 µM - 6-times it's EC_{50} value). The NA gene from the virus in the supernatant of the last passage was sequenced (Sanger method). The resulting sequencing form the NA gene was translated (A). Inhibitory activity of OST against NA of influenza viruses grown in the presence (black line) and absence (gray line) of Tritempo was measured as previously described (B).

A

```
Influenza without Tritempo  MNPNQKIITIGSVSLTIATICFLMQIAILVTTVTLHFKQY [ 40]
Influenza with Tritempo     ........................................ [ 40]

Influenza without Tritempo  ECDSPANNQVMPCEPIIIERNITEIVYLTNTTIEKEICPK [ 80]
Influenza with Tritempo     ........................................ [ 80]

Influenza without Tritempo  LVEYRKWSKPQCKITGFAPFSKDNSIRLSAGGDIWVTREP [120]
Influenza with Tritempo     ........................................ [120]

Influenza without Tritempo  YVSCDPGKCYQFALGQGTTLDNKHSNDTIHDRIPHRTLLM [160]
Influenza with Tritempo     ........................................ [160]

Influenza without Tritempo  NELGVPFHLGTRQVCIAWSSSSCHDGKAWLHVCVTGDDKN [200]
Influenza with Tritempo     ........................................ [200]

Influenza without Tritempo  ATASFIYDGRLVDSIGSWSQNILRTQESECVCINGTCTVV [240]
Influenza with Tritempo     ........................................ [240]

Influenza without Tritempo  MTDGSASGRADTRILFIEEGKIVHISPLSGSAQHVEECSC [280]
Influenza with Tritempo     .......P................................ [280]

Influenza without Tritempo  YPRYPGVRCICRDNWKGSNRPVVDINVKDYSIDSSYVCSG [320]
Influenza with Tritempo     ........................................ [320]

Influenza without Tritempo  LVGDTPRNNDRSSNSYCRNPNNERGNHGVKGWAFDDGNDV [360]
Influenza with Tritempo     ........................................ [360]

Influenza without Tritempo  WMGRTISKDSRSGYETFKVIGGWSTPNSKSQINRQVIVDS [400]
Influenza with Tritempo     ........................................ [400]

Influenza without Tritempo  DNRSGYSGIFSVEGKSCINRCFYVELIRGREQETRVWWTS [440]
Influenza with Tritempo     ........................................ [440]

Influenza without Tritempo  NSIVVFCGTSGTYGTGSWPDGADINLMPI* [470]
Influenza with Tritempo     ............................... [470]
```

B

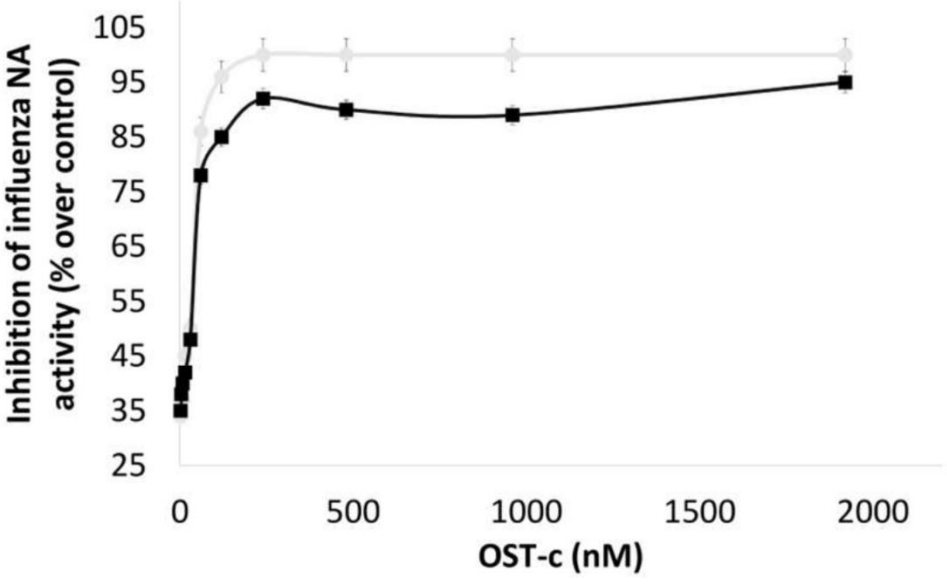

The results displayed in this work advances over a previously studied series of molecules from our group, the 1,2,3-Triazolyl-4-oxoquinolines (10). 1,2,3-Triazolyl-4-oxoquinolines pharmacophoric groups were a triazolic and cyclohexenyl moieties (10). Tritempo showed low cytotoxicity and improved anti-influenza activity, being more potently than the 1,2,3-Triazolyl-4-oxoquinolines. We have shown that 4-oxoquinolines alone do not possess anti-influenza activity (10). Our compound also inhibited the NA activity of different influenza types/subtypes, including OST-resistant strains, at nanomolar range and with no cross-resistance to the reference molecule. Therefore, the absence of a 4- oxoquinoline-like moiety in the Tritempo chemical structure may have allowed it fit better than 1,2,3-Triazolyl-4-oxoquinolines in the influenza NA. The triazolic-tempol nature of Tritempo may have docked into NA without the steric bumps from the 4-oxoquinolines moieties. Tritempo was previously described being an anti-inflammatory compound, a desirable complementary activity for a novel antiviral (15). Altogether our results suggest that Tritempo chemical structure is a promising one to the development of novel anti-influenza drugs.

Acknowledgements

Thanks are due to the Influenza Reagent Resource (IRR; https://www.influenzareagentresource.org/), the Centers for Disease Control (CDC/Atlanta; WHO Collaborating Center for influenza) and Hoffman-La Roche Inc., Basel, Switzerland for donating materials to conduct this investigation.

Funding

This work was supported by Conselho Nacional de Desenvolvimento e Pesquisa (CNPq), Fundação de Amparo à Pesquisa do Estado do Rio de Janeiro (FAPERJ).

References

1. Murphy BR, Webster RG. Orthomyxoviruses. 3rd ed. Fields BNKDMHlPMCRMMJLMTPRBSSE, editor. Philadelphia: Lappincott-Raven Publishers; 1996.
2. Damjanovic D, Small CL, Jeyanathan M, Jeyananthan M, McCormick S, Xing Z. Immunopathology in influenza virus infection: uncoupling the friend from foe. Clin Immunol. 2012;144(1):57-69.
3. Palese P, Shaw ML. Orthomyxoviridae: The viruses and their replication. Knipe DM, Howley PMe, editors. Philadelphia: Lippincott, Williams & Wilkins; 2007.
4. Tang JW, Shetty N, Lam TT, Hon KL. Emerging, novel, and known influenza virus infections in humans. Infect Dis Clin North Am. 2010;24(3):603-17.
5. Hurt AC. The epidemiology and spread of drug resistant human influenza viruses. Curr Opin Virol. 2014;8C:22-9.
6. Jefferson T, Jones M, Doshi P, Spencer EA, Onakpoya I, Heneghan CJ. Oseltamivir for influenza in adults and children: systematic review of clinical study reports and summary of regulatory comments. BMJ. 2014;348:g2545.
7. Fry AM, Gubareva LV. Understanding influenza virus resistance to antiviral agents; early warning signs for wider community circulation. J Infect Dis. 2012;206(2):145-7.
8. Hurt AC, Hardie K, Wilson NJ, Deng YM, Osbourn M, Leang SK, et al. Characteristics of a widespread community cluster of H275Y oseltamivir-resistant A(H1N1)pdm09 influenza in Australia. J Infect Dis. 2012;206(2):148-57.
9. Souza TM, Resende PC, Fintelman-Rodrigues N, Gregianini TS, Ikuta N, Fernandes SB, et al. Detection of Oseltamivir-Resistant Pandemic Influenza A(H1N1)pdm2009 in Brazil: Can Community Transmission Be Ruled Out? PLoS One. 2013;8(11):e80081.
10. Boechat FaC, Sacramento CQ, Cunha AC, Sagrillo FS, Nogueira CM, Fintelman-Rodrigues N, et al. 1,2,3-Triazolyl-4-oxoquinolines: A feasible beginning for promising chemical structures to inhibit oseltamivir-resistant influenza A and B viruses. Bioorg Med Chem. 2015;23(24):7777-84.
11. Wang Z, Wu B, Kuhen KL, Bursulaya B, Nguyen TN, Nguyen DG, et al. Synthesis and biological evaluations of sulfanyltriazoles as novel HIV-1 non-nucleoside reverse transcriptase inhibitors. Bioorg Med Chem Lett. 2006;16(16):4174-7.
12. Shamroukh AH, Ali MA. Anti-HAV activity of some newly synthesized triazolo[4,3-b]pyridazines. Arch Pharm (Weinheim). 2008;341(4):223-30.
13. Wittine K, Stipković Babić M, Makuc D, Plavec J, Kraljević Pavelić S, Sedić M, et al. Novel 1,2,4-triazole and imidazole derivatives of L-ascorbic and imino-ascorbic acid: synthesis, anti-HCV and antitumor activity evaluations. Bioorg Med Chem. 2012;20(11):3675-85.
14. Degtyarenko K, de Matos P, Ennis M, Hastings J, Zbinden M, McNaught A, et al. ChEBI: a database and ontology for chemical entities of biological interest. Nucleic Acids Res. 2008;36(Database issue):D344-50.
15. Queiroz RF, Jordão AK, Cunha AC, Ferreira VF, Brigagão MR, Malvezzi A, et al. Nitroxides attenuate carrageenan-induced inflammation in rat paws by reducing neutrophil infiltration and the resulting myeloperoxidase-mediated damage. Free Radic Biol Med. 2012;53(10):1942-53.

16. Scudiero DA, Shoemaker RH, Paull KD, Monks A, Tierney S, Nofziger TH, et al. Evaluation of a soluble tetrazolium/formazan assay for cell growth and drug sensitivity in culture using human and other tumor cell lines. Cancer Res. 1988;48(17):4827-33.

Influenza virus RNA polymerase may be activated inside the virion to enhance molecular diagnostic sensitivity

Carolina Q. Sacramento[1,2,3#], Natalia Fintelman-Rodrigues[1,2,3#], Milene Miranda[2], Marilda M. Siqueira[2], Thiago Moreno L. Souza[1,2,3*].

[#]These authors contributed equally to this work.

[1] Laboratório de Imunofarmacologia, Pavilhão Osório de Almeida, Instituto Oswaldo Cruz (IOC), Fundação Oswaldo Cruz (Fiocruz), Av. Brasil 4365, Manguinhos, Rio de Janeiro/RJ, Brasil.

[2] Laboratório de Vírus Respiratório e do Sarampo, Pavilhão Helio Peggy e Pereira, IOC, Fiocruz, Av. Brasil 4365, Manguinhos, Rio de Janeiro/RJ, Brasil.

[3] National Institute for Science and Technology on Innovation on Diseases of Neglected Populations (INCT/IDPN), Center for Technological Development in Health (CDTS), Fiocruz, Av. Brasil 4036, Manguinhos, Rio de Janeiro/RJ, Brasil.

[*] Corresponding author:

Thiago Moreno L. Souza, PhD

****

Fundação Oswaldo Cruz

Centro de Desenvolvimento Tecnológico em Saúde (CDTS)

Instituto Oswaldo Cruz (IOC)

Pavilhão Osório de Almeida, sala 16

Av. Brasil 4365, Manguinhos, Rio de Janeiro - RJ, Brasil, CEP 21060340

Tel.: +55 21 2562-1311

Email: tmoreno@cdts.fiocruz.br

Keywords: Influenza virus, RNA-dependent RNA polymerase, endogenous polymerase activity.

Abstract

Influenza A and B virions are packaged with their RNA polymerases to catalyze an RNA-dependent RNA polymerase activity. Since there is no evidence to rule in or out the permissiveness of influenza virions to triphosphate ribonucleotides, we functionally evaluated it. We found the means to stimulate influenza A and B RNA polymerase activity inside the virion, called natural endogenous RNA polymerase (NERP) activity. Stimulation of NERP activity increased up to $3\log_{10}$ viral RNA content, allowing the detection of influenza virus in otherwise undetectable clinical samples. NERP activation also improved our capacity to sequence misidentified regions of the influenza genome from clinical samples. By treating the samples with the ribavirin we inhibited NERP activity, which confirms our hypothesis and highlights that this assay could be used to screen antiviral drugs. Altogether, our data show that NERP activity could be explored to increase molecular diagnostic sensitivity and/or to develop antiviral screening assays.

Influenza A and B viruses are the main causes of acute respiratory infections. Influenza causes a major public health burden because of its high morbidity and mortality ratios (1). The annual global attack rate for influenza is estimated at 5 – 10 % in adults and 20 – 30 % in children (1). Despite these data, it is believed that almost 80 % of children below 5 years old are misdiagnosed, in both outpatient and inpatient settings (2). A false negative diagnosis may result in underestimation of influenza attack rates (3, 4), jeopardizing routine outbreak surveillance and even pandemic preparedness. That is, influenza A and B strains may display seasonal antigenic drifts, which are changes in the viral surface glycoproteins hemagglutinin (HA) and neuraminidase (NA) that allow the virus to escape from the host's memory immune response (5). Moreover, different subtypes of influenza A may mix their genomic segments, causing antigenic shifts that may lead to the emergence of strains with pandemic potential (6). Altogether, this information highlights that laboratory-based molecular surveillance for influenza is critical. Therefore, additional tools to enhance the molecular diagnosis of influenza are necessary.

It has already been described that some viruses, which contain their DNA/RNA polymerase within the virion, may be stimulated to produce an endogenous polymerase activity. For example, HIV reverse transcriptase (RT) may be activated by incubating virus particles with deoxynucleotides and Mg^{++} (7). Deoxynucleotides enter HIV virions through a channel created by the trimeric transmembrane protein gp41 (7). Influenza RNA polymerase is packaged within the virions (8), because this viral enzyme catalyzes an RNA-dependent RNA polymerase activity absent in the host cell. This is a common mechanism for negative sense RNA viruses. However, since there is no structural evidence to rule in or out the permissiveness of influenza virions to triphosphate ribonucleotides (NTPs), we functionally evaluated that.

To evaluate whether intravirion RNA polymerase activity was measurable for influenza, cell-free samples of influenza virus were stimulated to evaluate the natural endogenous RNA polymerase (NERP) activity. Samples containing influenza A and B were diluted 10-fold and incubated for 1 h at 37 ºC with a reaction mix containing 16 U RNase Out, 10 mM $MgCl_2$, and DMEM without serum to obtain a final volume of 40 µL. A second incubation period was performed for 2 h at 37 ºC with different concentrations of NTPs (from 300 to 2.3 µM) in a final volume of 50 µL. The final reaction was stopped by the lysis buffer of the viral RNA extraction mini kit. The total viral RNA was extracted according to the manufacturer instructions (Qiagen) and

subjected to one-step RT-PCR for quantification. The assays were carried out according to World Health Organization (WHO) recommendation (9, 10) and virus quantification was based on a standard curve method as previously described (11).

Indeed, the presence of NTPs/Mg^{++} enhanced the influenza RNA polymerase activity (Fig. 1). If virus input was high (> 1,000 $TCID_{50}$/mL), the induction of NERP activity was increased by approximately 1 log_{10} (Fig. 1(a) and (b)). Importantly, when virus inputs were lower (~ 100 $TCID_{50}$/mL), NERP activity enhanced virus loads more substantially, by 3 log_{10} (Fig. 1(a) and (b)). If the virus input was equivalent to 10 $TCID_{50}$/mL or lower, the ability to enhance virus detection by triggering the NERP activity was jeopardized, probably due to a limiting dilution of the virus.

Enzymatic activity is highly dependent on the substrate concentration. Therefore, to provide further evidence about the NERP activity, cell-free fractions of influenza containing high virus input (10,000 $TCID_{50}$/mL) were incubated with various concentrations of NTPs, the RNA polymerase substrate. Indeed, a saturable and Michaelian-shaped enzymatic curve was observed (Fig. 1(c)), reinforcing the existence of enzymatic behavior (Fig. 1(c)).

To further evaluate whether intravirion RNA polymerase activity is present in influenza subtypes other than A/H1N1pdm09, we also measured NERP activity inside influenza A/H3N2 and B viruses. We incubated 10,000 $TCID_{50}$/mL of cell-free influenza samples with NTPs/Mg^{++}, and next quantified influenza RNA levels by RT-PCR. Similar to the induction of NERP activity for influenza A/H1N1pdm09, viral RNA levels were enhanced at different magnitudes for influenza A/H3N2 and B viruses (Fig. 1(d)). These results functionally demonstrate that influenza A and B viruses are permissive to NTPs and Mg^{++}. Consequently, these stimuli triggered viral endogenous RNA polymerase activity.

To further confirm the stimulation of virus intrinsic RNA polymerase activity, samples were treated with ribavirin, a known pan-inhibitor of viral polymerases. Ribavirin treatment reduced the total RNA levels to their baseline, similar to the level quantified in samples without NTPs/Mg^{++} stimuli (Fig. 2). Altogether, our results reinforce the presence of RNA polymerase activity within virions. Moreover, our results also highlight that a NERP assay could be used as a method to screen compounds targeting influenza RNA polymerase.

We have demonstrated that the influenza virus possesses intrinsic RNA polymerase activity for laboratory-adapted strains of influenza. Considering the

importance of influenza diagnosis for public health, we evaluated whether NTPs/Mg^{++} stimuli could increase the sensitivity of influenza virus detection through RT-PCR in clinical samples. Forty clinical samples were collected from the influenza surveillance system from individuals with fever (>37.8°C) and respiratory influenza-like illness (9). Nasopharyngeal Dacron swabs or aspirates were processed and diagnosed in the Respiratory Viruses and Measles Laboratory at the Oswaldo Cruz Institute of the Oswaldo Cruz Foundation, the National Influenza Center (NIC) in Brazil. RNA was extracted from the samples, and one-step real-time RT-PCR assays were performed to diagnose and subtype influenza, according to the WHO recommendations (9). Our study has been approved by the Research Ethics Committee of the Evandro Chagas Clinical Research Institute (protocol number 00930112.7.0000.5262). The approval includes the retrospective use of clinical samples. All data were analyzed in an anonymous fashion.

The clinical samples were originally divided into categories in terms of their threshold cycle (C_t) values, namely: detectable viral loads (D), samples presenting C_t values lower than 40; borderline detection (B), samples with C_t values between 40 and 45; non-detectable viral loads from syndromic patients (NDS), samples from patients with influenza-like symptoms that presented Ct values higher than 45; non-detectable viral loads from non-syndromic patients (NDNS), samples from healthy individuals with C_t values higher than 45 used as negative controls. The results were compared with or without NTPs/Mg^{++} stimuli (Fig. 3). In the samples from all syndromic patients (including D, B and NDS), the stimulation with NTP/Mg^{++} increased the viral loads (Fig. 3(a)). In line with better enhancement of RNA levels in samples with low viral loads, the fold increase was more pronounced in NDS than in D and B samples (Fig. 3(a)). Of note, no increase in viral loads was observed in the samples from healthy individuals (NDNS) (Fig. 3(a)).

Moreover, to seek further evidence that NERP activity is specific, we sequenced the influenza NA gene (12, 13) from samples that received and did not receive NTP/Mg^{++} stimuli. Consensus sequences for NA were generated and aligned with an NA reference sequence, A/California/04/2009 (H1N1) (GenBank accession number: FJ966084). Interestingly, NERP increased the virus loads to levels that allowed us to uncover some misidentified nucleotides in the influenza genome (Fig. 3(b)). This information means that NERP activity is specific, unlikely to create molecular artifacts.

Influenza viruses continue to be a major public health concern. Annually, influenza is estimated to cause between 3 to 5 million cases of severe illness and to lead

to up to 500,000 deaths globally (1). Consequently, influenza is associated with considerable economic burden, from direct health-care costs, lost days of work or education and general social disruption across all age groups (14). Although the statistics associated with the influenza burden of disease are alarming, the possibility of enhancing diagnostic sensitivity may reveal that these numbers are still underestimated. Here, we show that the influenza virion from both A and B types is functionally permissive to the viral RNA polymerase substrate and cofactor (NTPs/Mg^{++}), leading to the enhancement of viral RNA content. The natural endogenous RNA polymerase activity that we describe here may have different applications, such as in increasing molecular diagnostic sensitivity and/or developing antiviral screening assays (15).

Some viruses carry their own RNA/DNA polymerase within the virions. This is necessary when the viral enzymes are endowed with distinguishable features when compared to cellular counterpart enzymes. As an example, HIV virions are packaged with the enzyme reverse transcriptase (RT), which possesses RNA-dependent DNA polymerase activity absent in the host cell. HIV virions are permissive to NTPs (8), presumably because of a channel formed by the envelope glycoprotein gp41 (7). For instance, influenza viruses are packaged with the viral RNA polymerase, which is an RNA-dependent RNA polymerase enzyme necessary to transcribe/replicate the negative sense viral genome and absent in the host. Since there is no structural evidence to rule in or out the permissiveness of influenza virions to NTPs, we functionally evaluated this activity. Indeed, we demonstrated that influenza is endowed with NERP activity. Considering that many viruses provoke cell lysis, releasing molecules such as nucleotides and Mg^{++} into the extracellular environment of the infected tissue, progeny virus particles could take advantage of the NERP activity to increase the amount of virus RNA.

In this article, we were more interested in demonstrating the existence of NERP activity and exploring the resultant potential to enhance molecular diagnostic sensitivity. Various human respiratory viruses may cause overlapping symptoms. Among these agents, influenza surveillance deserves especial attention because of the possibilities of antigenic drifts and shifts, which may drive public health concerns. Laboratory-based surveillance for influenza includes molecular assays, rapid diagnostic tests, immunofluorescence, viral culture and/or serology (16). These tests differ in their sensitivities (17, 18). Particularly, molecular assays, such as RT-PCR, have the highest sensitivity and specificity, but the time frame from onset of illness to sample collection

may jeopardize a precise diagnosis (17). Detectable viral RNA in respiratory tract samples may disappear quickly. We observed that NTPs/Mg^{++} stimuli specifically increased the sensitivity of influenza virus detection in clinical samples by $3log_{10}$. By increasing the RNA content, NERP activity allowed us to sequence missed nucleotides in the influenza genome from clinical samples.

Of note, during our investigation, we also used the pan-antiviral ribavirin to inhibit NERP activity, proving that it is carried out by the viral RNA polymerase. This result not only confirmed our hypothesis but also highlighted that this assay could be used to screen for antiviral drugs targeting influenza RNA polymerase activity (15).

Finally, the results presented here indicate that influenza RNA polymerase activity may be activated within the virion, helping to enhance laboratory-based molecular diagnosis of this virus.

Acknowledgements

Thanks are due to the Influenza Reagent Resource (IRR; https://www.influenzareagentresource.org/), the Centers for Disease Control (CDC/Atlanta; WHO Collaborating Center for Influenza) and Instituto de Tecnologia em Fármacos (Farmanguinhos) for donating materials used to conduct this investigation.

Funding

This work was supported by Conselho Nacional de Desenvolvimento e Pesquisa (CNPq), Fundação de Amparo à Pesquisa do Estado do Rio de Janeiro (FAPERJ).

Conflicts of interest

The authors declare no conflicts of interest.

References

1. **WHO**. Influenza (seasonal) Fact Sheet N°211 [Internet]. World Health Organization [online]. 2014.

2. **Poehling KA, Edwards KM, Weinberg GA, Szilagyi P, Staat MA, Iwane MK, et al.** The underrecognized burden of influenza in young children. N Engl J Med. 2006;355(1):31-40.

3. **CDC.** Influenza Signs and Symptoms and the Role of Laboratory Diagnostics 2015 [Available from: http://www.cdc.gov/flu/professionals/diagnosis/labrolesprocedures.htm.
4. **CDC**. Rapid Diagnostic Testing for Influenza: Information for Health Care Professionals 2015 [Available from: http://www.cdc.gov/flu/professionals/diagnosis/rapidclin.htm#table2.
5. **McHardy AC, Adams B.** The role of genomics in tracking the evolution of influenza A virus. PLoS Pathog. 2009;5(10):e1000566.
6. **Holmes EC.** RNA virus genomics: a world of possibilities. J Clin Invest. 2009;119(9):2488-95.
7. **Aguiar RS, Costa LJ, Pereira HS, Brindeiro RM, Tanuri A.** Development of a new methodology for screening of human immunodeficiency virus type 1 microbicides based on real-time PCR quantification. Antimicrob Agents Chemother. 2007;51(2):638-44.
8. **Das K, Aramini JM, Ma LC, Krug RM, Arnold E.** Structures of influenza A proteins and insights into antiviral drug targets. Nat Struct Mol Biol. 2010;17(5):530-8.
9. **WHO**, Network GIS. Manual for the laboraroty diagnosis and virological surveillance of influenza. 2011 [Available from: http://apps.who.int/iris/bitstream/10665/44518/1/9789241548090_eng.pdf.
10. **Szretter KJ, Balish AL, Katz JM.** Influenza: propagation, quantification, and storage. Curr Protoc Microbiol. 2006;Chapter 15:Unit 15G 1.
11. **Mesquita M, Fintelman-Rodrigues N, Sacramento CQ, Abrantes JL, Costa E, Temerozo JR, et al.** HIV-1 and its gp120 inhibits the influenza A(H1N1)pdm09 life cycle in an IFITM3-dependent fashion. PLoS One. 2014;9(6):e101056.
12. **Baillie GJ, Galiano M, Agapow PM, Myers R, Chiam R, Gall A, et al.** Evolutionary dynamics of local pandemic H1N1/2009 influenza virus lineages revealed by whole-genome analysis. J Virol. 2012;86(1):11-8.
13. **Souza TM, Resende PC, Fintelman-Rodrigues N, Gregianini TS, Ikuta N, Fernandes SB, et al.** Detection of oseltamivir-resistant pandemic influenza A(H1N1)pdm2009 in Brazil: can community transmission be ruled out? PLoS One. 2013;8(11):e80081.
14. **WHO**. Influenza 2016 [Available from: http://www.who.int/biologicals/vaccines/influenza/en/.
15. **Sacramento CQ, Fintelman-Rodrigues N, Marttorelli A, de Freitas CS, d e Melo GR, Ferreira AC, et al.** The ribavirin analog methyl 1-benzyl-1H-1,2,3-triazole-4-carboxylate inhibits influenza in vitro and in vivo replication. Accompanying manuscript. Journal of General Virology2017.
16. **WHO**. WHO recommendations on the use of rapid testing for influenza diagnosis. 2005 [Available from: http://www.who.int/influenza/resources/documents/RapidTestInfluenza_WebVersion.pdf.
17. **Binsaeed AA, Al-Khedhairy AA, Mandil AM, Shaikh SA, Qureshi R, Al-Khattaf AS, et al.** A validation study comparing the sensitivity and specificity of the new Dr. KSU H1N1 RT-PCR kit with real-time RT-PCR for diagnosing influenza A (H1N1). Ann Saudi Med. 2011;31(4):351-5.
18. **de Mello WA.** The role of laboratory diagnosis of influenza. Rev Pan-Amaz Saude. 2010;1(1):191-3

Figure Legends

Figure 1. Influenza virus possesses endogenous RNA polymerase (NERP) activity. Different inputs of cell-free influenza samples were incubated for 3 h at 37 ºC in the presence (NTPs/Mg^{++}, black) and absence (Nil, white) of stimuli of viral RNA polymerase activity, NTPs (150 μM) and $MgCl_2$ (10 mM). Influenza viral RNA levels were quantified through RT-PCR **(A)**. Fold increases of influenza RNA levels were calculated based on the ratio of RNA present in the samples stimulated or not by NTPs/$MgCl_2$ **(B)**. Cell-free influenza samples containing 10,000 $TCID_{50}$/mL of virus input were incubated with $MgCl_2$ (10 mM) and indicated concentrations of NTPs prior to influenza RNA quantification **(C)**. Cell-free influenza A/H1N1pdm09, A/H3N2 and B samples (10,000 $TCID_{50}$/mL) were stimulated with NTPs (150 μM) and $MgCl_2$ (10 mM) for 3 h at 37 ºC. Influenza RNA levels were quantified through RT-PCR. NERP activity is represented as a fold increase in RNA levels, calculated based on the ratio of RNA quantity present in the samples stimulated or not by NTPs/Mg^{++} **(D)**. *$p < 0.05$. **$p < 0.01$

Figure 2. Ribavirin inhibits influenza NERP activity. Cell-free influenza A/H1N1pdm09 (10,000 $TCID_{50}$/mL) were stimulated or not with NTPs (150 μM) and $MgCl_2$ (10 mM) in the presence of indicated concentrations of ribavirin triphosphate. NERP activity was measured by quantifying total viral RNA levels through RT-PCR. *$p < 0.05$.

Figure 3. Influenza NERP activity can be triggered in clinical samples. Clinical samples positive for influenza A/H1N1pdm09 virus were stimulated or not with NTPs (150 μM) and $MgCl_2$ (10 mM) for 3 h at 37 ºC prior to molecular detection of viral RNA. Samples were categorized as follows according to original RT-PCR (without NTP/Mg^{++} stimuli): detectable (D, Ct < 40), borderline (B, 40 < Ct < 45), non-detectable from syndromic patients (NDS, Ct ≥ 45) and non-detectable from non-syndromic individuals or healthy volunteers (NDNS, Ct ≥ 45). The fold increase in RNA levels from NTP/Mg^{++}-treated vs. –untreated samples is displayed. The dashed line above 1 means that NTP/Mg^{++} stimuli provided enhanced RNA levels. **(A)**. The NA genes of influenza viruses from clinical samples stimulated or not with NTPs/Mg^{++}

were sequenced. Dotted lines represent nucleotides identical to the reference sequence. Dashed lines represent nucleotides with no information **(B)**.

Figures

1

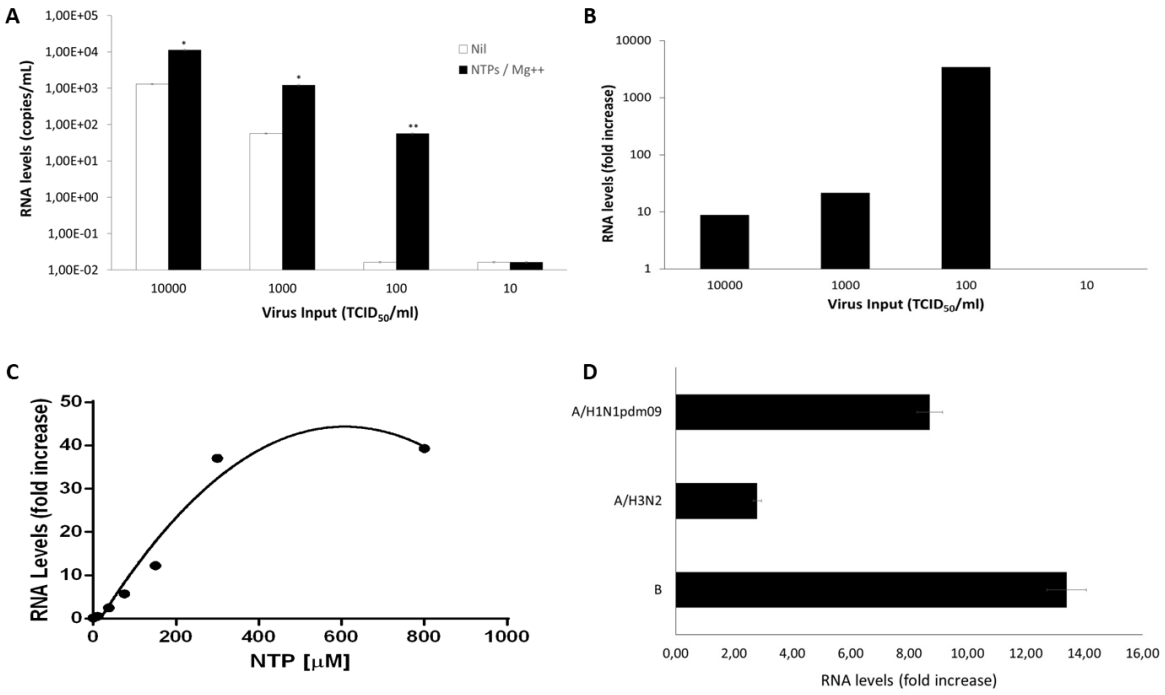

2

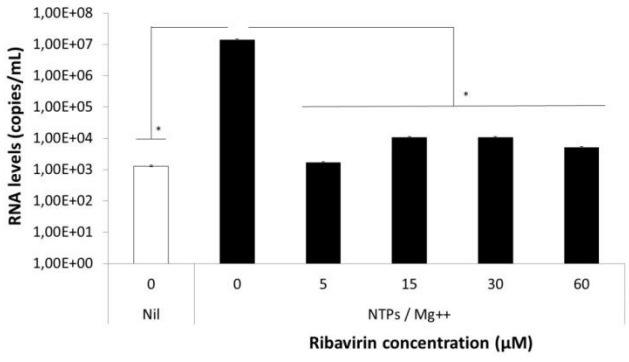

325 **3**

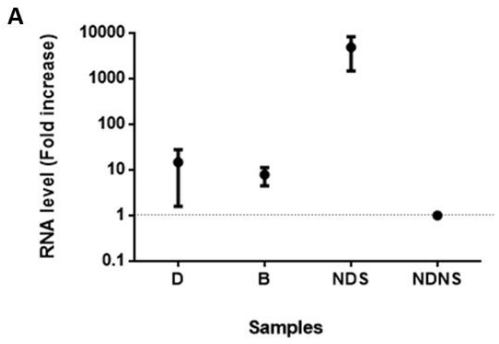

B

```
#A/California/04/2009(H1N1)              TCC GTG AAA TTA GCG GGC AAT TCC TCT CTC TGC CCT GTT AGT GGA TGG GCT ATA TAC AGT AAA GAC AAC AGT GTA AGA ATC GGT TCC AAG GGG GAT GTG
#A/Rio_de_Janeiro/13898/2009(H1N1)        ... ... ... ... ... ... ... ... ... M.. K.. .SK .K. ..K ... ... ... ... ... ... ... ... ... ... A.. ... ... ... ... ... ... ... ...
#A/Rio_de_Janeiro/13898/2009(H1N1)_+_NERP ... ... ... ... ... ... ... ... ... ... ... ... ... ... ... ... ... ... ... ... ... ... ... ... ... A.. ... ... ... ... ... ... ... ...
#A/Rio_de_Janeiro/6827/2009(H1N1)         --- --- --- --- --- --- --- --- --- --- --- --- --- --- --- --- --- --- --- --- --- --- --- --- --- --- --- --- --- --- --- --- --- ---
#A/Rio_de_Janeiro/6827/2009(H1N1)_+_NERP  ... ... ... ... ... ... ... ... ... ... ... ... ... ... ... ... ... ... ... ... ... ... ... ... ... A.. ... ... ... ... ... ... ... ...

#A/California/04/2009(H1N1)               TTT GTC ATA AGG GAA CCA TTC ATA TCA TGC TCC CCC TTG GAA TGC AGA ACC TTC TTC TTG ACT CAA GGG GCC TTG CTA AAT GAC AAA CAT TCC AAT GGA
#A/Rio_de_Janeiro/13898/2009(H1N1)        ... ... ... G.. ... ... ... ... ... ... ... ... ... ... ... ... ... ... ... ... ... ... ... ... ... ... ... ... ... ... ... ... ...
#A/Rio_de_Janeiro/13898/2009(H1N1)_+_NERP ... ... ... ... ... ... ... ... ... ... ... ... ... ... ... ... ... ... ... ... ... ... ... ... ... ... ... ... ... ... ... ... ... ...
#A/Rio_de_Janeiro/6827/2009(H1N1)         --- --- --- --- --- --- --- --- --- --- --- --- --- --- --- --- --- --- --- --- --- --- --- --- --- --- --- --- --- --- --- --- --- ---
#A/Rio_de_Janeiro/6827/2009(H1N1)_+_NERP  ... ... ... ... ... ... ... ... ... ... ... ... ... ... ... ... ... ... ... ... ... ... ... ... ... ... ... ... ... ... ... ... ... ...

#A/California/04/2009(H1N1)               ACC ATT AAA GAC AGG AGC CCA TAT CGA ACC CTA ATG AGC TGT CCT ATT GGT GAA GTT CCC TCT CCA TAC AAC TCA AGA TTT GAG TCA GTC GCT TGG TCA
#A/Rio_de_Janeiro/13898/2009(H1N1)        ... ... ... ... ... ... ... ... ... ... ... ... ... ... ... ... ... ... ... ... ... ... ... ... ... ... ... ... ... ... ... ... ... ...
#A/Rio_de_Janeiro/13898/2009(H1N1)_+_NERP ... ... ... ... ... ... ... ... ... ... ... ... ... ... ... ... ... ... ... ... ... ... ... ... ... ... ... ... ... ... ... ... ... ...
#A/Rio_de_Janeiro/6827/2009(H1N1)         --- --- --- --- --. ... ... ... ... ... ... ... ... ... ... ... ... ... ... ... ... ... ... ... ... ... ... ... ... ... ... ... ...
#A/Rio_de_Janeiro/6827/2009(H1N1)_+_NERP  ... ... ... ... ... ... ... ... ... ... ... ... ... ... ... ... ... ... ... ... ... ... ... ... ... ... ... ... ... ... ... ... ... ...
```

... Identical nucleotide
--- Undetermined nucleotide

326

327

328

The ribavirin analogue methyl 1-benzyl-1*H*-1,2,3-triazole-4-carboxylate inhibits influenza *in vitro* and *in vivo* replication

Carolina Q. Sacramento[1,2,6], Natalia Fintelman-Rodrigues[1,2,6], Andressa Marttorelli[1,2,6], Caroline S. de Freitas[1,2,6], Gabrielle R. de Melo[1,2,6], André C. Ferreira[1,2,6], Cristiana C. Garcia[2], Alexandre M. V. Machado[3], Andrea Surrage[1], Milene Miranda[2], Maria de Lourdes G. Ferreira[4], Luiz C. S. Pinheiro[4], Nubia Boechat[4], Fernando A. Bozza[5] and Thiago Moreno L. Souza[1,2,6*]

[1] Laboratório de Imunofarmacologia, Pavilhão Osório de Almeida, Instituto Oswaldo Cruz (IOC), Fundação Oswaldo Cruz (Fiocruz), Av. Brasil 4365, Manguinhos, Rio de Janeiro/RJ, Brasil.

[2] Laboratório de Vírus Respiratório e do Sarampo, Pavilhão Helio Peggy e Pereira, IOC, Fiocruz, Av. Brasil 4365, Manguinhos, Rio de Janeiro/RJ, Brasil.

[3] Imunologia de Doenças Virais, Centro de Pesquisas René Rachou, Fiocruz, Av. Augusto de Lima 1715, Belo Horizonte/MG, Brazil.

[4] Departamento de Síntese de Fármacos, Instituto de Tecnologia em Fármacos, Farmanguinhos, Fiocruz, Av. Brasil 4365, Rio de Janeiro/RJ, Brazil.

[5] Instituto Nacional de Infectologia, Fiocruz, Av. Brasil 4365, Manguinhos, Rio de Janeiro/RJ, Brasil.

[6] National Institute for Science and Technology on Innovation on Diseases of Neglected Populations (INCT/IDPN), Center for Technological Development in Health (CDTS), Fiocruz, Av. Brasil 4365, Manguinhos, Rio de Janeiro/RJ, Brasil.

***Corresponding author**

Thiago Moreno L. Souza, PhD

****

Fundação Oswaldo Cruz

Centro de Desenvolvimento Tecnológico em Saúde (CDTS)

Instituto Oswaldo Cruz (IOC)

Pavilhão Osório de Almeida, sala 16
Av. Brasil 4365, Manguinhos, Rio de Janeiro - RJ, Brasil, CEP 21060340
Tel.: +55 21 2562-1311
Email: tmoreno@cdts.fiocruz.br

Keywords: Influenza virus, RNA-dependent RNA polymerase, Anti-influenza drugs, Ribavirin analogue, Triazole

Abstract

Influenza virus represents one of the main causes of acute respiratory infections, and causes a major public health burden. Neuraminidase inhibitors (NAIs), such as oseltamivir, are the sole class of anti-influenza drugs in clinical use. Nevertheless, oseltamivir-resistant strains have been described, motivating the search for novel compounds with different targets. We aimed to study the anti-influenza activity of the ribavirin analogue, compound **5b**. Compound **5b** was less cytotoxic and more potent than ribavirin by inhibiting influenza replication on MDCKs. Our compound inhibits influenza RNA polymerase and disrupts the balance between the viral genome transcription and replication. Compound **5b** at a dose 200 mg/kg administered orally showed no toxicity *in vivo*. Our drug demonstrated immunomodulatory properties by reducing the production of influenza-dependent and influenza-independent pro-inflammatory cytokines *in vitro* and *in vivo*. Altogether our data suggest that compound **5b** is a potent inhibitor of influenza polymerase with desirable immunomodulatory properties. In addition, our results indicate that this compound`s chemical structure is promising for medicinal chemistry modifications and for the development of novel anti-influenza drugs.

Introduction

Influenza virus is one of the major causes of acute respiratory infections, leading to high levels of morbidity, mortality and public health burden worldwide (1). This *orthomyxovirus* causes seasonal infections, pandemic outbreaks and is also the most important aetiologic agent of severe acute respiratory infections (SARI) (2, 3). Annually, the global influenza infection rates are estimated from 3 to 5 million cases of severe illness, and approximately 250,000 to 500,000 deaths (4).

To control virus spread in the human population, vaccination and antiviral drugs may be used (5, 6). However, the existence of multiple zoonotic hosts (7), the time required to produce the vaccines against novel viruses, the costs of vaccine production and its recommendation only for groups of patients at high risk for serious influenza-related illnesses represent major limitations for the use of vaccines (8). On the other hand, anti-influenza drugs are now recommended for clinical use whenever possible (9). In addition, the stockpiling of anti-influenza drugs is a key issue in pandemic preparedness since the antigenic characteristics of the influenza strains that might cause future pandemic outbreaks are unpredictable (10, 11). Therefore, there is a great motivation for the continuous search for anti-influenza drugs. A desirable anti-influenza molecule would target any step of virus replication.

To enter the host cells, influenza binds to sialic acid residues on glycoproteins localized in the cellular plasma membrane. This is followed by endocytosis and the fusion of the viral envelope with the endocytic membrane in a viral protein M2-dependent manner (12). Next, viral ribonucleoproteins (RNP) composed of the RNA polymerase complex, viral RNA, nucleoprotein (NP) and nuclear export proteins (NEP) are released into the cytoplasm and transported to the cell nucleus, where the transcription and replication of the viral genome occur. Then, viral proteins are made and trafficked to the host cell plasma membrane for the assembly of new viruses. These particles bud through the cellular plasma membrane and are released via viral neuraminidase (NA) activity (13).

Neuraminidase inhibitors (NAIs), such as oseltamivir (OST), constitute the main licensed class of drugs available for clinical use against influenza (14). OST is the most used anti-influenza drug (15). Most countries stockpile OST for pandemic preparedness (10, 11). Nevertheless, circulating strains of influenza A(H1N1)pdm09 virus that are resistant to OST have been described, even in untreated individuals (16, 17). Therefore,

the identification of novel molecules targeting different viral proteins is pivotal because it may increase the number of options available to fight OST-resistant strains.

Ribavirin is a guanosine analogue with a broad spectrum of action against various RNA and DNA viruses, including influenza (18). Ribavirin targets the viral DNA/RNA polymerases and regulates cytokine production, despite its high cytotoxicity (19). We previously described that new ribavirin analogues, from the series of 1*H*-1,2,3-triazole nucleosides, are endowed with antiviral activity against influenza (20). Thus, in this work, we aimed to explore the mechanism of action of compound (2R,3R,4R)-2-((benzoyloxy)methyl)-5-(4-(methoxycarbonyl)-1*H*-1,2,3-triazol-1-yl)tetrahydrofuran-3,4-diyl dibenzoate **(5b)**, the most active analogue among the series of 1*H*-1,2,3-triazole nucleosides (20), and feasibility to turn this into a lead molecule for anti-influenza development.

Results

Potency against influenza replication and cytotoxicity of compound 5b. During our continuous screening of small molecule inhibitors of influenza replication, a series of 1*H*-1,2,3-triazole nucleoside ribavirin analogues emerged as potential hits (20). Among these, compound **5b** (Fig. 1), which contains a methyl carboxylate radical, was the most effective one, decreasing the viral RNA levels after treatment of influenza-infected cells (20).

We further explored the pharmacological activity of compound **5b** by performing yield-reduction assays, in which the supernatant of the infected and treated cultures are harvested and the virus infectivity was measured in additional rounds of infection. We confirmed that compound **5b** is endowed with anti-influenza activity. Compound **5b** presented an EC_{50} value of 0.07 ± 0.006 μM (Table 1). For reference, for ribavirin, this pharmacological parameter was 20.5 ± 3.0 μM (Table 1). We also evaluated compound **5b**`s cytotoxicity. Ribavirin`s cytotoxicity was approximately 10-times higher than for compound **5b** (Table 1). Based on the ratio between the CC_{50} and EC_{50}, the selective index (SI) values were calculated. Our compound`s SI is 3,000-fold higher when compared to ribavirin (Table 1), indicating its higher safety *in vitro*. Altogether, the results confirmed that the ribavirin analogue compound **5b** inhibits the *in vitro* replication of influenza.

Compound 5b inhibitory effect on viral RNA polymerase. Since our molecule is a modified nucleoside analogue, we next evaluated compound **5b**`s inhibitory effect towards influenza viral RNA polymerase activity. We used a new method to access influenza viruses endogenous (intra-virion) RNA polymerase activity (NERP) (21). As can be observed in Table 2 and Fig. 2, our compound was able to inhibit influenza virus RNA polymerase activity in a dose-dependent manner even with different concentrations of substrate, which demonstrates a different mechanism than classical nucleoside/nucleotide analogues.

Since compound **5b** inhibits influenza RNA polymerase activity, we further investigated whether viral RNA replication and transcription would be affected. MDCKs were infected with influenza virus for 1 h at 4 ºC to synchronize the adsorption. The temperature was increased to 37 ºC for 6 h, which is enough time for the viral RNPs to reach the nucleus (22). After that, the cells were treated with compound **5b** or ribavirin. After 24 h, the levels of influenza-related transcription and replication were measured. In Fig. 3, we can observe that normally (without treatments) the proportion of genomic/antigenomic viral RNA levels are superior to the influenza mRNA content. The treatments, either with compound **5b** or ribavirin, significantly disrupted the balance between the replication and transcription during the viral life cycle (Fig. 3). Ribavirin and its tested analogue reduced viral transcription by approximately 30 % (Fig. 3). Although an approximately 10-fold enhancement of the replication was observed (Fig. 3), these RNAs are likely to be defective – because of the observed diminishing during viral infectivity (Table 2). Altogether, the data from this section confirms that compound **5b** inhibits the RNA polymerase of influenza.

Compound 5b can modulate MCP-1, IL-6 and TNF-α levels. To verify if compound **5b** presents immunomodulatory activity, such as ribavirin (23), we evaluated our compound`s ability to modulate influenza-dependent and -independent (LPS-induced) pro-inflammatory cytokine production. The human pulmonary epithelial cell line (A549) was infected with influenza virus and treated with compound **5b**. After the 24 h-incubation period, the levels of chemokines and pro-inflammatory cytokines were measured. Treatment with compound **5b** modestly reduced the levels of IL-8 by 30 % (Fig. 4 (a)). More importantly, MCP-1 levels were substantially reduced by a 67 % (Fig. 4 (b)). Compound **5b** displayed similar results compared to the positive control, the

anti-inflammatory molecule dexamethasone (Fig. 4). Since we have shown above that compound **5b** directly inhibits viral replication, diminished viral replication could lead to the proposed anti-inflammatory activity of this molecule. To test whether compound **5b** is endowed with anti-inflammatory properties independent of influenza replication, we used a different *in vitro* model.

During influenza physiopathology, monocytes are attracted to the site of inflammation. Commonly, respiratory viruses disrupt tissue integrity and lead to initial inflammation, which is exacerbated by secondary bacterial infections (24). Thus, a desirable feature of the antiviral drugs would be additional anti-inflammatory activity for both virus-related and -unrelated insults. Human primary peripheral monocyte-derived macrophages (MDMs) were pre-treated with different concentrations of compound **5b** or the reference compound ribavirin for 30 minutes and were then stimulated with a bacterial product, LPS (a virus-independent inflammatory stimulus). After 24 h incubation, we observed that treatment with our compound significantly decreased the levels of IL-6 and TNF- α, similarly to ribavirin (Fig. 5). Our results confirm that compound **5b** is endowed with immunomodulatory properties, which is independent of its antiviral activity.

Compound 5b shows anti-influenza effects *in vivo*. We further studied whether compound **5b** possesses antiviral activity *in vivo*. At first, we observed no signs of toxicity in the Swiss outbred mice, an ideal model for initial pharmacological studies (25), after treatment with compound **5b**, even at doses of 200 mg/kg (Fig S1 and Table S1).

As authorized by the Animal Welfare Committee, our initial antiviral *in vivo* studies used an established model of influenza pathogenesis using a mouse adapted influenza virus inoculation. Thus, C57Bl/6 mice were inoculated intranasally with the influenza virus A/PR/8/34 H1N1 strain at 10^3 PFU. To choose the amount of drug to be used, we took the human dose of OST as a reference, and converted it to mice (26). This dose would provide a pragmatic go/no-go response to whether or not compound **5b** possesses *in vivo* antiviral activity. Animals were treated daily with 10 mg/kg of compound **5b** and monitored for up to 5 days.

As depicted in Fig. 6 (a), compound **5b** did not prevent influenza-induced weight loss, however it led to a 4-time reduction in influenza RNA levels in the lungs of infected animals (Fig. 6 (b)). Analysis on the bronchoalveolar lavage (BAL) at 5 days

post-infection (pi) demonstrated that the number of total leucocytes, mononuclear and polymorphonuclear cells, and total protein levels were significantly decreased in mice treated with compound **5b** compared with the non-treated influenza-infected group (Fig. 6 (c) – (f)), pointing out that treated mice benefit from a reduced cell mediated inflammatory response compared to untreated animals. Similarly, the total number of leucocytes in the peripheral blood is also reduced by treatment with compound **5b** (Fig. 6 (g)). Accordingly, compound **5b** prevented influenza-induced enhancement of pro-inflammatory cytokines in the BAL, such as TNF-α, IFN-γ, IL-6, and the chemokines KC and MCP-1 (Fig. 7 (a) – (f)).

We further examined the lungs of the mice (Fig. 7). The lungs of mice inoculated with influenza virus displayed large inflammatory infiltrate (Fig. 7 (b) and (e)) when compared to the control (Fig. 7 (a) and (d)), which is consistent with an acute infection. Importantly, infected and treated mice displayed airways and lung parenchyma that were more similar to control uninfected mice (Fig. 7 (c) and (f)). Our results indicate that the antiviral and anti-inflammatory activities of compound **5b** are preserved *in vivo* at a relevant pharmacological dose.

Discussion

Influenza viruses continue to threaten public health due to their high morbidity and mortality rates, despite annual vaccination (1, 8). In addition, influenza constantly imposes the threat of a pandemic outbreak because of its genetic variability and multiple zoonotic hosts (2, 3). Antiviral drugs against influenza are essential to fight both seasonal and pandemic infections. Considering the emergence of drug-resistant strains of influenza (16, 17), it is important to search for molecules that are able to inhibit the influenza life cycle at different steps than those molecules currently in clinical use. In this work, we demonstrated the *in vitro* and *in vivo* activity of a new 1*H*-1,2,3-triazole nucleoside, a ribavirin analogue, compound **5b**, that was previously described as having antiviral effects against influenza (20).

Compound **5b** inhibited influenza replication at micromolar concentrations and with very low cytotoxicity. Consequently, our compound presented a very safe range for use *in vitro*. Ribavirin, our reference compound, is approximately 10-times more cytotoxic and 300-times less potent than compound **5b** in our experimental conditions. Compared to OST, the anti-influenza drug currently in clinical use, our compound was

slightly less potent. Nevertheless, OST and compound **5b** present different mechanisms of action. While OST blocks the spread of influenza by inhibiting the viral enzyme NA, our compound reduces influenza replication by targeting the viral RNA polymerase. Importantly, approximately 2 % of circulating influenza strains are resistant to OST (16, 17). Thus, the effect of our compound on a different step of the virus life cycle may be of great interest as an alternative to OST.

Due to influenza RNA polymerase`s critical role during the virus replicative cycle and the fact that this enzyme has been highly conserved among all the strains and subtypes during evolution, it has become a promising target for the development of anti-influenza drugs in recent years. Other compounds that inhibit influenza RNA polymerase have been described (27). For example, favipiravir, a new antiviral drug with a strong inhibitory activity on the RNA-dependent RNA polymerase of most RNA virus genome (28, 29), has advanced to phase II clinical trials (USA) and phase III clinical trials (Japan).

Compound **5b** targets influenza virus RNA polymerase activity, inhibiting this enzyme activity in a dose-dependent manner, even with different concentrations of substrate, which notes a mechanism that is different than the classical nucleoside/nucleotide analogues (30). Influenza RNA polymerase is responsible for both the replication and transcription of viral genome (31). We also showed that compound **5b** inhibits influenza RNA polymerase in such a way that the balance between the synthesis of viral transcripts and replicons is disrupted. We believe this is an interesting finding because a great deal of light has been shed on the processes that regulate influenza transcription and replication (32). We observed a reduction in viral transcription by compound **5b**. We believe that because transcription was blocked, the viral genome was preferentially used by other processes, such as genomic and anti-genomic viral RNA synthesis.

During highly pathogenic cases of influenza virus infection (HPCIVI), exacerbated pro-inflammatory cytokine production is observed (also called cytokine storm), along with excessive inflammatory infiltrates and virus-induced tissue destruction (33). The ability to modulate pro-inflammatory response after an insult is also a desirable feature of novel antivirals. Compound **5b** significantly reduced the levels of the neutrophil and monocyte chemoattractant proteins IL-8 and MCP-1, respectively. Curiously, dexamethasone, a glucocorticoid used as a positive control did not inhibit IL-8 production. It could be expected since downregulation of the IL-8 levels

by dexamethasone is an early event (up to 5 h after dexamethasone treatment) and this drug can affect IL-8 mRNA stability, reducing its half-life from more than 8 h to approximately 78 minutes (34). We also evaluated whether compound **5b** as well as ribavirin can modulate LPS-stimulated macrophage cytokine secretion and observed a significant decrease in the production of TNF-α and IL-6. These data are of great importance since immunomodulation is expected to control the severity of virus-induced inflammatory complications during influenza infection.

In animal experiments, a single high oral dose of compound **5b** (200 mg/kg) showed no toxicity for Swiss mice. This was demonstrated by the absence of signs of toxicity, the maintenance of weight and motor activity and the coordination of the animals belonging to the treatment group. To access the antiviral effects of compound **5b** *in vivo*, we inoculated C57Bl/6 mice with a non-lethal dose of mouse-adapted influenza PR8 virus (10^3 PFU) and treated them with 10 mg/kg per day of compound **5b**. The dose chosen for the treatment of mice is equivalent to oseltamivir`s dose of 75 mg for human adults (80 kg), according to the body surface area calculation (26). Acute lung injury (ALI) and its more severe form, acute respiratory distress syndrome (ARDS), can be seen during HPCIVI. They are a common consequence of the cytokine storm in the lung alveolar environment and are characterized by an acute mononuclear/neutrophilic inflammatory response (33). Thus, the reduction of the recruitment of immune cells to the site of infection may help to ameliorate lung tissue injury caused by the influenza-induced cytokine storm. In addition, the regulation of pro- and anti-inflammatory cytokines production during influenza infection is critical to prevent the cytokine storm and to maintain lung immune homeostasis. One mechanism to diminish lung inflammation is by regulating the activation of specific cells types, such as alveolar macrophages (35).

The combination use of antiviral and immunomodulatory therapies is currently a popular approach in treating severe cases of influenza infection (36-38). Therefore, a novel anti-influenza drug with specific anti-inflammatory properties is a desirable feature. Based on the results of this work, compound **5b** possesses a potent antiviral effect, inhibiting influenza RNA polymerase with immunomodulatory properties *in vitro* and *in vivo* and constitutes a promising prototype for further development of novel antiviral drugs.

Materials and Methods

Cells, viruses and compounds. Madin-Darby Canine Kidney (MDCK) cells, donated by Influenza Reagent Resource (IRR; http://www.influenzareagentresource.org/) to the Brazilian National Influenza Center (NIC), were cultured in Dulbecco's Modified Eagle Medium (DMEM; Life Technologies, Grand Island, NY) and supplemented with 10 % foetal bovine serum (FBS; HyClone, Logan, UT, USA), 100 U/mL penicillin and 100 mg/mL streptomycin (Sigma-Aldrich). A549 human lung cancer cells (A549 cells; ATCC, USA) were maintained in a DMEM: Nutrient Mixture of F-12 1:1 (DMEM/F12; Life Technologies, Grand Island, NY) culture medium supplemented with 2 % FBS, 1 % L-glutamine (Life Technologies, Grand Island, NY) and penicillin/streptomycin. Both cell lines were cultured at 37 °C in a 5 % CO_2 atmosphere. Monocyte–derived macrophages (MDMs) were obtained through the adherence of peripheral blood mononuclear cells (PBMCs) previously isolated by density gradient centrifugation (Ficoll-Paque, GE Healthcare) from buffy coat preparations of blood from healthy donors to plastic. Briefly, 2.0 x 10^6 PBMCs were plated onto 48-well plates (NalgeNunc) in DMEM containing 10 % human serum (HS; Millipore) and penicillin/streptomycin. Cells were maintained at standard culture conditions for 6–7 days for monocyte differentiation into macrophages. Then, non-adherent cells were washed and the remaining macrophage layer was maintained in DMEM with 5 % HS.

Cell infection assays were performed with a laboratory-adapted influenza A strain (A/England/42/1972, H3N2). Influenza viruses were propagated in MDCK cells (39). For *in vivo* studies, we used a mouse-adapted PR8 virus, influenza A/Puerto Rico/8/34 (A/PR/8/34, H1N1 – kindly donated by Dr. Alexandre de Magalhães Vieira Machado from Centro de Pesquisas René Rachou, FIOCRUZ, Belo Horizonte/MG) (40) that was grown in MDCK cells. The viral stocks were aliquoted and stored at -70 °C for further studies. Titration of the viral stocks was performed using serial dilutions on MDCK monolayers with an agarose overlay for 72 h, and the plaque forming units (PFU) were counted.

Compound **5b** was synthetized using a previously described protocol (20). Ribavirin triphosphate and Oseltamivir carboxylate (OST-c) were purchased from Sierra Bioresearch (Tucson, AZ). All molecules were dissolved in 100 % dimethyl sulfoxide (DMSO) and, subsequently, diluted 10^4-fold in culture or reaction medium before each assay. The final DMSO concentrations showed no cytotoxicity.

Animals. Male Swiss-Webster or C57Bl/6 mice (20–30 g) were obtained from the Oswaldo Cruz Foundation breeding colony. The experiments performed in this work were approved by the Committee on the Use of Laboratory Animals of the Oswaldo Cruz Foundation (CEUA-FIOCRUZ, license L-050/15). The animals were maintained with free access to food and water and kept at 25–28 °C under a controlled 12 h light/dark cycle. Experiments were performed during the light phase of the cycle. The animals were allowed to adapt to the laboratory for at least 2 h before testing and were used only once. In all the infection procedures, animals were anaesthetized and kept under observation until they completely recovered. We anaesthetized the mice before euthanasia procedures for all the *in vivo* experiments. In the case of weight loss higher than 25 %, euthanasia was performed to alleviate animal suffering.

Cell viability assays. Monolayers of MDCKs (2 x 10^4 cell/well) in 96-well culture plates were incubated with the compounds at different concentrations for 72 h. Then, 2,3-Bis-(2-methoxy-4-nitro-5-sulfophenyl)-*2H*-tetrazolium-5-carboxanilide (XTT) at 5 mg/ml was added to the DMEM in the presence of 0.01 % *N*-Methylphenazinium methyl sulfate (PMS). After incubation for 4 h at 37 °C, the plates were read in a spectrophotometer at 492 nm and 620 nm (41). The 50 % cytotoxic concentration (CC_{50}) was calculated by performing a linear regression analysis on the dose–response curves generated from the data.

Yield Reduction Assay. Monolayers of MDCK cells (2 x 10^5 cell/well) in 24-well plates were infected with influenza at an MOI of 0.05 for 1 h at 37ºC. Cells were washed to remove residual virus and various concentrations of the compounds were added. After 24 h, the viruses in the supernatant were harvested and titrated by end-point 50 % cell culture infective dose ($TCID_{50}$/mL) using MDCK cells (42). For comparison, the reference compound ribavirin was used as a positive control. Linear regression of the dose-response curve was performed to determine the 50 % inhibitory effect on the viral replication (EC_{50}) for the tested compound.

Viral RNA polymerase inhibition assay. Cell-free influenza virus samples were stimulated to evaluate the inhibitory effect of compound **5b** on the natural endogenous RNA polymerase (NERP) activity (21). In summary, 10-fold dilutions of cell-free influenza samples were incubated for 1 h at 37 ºC with a reaction mix containing 16 U

of RNAse out, 10 mM $MgCl_2$, and different concentrations of compound **5b**. A second incubation period was performed for 2 h at 37 ºC with 150 µM of nucleoside triphosphate (NTPs). The final reaction was stopped, total virus RNA was extracted with the viral RNA mini kit (Qiagen Inc, CA) and the virus was quantified through one-step RT-PCR using Superscript III/ Platinum Taq, as previously described (39). All reagents for real time RT-PCR, including primers, probes and enzymes, were used as recommended by the World Health Organization (WHO) (43). Kinetic parameters, such as the maximal velocity (V_{max}) and Michaelis constant (K_M), were calculated using Sigma Plot 12.0.

Inhibition of viral RNA replication and transcription. Monolayers of MDCK cells were infected with influenza (MOI of 1) for 1 h at 4 ^{o}C, a condition that only allows virus adsorption. Cells were washed with PBS and incubated with warm medium for 6 h at 37 ºC to allow for the influenza RNPs to reach the cell nucleus. After the second incubation period, cells were treated with 30 µM of compound **5b** and lysed with buffer A (10 mM of HEPES, 1.5 mM of $MgCl_2$, 10 mM of KCl, 0.5 % NP-40, 1 mM of DTT, 0.5 mM of PMSF) 24 hours post-infection (hpi) (22). The cell lysate was centrifuged for 10 minutes at 1000 x *g*, allowing the separation of the nuclear (pellet) and non-nuclear fractions (supernatant). We confirmed the purity of the nuclear RNA preparation as previously described (22). The total RNA of the nuclear fraction was extracted as previously mentioned. cDNA was synthetized with SuperScript III (Life Technologies) using oligo.dT (Life Technologies) or UNI-12 (59-AGCRAAAGCAGG-39) as the primers for first-strand synthesis, for 1 h at 45 ºC. Oligo.dT and UNI-12 primers allow the retrotranscription of the messenger RNA (mRNA) and total influenza RNA, respectively. Real time PCR assays were performed to amplify the influenza gene M1 in order to quantify both the total RNA and mRNA. As a control, the total RNA and mRNA were also measured in the influenza-infected cells treated with ribavirin. The replication and transcription processes were measured through the levels of viral genomic/antigenomic RNA and mRNA, respectively. The levels of genomic/antigenomic RNA were obtained by subtracting the levels of total influenza RNA minus the mRNA counted in the real time PCR reaction.

Cytokine and Chemokine Measurements. The levels of cytokines and chemokines were measured using DuoSet® ELISA Development System (R&D Systems, Inc.) assays from the supernatants of the cultures. MDMs were pre-treated with different concentrations of compound **5b** or the reference compound ribavirin for 30 minutes and then were stimulated with 10 ng/mL of LPS (Sigma-Aldrich). After 24 h-incubation, the level of the cytokines and chemokines were measured by ELISA.

The levels of influenza-induced pro-inflammatory cytokines were quantified from the supernatants of A549 cultures. A549 cells were infected with the influenza virus A/England/42/1972, H3N2 (MOI of 0.05 for 1 h at 37ºC) and treated with 15 µM of compound **5b** or 10 µg/mL of dexamethasone (used as a positive control). After a 24 h incubation, the levels of the cytokines and chemokines were measured by ELISA.

***In vivo* antiviral activity.** C57Bl/6 mice were anaesthetized with 15 mg/kg of ketamine and 0.6 mg/kg of xylazine and inoculated intranasally with PBS (mock), or 10^3 PFU of PR8 influenza virus in 25 µl of PBS (44). At least, five mice were used per group: mock-infected; influenza-infected and treated with vehicle; and influenza-infected and treated with compound **5b**. Mice were treated with 10 mg/kg/day orally for 5 days.

At day 5 after infection, the mice were anaesthetized, and the blood was collected by retro orbital puncture for the total and differential leukocyte counts. After blood collection, mice were euthanized with an overdose of ketamine/xylazine solution. Subsequently, bronchoalveolar lavage (BAL) from both lungs was harvested by washing the lungs three times with two 1-ml aliquots of PBS (45). After centrifugation, the pellet was used for total and differential leukocytes counts. The supernatant of the centrifuged BAL was used for the cytokines, chemokines and total protein measurements. After BAL harvesting, the lungs were perfused with 5 ml of PBS to remove the circulating blood. The right lobes were removed in sterile conditions and frozen for quantitative RT-PCR assay to measure the viral loads and the left lobes were fixed for analysis of the histopathological changes.

For molecular detection of viral RNA levels, the lung tissue was homogenized in PBS. The total RNA was extracted using RNeasy Mini Kits (Qiagen Inc, CA) according to the manufacturer's instructions and quantified through one-step RT-PCR using Superscript III/ Platinum Taq, as previously described (39). The standard curve method was employed for virus quantification. We used the PET26b+ plasmid (Novagen,

Darmstadt, DE) containing the influenza M1 synthetic gene insert (Genescript, Grand Cayman, KY) for this absolute quantification (22). Quantification was expressed as the copies/mL. For reference on the cell amounts used, the housekeeping gene RNAse P was amplified (46). The Ct values for this target were compared for those obtained at different cell amounts, 10^7 to 10^2, for calibration.

For histopathological analysis, the lungs were fixed in formalin and embedded in paraffin. Lung sections of 5-mm thickness were stained with haematoxylin-eosin (47). The slides containing the lung sections were scanned using the Panoramic Desk scanner (3DHISTECH, Budapest, Hungary) and the analysis of the tissue was performed through the software Panoramic Viewer 1.15.4 (3DHISTECH Ltd).

Total leukocytes from the blood and BAL (diluted in Turk's 2 % acetic acid fluid) were counted using a Neubauer chamber. Differential counts were performed in cytospins (Cytospin3, Shandon, CA, USA) and stained by the May-Grünwald-Giemsa method. The total protein concentration in the BAL was measured using a BCA protein assay kit (Thermo Scientific, Waltham, MA, USA), according to manufacturer's instructions. The levels of cytokines and chemokines were assessed in the BAL by ELISA according to the manufacturer's instructions (R&D Systems Duo set kits, Minneapolis, USA).

Statistical analysis. All assays were performed and codified by one professional. Subsequently, a different professional analysed the results before the identification of the experimental groups. This approach was used to keep the pharmacological assays blind. All experiments were carried out at least three times independently, including technical replicates in each assay. The dose-response curves were used to calculate the EC_{50} and CC_{50} values generated by Excel for Windows. The equations to fit the best curve were generated based on the internal parameters of the SigmaPlot 12.0 enzyme kinetics mode. The significance of the survival curves was evaluated using the Log-rank (Mantel-Cox) test. *P* values <0.05 were considered statistically significant.

Acknowledgements

We would like to thank the Influenza Reagent Resource (IRR; https://www.influenzareagentresource.org/) and the Centers for Disease Control (CDC/Atlanta; WHO Collaborating Center for Influenza) for donating materials to conduct this investigation.

Funding

This work was supported by Conselho Nacional de Desenvolvimento e Pesquisa (CNPq) and Fundação de Amparo à Pesquisa do Estado do Rio de Janeiro (FAPERJ).

Conflicts of interest

The authors declare no conflicts of interest.

References

1. **Damjanovic D, Small CL, Jeyanathan M, Jeyananthan M, McCormick S, Xing Z.** Immunopathology in influenza virus infection: uncoupling the friend from foe. *Clin Immunol.* 2012;144(1):57-69.
2. **Murphy BR, Webster RG.** Orthomyxoviruses. 3rd ed. Fields, editor. Philadelphia: Lappincott-Raven Publishers; 1996.
3. **Tang JW, Shetty N, Lam TT, Hon KL.** Emerging, novel, and known influenza virus infections in humans. I*nfect Dis Clin North Am.* 2010;24(3):603-17.
4. Influenza (seasonal) Fact Sheet N°211 [Internet]. World Health Organization [online]. 2014.
5. **Grohskopf LA, Olsen SJ, Sokolow LZ, Bresee JS, Cox NJ, Broder KR, et al.** Prevention and control of seasonal influenza with vaccines: recommendations of the Advisory Committee on Immunization Practices (ACIP) -- United States, 2014-15 influenza season. *MMWR Morb Mortal Wkly Rep.* 2014;63(32):691-7.
6. **Fiore AE, Fry A, Shay D, Gubareva L, Bresee JS, Uyeki TM.** Antiviral agents for the treatment and chemoprophylaxis of influenza --- recommendations of the Advisory Committee on Immunization Practices (ACIP). *MMWR Recomm Rep.* 2011;60(1):1-24.
7. **Manz B, Schwemmle M, Brunotte L.** Adaptation of avian influenza a virus polymerase in mammals to overcome the host species barrier. *J Virol.* 2013;87(13):7200-9.
8. **WHO**. Recommended composition of influenza virus vaccines for use in the 2014 southern hemisphere influenza season. *Wkly Epidemiol Rec.* 2013;88(41):437-48.
9. **Muthuri SG, Myles PR, Venkatesan S, Leonardi-Bee J, Nguyen-Van-Tam JS.** Impact of neuraminidase inhibitor treatment on outcomes of public health importance during the 2009-2010 influenza A(H1N1) pandemic: a systematic review and meta-analysis in hospitalized patients. *J Infect Dis.* 2013;207(4):553-63.
10. **Balicer RD, Huerta M, Davidovitch N, Grotto I.** Cost-benefit of stockpiling drugs for influenza pandemic. *Emerg Infect Dis.* 2005;11(8):1280-2.
11. **Patel A, Gorman SE.** Stockpiling antiviral drugs for the next influenza pandemic. *Clin Pharmacol Ther.* 2009;86(3):241-3.
12. **Kollerova E, Betakova T.** Influenza viruses and their ion channels. *Acta Virol.* 2006;50(1):7-16.
13. **Das K, Aramini JM, Ma LC, Krug RM, Arnold E.** Structures of influenza A proteins and insights into antiviral drug targets. *Nat Struct Mol Biol.* 2010;17(5):530-8.
14. **Hurt AC.** The epidemiology and spread of drug resistant human influenza viruses. *Curr Opin Virol.* 2014;8C:22-9.
15. J**efferson T, Jones M, Doshi P, Spencer EA, Onakpoya I, Heneghan CJ.** Oseltamivir for influenza in adults and children: systematic review of clinical study reports and summary of regulatory comments. *BMJ*. 2014;348:g2545.

16. **Fry AM, Gubareva LV.** Understanding influenza virus resistance to antiviral agents; early warning signs for wider community circulation. *J Infect Dis.* 2012;206(2):145-7.
17. **Hurt AC, Hardie K, Wilson NJ, Deng YM, Osbourn M, Leang SK, et al.** Characteristics of a widespread community cluster of H275Y oseltamivir-resistant A(H1N1)pdm09 influenza in Australia. *J Infect Dis.* 2012;206(2):148-57.
18. **Sidwell RW, Huffman JH, Khare GP, Allen LB, Witkowski JT, Robins RK.** Broad-spectrum antiviral activity of Virazole: 1-beta-D-ribofuranosyl-1,2,4-triazole-3-carboxamide. *Science*. 1972;177(4050):705-6.
19. **Paeshuyse J, Dallmeier K, Neyts J.** Ribavirin for the treatment of chronic hepatitis C virus infection: a review of the proposed mechanisms of action. *Curr Opin Virol.* 2011;1(6):590-8.
20. **Lourdes G. Ferreira M, Pinheiro LCS, Santos-Filho O, Peçanha MDS, Sacramento CQ, Machado V, et al.** Design, synthesis, and antiviral activity of new 1H-1,2,3-triazole nucleoside ribavirin analogs. *Medicinal Chemistry Research.* 2013;23:1501-11.
21. **Sacramento CQ, Fintelman-Rodrigues N, Miranda MD, Siqueira MM, Souza TML.** Influenza virus RNA polymerase may be activated inside the viron to enhance diagnostic sensitivity. Accompaning Manuscript. *Journal of General Virology*, 2017.
22. **Mesquita M, Fintelman-Rodrigues N, Sacramento CQ, Abrantes JL, Costa E, Temerozo JR, et al.** HIV-1 and its gp120 inhibits the influenza A(H1N1)pdm09 life cycle in an IFITM3-dependent fashion. *PLoS One.* 2014;9(6):e101056.
23. C**rotty S, Cameron C, Andino R.** Ribavirin's antiviral mechanism of action: lethal mutagenesis? *J Mol Med* (Berl). 2002;80(2):86-95.
24. **Vareille M, Kieninger E, Edwards MR, Regamey N.** The airway epithelium: soldier in the fight against respiratory viruses. *Clin Microbiol Rev.* 2011;24(1):210-29.
25. **Chia R, Achilli F, Festing MF, Fisher EM.** The origins and uses of mouse outbred stocks. *Nat Genet.* 2005;37(11):1181-6.
26. **Nair AB, Jacob S.** A simple practice guide for dose conversion between animals and human. *J Basic Clin Pharm.* 2016;7(2):27-31.
27. **Wu X, Sun Q, Zhang C, Yang S, Li L, Jia Z.** Progress of small molecular inhibitors in the development of anti-influenza virus agents. *Theranostics*. 2017;7(4):826-45.
28. **Furuta Y, Takahashi K, Fukuda Y, Kuno M, Kamiyama T, Kozaki K, et al.** In vitro and in vivo activities of anti-influenza virus compound T-705. *Antimicrob Agents Chemother*. 2002;46(4):977-81.
29. **Rocha-Pereira J, Jochmans D, Dallmeier K, Leyssen P, Nascimento MS, Neyts J.** Favipiravir (T-705) inhibits in vitro norovirus replication. *Biochem Biophys Res Commun.* 2012;424(4):777-80.
30. **Jordheim LP, Durantel D, Zoulim F, Dumontet C.** Advances in the development of nucleoside and nucleotide analogues for cancer and viral diseases. *Nat Rev Drug Discov*. 2013;12(6):447-64.
31. **Boivin S, Cusack S, Ruigrok RWH, Hart DJ.** Influenza A Virus Polymerase: Structural Insights into Replication and Host Adaptation Mechanisms. *J Biol Chem.* 2010;285(37):28411–7.
32. **Te Velthuis AJ, Fodor E.** Influenza virus RNA polymerase: insights into the mechanisms of viral RNA synthesis. *Nat Rev Microbiol.* 2016;14(8):479-93.
33. **Tisoncik JR, Korth MJ, Simmons CP, Farrar J, Martin TR, Katze MG.** Into the eye of the cytokine storm. *Microbiol Mol Biol Rev.* 2012;76(1):16-32.
34. **Chang MM, Juarez M, Hyde DM, Wu R.** Mechanism of dexamethasone-mediated interleukin-8 gene suppression in cultured airway epithelial cells. *Am J Physiol Lung Cell Mol Physiol.* 2001;280(1):L107-15.
35. **Snelgrove RJ, Goulding J, Didierlaurent AM, Lyonga D, Vekaria S, Edwards L, et al.** A critical function for CD200 in lung immune homeostasis and the severity of influenza infection. *Nat Immunol.* 2008;9(9):1074-83.

36. **Souza TM, Salluh JI, Bozza FA, Mesquita M, Soares M, Motta FC, et al.** H1N1pdm influenza infection in hospitalized cancer patients: clinical evolution and viral analysis. *PLoS One.* 2010;5(11):e14158.
37. **Brun-Buisson C, Richard JM, Mercat A, Thie´baut ACM, Brochard L.** Early Corticosteroids in Severe Influenza A/H1N1 Pneumonia and Acute Respiratory Distress Syndrome. *J Respir Crit Care Med.* 2011;183:1200–6.
38. **Tavares LP, Teixeira MM, Garcia CC.** The inflammatory response triggered by Influenza virus: a two edged sword. *Inflamm Res.* 2017;66(4):283-302.
39. **Szretter KJ, Balish AL, Katz JM.** Influenza: propagation, quantification, and storage. *Curr Protoc Microbiol.* 2006;Chapter 15:Unit 15G 1.
40. **Thangavel RR, Bouvier NM.** Animal models for influenza virus pathogenesis, transmission, and immunology. *J Immunol Methods.* 2014;410:60-79.
41. **Scudiero DA, Shoemaker RH, Paull KD, Monks A, Tierney S, Nofziger TH, et al.** Evaluation of a soluble tetrazolium/formazan assay for cell growth and drug sensitivity in culture using human and other tumor cell lines. *Cancer Res.* 1988;48(17):4827-33.
42. **WHO, CDC.** Serological Diagnosis of Influenza by Microneutralization Assay. 2010.
43. **WHO**, **Network GIS.** Manual for the laboraroty diagnosis and virological surveillance of influenza. 2011 [Available from: http://apps.who.int/iris/bitstream/10665/44518/1/9789241548090_eng.pdf.
44. **Barbosa RP, Salgado AP, Garcia CC, Filho BG, Gonçalves AP, Lima BH, et al.** Protective immunity and safety of a genetically modified influenza virus vaccine. *PLoS One*. 2014;9(6):e98685.
45. d**e Oliveira DB, Almeida GM, Guedes AC, Santos FP, Bonjardim CA, Ferreira PC, et al.** Basal Activation of Type I Interferons (Alpha2 and Beta) and 2'5'OAS Genes: Insights into Differential Expression Profiles of Interferon System Components in Systemic Sclerosis. *Int J Rheumatol.* 2011;2011:275617.
46. **Coelho SVA, Neris RLS, Papa MP, Schnellrath LC, Meuren LM, Tschoeke DA, et al.** Development of standard methods for Zika virus propagation, titration, and purification. *J Virol Methods.* 2017;246:65-74.
47. **Thumwood CM, Hunt NH, Clark IA, Cowden WB.** Breakdown of the blood-brain barrier in murine cerebral malaria. *Parasitology*. 1988;96 (Pt 3):579-89.

606 **Figure Legends**

607

608 **Fig. 1. The chemical structure of compound 5b.**

609

610 **Fig. 2. Effect of compound 5b on the kinetic parameters of influenza A virus RNA**
611 **polymerase.** Indicated inputs of cell-free virus were incubated for 1 h at 37 ºC with a
612 reaction mix containing 16 U of RNAse, 10 mM of $MgCl_2$, and different concentrations
613 of compound **5b**. Next, 150 µM of nucleoside triphosphate (NTPs) was added. After 2 h
614 at 37 ºC, the reaction was stopped, and total RNA was extracted and quantified through
615 RT-PCR. Data are presented as the mean ± SEM of 5 independent experiments
616 performed with technical replicates. $^{*}p < 0.05$ (treatment vs no treatment).

617

618 **Fig. 3. Compound 5b`s effect on influenza virus RNA transcription and**
619 **replication.** MDCK were infected for 1 h at 4 ºC. Unbounded viral particles were
620 washed out, and the temperature was shifted to 37 ºC for 6 h. Next, the cells were
621 treated for 24 h. Finally, cells were lysed, and the influenza-related total and mRNA
622 were measured. Replication is determined by total influenza RNA content (UNI-12-
623 dependent cDNA synthesis) minus the influenza mRNA levels (oligo.dT-dependent
624 cDNA synthesis). Transcription is determined by measurement of influenza mRNA
625 levels. Data are presented as the mean ± SEM of 5 independent experiments performed
626 with technical replicates. * and $^{\#}p < 0.05$ (treatment *vs* no treatment).

627

628 **Fig. 4. Modulation of influenza-induced chemokine production by the treatment**
629 **with compound 5b.** A549 cells were infected with influenza virus (1 h, 37 ºC) and
630 treated with 15 µM of compound **5b**. After 24 h, culture supernatants were collected and
631 the levels of influenza-induced chemokines IL-8 (a) and MCP-1 (b) were quantified by
632 ELISA. $^{*}p<0.05$ (treatment *vs* untreated control).

633

634 **Fig. 5. Modulation of influenza-independent pro-inflammatory cytokine**
635 **production by compound 5b.** MDMs were pre-treated with 30, 60 or 120 µM of
636 compound **5b** or 60, 120 or 240 µM of ribavirin (used as a positive control) for 30
637 minutes and stimulated with 10 ng/ml of LPS. The levels of IL-6 ((a) and (b)) and TNF-

α ((c) and (d)) are displayed 24 h after LPS treatment. $^{\#}p < 0.05$ (LPS stimulus *vs* non-stimulated); $^{*}p < 0.05$ (treatment *vs* no treatment)

Fig. 6. Influenza-induced cell-mediated inflammation is modulated by treatment with compound 5b. C57BL/6 mice were inoculated with PBS (mock, n=5) or infected intranasally with 10^3 PFU of influenza PR8 virus (influenza, n=4). A group of infected animals were treated daily with an oral dose of compound **5b** at 10 mg/kg (n=5). Animals were monitored and weighed for up to 5 days (a). At day 5 post-infection, a group of animals were euthanized and lung and bronchoalveolar lavage was collected for different analysis. Influenza RNA levels were quantified in the lungs through quantitative RT-PCR (b). Total leucocytes (c), mononuclear (d) and polymorphonuclear (e) cell counts were performed in BAL. Total protein levels were also quantified in the BAL (f) and total leucocytes numbers were determined in the peripheral blood (g). $^{*}p < 0.05$ compared to the mock; $^{\#}p < 0.05$ compared to the influenza-infected group.

Fig. 7. Pro-inflammatory cytokines are decreased in the BAL of mice treated with compound 5b. C57BL/6 mice were inoculated with PBS (mock, n=5) or infected intranasally with 10^3 PFU of influenza PR8 virus (influenza, n=4). A group of infected animals were treated daily with an oral dose of 10 mg/kg of compound **5b** (n=5). At day 5, a group of animals were euthanized, the BAL was collected for cytokines and chemokines measurement in the BAL. TNF-α (a), IFN-γ (b), IL-6 (c), KC (d), MCP-1 (e) and IL-10 (f) levels were determined by ELISA. $^{*}p < 0.05$ compared to the mock; $^{\#}p < 0.05$ compared to influenza-infected group.

Fig. 8. Lung inflammation induced by influenza infection is reduced after treatment with compound 5b. C57BL/6 mice were inoculated with PBS (mock, panels (a) and (d)) or infected intranasally with 10^3 PFU of influenza PR8 virus (influenza, panels (b) and (e)) (n = 4–5 in each group). Influenza-infected animals were treated orally with 10 mg/kg/day of compound **5b** (compound **5b**, panels (c) and (f)). Mice were euthanized at day 5, and the lungs were removed and stained with haematoxylin-eosin. The sections were scanned, and the photomicrographs were obtained through

Panoramic Viewer software (x1 or x10 magnification). The scale bars indicate a size of 2000 µm (panels (a)-(c)) or 200 µm (panels (d)-(f)). $^{*}p < 0.05$ (influenza *vs* mock), $^{\#}p < 0.05$ (compound **5b** *vs* influenza).

Figures

1

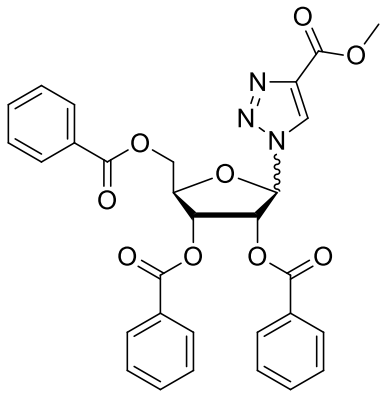

2

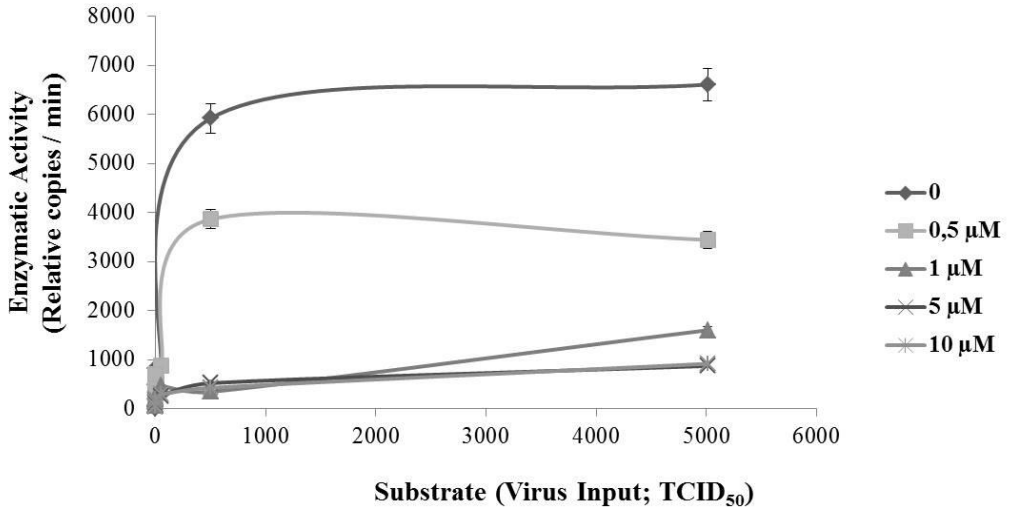

687 **3**

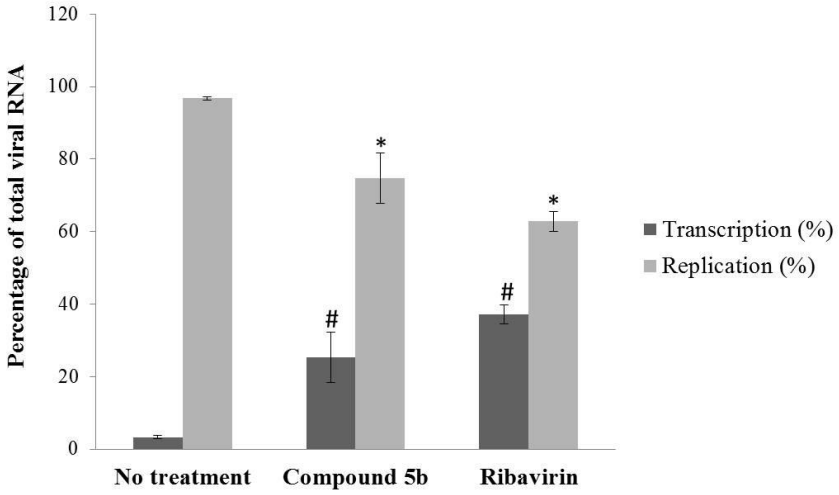

688

689

690 **4**

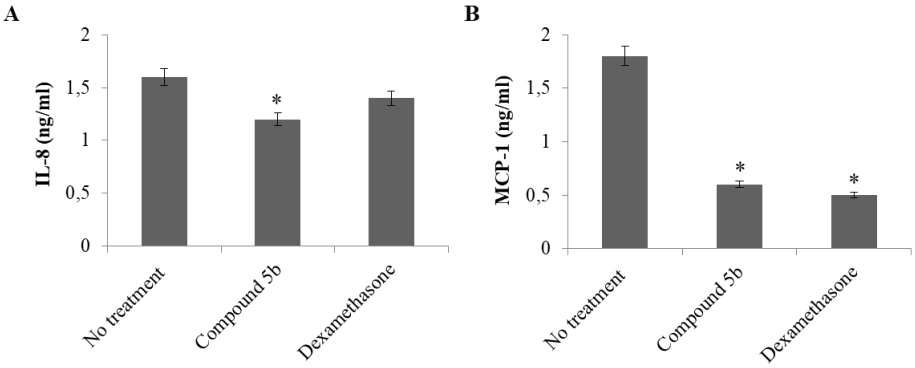

691

692

693

694

695

696

697

698

699

700

5

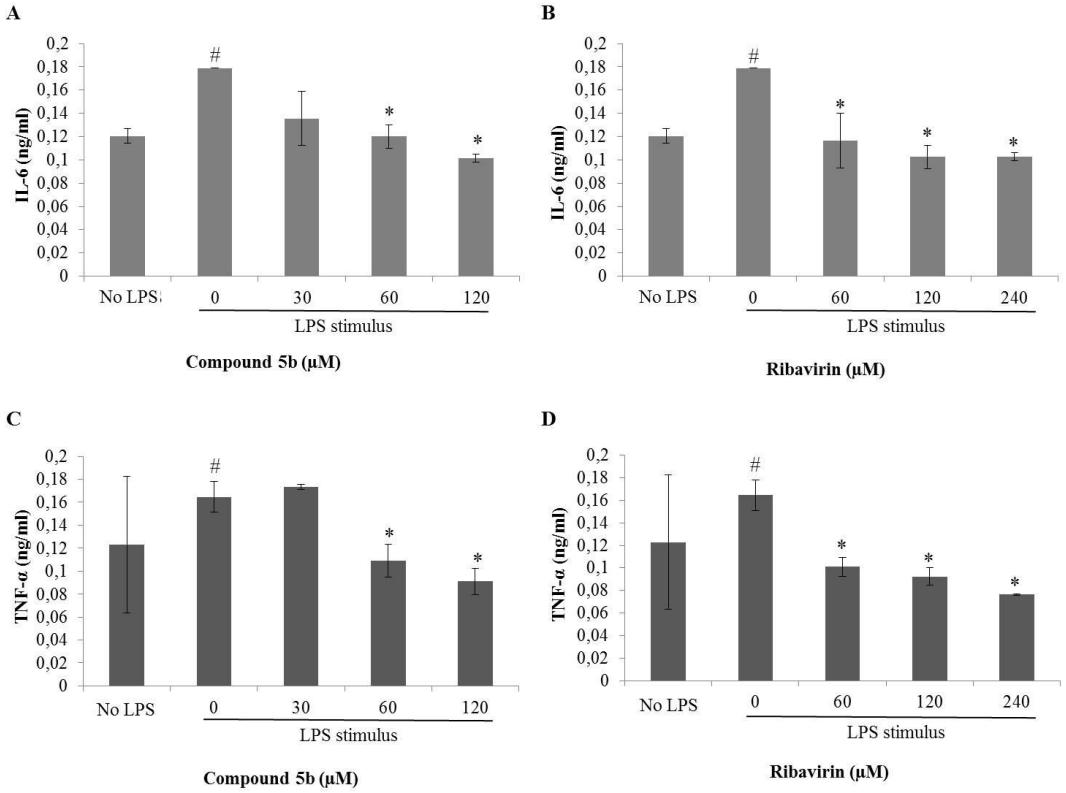
A
B
C
D
IL-6 (ng/ml)
TNF-α (ng/ml)
No LPS
LPS stimulus
Compound 5b (μM)
Ribavirin (μM)

6

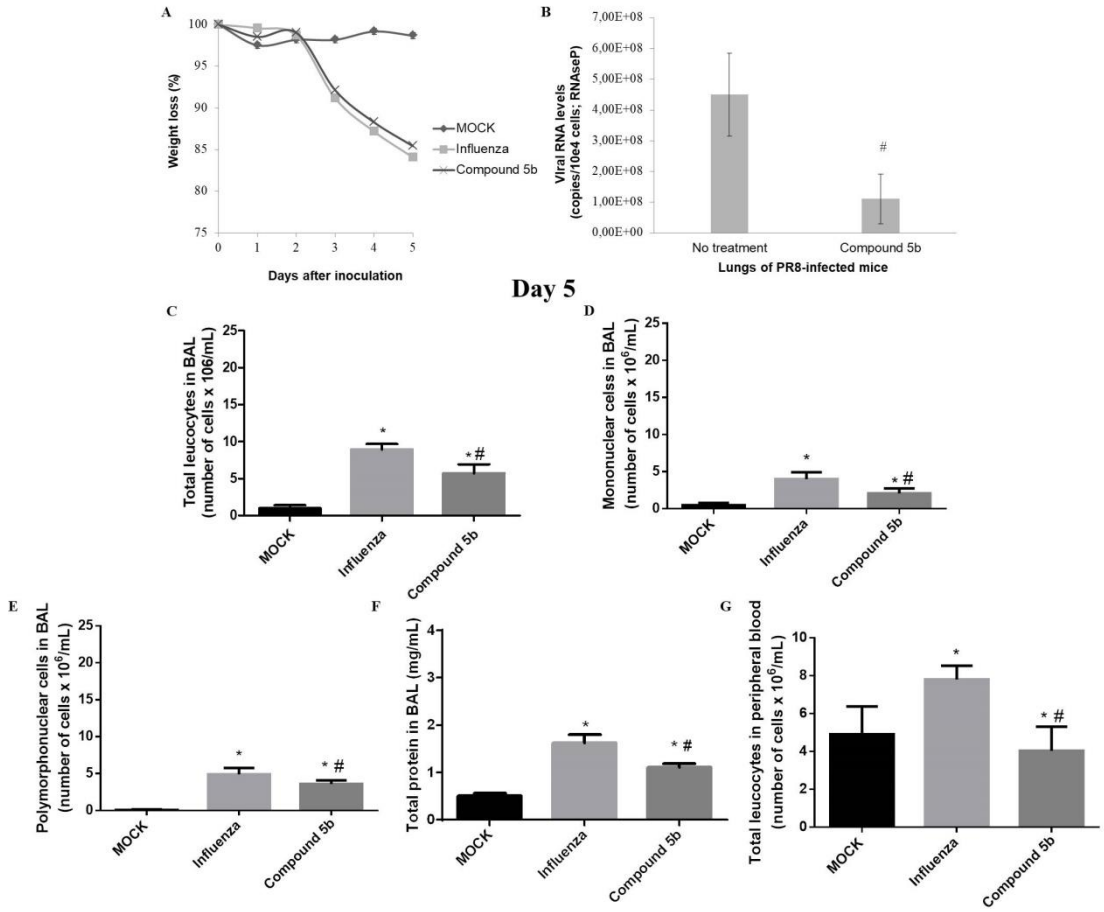
A
Weight loss (%)
Days after inoculation
MOCK
Influenza
Compound 5b
B
Viral RNA levels (copies/10e4 cells; RNAseP)
No treatment
Compound 5b
Lungs of PR8-infected mice
Day 5
C
Total leucocytes in BAL (number of cells x 106/mL)
D
Mononuclear celss in BAL (number of cells x 10^6/mL)
E
Polymorphonuclear cells in BAL (number of cells x 10^6/mL)
F
Total protein in BAL (mg/mL)
G
Total leucocytes in peripheral blood (number of cells x 10^6/mL)

7

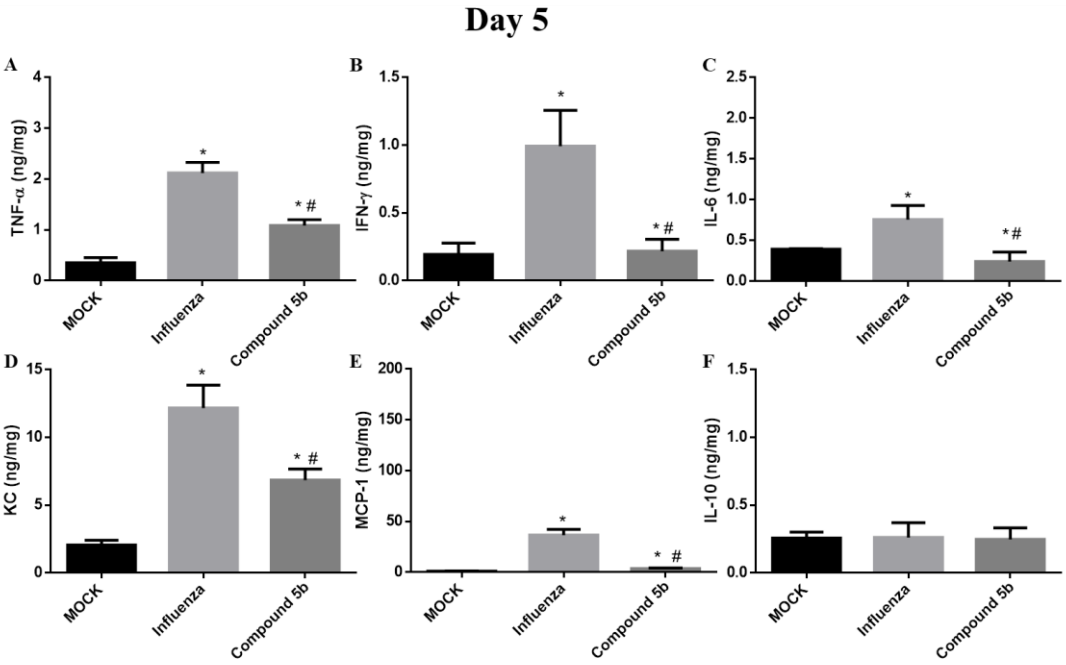
Day 5
A
TNF-α (ng/mg)
B
IFN-γ (ng/mg)
C
IL-6 (ng/mg)
D
KC (ng/mg)
E
MCP-1 (ng/mg)
F
IL-10 (ng/mg)
MOCK
Influenza
Compound 5b

8

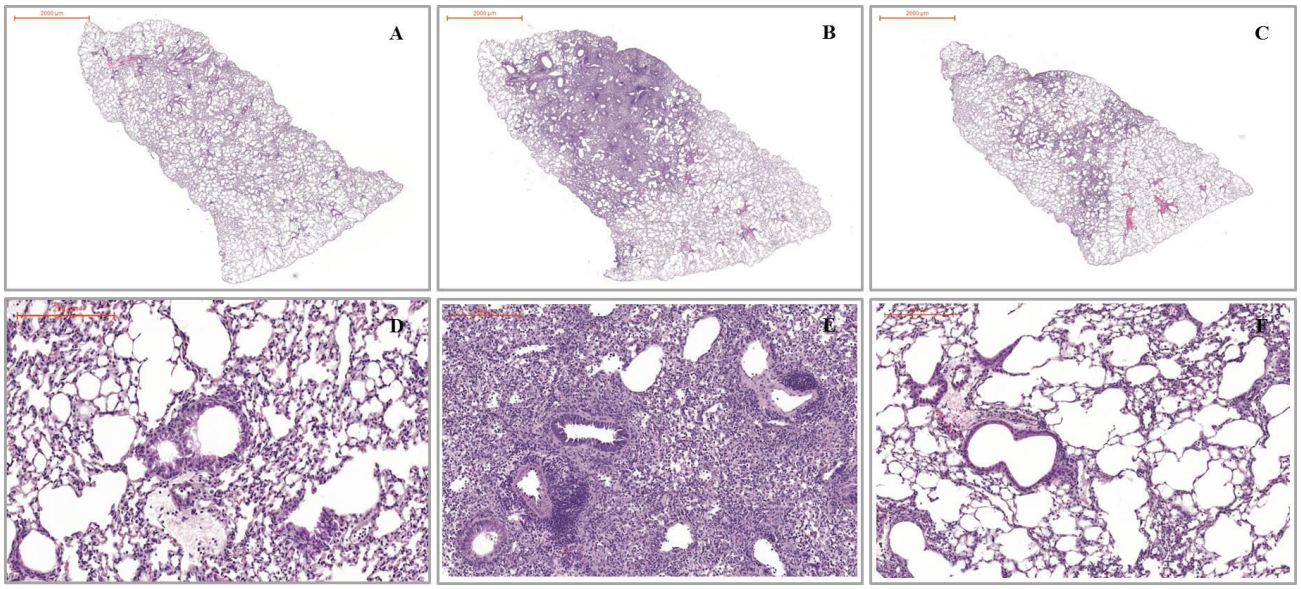

Tables

Table 1. Compound 5b`s cytotoxicity and antiviral potency against influenza A/H3N2 virus.

Compounds	CC_{50} (μM)	EC_{50} (μM)	SI (CC_{50}/IC_{50})
5b	> 1,000	0.07	> 14,000
Ribavirin	94.2	20.5	4.6

Table 2. Estimated kinetic parameters of influenza NERP with different concentrations of compound 5b.

	Compound 5b (μM)		
	0	**1**	**5**
$K_{M\ (substrate\ input\ TCID50)}$	0.084	0.024	0.017
$V_{max\ (copies/min)}$	6609	1602	875

Supplementary Material

The ribavirin analogue methyl 1-benzyl-1*H*-1,2,3-triazole-4-carboxylate inhibits influenza *in vitro* and *in vivo* replication

Carolina Q. Sacramento, Natalia Fintelman-Rodrigues, Andressa Marttorelli, Caroline S. de Freitas, Gabrielle R. de Melo, André C. Ferreira, Cristiana C. Garcia, Alexandre M. V. Machado, Andrea Surrage, Milene Mesquita, Maria de Lourdes G. Ferreira, Luiz C. S. Pinheiro, Nubia Boechat, Fernando A. Bozza and Thiago Moreno L. Souza

Results

Compound 5b showed no toxicity *in vivo*. Swiss mice treated with compound **5b** or ribavirin were monitored for up to 7 days after treatment. As shown in Fig. S1 (a), there was a 100% survival and no weight loss in comparison with the untreated animals or ribavirin-treated group. During the monitoring period, we did not observe signs of toxicity, such as lethargy, prostration, hunching, hyperactivity, and ruffled fur. At day 7, the general locomotor activity and motor coordination of the animals was evaluated on the open field and rotarod tests, respectively. The treatment caused no impairment on both the motor activity and coordination of the animals (Fig. S1 (b), (c)). We also performed haematological and biochemical dosages of the peripheral blood of the mice collected 7 days post-treatment. We did not observe alterations in the peripheral blood levels of mice treated with compound **5b** (Table S1). Altogether these data demonstrate that compound **5b** shows no toxicity and is safe for use in an experimental mouse model.

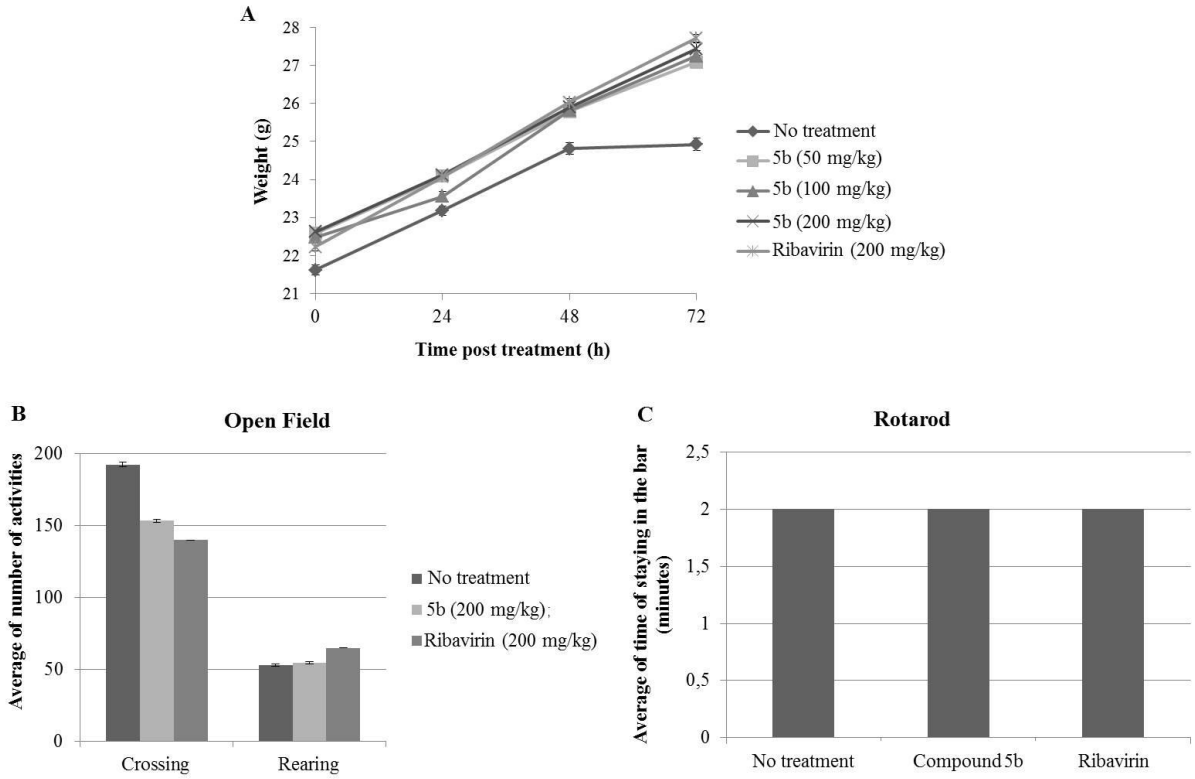

Fig. S1. Treatment with compound 5b showed no toxicity *in vivo*. Swiss-Webster mice were treated with a single oral high dose of compound **5b** in different concentrations (50, 100 and 200 mg/kg) and monitored for up to 7 days. Animals were weighed for 3 days (a) and at day 7, the general locomotor activity and motor coordination of the animals was evaluated on an open field (b) and with rotarod (c) tests. During the open field test, the animals were kept in the arena for 5 minutes, and we registered the number of crossings and rearings. The results are expressed as the mean number of activities. For the rotarod test, the animals were kept on the rotating bar for 2 minutes, and the length of stay was measured 3 times for each animal. The results are expressed as the mean of the length of stay.

Table S1. Haematological and biochemical parameters evaluated in the peripheral blood of Swiss mice treated with compound 5b.

Blood Parameters*		
	Mock	**Compound 5b 200 mg/kg**
	(Mean ± SD) (n=5)	**(Mean ± SD) (n=5)**
RBC (millions/mm^3)	8,86 ± 0,25	9,14 ± 0,21
HGB (g/dL)	14,82 ± 0,33	14,64 ± 0,35
HCT (%)	53,16 ± 1,89	52,98 ± 1,56
MCV (*f*m^3)	60,04 ± 2,03	57,92 ± 1,27
MCH (pg)	16,74 ± 0,57	16,02 ± 0,27
MCHC (g/dL)	27,86 ± 0,65	27,64 ± 0,23
WBC (thousand/mm^3)	7,16 ± 1,58	6,7 ± 1,75
EOS (%)	0	0
BAS (%)	0	0
NEU (ban) (%)	0	0
NEU (seg) (%)	0	0
LYM (%)	0	0
MON (%)	0	0
ATYP LYM (%)	0	0
PLT (thousand/mm^3)	1206,8 ± 201,83	1376,6 ± 447,73
Biochemical Parameters*		
	Mock (Mean ± SD) (n=5)	**Compound 5b 200 mg/kg (Mean ± SD) (n=5)**
Total bilirubin (mg/dL)	0,42 ± 0,07	0,4 ± 0,07
Uric acid (mg/dL)	1,56 ± 0,11	2,07 ± 0,19
Calcium (mg/dL)	10,24 ± 0,15	9,82 ± 0,16
ALT (U/L)	60,4 ± 0,62	53,5 ± 0,84
Urea (mg/dL)	54,76 ± 0,55	43,92 ± 0,67
Chloride (mmol/L)	82,2 ± 1,36	103,5 ± 0,4
Alkaline phosphatase (U/L)	214 ± 2,25	274,75 ± 2,16
AST (U/L)	99,4 ± 1,36	82,0 ± 1,11
Glucose (mg/dL)	140 ± 1,07	146,25 ± 1,03

*All values are in accordance with reference values for Swiss mice blood and biochemical parameters.

RBC: Red blood cells; HGB: Haemoglobin; HCT: Haematocrit; MCV: Mean volume of erythrocytes; MCH: Mean content of haemoglobin in single erythrocytes; MCHC: Mean concentration of haemoglobin in erythrocytes; WBC: White blood cells; EOS: Eosinophils; BAS: Basophils; NEU (ban / seg): Bands and segmented neutrophils;

LYM: Lymphocytes; MON: Monocytes; ATYP LYM: Atypical lymphocytes; PLT: Platelets; ALT: Alanine aminotransferase; AST: Aspartate aminotransferase.

Materials and Methods

***In vivo* toxicity determination.** Male Swiss-Webster mice were treated with a single oral dose of compound **5b** in different concentrations to evaluate their toxicity. Five mice were used per treatment group: untreated controls; mice treated with 50, 100 or 200 mg/kg of compound **5b**; or mice treated with 200 mg/kg of ribavirin. Animals were weighed immediately prior to treatment and again 3 days post-drug-exposure. Mice were observed for signs of toxicity (lethargy, prostration, hunching, hyperactivity, and ruffled fur) and death over the course of 7 days. At day 7, the general locomotor activity and motor coordination of the animals was evaluated on the open field (1) and in the rotarod (2) tests. After the tests animals were anaesthetized and euthanized, the stomach and intestines were collected and visually analysed for signs of toxicity. We also collected peripheral blood and performed haematological and biochemical dosages.

References

1. Bailey KR, Crawley JN. Methods of Behavior Analysis in Neuroscience. 2nd Edition ed. Buccafusco JJ, editor: Boca Raton (FL): CRC Press/Taylor & Francis; 2009.
2. Deacon RM. Measuring motor coordination in mice. J Vis Exp. 2013(75):e2609.

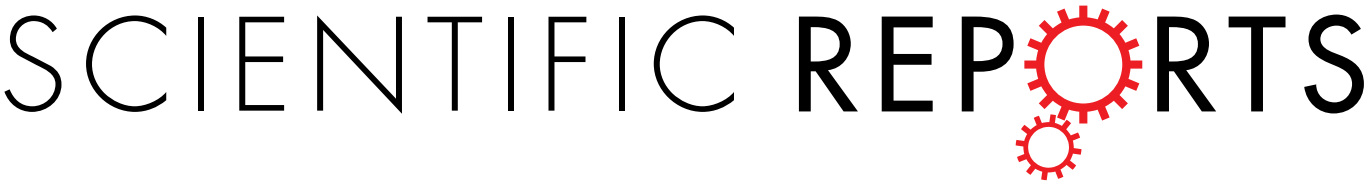

OPEN

The clinically approved antiviral drug sofosbuvir inhibits Zika virus replication

Received: 18 October 2016
Accepted: 13 December 2016
Published: 18 January 2017

Carolina Q. Sacramento[1,2,3,*], Gabrielle R. de Melo[1,2,3,*], Caroline S. de Freitas[1,2,3,*], Natasha Rocha[1,2,3,*], Lucas Villas Bôas Hoelz[4], Milene Miranda[5,6], Natalia Fintelman-Rodrigues[1,2,3], Andressa Marttorelli[1,2,3], André C. Ferreira[1,2,3], Giselle Barbosa-Lima[1,2,3], Juliana L. Abrantes[1,2,7], Yasmine Rangel Vieira[1,2,3], Mônica M. Bastos[4], Eduardo de Mello Volotão[8], Estevão Portela Nunes[2], Diogo A. Tschoeke[6,9,10], Luciana Leomil[6,9], Erick Correia Loiola[11], Pablo Trindade[11], Stevens K. Rehen[7,11], Fernando A. Bozza[1,2], Patrícia T. Bozza[1], Nubia Boechat[4], Fabiano L. Thompson[6,9], Ana M. B. de Filippis[12], Karin Brüning[13] & Thiago Moreno L. Souza[1,2,3]

Zika virus (ZIKV) is a member of the *Flaviviridae* family, along with other agents of clinical significance such as dengue (DENV) and hepatitis C (HCV) viruses. Since ZIKV causes neurological disorders during fetal development and in adulthood, antiviral drugs are necessary. Sofosbuvir is clinically approved for use against HCV and targets the protein that is most conserved among the members of the *Flaviviridae* family, the viral RNA polymerase. Indeed, we found that sofosbuvir inhibits ZIKV RNA polymerase, targeting conserved amino acid residues. Sofosbuvir inhibited ZIKV replication in different cellular systems, such as hepatoma (Huh-7) cells, neuroblastoma (SH-Sy5y) cells, neural stem cells (NSC) and brain organoids. In addition to the direct inhibition of the viral RNA polymerase, we observed that sofosbuvir also induced an increase in A-to-G mutations in the viral genome. Together, our data highlight a potential secondary use of sofosbuvir, an anti-HCV drug, against ZIKV.

Zika virus (ZIKV) is a member of the *Flaviviridae* family, which includes several agents of clinical significance, such as dengue (DENV), hepatitis C (HCV), West Nile (WNV) and Japanese encephalitis (JEV) viruses. This emerging pathogen is an enveloped positive-sense single-stranded RNA virus. Although ZIKV is an arthropod-borne virus (arbovirus) transmitted by mosquitos of the genus *Aedes*[1], transmission through sexual contact has been described[2]. The perception that ZIKV causes a mild and self-limited infection[3,4] has been jeopardized in recent years, with outbreaks in the Pacific Islands and the Americas[1,5]. For instance, ZIKV spread explosively across the Brazilian territory and to neighboring countries in 2015, infecting more than 4 million people[6]. As the ZIKV epidemic has scaled up, the virus has been associated with congenital malformations, including microcephaly, and a broad range of neurological disorders in adults, including Guillain-Barré syndrome (GBS)[7,8]. These morbidities associated with ZIKV infection led the World Health Organization (WHO) to declare the Zika outbreak to be a public health emergency of international concern.

[1]Laboratório de Imunofarmacologia, Instituto Oswaldo Cruz (IOC), Fundação Oswaldo Cruz (Fiocruz), Rio de Janeiro, RJ, Brazil. [2]Instituto Nacional de Infectologia (INI), Fiocruz, Rio de Janeiro, RJ, Brazil. [3]National Institute for Science and Technology on Innovation on Neglected Diseases (INCT/IDN), Center for Technological Development in Health (CDTS), Fiocruz, Rio de Janeiro, RJ, Brazil. [4]Instituto de Tecnologia de Fármacos (Farmanguinhos), Fiocruz, Rio de Janeiro, RJ, Brazil. [5]Laboratório de Vírus Respiratório e do Sarampo, IOC, Fiocruz, Rio de Janeiro, RJ, Brazil. [6]Instituto de Biologia, Universidade Federal do Rio de Janeiro (UFRJ), Rio de Janeiro, RJ, Brazil. [7]Instituto de Ciências Biomédicas, Universidade Federal do Rio de Janeiro, Rio de Janeiro, RJ, Brazil. [8]Laboratório de Virologia Comparada e Ambiental, IOC, Fiocruz, Rio de Janeiro, RJ, Brazil. [9]SAGE –COPPE, UFRJ, Rio de Janeiro, RJ, Brazil. [10]Núcleo em Ecologia e Desenvolvimento Sócio-Ambiental de Macaé (NUPEM), Universidade Federal do Rio de Janeiro, Macaé, Rio de Janeiro, Brazil. [11]D'Or Institute for Research and Education (IDOR), Rio de Janeiro, RJ, Brazil. [12]Laboratório de Flavivírus, IOC, Fiocruz, Rio de Janeiro, RJ, Brazil. [13]BMK Consortium: Blanver Farmoquímica Ltda; Microbiológica Química e FarmacêuticaLtda; Karin Bruning & Cia, Ltda, Brazil. *These authors contributed equally to this work. Correspondence and requests for materials should be addressed to T.M.L.S. (email: tmoreno@cdts.fiocruz.br)

Antiviral treatments against ZIKV are therefore necessary not only to mitigate ZIKV-associated morbidities but also to impair the chain of transmission. Some broad-spectrum antivirals, such as interferons (IFNs), ribavirin and favipiravir, are not suitable for use against ZIKV because they can be harmful to pregnant women[9]. Alternatively, others have studied the use of Food and Drug Administration (FDA)-approved small molecule drugs against ZIKV[10–15]. Overall, these drugs might exert their anti-ZIKV activity at least in part by interfering with the cellular pathways important for ZIKV replication[10–15].

The gene encoding the viral RNA polymerase shows the highest degree of conservation among the members of the *Flaviviridae* family[16], and the clinically approved anti-HCV drug sofosbuvir targets this protein. Sofosbuvir is an uridine nucleotide prodrug, which is triphosphorylated within cells to target the viral RNA polymerase[17]. Sofosbuvir is a class B FDA-approved drug. Moreover, Australia's regulatory agency on drug administration, the Therapeutic and Goods Administration (TGA), categorizes sofosbuvir as class B1: "Drugs which have been taken by only a limited number of pregnant women and women of childbearing age, without an increase in the frequency of malformation or other direct or indirect harmful effects on the human fetus having been observed." Altogether, this information motivated us to investigate whether the chemical structure of sofosbuvir possesses anti-ZIKV activity. In the interest of disseminating public health information, we disclosed a preprint of our data showing the anti-ZIKV activity of sofosbuvir[18]. In the present investigation, we further studied the pharmacology of sofosbuvir in neuronal and non-neuronal cell types. We observed a direct inhibition of the viral RNA polymerase and an increase in A-to-G mutations in the viral genome due to sofosbuvir treatment, highlighting a potential secondary use of sofosbuvir.

Materials and Methods

Reagents. The antiviral sofosbuvir (β-d-2′-deoxy-2′-α-fluoro-2′-β-C-methyluridine) was donated by the BMK Consortium: Blanver Farmoquímica Ltda; Microbiológica Química e Farmacêutica Ltda; Karin Bruning & Cia. Ltda, (Taboão da Serra, São Paulo, Brazil). Ribavirin was received as a donation from the Instituto de Tecnologia de Farmacos (Farmanguinhos, Fiocruz). Sofosbuvir triphosphate (STP) (β-d-2′-deoxy-2′-α-fluoro-2′-β-C-methyluridine triphosphate), ribavirin triphosphate (RTP) and AZT triphosphate (AZT-TP) were purchased (Codontech.org, CA and Sierra Bioresearch, AZ). Interferon-alpha was purchased from R&D Bioscience. All small molecule inhibitors were dissolved in 100% dimethylsulfoxide (DMSO) and subsequently diluted at least 10^4-fold in culture or reaction medium before each assay. The final DMSO concentrations showed no cytotoxicity. The materials for cell culture were purchased from Thermo Scientific Life Sciences (Grand Island, NY), unless otherwise mentioned.

Cells. Human neuroblastoma (SH-Sy5y; ATCC) and baby hamster kidney (BHK-21) cells were cultured in MEM:F-12 (1:1) and MEM, respectively. African green monkey kidney (Vero) and human hepatoma (Huh-7) cells were cultured in DMEM. *Aedes albopictus* cells (C6/36) were grown in L-15 medium supplemented with 0.3% tryptose phosphate broth, 0.75 g/L sodium bicarbonate, 1.4 mM glutamine, and nonessential amino acids. The culture medium of each cell type was supplemented with 10% fetal bovine serum (FBS; HyClone, Logan, Utah), 100 U/mL penicillin, and 100 μg/mL streptomycin[19,20]. The mammalian cells were incubated at 37 °C in 5% CO_2, whereas the mosquito cells were maintained at 26 °C. Passages of the SH-sy5y cells included both adherent and non-adherent cells.

Virus. ZIKV was isolated from a serum sample of a confirmed case from Rio de Janeiro, Brazil. This sample was received and diagnosed by the Reference Laboratory for Flavivirus, Fiocruz, Brazilian Ministry of Health, as part of the surveillance system against arboviruses[3]. Brazilian ZIKV was originally isolated in C6/36 cells, titered by plaque-forming assays and further passaged at a multiplicity of infection (MOI) of 0.01. The virus was passaged by inoculating C6/36 cells for 1 h at 26 °C. Next, the residual virus particles were removed by washing with phosphate-buffered saline (PBS), and the cells were cultured for an additional 9 days. After each period, the cells were lysed by freezing and thawing and centrifuged at 1,500 × *g* at 4 °C for 20 min to remove cellular debris.

ZIKV was purified between fractions of 50% and 20% sucrose. The sucrose gradients were made in 40 mL ultracentrifuge tubes (Ultra-clear; Beckman, Fullerton, CA) in PBS without Ca^{++} and Mg^{++} (pH 7.4). The tubes were allowed to stand for 2 h at room temperature. Up to 20 mL of virus was added to each tube and centrifuged in an SW 28 rotor (Beckman) at 10,000 rpm for 4 h at 4 °C. The fractions were collected and assayed for total protein and for virus-induced hemagglutination (HA) analysis using turkey red blood cells (Fitzgerald Industries International, North Acton, MA). The fractions displaying HA activity (≥16 UHA/50 μL) were pooled and dialyzed against PBS without Ca^{++} and Mg^{++} (pH 7.4) and 10% sucrose overnight at 4 °C. The virus pools were filtered through 0.22-μm membranes (Chemicon, Millipore, Bedford, NY). The infectious virus titers were determined by plaque assays in BHK-21 cells, and the virus was stored at −70 °C for further studies.

Cytotoxicity assay. Monolayers of 10^4 BHK-21, 5×10^4 SH-Sy5y, 1.5×10^4 Vero or 1.5×10^4 Huh-7 cells in 96-well plates were treated for 5 days with various concentrations of sofosbuvir or ribavirin as a control. Then, 5 mg/ml 2,3-bis-(2-methoxy-4-nitro-5-sulfophenyl)-2*H*-tetrazolium-5-carboxanilide (XTT) in DMEM was added to the cells in the presence of 0.01% of N-methyl dibenzopyrazine methyl sulfate (PMS). After incubating for 4 h at 37 °C, the plates were read in a spectrophotometer at 492 nm and 620 nm[21]. The 50% cytotoxic concentration (CC_{50}) was calculated by a non-linear regression analysis of the dose–response curves.

Plaque-forming assay. Monolayers of BHK-21 cells in 6-well plates were exposed to different dilutions of the supernatant from the yield-reduction assays for 1 h at 37 °C. Whenever virus yields were extremely low, viral particles from the supernatants were concentrated through 80-kDa centrifugal exclusion filters (Merk Millipore, Darmstadt, Germany) prior to plaque-forming assay. Next, the cells were washed with PBS, and culture medium containing 1% FBS and 3% carboxymethylcellulose (Fluka) (overlay medium) was added to cells. After 5 days at

37 °C, the monolayers were fixed with 10% formaldehyde in PBS and stained with a 0.1% solution of crystal violet in 70% methanol, and the virus titers were calculated by scoring the plaque-forming units (PFU).

Yield-reduction assay. Monolayers of 10^4 BHK-21, 5×10^4 SH-Sy5y, 1.5×10^4 Vero or 1.5×10^4 Huh-7 cells in 96-well plates were infected with ZIKV at the indicated MOIs for 1 h at 37 °C. The cells were washed with PBS to remove residual viruses, and various concentrations of sofosbuvir, or interferon-alpha as a positive control, in culture medium with 1% FBS were added. After 24 h, the cells were lysed, the cellular debris was cleared by centrifugation, and the virus titers in the supernatant were determined as PFU/mL. A non-linear regression analysis of the dose-response curves was performed to calculate the concentration at which each drug inhibited the plaque-forming activity of ZIKV by 50% (EC_{50}).

Preparation of ZIKV RNA polymerase. ZIKV RNA polymerase (ZVRP) was obtained from ZIKV-infected BHK-21 cells. The cells were infected with ZIKV at an MOI of 10 for 24 h, lysed with buffer A [containing 0.25 M potassium phosphate (pH 7.5), 10 mM 2-mercaptoethanol (2-ME), 1 mM EDTA, 0.5% Triton X-100, 0.5 mM phenylmethane sulfonyl fluoride (PMSF) and 20% glycerol], sonicated and centrifuged at $10{,}000 \times g$ for 10 min at 4 °C. The resulting supernatant was further centrifuged at $100{,}000 \times g$ for 90 min at 4 °C and passed through two ion-exchange columns, DEAE- and phospho-cellulose[19]. Alternatively, the ZIKV NS5 region encoding the nucleotides responsible for the RNA-dependent RNA polymerase (RDRP) activity were cloned into the pET-41b+ vector (Novagen) between the BamHI and SacI sites. ZVRP expression was induced by adding isopropyl β-D-1-thiogalactopyranoside (IPTG) to the *E. coli* strain BL21. The cells were lysed in buffer A, and the N-terminal GST-tag was used to purify the protein using a GST spin purification kit (ThermoFisher Scientific) according to the manufacturer's instructions.

RNA polymerase inhibition assay. ZVRP inhibition assays were adapted from a previous publication[22]. The reaction mixture for ZVRP activity measurements was composed of 50 mM HEPES (pH 7.3), 0.4 mM of each ribonucleotide (ATP, GTP, CTP and labelled UTP), 0.4 mM dithiothreitol, 3 mM $MgCl_2$, and 500 ng of ZIKV genomic RNA or cell extracts. The ZIKV RNA was obtained using a QIAmp viral RNA mini kit (Qiagen, Dusseldorf, Germany) according to the manufacturer's instructions, except for the use of the RNA carrier. The reaction mixtures were incubated for 1 h at 30 °C in the presence or absence of the drugs. The reactions were stopped with addition of EDTA at a final concentration of 10 mM.

The labeled UTP mentioned above represents an equimolar ratio between biotinylated-UTP and digoxigenin-UTP (DIG-UTP) (both from Roche Life Sciences, Basel, Switzerland). The detection of incorporated labeled UTP nucleotides was performed by an amplified luminescent proximity homogeneous assay (ALPHA; PerkinElmer, Waltham, MA). In brief, streptavidin-donor and anti-DIG-acceptor beads were incubated with the stopped reaction mixture for 2 h at room temperature. Then, the plates containing the mixtures were read in an EnSpire® multimode plate reader (PerkinElmer). Different types of blank controls were used, such as reaction mixtures without cellular extracts and a control reaction mixture without inhibitor and beads. In addition, the extract from mock-infected cells was also assayed to evaluate the presence of RNA-dependent RNA polymerase activity unrelated to ZIKV. Non-linear regression curves were generated to calculate the IC_{50} values for the dose-response effects of the compounds.

Antiviral activity in human induced pluripotent stem (iPS) cell-derived neural stem cells (NSCs) and brain organoids. NSCs and brain organoids derived from human iPS cells were prepared as previously described[23]. The NSCs (20×10^3 cells/well in a 96-well plate) were infected at MOIs of either 1.0 or 10 for 2 h at 37 °C. Next, the cells were washed, and fresh medium containing sofosbuvir was added. The cells were treated daily with sofosbuvir at the indicated concentrations. The NSCs were observed daily for 8 days after infection. Virus titers were determined from the culture supernatant using a plaque-forming assay. The cell supernatant was also used for ZIKV genome analysis. Cell death was measured by adding 2 μM CellEvent caspase-3/7 reagent and the fluorescent dye ethidium homodimer[23] at days 4 and 8, when the culture supernatants were collected. Images were acquired with an Operetta high-content imaging system with a 20x objective and high numerical apertures (NA) (PerkinElmer, USA). The data were analyzed using the high-content image analysis software Harmony 5.1 (PerkinElmer, USA). Seven independent fields were evaluated from triplicate wells per experimental condition.

Brain organoids were infected with ZIKV at 3×10^5 PFU/mL for 2 h, and the medium containing virus particles was then replaced with fresh medium. Sofosbuvir was added to the fresh medium daily for one week. The culture supernatant was collected to monitor virus infectivity and for RNA sequencing.

Comparative molecular modeling. The amino acid sequence encoding ZVRP (UniProtKB ID: B3U3M3) was obtained from the EXPASY proteomic portal[24] (http://ca.expasy.org/). The template search was performed using the Blast server (http://blast.ncbi.nlm.nih.gov/Blast.cgi) with the Protein Data Bank[25] (PDB; http://www.pdb.org/pdb/home/home.do) as the database and the default options. The T-COFFEE algorithm was used to generate a multiple alignment between the amino acid sequences of the template proteins and ZVRP. Subsequently, the construction of the SFV-ZVRP complex was performed using MODELLER 9.16 software[26], which employs spatial restriction techniques based on the 3D-template structure. The preliminary model was refined in the same software, using three cycles of the default optimization protocol. The structural evaluation of the model was then performed using two independent algorithms in the SAVES server (http://nihserver.mbi.ucla.edu/SAVES_3/): PROCHECK software[27] (stereochemical quality analysis) and VERIFY 3D[28] (compatibility analysis between the 3D model and its own amino acid sequence by assigning a structural class based on its location and environment and by comparing the results with those of crystal structures).

Genome assembly. A 0.3-mL aliquot of supernatant containing ZIKV (at least 2×10^5 PFU) was filtered through 0.22-μm filters to remove residual cells. The viral RNA was extracted using a QIAamp Viral RNA Mini Kit (Qiagen®) with RNase-free DNase (Qiagen®) treatment, omitting carrier RNA. Double-stranded cDNA libraries were constructed using a TruSeq Stranded Total RNA LT kit (Illumina®) with Ribo-zero treatment according to the manufacturer's instructions. The library size distribution was assessed using a 2100 Bioanalyzer (Agilent®) with a High Sensitivity DNA kit (Agilent®), and the quantification was performed using a 7500 Real-time PCR System (Applied Biosystems®) with a KAPA Library Quantification Kit (Kapa Biosystems). Paired-end sequencing (2×300 bp) was performed with a MiSeq Reagent kit v3 (Illumina®). The sequences obtained were preprocessed using the PRINSEQ software to remove reads smaller than 50 bp and sequences with scores of lower quality than a Phred quality score of 20. Paired-End reAd merger (PEAR) software was used to merge and extend the paired-end Illumina reads using the default parameters[29,30]. The extended reads were analyzed against the Human Genome Database using the DeconSeq program, with an identity and coverage cutoff of 70%, to remove human RNA sequences[31]. Non-human reads were analyzed against all GenBank viral genomes (65 052 sequences) using the BLAST software with a 1e-5 e-value cutoff. The sequences rendering a genome were assembled with SPAdes 3.7.1 software[32] followed by a reassembly with the CAP3 program[33].

Sequence comparisons. The sequences encoding the C-terminal portion of the RNA polymerase from members of the *Flaviviridae* family were acquired from the complete sequences deposited in GenBank. An alignment was performed using the ClustalW algorithm in the Mega 6.0 software. The sequences were analyzed using the neighbor-joining method with pairwise deletion and a bootstrap of 1,000 replicates, and the *P* distances were registered. The sequences were also analyzed for the mean evolutionary rate.

Statistical analysis. All assays were performed and codified by one professional. Subsequently, a different professional analyzed the results before the identification of the experimental groups. This approach was used to keep the pharmacological assays blind. All experiments were carried out at least three independent times, including technical replicates in each assay. The dose-response curves used to calculate the EC_{50} and CC_{50} values were generated by Excel for Windows. The dose-response curves used to calculate the IC_{50} values were produced by Prism GraphPad software 5.0. The equations to fit the best curve were generated based on R^2 values ≥ 0.9. ANOVA tests were also used, with P values < 0.05 considered statistically significant. The statistical analyses specific to each software program used in the bioinformatics analysis are described above.

Results

Sofosbuvir fits into the ZVRP predicted structure. The RNA polymerase structures from WNV (PDB #2HFZ)[34], JEV (PDB #4K6M)[35], DENV (PDB #5DTO)[36] and HCV (PDB #4WTG)[37] share 72, 70, 68, and 25% sequence identity, respectively, with the orthologous ZIKV enzyme. Despite its relatively low sequence identity to ZIKV, the HCV enzyme structure is complexed with sofosbuvir, and the amino acids residues that interact with the drug are highly conserved (approximately 80%) among the members of the *Flaviviridae* family[37]. The region encoding the C-terminal portion of the *Flaviviridae* RNA polymerase contains around 800 amino acid residues. Of these, we have highlighted in yellow those that are identical among members of the *Flaviviridae* family (see Supplementary Material 1). The residues critical for RDRP activity are conserved among different viral species and strains, including an African ZIKV strain from the 1950 s and those circulating currently, DENV and different genotypes of HCV (see Supplementary Material 1)[38].

Based on the HCV RNA-dependent RNA polymerase domains, we constructed a 3D model of the orthologous ZIKV enzyme (Fig. 1). Sofosbuvir was predicted to be located among the palm and fingers region of ZIKV RNA polymerase (Fig. 1A), an area important for coordinating the incorporation of incoming nucleotides into the new strand of RNA[37]. Consequently, the amino acid residues relevant to the sofosbuvir interaction are some of those critical for natural nucleotide incorporation and thus RDRP activity (Fig. 1B)[37].

Sofosbuvir inhibits ZVRP in a dose-dependent fashion. Next, we evaluated whether sofosbuvir triphosphate (STP), the bioactive compound, could inhibit ZIKV RDRP activity. Fractions containing the ZIKV RDRP activity were partially purified from infected cells[19]. STP inhibited ZIKV RDRP activity with an IC_{50} value of $0.38 \pm 0.03\,\mu M$ (Fig. 2A). Ribavirin-triphosphate (RTP) and AZT-TP were used as positive and negative controls, respectively (Fig. 2A). RTP and AZT-TP exhibited IC_{50} values of 0.21 ± 0.06 and $>10\,\mu M$, respectively (Fig. 2A). Moreover, the recombinant expression of the C-terminal portion of ZVRP confirmed the STP antiviral activity, with an IC_{50} value of $0.61 \pm 0.08\,\mu M$ (Fig. 2B). The AZT-TP and RTP IC_{50} values for recombinant ZVRP were >10 and $0.62 \pm 0.05\,\mu M$, respectively (Fig. 2B). Of note, the small discrepancy observed in the STP IC_{50} values against the partially purified and recombinant ZVRP could be because the total protein content was used to normalize the assay conditions; therefore, the purified recombinant preparation possessed a higher specific activity. Altogether, the data from Fig. 2 confirmed the molecular modeling prediction that sofosbuvir docks onto the ZVRP structure, revealing that the chemical structure of sofosbuvir inhibits ZIKV RDRP activity.

Sofosbuvir inhibits ZIKV replication in a cell lineage-, MOI- and dose-dependent manner. Before investigating ZIKV susceptibility to sofosbuvir using cell-based assays, a Brazilian ZIKV isolate was characterized for further use as a reference strain for the experimental virology. The full-length viral genome was sequenced (GenBank accession #KX197205), and the characteristic plaque-forming units (PFU) and cytopathic effects (CPE) were determined in BHK-21 cells (see Supplementary Fig. S1). Another concern was to establish whether another plaque-forming viral agent was co-isolated with ZIKV, which could result in a misleading interpretation of the antiviral activity. A metagenomic analysis revealed that ZIKV was the only full-length genome of a plaque-forming virus detected in BHK-21 cells (see Supplementary Material 2).

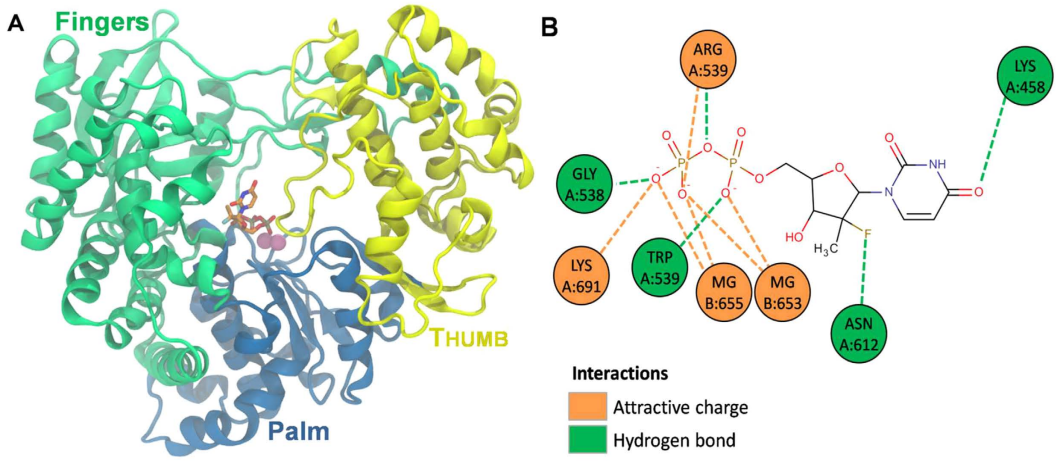

Figure 1. Putative ZIKV RNA polymerase in complex with sofosbuvir. Based on the crystal structure of the HCV RNA polymerase in complex with sofosbuvir diphosphate (PDB accession #4WTG), the putative structure of the ZVRP was constructed. Using the T-COFFEE server, the amino acid sequence of the ZVRP (UniProtKB ID: B3U3M3) was aligned with orthologous RNA polymerases from other members of the *Flaviviridae* family, specifically hepatitis C virus (HCV; PDB #4WTG, West Nile virus (WNIV; PDB #2HFZ), Japanese encephalitis virus (JEV; PDB #4K6M), and dengue virus (DENV; PDB #5DTO). The MODELLER 9.16 software was used to build a 3D model of ZIKV RNA polymerase, with subsequent refinement performed using three cycles of the default optimization protocol. The structural evaluation of the model was performed using two independent algorithms, PROCHECK software and VERIFY 3D. (**A**) The 3D model of ZIKV RNA polymerase is presented. (**B**) The residues presumably required for the interaction of ZVRP with sofosbuvir and Mg^{++} ions.

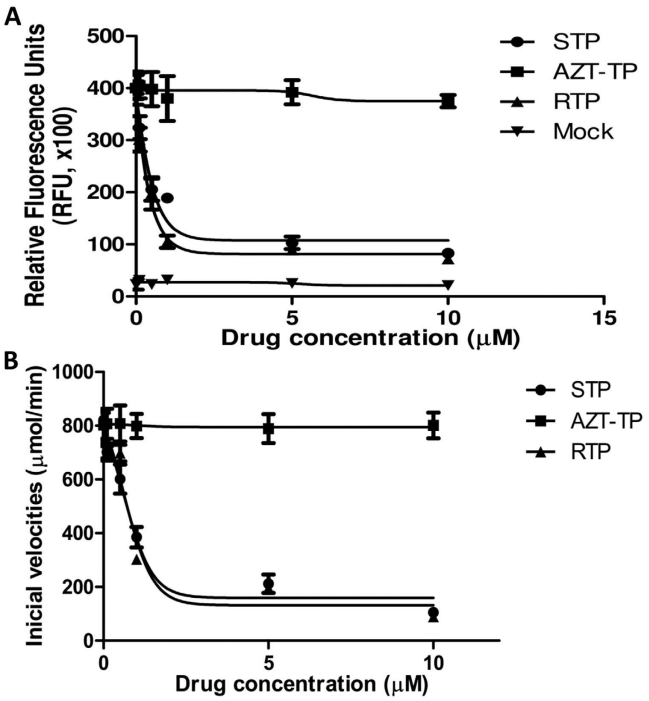

Figure 2. Sofosbuvir inhibits ZIKV RDRP activity. Cell extracts from ZIKV-infected cells (**A**) or recombinant ZVRP (**B**) were assayed for RDRP activity using viral RNA as the template and labeled UTP as the tracer. Biotinylated-UTP and digoxigenin-UTP were detected by ALPHA technology using an EnSpire® multimode plate reader (PerkinElmer). The molecules assayed were sofosbuvir triphosphate (STP), ribavirin triphosphate (RTP) and AZT triphosphate (AZT-TP). As a control, the RDRP activity was measured in extracts from mock-infected cells (mock). The data represent means ± SEM of five independent experiments.

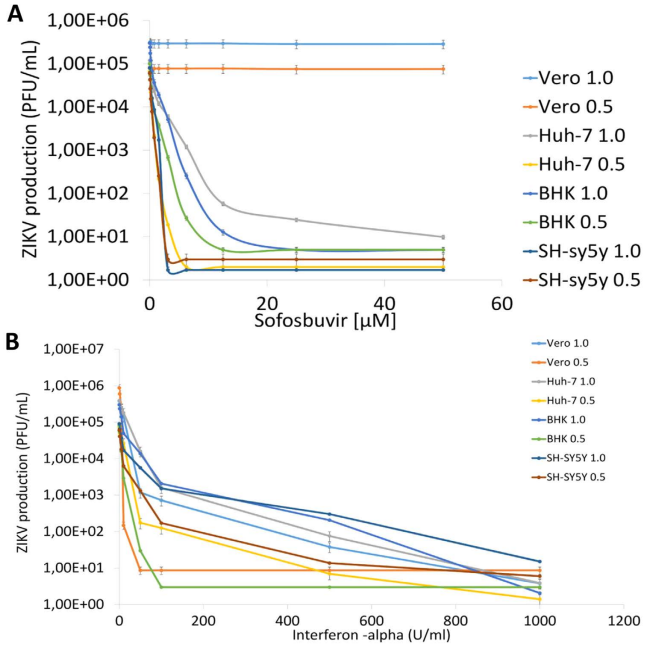

Figure 3. The antiviral activity of sofosbuvir against ZIKV. BHK-21, SH-sy5y, Huh-7 or Vero cells were infected with ZIKV at the indicated MOIs and exposed to various concentrations of sofosbuvir (**A**) or IFN-alpha (**B**), and the viral replication was measured by plaque-forming assays after 24 h of infection. The data represent means ± SEM of three independent experiments.

	Sofosbuvir			Ribavirin			IFN-alpha*		
	EC_{50}	CC_{50}	SI	EC_{50}	CC_{50}	SI	EC_{50}	CC_{50}	SI
BHK	1.9 ± 0.2	360 ± 43	184	5.3 ± 0.8	177 ± 22	33	7.3 ± 0.3	ND	NA
SH-sy5y	1.1 ± 0.2	421 ± 34	384	2.9 ± 0.4	300 ± 21	103	9.8 ± 1.2	ND	NA
Huh-7	0.41 ± 0.04	381 ± 25	1191	6.9 ± 0.8	284 ± 12	41	8.2 ± 0.3	ND	NA
Vero	>50	512 ± 43	NA	5.5 ± 0.04	321 ± 41	58	9.1 ± 0.2	ND	NA

Table 1. Antiviral activity and cytotoxicity of sofosbuvir at an MOI of 1.0. *Values are expressed as U/ml, ND – Not determined, NA – Not Applicable.

	Sofosbuvir			Ribavirin			IFN-alpha*		
	EC_{50}	CC_{50}	SI	EC_{50}	CC_{50}	SI	EC_{50}	CC_{50}	SI
BHK	1.7 ± 0.1	360 ± 43	212	3.1 ± 0.6	177 ± 22	57	2.8 ± 0.3	ND	NA
SH-sy5y	0.65 ± 0.08	421 ± 34	648	1.2 ± 0.2	300 ± 21	31	4.9 ± 0.6	ND	NA
Huh-7	0.12 ± 0.03	381 ± 29	929	3.8 ± 0.04	284 ± 19	23	3.4 ± 0.1	ND	NA
Vero	>50	512	NA	3.3 ± 0.08	321 ± 56	97	8.3 ± 0.2	ND	NA

Table 2. Antiviral activity and cytotoxicity of sofosbuvir at an MOI of 0.5. *Values are expressed as U/ml, ND – Not determined, NA – Not Applicable.

The sofosbuvir phosphoramidate prodrug must be converted to its triphosphate analog in the cellular environment to become active. Despite a general perception that this process is an exclusive feature of hepatocytes[17], sofosbuvir may also become active within neuroepithelial stem cells[39]. Indeed we investigated whether sofosbuvir inhibits ZIKV replication in different cellular systems. BHK-21, SH-Sy5y, Huh-7 or Vero cells were inoculated at different MOIs and treated with various concentrations of sofosbuvir. The supernatants from these cells were collected, and the infectious virus progeny were titered. Sofosbuvir induced an MOI- and dose-dependent inhibition of ZIKV replication (Fig. 3A, Tables 1 and 2, and see Supplementary Fig. S2A–D). The potency and efficiency to inhibit ZIKV replication were higher in Huh-7 and SH-Sy5y cellsthan in BHK-21 cells (Fig. 3A and Table 1 and 2, and see Supplementary Fig. S2A–C). Of note, even high concentrations of sofosbuvir did not inhibit ZIKV replication in Vero cells, indicating a cell-dependent inhibition of ZIKV replication (Fig. 3A and Tables 1 and 2, and see Supplementary Fig. S2D). IFN-alpha and ribavirin were used as positive controls to inhibit ZIKV replication (Fig. 3B and Tables 1 and 2, and see Supplementary Fig. S2A–D).

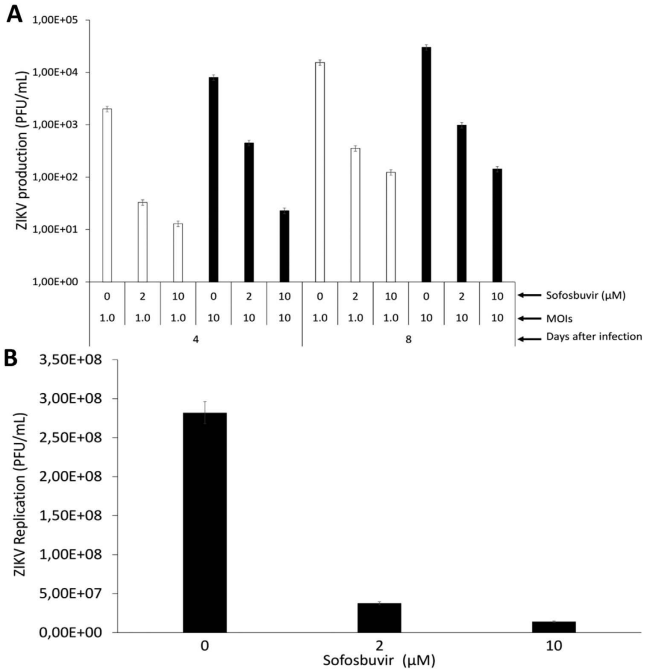

Figure 4. Sofosbuvir inhibits ZIKV replication in human iPS cell-derived NSCs and brain organoids. NSCs (**A**) were infected at the indicated MOIs and brain organoids (**B**) were infected with 5×10^7 PFU/mL of ZIKV. The ZIKV-infected cells were treated with the indicated concentrations of sofosbuvir for different periods of time post infection. At the indicated time points, the culture supernatants were collected, and the virus was titered by plaque-forming assays. The data represent means ± SEM of five independent experiments. The virus production in the presence of the treatments was significantly reduced when compared to untreated cells ($P < 0.01$).

The sofosbuvir cytotoxicity was also cell type-dependent (Tables 1 and 2). Our results indicate that the selectivity index (SI; which represents the ratio between the CC_{50} and EC_{50} values) for sofosbuvir varied from 184 to 1191 (Tables 1 and 2) – being safer at an MOI of 0.5 in the hepatoma and neuroblastoma cell lines. For comparison, the SI values for sofosbuvir were almost 30 times higher than for ribavirin (Table 1). Our data indicate that the sofosbuvir chemical structure possesses anti-ZIKV activity.

Sofosbuvir inhibits ZIKV replication in human primary NSCs and brain organoids. Since the results regarding the pharmacologic activity of sofosbuvir against ZIKV replication in lineage cells were promising, we next investigated whether sofosbuvir could be neuroprotective in a cellular model that corresponds to the early stages of brain development[23]. Human iPS cell-derived neural stem cells (NSCs) were infected with ZIKV and treated with sofosbuvir. Sofosbuvir produced a pronounced inhibition of ZIKV replication in NSCs challenged with MOIs of 1.0 or 10 after 4 to 8 days of infection (Fig. 4A), as only marginal virus titers were detected in sofosbuvir-treated cells. This drastic reduction in viral replication in sofosbuvir-treated NSCs impaired ZIKV-mediated neuropathogenesis by inducing cell death. Whereas ZIKV-infected NSCs exhibited considerable levels of caspase-3/7 activation and plasma membrane permeability at 8 days post infection, sofosbuvir significantly protected these cells from death (Fig. 5, and see Supplementary Figs S3 and S4).

Subsequently, we used ZIKV-infected brain organoids as a three-dimensional model to assess the antiviral activity of sofosbuvir. Brain organoids have been used as a sophisticated cellular model to evaluate the impact of ZIKV on early brain development and as a translational system for in-depth investigations of the cellular and molecular events related to microcephaly[23]. We again observed a pronounced reduction of ZIKV production due to sofosbuvir treatment (Fig. 4B). Altogether, these data indicate that sofosbuvir is effective against ZIKV in neuronal cell systems relevant to the physiopathology of the virus.

Observational analysis of mutations in the ZIKV genome associated with sofosbuvir treatment. Systematically, we observed that sofosbuvir was more effective in reducing ZIKV infectivity than viral RNA levels in the supernatant of the cultures (Fig. 6). Independent of whether sofosbuvir activity was measured in ZIKV-infected Huh-7 cells, NSCs or BHK-21 cells, a concentration of 2 μM of this drug was in general almost two times more potent in inhibiting ZIKV-induced cell death and viral infectivity than viral RNA production (Fig. 6). These data suggest that virus particles containing genomic RNA may be produced under sofosbuvir treatment but that these particles are unable to efficiently infect new cells and produce cytopathogenicity.

We thus sequenced the ZIKV genome from infected Huh-7 cells, NSCs and brain organoids treated with sofosbuvir at 2 μM, a concentration that does not allow for viral RNA extinction. The frequencies of the overall transition mutations in sofosbuvir-treated sequences was significantly increased when compared to

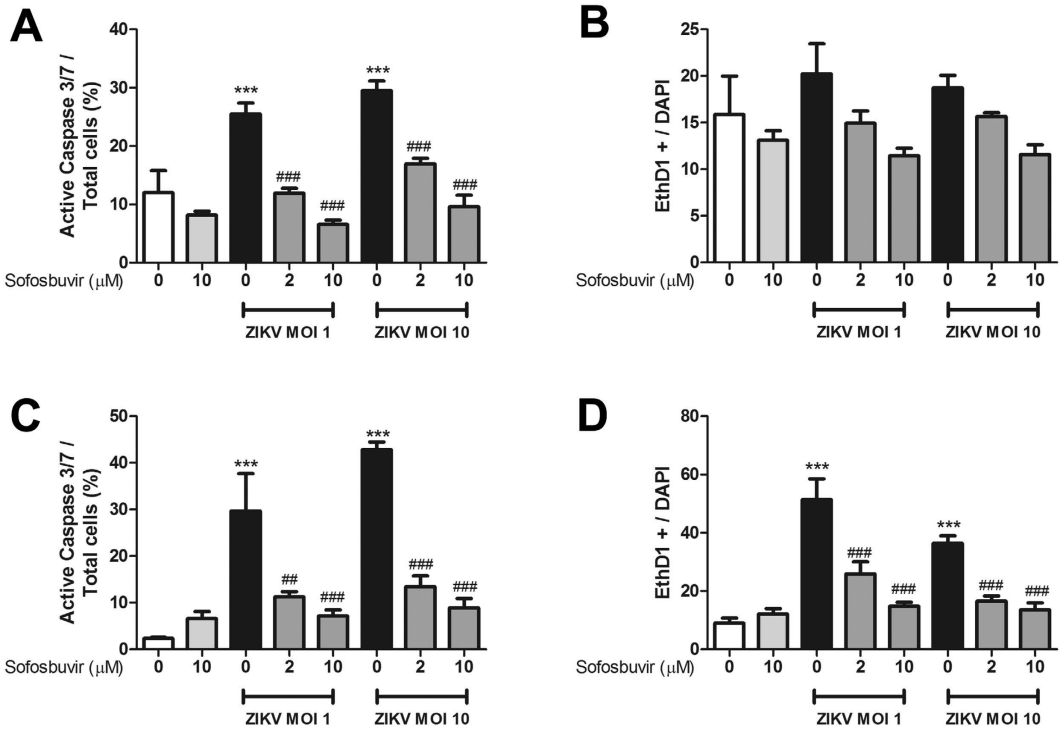

Figure 5. Sofosbuvir protects human iPS cell-derived NSCs from ZIKV-induced cell death. NSCs were labeled for activated caspase-3/7 (**A,C**) and cell permeability (**B,D**) 4 or 8 days after infection. The data represent means ± SEM of five independent experiments. ***indicates $P < 0.001$ for the comparison between the mock- and ZIKV-infected cells. ###Indicates $P < 0.001$ and ##Indicates $P < 0.01$ for the comparison between the ZIKV-infected cells treated with or without sofosbuvir.

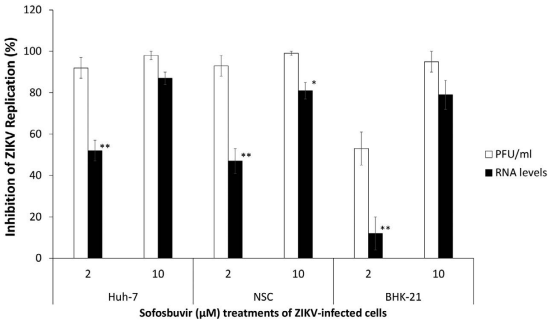

Figure 6. Inhibition of ZIKV-related infectivity and RNA production by sofosbuvir. ZIKV-infected Huh-7 cells, NSCs and BHK-21 cells were treated with or without sofosbuvir. The culture supernatants were collected 24 h after infection to determine the virus infectivity by plaque-forming assays and the viral RNA loads by real time RT-PCR analysis. The data are presented as the percentage over the control (untreated cells). *Indicates a significant difference ($P < 0.05$) between the black and white bars. **Indicates a significant difference ($P < 0.01$) between the black and white bars.

control sequences ($P < 0.05$) for all infected host cell models (Table 3). More specifically, the increased mutation frequency was greater for A-to-G changes, which represented 80 ± 5% of all transition mutations in the sofosbuvir-treated sequences (Table 3). In addition, A-to-G mutations were approximately five times more abundant in sofosbuvir-treated sequences than in control sequences (Table 3). Of note, there were no significant differences in the frequencies of other transitions and transversions between sofosbuvir-treated and control sequences. Our observations indicate that in addition to its direct inhibition of the ZIKV RNA polymerase, sofosbuvir may also increase mutations in the viral genome.

Discussion

ZIKV is a member of the *Flaviviridae* family, along with other clinically relevant viruses such as DENV, WNV, JEV and HCV. In this family, ZIKV was considered to be a virus causing only mild and self-limited infections[4]. However, based on clinical evidence and experimental data, ZIKV infection has been associated with

Mutation Type	Number of mutations						Frequency per 1000 nucleotides[€]					
	Huh-7		NSC		Organoid		Huh-7		NSC		Organoid	
	Control	SFV	Control	SFV	Control	SFV	Control	SFV	Control	SFV	Control	SFV
All Mutations	11	19	13	22	15	27	0.210	0.363	0.248	0.420	0.287	0.516
Transitions	8	15	7	16	12	22	0.153	0.287*	0.134	0.306*	0.229	0.420*
A-to-G	2	13	3	12	4	18	0.038	0.248*	0.057	0.229*	0.076	0.344*
Transversions	3	4	6	6	3	5	0.057	0.076	0.115	0.115	0.057	0.096

Table 3. Mutations in the ZIKV sequence from viruses propagated in cells treated with 2 μM sofosbuvir. [€]With respect to 52347 nucleotides analyzed, SFV – sofosbuvir, $*P < 0.05$ SFV vs control.

neurological-related morbidities, with impacts on the development of the human nervous system and neurological complications in adults[7,8,23,40–43]. Antiviral treatment options are thus required to block viral replication. Here, we show that uridine nucleotide analog anti-HCV drug sofosbuvir possesses anti-ZIKV activity.

Several ongoing studies have demonstrated the anti-ZIKV activity of clinically approved drugs[10–15,18]. Here, we show that sofosbuvir-triphosphate inhibits ZVRP in a dose-dependent fashion. The predicted ZVRP structure suggests that sofosbuvir binds to amino acid residues that are critical for ribonucleotide incorporation, such as Arg473, Gly538, Trp539, and Lys691. The fluoride radical in the sofosbuvir ribosyl moiety is coordinated by Asn612, an interaction that is involved with the drug selectivity to the viral RDRP, which may avoid nonspecific effects towards the cellular DNA-dependent RNA polymerase. Lys458 seems to be the docking residue for the uridine analog.

Next, using cell-based assays, we demonstrated that sofosbuvir inhibits ZIKV replication in BHK-21, SH-Sy5y and Huh-7 cells. Although ZIKV replication was susceptible to sofosbuvir in these cells, the magnitude of antiviral potency and efficiency varied among these cells. Taking as a reference an MOI of 1.0, the potency of antiviral activity observed in hepatoma cells was five times higher, and in neuroblastoma cells was two times higher, than that observed in BHK-21 cells. This is consistent with the demonstration that sofosbuvir converts to its bioactive form in liver cells[17]. Most recently, another group also demonstrated that sofosbuvir may become active in human neuroepithelial stem cells using functional assays against ZIKV[39]. Indeed, we further confirmed that human iPS cell-derived NSCs and brain organoids can be protected by sofosbuvir, even when these cells are challenged with exceedingly high MOIs. Brain organoids represent a translational three-dimensional cell culture model for the study of ZIKV-associated microcephaly[23]. Therefore, the antiviral activity observed by sofosbuvir using human neural progenitors and brain organoids represents a pragmatic demonstration of the potential secondary use of this clinically approved anti-HCV drug, because it impairs ZIKV neuropathogenesis, as shown here and by others[39].

On the other hand, we observed no inhibition of viral replication with even 50 μM of sofosbuvir in Vero cells. Similarly, in a recent study from Eyer *et al.*[12], African ZIKV susceptibility to sofosbuvir was screened in Vero cells, and this compound did not emerge as a potential hit. Although Eyer *et al.*[12] and our group used different viral strains, we obtained similar results in Vero cells. Interestingly, sofosbuvir is a substrate for glycoprotein-P[44]. Proteomic data indicate that Vero cells express this multi-drug resistance ABC-transporter, which may cause the efflux of sofosbuvir from the cell[45–47].

Using different read outs to monitor sofosbuvir anti-ZIKV activity, we observed that this drug reduced virus infectivity more than it inhibited the production of viral RNA. Unlike most antiviral nucleoside analogs[48] and despite the presence of the 3′-OH radical in its chemical structure[37], sofosbuvir acts as a chain terminator. To impair the incorporation of the incoming nucleotides, the 2′-F radical disrupts the hydrogen bonding network[37]. Similarly, the 2′-F in sofosbuvir forms a hydrogen bond with Asn612, which may disrupt the hydrogen bonding of incoming nucleotides to ZIKV RNA polymerase. Indeed, our results indicate that sofosbuvir directly inhibits the viral RNA polymerase. In addition to this mechanism, ZIKV genome sequences from sofosbuvir-treated cells had an increased rate of A-to-G mutations when compared to untreated cells. It is plausible to interpret that both the direct inhibition of ZIKV RNA polymerase and induction of mutations in the viral genome may be triggered by sofosbuvir. For instance, ribavirin, another ribonucleoside analog, may inhibit viral replication by direct targeting the viral RNA polymerase and by the induction of error-prone replication[49,50].

ZIKV-associated microcephaly and GBS highlight that antiviral interventions are urgently needed. Our data reveal that a clinically approved drug possesses antiviral activity against ZIKV and is active in cells derived from peripheral organs and the CNS. Sofosbuvir may induce error-prone ZIKV replication. Together, our data highlight the potential secondary use of sofosbuvir, an anti-HCV drug, against ZIKV.

References

1. Musso, D. & Gubler, D. J. Zika Virus. *Clin Microbiol Rev* **29,** 487–524 (2016).
2. Musso, D. *et al.* Potential sexual transmission of Zika virus. *Emerg Infect Dis* **21,** 359–361 (2015).
3. Dick, G. W., Kitchen, S. F., Haddow, A. J. & Zika virus, I. Isolations and serological specificity. *Trans R Soc Trop Med Hyg* **46,** 509–520 (1952).
4. Cerbino-Neto, J. *et al.* Clinical Manifestations of Zika Virus Infection, Rio de Janeiro, Brazil, 2015. *Emerg Infect Dis* **22** (2016).
5. Faria, N. R. *et al.* Zika virus in the Americas: Early epidemiological and genetic findings. *Science* **352,** 345–349 (2016).
6. Solomon, T., Baylis, M. & Brown, D. Zika virus and neurological disease-approaches to the unknown. *Lancet Infect Dis* **16,** 402–404 (2016).
7. Calvet, G. *et al.* Detection and sequencing of Zika virus from amniotic fluid of fetuses with microcephaly in Brazil: a case study. *Lancet Infect Dis* **16,** 653–660 (2016).
8. Cao-Lormeau, V. M. *et al.* Guillain-Barré Syndrome outbreak associated with Zika virus infection in French Polynesia: a case-control study. *Lancet* **387,** 1531–1539 (2016).
9. Chutaputti, A. Adverse effects and other safety aspects of the hepatitis C antivirals. *J Gastroenterol Hepatol* **15,** E156–163 (2000).

10. Delvecchio, R. *et al.* Chloroquine inhibits Zika Virus infection in different cellular models. *BioRxiv*, 10.1101/051268 (2016).
11. Zmurko, J. *et al.* The Viral Polymerase Inhibitor 7-Deaza-2′-C-Methyladenosine Is a Potent Inhibitor of *In Vitro* Zika Virus Replication and Delays Disease Progression in a Robust Mouse Infection Model. *PLoS Negl Trop Dis* **10,** e0004695, 10.1371/journal.pntd.0004695 (2016).
12. Eyer, L. *et al.* Nucleoside inhibitors of Zika virus. *J Infect Dis* **214,** 707–711 (2016).
13. Barrows, N. J. *et al.* A Screen of FDA-Approved Drugs for Inhibitors of Zika Virus Infection. *Cell Host Microbe* **20,** 259–270 (2016).
14. Elfiky, A. A. Zika viral polymerase inhibition using anti-HCV drugs both in market and under clinical trials. *J Med Virol* **88,** 2044–2051 (2016).
15. Xu, M. *et al.* Identification of small-molecule inhibitors of Zika virus infection and induced neural cell death via a drug repurposing screen. *Nat Med* **22,** 1101–1107 (2016).
16. Piperno, A., Cordaro, M., Scala, A. & Iannazzo, D. Recent highlights in the synthesis of anti-HCV ribonucleosides. *Curr Med Chem* **21,** 1843–1860 (2014).
17. Bhatia, H. K., Singh, H., Grewal, N. & Natt, N. K. Sofosbuvir: A novel treatment option for chronic hepatitis C infection. *J Pharmacol Pharmacother* **5,** 278–284 (2014).
18. Sacramento, C. Q. *et al.* The clinically approved antiviral drug sofosbuvir impairs Brazilian zika virus replication. *BioRxiv*, 10.1101/061671 (2016).
19. Souza, T. M. L. *et al.* Inhibition of HSV-1 replication and HSV DNA polymerase by the chloroxoquinolinic ribonucleoside 6-chloro-1,4-dihydro-4-oxo-1-(beta-D-ribofuranosyl) quinoline-3-carboxylic acid and its aglycone. *Antiviral Research* **77,** 20–27 (2008).
20. Hottz, E. D. *et al.* Platelets mediate increased endothelium permeability in dengue through NLRP3-inflammasome activation. *Blood* **122,** 3405–3414 (2013).
21. Lu, J. *et al.* The IFITM proteins inhibit HIV-1 infection. *J Virol* **85,** 2126–2137 (2011).
22. Tan, B. H. *et al.* Recombinant dengue type 1 virus NS5 protein expressed in Escherichia coli exhibits RNA-dependent RNA polymerase activity. *Virology* **216,** 317–325 (1996).
23. Garcez, P. P. *et al.* Zika virus impairs growth in human neurospheres and brain organoids. *Science* **352,** 816–818 (2016).
24. Gasteiger, E. *et al.* ExPASy: The proteomics server for in-depth protein knowledge and analysis. *Nucleic Acids Res* **31,** 3784–3788 (2003).
25. Dutta, S. *et al.* Data deposition and annotation at the worldwide protein data bank. *Mol Biotechnol* **42,** 1–13 (2009).
26. Sali, A. & Blundell, T. L. Comparative protein modelling by satisfaction of spatial restraints. *J Mol Biol* **234,** 779–815 (1993).
27. Laskowski, R. A., MacArthur, M. W., Moss, D. S. & Thornton, J. M. PROCHECK: a program to check the stereochemical quality of protein structures. *Journal of Applied Crystallography* **26,** 283–291 (1993).
28. Eisenberg, D., Lüthy, R. & Bowie, J. U. VERIFY3D: assessment of protein models with three-dimensional profiles. *Methods Enzymol* **277,** 396–404 (1997).
29. Schmieder, R. & Edwards, R. Quality control and preprocessing of metagenomic datasets. *Bioinformatics* **27,** 863–864 (2011).
30. Zhang, J., Kobert, K., Flouri, T. & Stamatakis, A. PEAR: a fast and accurate Illumina Paired-End reAd mergeR. *Bioinformatics* **30,** 614–620 (2014).
31. Schmieder, R. & Edwards, R. Fast identification and removal of sequence contamination from genomic and metagenomic datasets. *PLoS One* **6,** e17288, 10.1371/journal.pone.0017288 (2011).
32. Nurk, S. *et al.* Assembling single-cell genomes and mini-metagenomes from chimeric MDA products. *J Comput Biol* **20,** 714–737 (2013).
33. Huang, X. & Madan, A. CAP3: A DNA sequence assembly program. *Genome Res* **9,** 868–877 (1999).
34. Malet, H. *et al.* Crystal structure of the RNA polymerase domain of the West Nile virus non-structural protein 5. *J Biol Chem* **282,** 10678–10689 (2007).
35. Lu, G. & Gong, P. Crystal Structure of the full-length Japanese encephalitis virus NS5 reveals a conserved methyltransferase-polymerase interface. *PLoS Pathog* **9,** e1003549, 10.1371/journal.ppat.1003549 (2013).
36. Zhao, Y. *et al.* Molecular basis for specific viral RNA recognition and 2′-O-ribose methylation by the dengue virus nonstructural protein 5 (NS5). *Proc Natl Acad Sci USA* **112,** 14834–14839 (2015).
37. Appleby, T. C. *et al.* Viral replication. Structural basis for RNA replication by the hepatitis C virus polymerase. *Science* **347,** 771–775 (2015).
38. Ferron, F., Bussetta, C., Dutartre, H. & Canard, B. The modeled structure of the RNA dependent RNA polymerase of GBV-C virus suggests a role for motif E in Flaviviridae RNA polymerases. *BMC Bioinformatics* **6,** 255, 10.1186/1471-2105-6-255 (2005).
39. Onorati, M. *et al.* Zika Virus Disrupts Phospho-TBK1 Localization and Mitosis in Human Neuroepithelial Stem Cells and Radial Glia. *Cell Rep* **16,** 2576–2592 (2016).
40. Brasil, P. *et al.* Zika Virus Infection in Pregnant Women in Rio de Janeiro - Preliminary Report. *N Engl J Med* **4,** 10.1056/NEJMoa1602412 (2016).
41. Driggers, R. W. *et al.* Zika Virus Infection with Prolonged Maternal Viremia and Fetal Brain Abnormalities. *N Engl J Med* **374,** 2142–2151 (2016).
42. Rasmussen, S. A., Jamieson, D. J., Honein, M. A. & Petersen, L. R. Zika Virus and Birth Defects - Reviewing the Evidence for Causality. *N Engl J Med* **19,** 1981–1987 (2016).
43. Smith, D. W. & Mackenzie, J. Zika virus and Guillain-Barré syndrome: another viral cause to add to the list. *Lancet* **387,** 1486–1488 (2016).
44. Gilead. *Product Monograph Pr SOVALDI®* (*sofosbuvir*) *Tablets 400 mg sofosbuvir Antiviral Agent* http://www.gilead.ca/pdf/ca/sovaldi_pm_english.pdf (2015; acessed on 09/12/2016).
45. Zhong, L. *et al.* Quantitative proteomics study of the neuroprotective effects of B12 on hydrogen peroxide-induced apoptosis in SH-SY5Y cells. *Sci Rep* **6,** 22635, 10.1038/srep22635 (2016).
46. Guo, D., Zhu, Q., Zhang, H. & Sun, D. Proteomic analysis of membrane proteins of vero cells: exploration of potential proteins responsible for virus entry. *DNA Cell Biol* **33,** 20–28 (2014).
47. Guo, H. C. *et al.* Quantitative Proteomic Analysis of BHK-21 Cells Infected with Foot-and-Mouth Disease Virus Serotype Asia 1. *PLoS One* **10,** e0132384, 10.1371/journal.pone.0132384 (2015).
48. De Clercq, E. A cutting-edge view on the current state of antiviral drug development. *Med Res Rev* **33,** 1249–1277 (2013).
49. Day, C. W. *et al.* Error-prone replication of West Nile virus caused by ribavirin. *Antiviral Res* **67,** 38–45 (2005).
50. Leyssen, P., De Clercq, E. & Neyts, J. The anti-yellow fever virus activity of ribavirin is independent of error-prone replication. *Mol Pharmacol* **69,** 1461–1467 (2006).

Acknowledgements

Thanks are due to Drs Carlos M. Morel, Marcio L. Rodrigues, Renata Curi and Fabrícia Pimenta for their strong advisement and support regarding the technological development underlying this project. This work was supported by Conselho Nacional de Desenvolvimento e Pesquisa (CNPq), Fundação de Amparo à Pesquisa do Estado do Rio de Janeiro (FAPERJ).

Author Contributions

C.Q.S., G.R.deM., N.R., L.V.B.H., M.M., C.S.deF., N.F.-R., A.M., A.C.F., G.B.-L., J.L.A., Y.R.V., E.deM.V., E.N.P., D.A.T., L.L., E.C.L and P.T. – experimental execution and analysis S.K.R., M.M.B., F.A.B., P.T.B., N.B., F.L.T., A.M.B.deF., K.B. and T.M.L.S. – data analysis, manuscript preparation and revision. K.B. and T.M.L.S. – conceptualized the study All authors revised and approved the manuscript.

Additional Information

Supplementary information accompanies this paper at http://www.nature.com/srep

Competing financial interests: The authors declare no competing financial interests.

How to cite this article: Sacramento, C. Q. *et al.* The clinically approved antiviral drug sofosbuvir inhibits Zika virus replication. *Sci. Rep.* **7**, 40920; doi: 10.1038/srep40920 (2017).

Publisher's note: Springer Nature remains neutral with regard to jurisdictional claims in published maps and institutional affiliations.

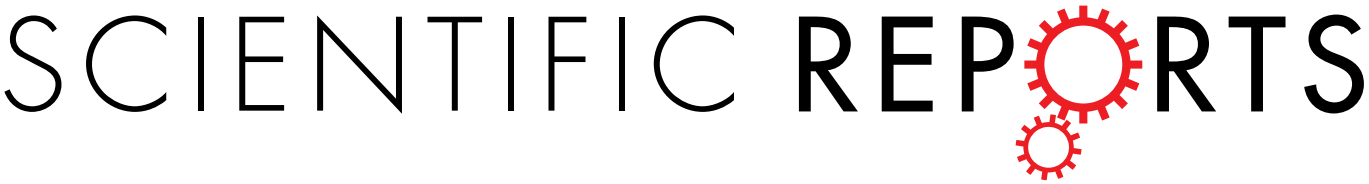

OPEN

Sofosbuvir protects Zika virus-infected mice from mortality, preventing short- and long-term sequelae

Received: 8 May 2017
Accepted: 28 July 2017
Published online: 25 August 2017

André C. Ferreira[1], Camila Zaverucha-do-Valle[1,2], Patrícia A. Reis[1], Giselle Barbosa-Lima[2], Yasmine Rangel Vieira[2], Mayara Mattos[1], Priscila de Paiva Silva[1], Carolina Sacramento[1], Hugo C. de Castro Faria Neto[1], Loraine Campanati[3], Amilcar Tanuri[4], Karin Brüning[5], Fernando A. Bozza[1,2], Patrícia T. Bozza[1] & Thiago Moreno L. Souza[1,2,6]

Zika virus (ZIKV) causes significant public health concerns because of its association with congenital malformations, neurological disorders in adults, and, more recently, death. Considering the necessity to mitigate ZIKV-associated diseases, antiviral interventions are an urgent necessity. Sofosbuvir, a drug in clinical use against hepatitis C virus (HCV), is among the FDA-approved substances endowed with anti-ZIKV activity. In this work, we further investigated the *in vivo* activity of sofosbuvir against ZIKV. Neonatal Swiss mice were infected with ZIKV (2×10^7 PFU) and treated with sofosbuvir at 20 mg/kg/day, a concentration compatible with pre-clinical development of this drug. We found that sofosbuvir reduced acute levels of ZIKV from 60 to 90% in different anatomical compartments, such as the blood plasma, spleen, kidney, and brain. Early treatment with sofosbuvir doubled the percentage and time of survival of ZIKV-infected animals. Sofosbuvir also prevented the acute neuromotor impairment triggered by ZIKV. In the long-term behavioural analysis of ZIKV-associated sequelae, sofosbuvir prevented loss of hippocampal- and amygdala-dependent memory. Our results indicate that sofosbuvir inhibits ZIKV replication *in vivo*, which is consistent with the prospective necessity of antiviral drugs to treat ZIKV-infected individuals.

Zika virus (ZIKV) is an enveloped, positive-sense, single stranded RNA pathogen that belongs to the *Flaviviridae* family. ZIKV is transmitted by mosquitoes, similar to several other arboviruses of the *Flavivirus* genus, such as dengue virus (DENV). ZIKV re-emerged in the last few years and was revealed to be a unique pathogen[1]. ZIKV is spread through sexual and physical contact, as well as vertically[1]. The main wave of Zika epidemics in the Americas occurred from the middle of 2015 to the beginning of 2016, when the World Health Organization (WHO) declared this outbreak as a public health emergency of international concern. This relevant apprehension was raised due to ZIKV's association with congenital malformations, including microcephaly, and a broad range of neurological disorders in adults, including Guillain-Barré syndrome[2,3]. With the number of cases rising, Zika-associated deaths have also been reported[4,5]. Considering the necessity to mitigate ZIKV-associated morbidities, antiviral interventions against this virus are an urgent necessity.

Different studies have been published on the repositioning of Food and Drug Administration (FDA)-approved molecules to treat ZIKV infection[6–11]. Over 30 FDA-approved molecules are endowed with anti-ZIKV activity.

[1]Laboratório de Imunofarmacologia, Instituto Oswaldo Cruz (IOC), Fundação Oswaldo Cruz (Fiocruz), Rio de Janeiro, RJ, Brazil. [2]Instituto Nacional de Infectologia (INI), Fiocruz, Rio de Janeiro, RJ, Brazil. [3]Instituto de Ciências Biomédicas, Universidade Federal do Rio de Janeiro, Rio de Janeiro, RJ, Brazil. [4]Instituto de Biologia, Universidade Federal do Rio de Janeiro (UFRJ), Rio de Janeiro, RJ, Brazil. [5]BMK Consortium: Blanver Farmoquímica Ltda; Microbiológica Química e Farmacêutica Ltda, Karin Bruning & Cia. Ltda, Taboão da Serra, SP, Brazil. [6]National Institute for Science and Technology on Innovation on Neglected Diseases (INCT/IDN), Center for Technological Development in Health (CDTS), Fiocruz, Rio de Janeiro, RJ, Brazil. André C. Ferreira, Camila Zaverucha-do-Valle and Patrícia A. Reis contributed equally to this work. Correspondence and requests for materials should be addressed to T.M.L.S. (email: tmoreno@cdts.fiocruz.br)

Among them, we and others have shown that sofosbuvir, a clinically approved anti-hepatitis C virus (HCV), targets ZIKV RNA polymerase, leading to inhibition of virus replication in cellular types important for the pathogenesis of this emergent agent, such as human brain organoids, neural stem cells, and neuroepithelial stem cells[12–14]. Therefore, sofosbuvir may represent a selective option to treat Zika. Nevertheless, more detailed analyses of sofosbuvir's anti-ZIKV activity *in vivo* are necessary.

Different animal models of Zika virus infection have been reported recently[15]. Many of these models, from immunocompromised to immunocompetent neonatal mice, among others, are relevant for antiviral testing[15]. In general, for pharmacological studies, outbred animals, such as Swiss mice, represent a consistent model. These animals display broader responses often found in heterogeneous populations[16], such as humans. Indeed, ZIKV infection in Swiss neonatal mouse models has been characterized since 1950[15,17–19]. Another advantage of neonatal mouse models is the opportunity to further examine behavioural sequelae induced by the infection and whether treatments could overcome/prevent this phenotype.

In this study, we show that sofosbuvir protects ZIKV-infected animals from mortality by a very significant viral challenge. This was associated with a decrease in viral RNA levels in different tissues and prevention of acute neuromotor and long-term memory sequelae.

Material and Methods

Reagents. The antiviral drug sofosbuvir (β-D-2′-deoxy-2′-α-fluoro-2′-β-C-methyluridine) was donated by the BMK Consortium: Blanver Farmoquímica Ltda; Microbiológica Química e Farmacêutica Ltda; Karin Bruning & Cia. Ltda, (Taboão da Serra, São Paulo, Brazil). Drugs were dissolved in 100% dimethylsulfoxide (DMSO) 1:10 (mass/volume), followed by the appropriate dilutions in PBS or culture medium (DMEM) to treat the animals. The final DMSO concentrations showed no toxicity to the animals. Other materials were purchased from Thermo Scientific Life Sciences (Grand Island, NY) unless otherwise mentioned.

Cells. African green monkey kidney (Vero) cells were cultured in DMEM. The culture medium was supplemented with 10% foetal bovine serum (FBS; HyClone, Logan, Utah), 100 U/mL penicillin, and 100 µg/mL streptomycin. Cells were kept at 37 °C in 5% CO_2.

Virus. ZIKV African (MR766) and Brazilian (GenBank accession #KX19720513) strains were propagated in Vero cells (E6 subtype). Vero cells were infected at a multiplicity of infection (MOI) of 0.01 at 37 °C for 1 h. Next, unadsorbed virus particles were removed by washing with phosphate-buffered saline (PBS), and the cells were cultured at 70% confluency for an additional 5 to 7 days in medium with 1% FBS. After each period, the cells were lysed by freezing and thawing and centrifuged at 1,500 × *g* at 4 °C for 20 min to remove cellular debris. The virus was stored at −70 °C for further studies. Detailed protocols to grow the stock virus strains at titers ~10^9 PFU/mL have been described by us previously[13,20].

Plaque-forming assay. Monolayers of Vero cells in 6-well plates were exposed to different dilutions of the supernatant containing virus for 1 h at 37 °C. Next, the cells were washed with PBS, and DMEM containing 1% FBS and 3% carboxymethylcellulose (Fluka) (overlay medium) was added to the cells. After 5 days at 37 °C, the monolayers were fixed with 10% formaldehyde in PBS and stained with a 0.1% solution of crystal violet in 70% methanol. The virus titers were then calculated by scoring the plaque-forming units (PFU).

Molecular detection of virus RNA levels. Total RNA from culture, extract-containing organs in PBS, or plasma was extracted using QIAamp Viral RNA or RNeasy Mini Kits (Qiagen®), according to manufacturer's instructions. Quantitative RT-PCR was performed using QuantiTect or QuantiNova Probe RT-PCR Kit (Quiagen®) in an ABI PRISM 7300 Sequence Detection System (Applied Biosystems). Amplifications were carried out in 25 µL reaction mixtures containing 2 × reaction mix buffer, 50 µM of each primer, 10 µM of probe, and 5 µL of RNA template. Primers, probes, and cycling conditions recommended by the Centers for Disease Control and Prevention (CDC) protocol were used to detect the ZIKV[21]. The standard curve method was employed for virus quantification. For reference on the cell amounts used, the housekeeping gene RNAse P was amplified[20]. The Ct values for this target were compared to those obtained to different cell amounts, 10^7 to 10^2, for calibration.

Animals. Swiss albino mice (*Mus musculus*) (pathogen-free) from the Oswaldo Cruz Foundation breeding unit (Instituto de Ciência e Tecnologia em Biomodelos (ICTB)/Fiocruz) were used for these studies. The animals were kept at a constant temperature (25 °C) with free access to chow and water in a 12-h light/dark cycle. The experimental laboratory received pregnant mice (at approximately the 14th gestational day) from the breeding unit. Pregnant mice were observed daily until delivery to accurately determine the postnatal day. We established a litter size of 10 animals for all experimental replicates.

The Animal Welfare Committee of the Oswaldo Cruz Foundation (CEUA/FIOCRUZ) approved and covered (license number L-016/2016) the experiments in this study. The procedures described in this study were in accordance with the local guidelines and guidelines published in the National Institutes of Health Guide for the Care and Use of Laboratory Animals. The study is reported in accordance with the ARRIVE guidelines for reporting experiments involving animals[22].

Experimental infection and treatment. Three-day-old Swiss mice were infected intraperitoneally with 2×10^7 PFU of virus[18,23], unless otherwise mentioned. Treatments with sofosbuvir were carried out with sofosbuvir at 20 mg/kg/day intraperitoneally. Treatment started one day prior to infection (pretreatment) or two days after infection (late treatment). In both cases, treatment was conducted for 7 days. For comparisons, mock-infected and mock-treated groups of animals were used as controls. Animals were monitored daily for survival, weight gain, and virus-induced short-term sequelae (righting in up to 60 seconds) (Supplementary Video).

Blood was collected by cardiac puncture and placed on citrate-containing tubes for plasma separation. Tissues (spleen, kidney, and brain) were collected. Initially, the tissues were analysed macroscopically for the presence of pathological signs. Whenever possible, the pathological signs were quantified by counting per verified tissue/organs. Alternatively, tissues were lysed (RLT buffer; Qiagen) and homogenized with a Potter-Elvehjem homogenizer (Teflon pestle and glass mortar). Homogenates were cleared by centrifugation, and total RNA was extracted.

If necessary to alleviate animal suffering, euthanasia was performed. The criteria were the following: i) differences in weight gain between infected and control groups > 50%, ii) ataxia, iii) loss of gait reflex, iv) absence of righting reflex within 60 seconds, and v) separation, with no feeding, of moribund offspring by the female adult mouse.

Behavioural tests. To test the righting reflex, animals were tested daily during the course of acute infection. Animals were held in a supine position with all four paws facing up in the air for 5 seconds. Then, animals were released, and the time the animal took to flip over onto its stomach with all four paws touching the surface was measured. A maximum of 60 seconds was given for each trial, and animals were tested twice a day with a 5-minute minimum interval between trials. For each animal, the lowest time was plotted in the graph. Animals that failed the test were included in the graph with a time of 60 seconds. Please see the Supplementary Video.

Animals at 6 to 8 weeks of age were assayed for long-term sequelae by different tests. The Morris water maze (MWM) is a behavioural task to evaluate hippocampal-dependent learning and spatial memory. The water maze comprised a black circular pool (100 cm in diameter) that was conceptually divided into four equal, but imaginary, quadrants for the purpose of data analysis. The water temperature was 25 °C. A platform (10 cm^2), which was hidden from the mouse's view, was located 2 cm beneath the surface of the water, allowing the mouse to easily climb onto it once its presence was detected. The water maze was located in a well-lit white room with several posters and other distal visual stimuli hanging on the walls to provide spatial cues. Training on the hidden platform (spatial) version of the MWM was carried out on 4 consecutive days. On day 5, when the platform was removed, memory was evaluated.

An amygdala-dependent aversive memory assay (freezing test) was conducted in a chamber with 3 dark walls and clear frontal wall and lid (28 × 26 × 23 cm). The floor of the chamber consisted of 20 parallel stainless steel grid bars, each measuring 4 mm in diameter and spaced 7 cm apart. The grid was connected to a shock generator device (Insight LTDA, Brazil). A training session consisted of placing the mouse in the chamber and allowing a 3-min acclimation period. After, mice received two foot shocks (0.6 mA, 3 s with one interval of 30 s) and were then returned to their home cages. Twenty-four hours later, mice were exposed to the same environment without shock stimuli for 3 min. Memory was assessed and expressed as the percentage of time that mice spent freezing (considered crouching without movement of the head except when associated with breathing).

Statistical analysis. Significance of survival curves was evaluated using the Log-rank (Mantel-Cox) test. Behavioural tests were analysed with ANOVA, followed by Tukey's post hoc test using Graphpad Prism software 7.0. Odds ratios (OR) and 95% confidence intervals (CI) were calculated by Fisher's exact test with Lancaster's mid-P correction using OpenEpi software[24] for comparisons of mortality among groups. *P* values of 0.05 or less were considered statistically significant.

Results

Sofosbuvir enhances the survival of ZIKV-infected mice. To evaluate whether sofosbuvir, at a concentration compatible with the pre-clinical/clinical studies for drug approval[25], protects ZIKV-infected mice, we first determined the strain and dose of virus to be used. Upon intraperitoneal infection, we found that the African strain induced greater mortality than the Brazilian virus (Figure S1A), in line with previous studies[19,26]. Subsequently, we determined that the dose of 2×10^7 PFU of African ZIKV was severe enough to drive mouse mortality within a week or less (Figure S1B). The next experiments were conducted using this condition.

Sofosbuvir significantly protected pretreated infected mice from ZIKV-induced mortality (Fig. 1A). Virtually all ZIKV-infected mice died up to 7 days after infection, whereas 40% of sofosbuvir-treated ZIKV-infected animals survived (Fig. 1A). Along with the survival curves, we evaluated the weight gain of pretreated animals during the time course of the assay. ZIKV-infected animals had impaired postnatal development, whereas the weight gain of sofosbuvir-treated ZIKV-infected mice was indistinguishable from uninfected controls (Fig. 1B).

Postponing the treatment to the second day after infection still preserved some level of protection to ZIKV-infected mice (Fig. 1C). Untreated ZIKV-infected mice died at 8 days post-infection, whereas 25% of the mice receiving late treatment with sofosbuvir survived (Fig. 1C). With respect to the postnatal development of ZIKV-infected mice, treated animals gained more weight than untreated mice (Fig. 1D).

Remarkably, treatment regimens resulted in enhanced survival when compared to the absence of treatment. Nevertheless, pretreatment may be considered more effective. Pretreatment decreased the mortality rates and increased the mean time of survival (T_{50}) when compared to late treatments (Table 1). To statistically compare different experimental groups with respect to mortality risk, odds ratios (OR) for this outcome were calculated. Comparing no treatment with sofosbuvir-treated mice (irrespective of timing) had a reduced mortality risk (OR = 0.198) (Fig. 2). However, compared with no treatment, pretreatment was more effective than the late regimen (no vs. pre: OR = 0.098; no vs. late OR = 0.220) (Fig. 2). The comparison between late vs pretreatment also revealed the benefits of earlier interventions (OR = 0.648) (Fig. 2). Our results show that sofosbuvir treatment is associated with reduced mortality in infected mice. Although potential benefits from sofosbuvir treatment were observed regardless of when animals received the intervention, earlier administration resulted in substantially improved antiviral results.

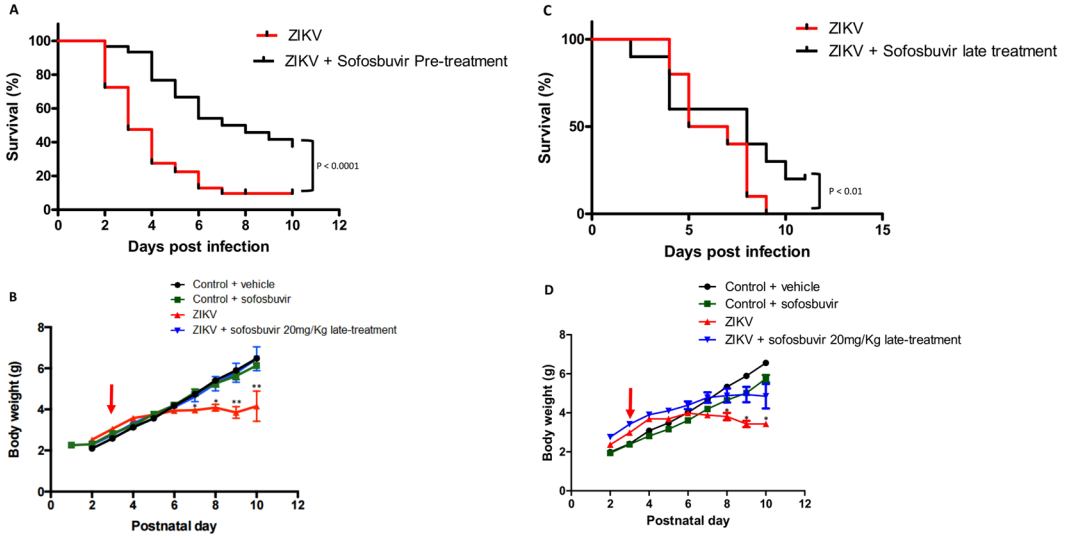

Figure 1. Treatment with Sofosbuvir increases survival and inhibits weight loss of ZIKV-infected mice. Three-day-old Swiss mice were infected with ZIKV (2×10^7 PFU) and treated with sofosbuvir either 1 day before (**A** and **B**) or 2 days after infection (**C** and **D**). Survival (**A** and **C**) and weight variation (**B** and **D**) were assessed during the course of treatment (7 days). The red arrow indicates when animals were infected. Survival was statistically assessed by Log-rank (Mentel-Cox) test. Differences in weight are displayed as the means ± SEM, and two-way ANOVA for each day was used to assess the significance. Independent experiments were performed with at least 10 mice/group (n = 50). *P < 0.01; **P < 0.001.

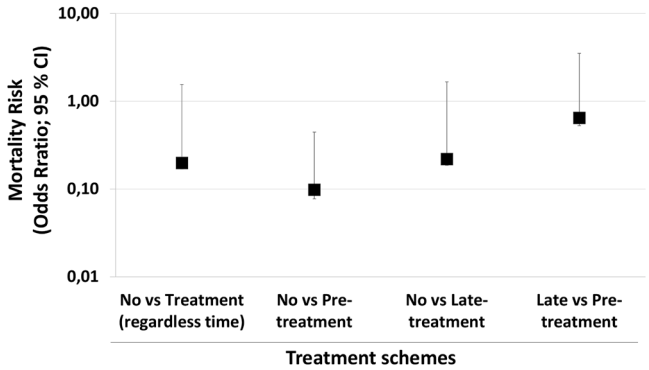

Figure 2. Sofosbuvir reduces the risk mortality of ZIKV-infected mice. Taking the data from Fig. 1A,C as reference, the odds ratio for mortality risk (with 95% confidence interval; CI) was calculated by Fisher's exact test with Lancaster's mid-P correction. All comparisons were statistically significant, with P < 0.001.

	Treatment Schemes			
	Pre		Late	
	Nil	Sofosbuvir	Nil	Sofosbuvir
Mortality (%)	95	40	100	25
T50 (Days)	3	7	5	7

Table 1. Percentage of mortality and mean survival time of sofosbuvir-treated ZIKV-infected mice.

Sofosbuvir decreases ZIKV loads during acute infection. Since sofosbuvir inhibits ZIKV replication, enhanced survival due to this treatment was presumably associated with reduction in viral levels during acute infection. We evaluated this hypothesis and measured the magnitude of virus inhibition *in vivo*. To do so, sofosbuvir-treated ZIKV-infected animals were euthanized daily from the first to the fifth day after infection. Next, viral loads were measured in different tissues (Fig. 3). We observed that sofosbuvir reduced the mice viraemia by over 90%, especially during the first 3 days after infection, when an exponential increase in viral levels in the plasma was observed (Fig. 3A). Sofosbuvir reduced the peak of virus detection by up to 60% between 2

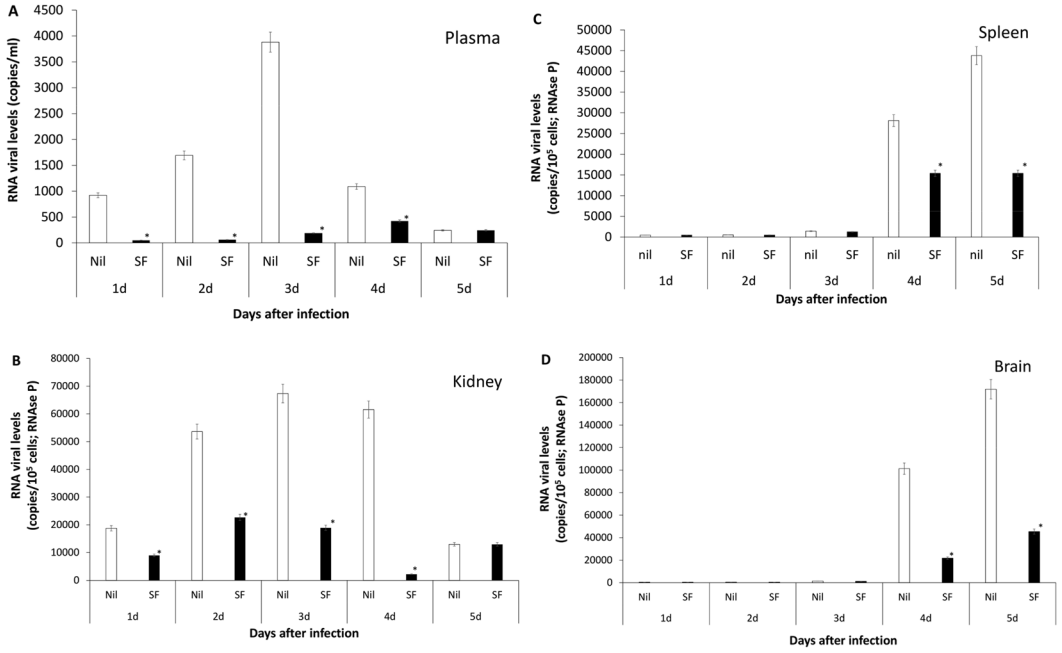

Figure 3. Sofosbuvir-dependent inhibition of ZIKV replication reduces viral loads in different anatomical compartments during acute infection. Three-day-old Swiss mice were infected with ZIKV (2×10^7 PFU) and treated with sofosbuvir (SF) or not (nil) beginning 1 day before infection. At indicated days after infection, animals were euthanized, and ZIKV RNA levels were measured in the plasma (**A**), kidney (**B**), spleen (**C**), and brain (**D**). The results are displayed as the means ± SEM (at least three technical replicates from at least three mice per group per day were assayed). Student's t test was used to compare the viral levels from SF- vs. mock-treated mice. *$P < 0.01$.

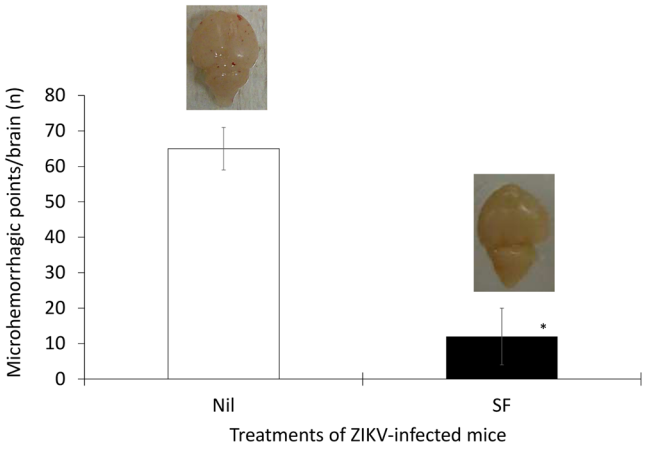

Figure 4. Sofosbuvir decreases the degree of microhaemorrhage in the brains of ZIKV-infected mice. Three-day-old Swiss mice were infected with ZIKV (2×10^7 PFU) and treated with sofosbuvir (SF) or not (nil) beginning 1 day before infection. At the fifth day after infection, animals were euthanized and whole brain collected to quantify the microhaemorrhagic foci. The means ± SEM of at least three mice per group are displayed. Student's t test was used to compare the viral levels of SF- vs. mock-treated mice. *$P < 0.01$. The insets are representative brains of untreated and treated mice.

and 4 days post-infection in the kidney (Fig. 3B). Virus detection in the spleen and brain was abundant at 4 to 5 days after infection, and sofosbuvir treatment reduced virus levels in these tissues by up to 80% (Fig. 3C,D). Remarkably, during this experiment, we observed that ZIKV-infected animals had foci of cerebral microhaemorrhage. Sofosbuvir prevented/reduced ZIKV-induced microhaemorrhage by over 90% (Fig. 4) in pretreated animals.

Altogether, our results indicate that the effects of sofosbuvir on mouse survival were indeed followed by a reduction in virus detection in different anatomical compartments.

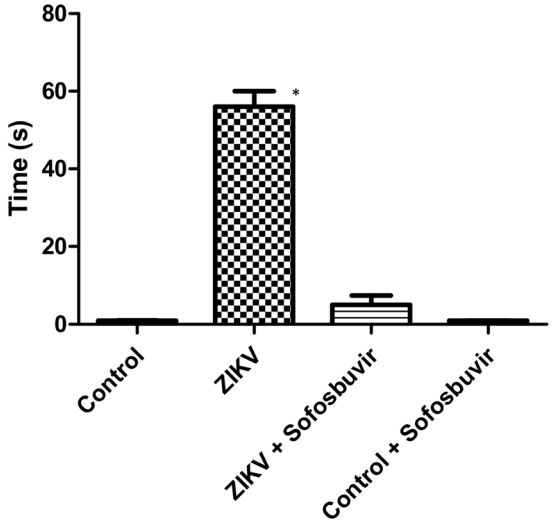

Figure 5. Sofosbuvir prevents neuromotor impairment in ZIKV-infected mice. Three-day-old Swiss mice were infected with ZIKV (2×10^7 PFU) and treated with sofosbuvir (SF) or not (nil) beginning 1 day before infection. At the fifth day after infection, animals were tested for righting (Supplementary Video). Animals were turned backwards and allowed up to 60 s to return to the upright position. The results are presented as the means ± SEM. This was a routine measure and at least 10 animals per group were analysed. Student's t test was used to compare untreated ZIKV-infected mice with other groups individually. *$P < 0.01$.

Sofosbuvir prevents short- and long-term sequelae in ZIKV-infected mice. The neonatal animal model may represent a relevant model to evaluate short, and especially, long-term behavioural sequelae after infection. Consistently, we observed an acute neuromotor impairment in ZIKV-infected mice (Supplementary Video). To determine the magnitude of this injury and the benefits of sofosbuvir use, we applied the righting test reflex for up to 60 seconds. ZIKV-infected animals, untreated with sofosbuvir, took 12 times longer to stay in the upright position than sofosbuvir-treated animals or controls (Fig. 5). Sofosbuvir-treated ZIKV-infected mice and the controls were statistically indistinguishable (Fig. 5). Our data indicate that sofosbuvir protects animals from ZIKV-associated acute neuromotor impairment.

Moreover, some ZIKV-infected mice did not succumb to the infection (Fig. 1A). We kept convalescent mice from acute ZIKV infection for 6 to 8 weeks to further monitor behavioural sequelae. We applied the Morris water maze test to assess hippocampal learning and memory. On the learning tests, training to find a platform 2 cm beneath the surface of the water was carried out for 4 days. Healthy control animals and survivors from ZIKV infection responded similarly to learning, independently of whether infected animals were treated (Fig. S2). On the 5th day after training, the platform was removed, and memory was evaluated by measuring the time to stay in the platform's quadrant (latency). Untreated ZIKV-infected mice did not stay on the quadrant where the platform had been previously located in comparison to control (uninfected) and sofosbuvir-treated ZIKV-infected mice (Fig. 6A).

Subsequently, an amygdala-dependent aversive memory test was performed (freezing test). This test consists of two foot shocks on mice. On the next day, mice are exposed to the same environment without a shock, when latency is measured. Our data showed that untreated ZIKV-infected animals lost the aversive memory, whereas the sofosbuvir-treated ZIKV-infected mice and healthy controls behaved normally (Fig. 6B). Our results indicate that, in addition to the increase in survival by sofosbuvir, this drug also prevents ZIKV-induced behavioural sequelae at the levels of neuromotor impairment and memory loss.

Discussion

In recent years, the risk perception on ZIKV infection has increased substantially. Although Zika fever is a mild and self-limiting disease in most cases[27], ZIKV-associated morbidities have been described[2,3]. Since 2013/2014, ZIKV has spread explosively across immunologically naïve populations throughout the world, especially in the Americas[28]. For instance, in Brazil during 2015, it is estimated that over 4 million people were affected by this virus[29]. Major concerns were raised due to the association of ZIKV infection with neurological disorders during foetal development and adulthood[2,3]. More recently, Zika-associated deaths have also been reported[4,5]. We and others have shown that sofosbuvir, a clinically approved drug against HCV, shows strong antiviral activity against ZIKV[12–14]. In particular, we showed that sofosbuvir is functionally active against ZIKV in cells derived from peripheral organs and the CNS by targeting viral RNA polymerase[13]. To advance the pre-clinical development of sofosbuvir as an anti-ZIKV drug, we further examined whether this uridine analogue is active *in vivo*.

Pharmacological studies on animal models with representative genetic heterogeneity, such as Swiss outbred mice, may allow further exploration of the generated data to a broader population[16]. The neonatal mouse model of ZIKV infection, at postnatal days 0 and 1, has been characterized to study viral physiopathology on the nervous system[18]. The authors considered that C57BL/6 and Swiss mice responded similarly to ZIKV[18]. We chose the

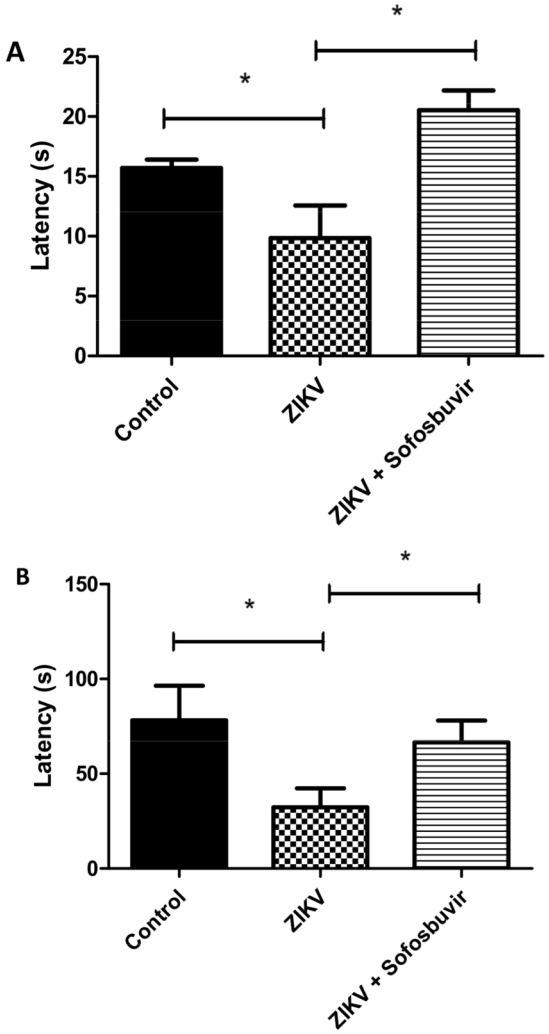

Figure 6. Sofosbuvir prevents memory loss in animals that survive ZIKV infection. Animals that survived from ZIKV neonatal infection, untreated or pretreated with sofosbuvir, were kept and tested for behavioural sequelae in learning and memory after 60 days. The time to find the platform, according to MWM test, was assessed. Trial in the absence of the platform was conducted (**A**) (*$P < 0.05$, Student's t test). In panel A, latency represents the time spent exploring the quadrant where the platform was located before removal, and the data are expressed as the means ± SEM (n = 5 to 8 per experimental group). Aversive memory was evaluated by freezing behaviour 24 h post-training session, whereas mice were allowed to explore the aversive environment during 180 s followed by two foot shocks (0.6 mA, 3 s) (**B**). In panel B, latency represents the time spent without movement (freezing) during 180 s, and the data are expressed as the means ± SEM (n = 5 to 8 per experimental group).

outbred animal model because it may represent a more natural system. For logistic reasons, it was unfeasible to use the day 0 or 1 neonatal mouse model[18]. Under our conditions, it was necessary to have enough time to accommodate the animals after birth in the experimental laboratory and then pretreat 1 day before infection. Thus, we infected 3-day-old Swiss mice to monitor the benefits of sofosbuvir treatment on the survival of ZIKV-infected animals. Of note, we did not aim to compare the cellular and molecular aspects of postnatal neurodevelopment nor physiopathology of ZIKV infection with previous works[18] because we used older neonatal mice. Older animals displayed limited susceptibility to ZIKV infection when compared to the work of van den Pol *et al.*[18]. Although we used a severe virus challenge throughout our investigation, a similar dose of virus has been used by a different route of inoculation (intracranially) to investigate the physiopathology of ZIKV infection in the brain[23].

Treatments with sofosbuvir were carried out at 20 mg/kg/day because this dose was administered to mice during preclinical development. The studies using this dose supported the clinical dossier to approve the safe and effective use of sofosbuvir in humans at 400 mg/day to treat HCV infection[25]. Thus, as a proof of concept, our findings consistently show that sofosbuvir, at a pragmatic concentration, possesses antiviral activity robust enough to provide protection against severe doses of virus. Under our conditions, less than 5% of all the animals assayed survived. Sofosbuvir increased the time of survival and reduced the mortality of infected animals. We also identified an associated likelihood of decreased mortality when comparing pretreatment with late initiation of treatment

(2 days after infection). These data may provide two important general notions: i) earlier sofosbuvir administration to ZIKV-infected mice leads to better antiviral results and reduced mortality; and ii) regardless of timing, it is more opportune to administer sofosbuvir rather than leave the animals without treatment for the sake of survival. This narrow and early time frame for antiviral intervention is common to other acute viral infections[30]. Mortality to pandemic influenza, for example, is reduced if neuraminidase inhibitors are administered early in the time course of infection, preferentially within 2.5 days of infection[30]. Sofosbuvir-treated animals had reduced mortality risk and also lived longer.

Moreover, sofosbuvir pretreatment prevented ZIKV mortality, suggesting its potential use for pre-exposure prophylaxis. We envision that prophylactic activity is a distinguishable feature of sofosbuvir against Zika. If safe, prophylactic drugs could be used by individuals at high risk of complications by a given infectious agent. Pregnant women and their babies are at the highest risk of ZIKV-associated morbidities. Sofosbuvir has a record of safety, even when the indiscriminate use of this substance occurred in limited numbers of pregnant women[31]. In addition, more accurate clinical-based evidence may start to emerge in late 2018 because a clinical trial of sofosbuvir on pregnant women is ongoing[32].

ZIKV detection in the kidney, urine, plasma, and spleen before reaching the brain[33–35] has been associated as a hallmark of the natural history of ZIKV infection. Sofosbuvir effects on survival were associated with an inhibition of acute virus infection and spread through different anatomical compartments. Since sofosbuvir reduced acute virus loads, sofosbuvir-treated ZIKV-infected animals displayed fewer foci of brain microhaemorrhage when compared to their untreated counterparts. Moreover, sofosbuvir-treated mice responded properly to neuromotor reflexes (righting), whereas untreated ZIKV-infected animals had severe impairment of this parameter.

In the long-term analysis of animals that survived, we noticed that ZIKV-infected animals had behavioural sequelae compatible with memory impairment. This is consistent with virus-induced cell death and cerebral inflammation in memory-forming areas[14,18,23,36,37]. Sofosbuvir-treated ZIKV-infected mice survived longer and in more numbers than untreated animals. The surviving animals were also healthier, responding to memory testing behaviour consistent with uninfected control mice.

Altogether, our results indicate that sofosbuvir treatment at a pharmacologically relevant concentration inhibits ZIKV replication *in vivo*, reducing mortality and blocking behavioural sequelae in the short- and long-term analysis. These results are an important proof of concept and are consistent with a prospective necessity of antiviral drugs to treat ZIKV-infected individuals.

References

1. Song, B. H., Yun, S. I., Woolley, M. & Lee, Y. M. Zika virus: history, epidemiology, transmission, and clinical presentation. *J. Neuroimmunol.* **308**, 50–64 (2017).
2. Calvet, G. *et al*. Detection and sequencing of Zika virus from amniotic fluid of fetuses with microcephaly in Brazil: a case study. *Lancet Infect. Dis.* **16**, 653–660 (2016).
3. Cao-Lormeau, V. M. *et al*. Guillain-Barre Syndrome outbreak associated with Zika virus infection in French Polynesia: a case-control study. *Lancet* **387**, 1531–1539 (2016).
4. Azevedo, R. S. *et al*. Zika virus epidemic in Brazil. I. Fatal disease in adults: clinical and laboratorial aspects. *J. Clin. Virol.* **85**, 56–64 (2016).
5. Swaminathan, S., Schlaberg, R., Lewis, J., Hanson, K. E. & Couturier, M. R. Fatal Zika virus infection with secondary nonsexual transmission. *N. Engl. J. Med.* **375**, 1907–1909 (2016).
6. Delvecchio, R. *et al*. Chloroquine inhibits Zika virus infection in different cellular models. *bioRxiv preprint*. doi:10.1101/051268 (2016).
7. Zmurko, J. *et al*. The viral polymerase inhibitor 7-deaza-2′-C-methyladenosine is a potent inhibitor of *in vitro* Zika virus replication and delays disease progression in a robust mouse infection model. *PLoS Negl. Trop. Dis.* **10**, e0004695 (2016).
8. Eyer, L. *et al*. Nucleoside inhibitors of Zika virus. *J. Infect. Dis.* **214**, 707–711 (2016).
9. Barrows, N. J. *et al*. A screen of FDA-approved drugs for inhibitors of zika virus infection. *Cell Host Microbe* **20**, 259–270 (2016).
10. Elfiky, A. A. Zika viral polymerase inhibition using anti-HCV drugs both in market and under clinical trials. *J. Med. Virol.* **88**, 2044–2051 (2016).
11. Xu, M. *et al*. Identification of small-molecule inhibitors of Zika virus infection and induced neural cell death via a drug repurposing screen. *Nat. Med.* **22**, 1101–1107 (2016).
12. Bullard-Feibelman, K. M. *et al*. The FDA-approved drug sofosbuvir inhibits Zika virus infection. *Antiviral Res.* **137**, 134–140 (2017).
13. Sacramento, C. Q. *et al*. The clinically approved antiviral drug sofosbuvir inhibits Zika virus replication. *Sci. Rep.* **7**, 40920 (2017).
14. Onorati, M. *et al*. Zika virus disrupts phospho-TBK1 localization and mitosis in human neuroepithelial stem cells and radial glia. *Cell Rep.* **16**, 2576–2592 (2016).
15. Morrison, T. E. & Diamond, M. S. Animal models of Zika virus infection, pathogenesis, and immunity. *J. Virol.* **91**, e00009–00017 (2017).
16. Chia, R., Achilli, F., Festing, M. F. & Fisher, E. M. The origins and uses of mouse outbred stocks. *Nat. Genet.* **37**, 1181–1186 (2005).
17. Fernandes, N. C. *et al*. Experimental Zika virus infection induces spinal cord injury and encephalitis in newborn Swiss mice. *Exp. Toxicol. Pathol.* **69**, 63–71 (2017).
18. van den Pol, A. N., Mao, G., Yang, Y., Ornaghi, S. & Davis, J. N. Zika virus targeting in the developing brain. *J. Neurosci.* **37**, 2161–2175 (2017).
19. Stauft, C. B., Gorbatsevych, O., Cello, J., Wimmer, E. & Futcher, B. Comparison of African, Asian, and American Zika viruses in Swiss Webster mice: virulence, neutralizing antibodies, and serotypes. *bioRxiv*, doi:10.1101/075747, 075747 (2016).
20. Coelho, S. V. A. *et al*. Development of standard methods for Zika virus propagation, titration, and purification. *J. Virol. Methods* **246**, 65–74 (2017).
21. Centers for Disease Control and Prevention (CDC). Revised diagnostic testing for Zika, chikungunya, and dengue viruses in US Public Health Laboratories. https://www.cdc.gov/zika/pdfs/denvchikvzikv-testing-algorithm.pdf (2016).
22. Kilkenny, C., Browne, W. J., Cuthill, I. C., Emerson, M. & Altman, D. G. Improving bioscience research reporting: the ARRIVE guidelines for reporting animal research. *Osteoarth. Cartil.* **20**, 256–260 (2012).
23. Huang, W. C., Abraham, R., Shim, B. S., Choe, H. & Page, D. T. Zika virus infection during the period of maximal brain growth causes microcephaly and corticospinal neuron apoptosis in wild type mice. *Sci. Rep.* **6**, 34793 (2016).
24. Dean, A. G., Sullivan, K. M. & Soe, M. M. OpenEpi: open source epidemiologic statistics for public health. www.OpenEpi.com (2014).

25. European Medicines Agency, EMA. Sovaldi. http://www.ema.europa.eu/docs/en_GB/document_library/EPAR__Public_assessment_report/human/002798/WC500160600.pdf (2013).
26. Simonin, Y. *et al*. Zika virus strains potentially display different infectious profiles in human neural cells. *EBioMedicine* **12**, 161–169 (2016).
27. Cerbino-Neto, J. *et al*. Clinical manifestations of Zika virus infection, Rio de Janeiro, Brazil, 2015. *Emerg. Infect. Dis.* **22**, 1318–1320 (2016).
28. Metsky, H. C. *et al*. Zika virus evolution and spread in the Americas. *Nature* **546**, 411–415 (2017).
29. Solomon, T., Baylis, M. & Brown, D. Zika virus and neurological disease-approaches to the unknown. *Lancet Infect. Dis.* **16**, 402–404 (2016).
30. Muthuri, S. G. *et al*. Effectiveness of neuraminidase inhibitors in reducing mortality in patients admitted to hospital with influenza A H1N1pdm09 virus infection: a meta-analysis of individual participant data. *Lancet Respir. Med.* **2**, 395–404 (2014).
31. Au-TGA, Australian Therapeutic Goods and Administration. Australian public assessment report for ledipasvir/sofosbuvir. https://www.tga.gov.au/auspar/auspar-sofosbuvir-ledipasvir (2015).
32. Study of Hepatitis C treatment during pregnancy - full text view - ClinicalTrials.gov. https://clinicaltrials.gov/ct2/show/NCT02683005 (2017).
33. Hirsch, A. J. *et al*. Zika virus infection of rhesus macaques leads to viral persistence in multiple tissues. *PLoS Pathog.* **13**, e1006219 (2017).
34. Dowall, S. D. *et al*. A susceptible mouse model for Zika virus infection. *PLoS Negl. Trop. Dis.* **10**, e0004658 (2016).
35. Paz-Bailey, G. *et al*. Persistence of Zika virus in body fluids - preliminary report. *N. Engl. J. Med.* doi:10.1056/NEJMoa1613108 (2017).
36. Garcez, P. P. *et al*. Zika virus impairs growth in human neurospheres and brain organoids. *Science* **352**, 816–818 (2016).
37. Retallack, H. *et al*. Zika virus cell tropism in the developing human brain and inhibition by azithromycin. *Proc. Natl. Acad. Sci. USA.* **113**, 14408–14413 (2016).

Acknowledgements

Thanks are due to Drs. Carlos M. Morel, Marcio L. Rodrigues, Renata Curi, and Fabrícia Pimenta for their strong advisement and support regarding the technological development underlying this project. This work was supported by Conselho Nacional de Desenvolvimento e Pesquisa (CNPq), Fundação de Amparo à Pesquisa do Estado do Rio de Janeiro (FAPERJ). The BMK consortium did not provide funding for this project.

Author Contributions

Experimental execution and analysis – A.C.F., C.Z.V., P.A.R., G.B.-L., Y.R.V., M.M., P.P.S., and C.S. Provided critical material – K.B. Data analysis, manuscript preparation, and revision – A.C.F., C.Z.V., P.A.R., G.B.-L., Y.R.V., M.M., P.P.S., C.S., H.C.C.F.N., L.C., A.T., F.A.B., P.T.B., and T.M.L.S. Conceptualized the study – A.C.F., C.Z.V., P.A.R., K.B., F.A.B., P.T.B., and T.M.L.S. All authors revised and approved the manuscript.

Additional Information

Supplementary information accompanies this paper at doi:10.1038/s41598-017-09797-8

Competing Interests: K.B. is a member of the consortium BMK, which manufactures sofosbuvir.

Publisher's note: Springer Nature remains neutral with regard to jurisdictional claims in published maps and institutional affiliations.